Optimal Assessment of Using Solar and Wind Power for Desalination on the Eastern Coast of Saudi Arabia

by

Basel Ismail

A Thesis Presented to the

FACULTY OF THE COLLEGE OF GRADUATE STUDIES

KING FAHD UNIVERSITY OF PETROLEUM & MINERALS

DHAHRAN, SAUDI ARABIA

In Partial Fulfillment of the
Requirements for the Degree of

MASTER OF SCIENCE

In

MECHANICAL ENGINEERING

September, 1992

Order Number 1354084

Optimal assessment of using solar and wind power for desalination on the Eastern Coast of Saudi Arabia

Ismail, Basel, M.S.

King Fahd University of Petroleum and Minerals (Saudi Arabia), 1992

U·M·I
300 N. Zeeb Rd.
Ann Arbor, MI 48106

OPTIMAL ASSESSMENT OF USING SOLAR AND WIND POWER FOR DESALINATION ON THE EASTERN COAST OF SAUDI ARABIA

BY

BASEL ISMAIL

A Thesis Presented to the

FACULTY OF THE COLLEGE OF GRADUATE STUDIES

KING FAHD UNIVERSITY OF PETROLEUM & MINERALS

DHAHRAN, SAUDI ARABIA

In Partial Fulfillment of the
Requirements for the Degree of

MASTER OF SCIENCE
In
MECHANICAL ENGINEERING

SEPTEMBER, 1992

KING FAHD UNIVERSITY OF PETROLEUM & MINERALS

DHAHRAN, SAUDI ARABIA

This thesis, written by

Basel Ismail A. Ismail

under the direction of his thesis committee, and approved by all the members, has been presented to and accepted by the Dean, College of Graduate Studies, in partial fulfillment of the requirements for the degree of

MASTER OF SCIENCE IN MECHANICAL ENGINEERING

Thesis Committee

Chairman (Dr. F. A. Al-Sulaiman)

Member (Dr. S. A. M. Said)

Member (Dr. A. A. Al-Farayedhi)

Dr. M. O. Budair
Department Chairman

Dr. Ala M. Rabeh
Dean College of Graduate Studies

Date : 17 - 10 - 92

To My Beloved Parents, Sisters, Brothers

and to Those Who Shared Their Care and Concern

ACKNOWLEDGEMENTS

Praise and gratitude be to Allah, the Almighty, with Whose gracious help, it was possible to accomplish this work.

Acknowledgement is due to the King Fahd University of Petroleum and Minerals for providing support to this work.

I wish to express my deep appreciation to my major thesis advisor Dr. Faleh A. Al-Sulaiman for his constant cooperation in the development of the present work, and for the many hours of attention he devoted to the development of this student. He was always kind and sympathetic to me. Working with him was indeed a wonderful experience which I thoroughly enjoyed.

I am also grateful to other members of my thesis committee Dr. Abdul-Ghani Al-Frayedhi and Dr. Syed A.M. Said for their interest, help, and advice.

I also want to thank Dr. Abdul-Ali A.F.M. for his contribution in my scholastic development in the area of solar energy which helped me in my thesis work. I am also greatly indebted to other faculty of Mechanical Engineering Department.

I wish to extend thanks to my karate team, friends and fellow graduate students for their moral support and the memorable days we shared together.

TABLE OF CONTENTS

LIST OF TABLES

LIST OF FIGURES

NOMENCLATURE

A	:	available energy, kJ
$\dot{A}$	:	availability rate, kW
$\dot{A}_{supply}$	:	total rate of available energy supplied into the system, kW
$\dot{A}_{products}$	:	total rate of available energy in useful products, kW
$\dot{A}_s$	:	rate of available energy destroyed within the system, kW
A_c	:	collector face area, m^2
$(A_c)_{opt}$	:	optimum collector area of PV system, m^2
BW	:	brackish water
CC	:	capital cost, $
$(C_B)_{opt}$	:	optimum electrical storage capacity of the batteries, kWh
C_p	:	specific heat of brine, $kJ/kg.K$
c_p	:	power coefficient of WEC
e	:	rate of exergy, kW
ED	:	electrodialysis process
f_c	:	corrected solar fraction
f_s	:	monthly average solar fraction
f_w	:	monthly average wind fraction
FR	:	freezing process
F_R	:	heat removal factor

h	:	enthalpy per unit mass, kJ/kg
h_{fg}	:	latent heat of evaporating brine, $W/m^2.K$
H	:	enthalpy, kJ
$\overline{H}_H$	:	monthly average daily solar radiation falling on a horizontal surface, MJ/m^2
$\overline{H}_{dH}$	:	monthly average daily diffuse radiation falling on a horizontal surface, MJ/m^2
$\overline{H}_{OH}$	:	monthly average daily extraterresterial radiation falling on a horizontal surface, MJ/m^2
$\overline{H}_T$	:	monthly average daily radiation falling on a tilted surface, MJ/m^2
i	:	normalized irreversibility, kW/kg
$\dot{I}$	:	rate of irreversibility, kW
IR	:	interest rate
$\overline{I}_T$	:	monthly daily average hourly radiation falling on a tilted surface, MJ/m^2
$\overline{K}_T$	:	monthly average clearness index
L	:	monthly average load required by MES, GJ
L_m	:	monthly average load required by RO, kW
$\dot{m}_p$	:	product water flow rate, kg/s
MC	:	maintenance coefficient
MES	:	multi-effect stack process

MSF	:	multi-stage flash process
n	:	number of effects in MES
N_i	:	moles of an ith component
P	:	pressure, bar
PC	:	production capacity, m^3/day
P_e	:	electrical load required by MES, kW
P'_e	:	electrical load provided by one WEC machine, kW
P_t	:	thermal load required by MES, kW
ppm	:	particles per million
PR	:	performance ratio (factor) of desalination processes
pv	:	present value, $
$\dot{Q}$	:	rate of heat consumption, kW
$\dot{Q}_{C.V.}$	:	rate of heat within a control volume, kW
Q_{st}	:	storage tank heat losses, GJ
r_d	:	ratio of hourly diffuse radiation to daily diffuse radiation
$r_{d,n}$	:	noon ratio of hourly diffuse radiation to daily diffuse radiation
r_t	:	ratio of hourly total radiation to daily total radiation
$r_{t,n}$	:	noon ratio of hourly total radiation to daily total radiation
$\overline{R}$	:	ratio of radiation falling on a tilted surface to that on a horizontal surface for the average day
RO	:	reverse osmosis process
$R_{b,n}$	:	beam radiation conversion factor at noon

R_c	:	recovery/conversion ratio (ratio of product water to feedwater)
R_n	:	noon total geometric factor
s	:	entropy per unit mass, kJ/kg.K
S	:	entropy, kJ/K
$\dot{S}$	:	rate of entropy, kW/K
SEC	:	specific energy consumption, kWh/m^3
$(STL)_{opt}$	:	system's optimum total cost, $
$\overline{T}_a$	:	monthly average daily ambient temperature, K
$\overline{T}_{min}$	:	monthly average minimum required temperature, K
$\overline{T}_s$	:	monthly average storage tank temperature, K
T_{WF}	:	temperature weighting factor, K
$(UA)_s$	:	heat loss coefficient-area product of the storage tank, $W/°C$
UC	:	unitary cost
U_L	:	overall heat loss coefficient, $W/m^2.°C$
V	:	total volume of the storage tank, m^3
VC	:	vapor compression process
$\overline{V}_w$	:	monthly average wind speed, m/s
$WECS$	:	wind energy conversion system
X'	:	dimensionless group
$\overline{X}_{c,min}$	:	critical radiation level at the minimum useful temperature
y	:	number of years
Y	:	dimensionless group

Greek Symbols

α	:	ratio of the rated power, p_{r_r} of the WEC to the required power. p_r
β	:	tilt angle of the solar collector
$\bar{\delta}$	:	declination angle of an average day of the month
η	:	thermal conversion efficiency
η_{II}	:	second-law efficiency
σ	:	salinity, g/kg
φ	:	location latitude, degrees
$\bar{\varphi}_{max}$	:	average maximum utilizability factor
$(\overline{\tau\alpha})$	:	transmittance-absorptance product

THESIS ABSTRACT

NAME OF STUDENT : *BASEL ISMAIL A. ISMAIL*

TITLE OF STUDY : *Optimal Assessment of Using Solar and Wind Power for Desalination on the Eastern Coast of Saudi Arabia*

MAJOR FIELD : *Mechanical Engineering*

DATE OF DEGREE : *September, 1992*

In order to select the desalination process that is best suited for coupling with solar and wind power on Dhahran area, located on the Eastern Coast of Saudi Arabia, several desalination processes were evaluated and compared with regard to their, energy requirements, technical performances, and economics. Further comparison was made based on the second-law of thermodynamics. Based on this comparison, the reverse osmosis (RO) and multi-effect stack (MES) processes were selected.

Three cost-effective designs were proposed. The present value method was used for the economics analysis of these designs. It was found that the augmented solar/wind-powered MES system is economically feasible for desalting seawater with unit distilled water cost ranging between 9.5-15 $/m^3, whereas, the autonomous wind-powered RO system is favoured for desalting brackish water with unit distilled water cost ranging between 0.87-1.85 $/m^3.

MASTER OF SCIENCE DEGREE

KING FAHD UNIVERSITY OF PETROLEUM AND MINERALS

Dhahran, Saudi Arabia

September, 1992

خلاصة الرسالة

إسم الطالب :- باسل اسماعيل عبد اسماعيل
عنوان الرساله :- تقييم أمثل في إستخدام الطاقة الشمسية والطاقة الهوائية لأغراض تحلية المياه المالحة على الساحل الشرقي للمملكة العربية السعودية
التخصص :- هندسة ميكانيكية
تاريخ الدرجة :- سبتمبر ١٩٩٢م

لكي يتم اختيار طريقة التحلية الأفضل للإقتران بمصدري الطاقة الشمسية والهوائية في منطقة الظهران والواقعة على الساحل الشرقي للمملكة العربية السعودية ، فقد تم تقييم عدد من طرق التحلية المعروفة ومقارنتها من حيث كمية الطاقة المطلوبه للتشغيل ونوعيتها والآداء التقني والإقتصادي. علاوةً على ذلك فقد عُملت مقارنة أخرى بين طرق التحلية على أساس القانون الثاني للديناميكا الحرارية. إستناداً لهذه المقارنات فقد تم اختيار طريقة التناضح العكسي (RO) وطريقة التأثير المتعدد (MES).

بعد ذلك أقترحت ثلاثة تصاميم فاعلية التكلفة من حيث النظرة الإقتصاديه ، وقد تم استخدام طريقة القيمة الحاضرة للتحليل الإقتصادي لهذه التصاميم ، وكنتيجة لهذه الدراسة فقد وُجد بأن التصميم المتعلق بطريقة ـ التأثير المتعدد ـ والمشغلة بمصدري الطاقة الشمسية والهوائية معاً (بنسب متفاوتة) هو أكثر ملاءَمة اقتصادية لتحلية مياه البحر بتكلفة اجمالية تتراوح ما بين ٩,٥ـ ١٥ دولاراً للمتر المكعب الواحد من الماءالمقطر، بينما التصميم المتعلق بطريقة التناضح العكسي والمشغل بالطاقة الهوائية فقط هو أكثر ملاءَمة اقتصادية لتحلية مياه الآبار المالحة بتكلفة اجمالية تتراوح ما بين ٠,٨٧ـ ١,٨٥ دولاراً للمتر المكعب الواحد من الماء المقطر.

درجة الماجستير في العلوم

جامعة الملك فهد للبترول والمعادن

الظهران، المملكة العربية السعودية

سبتمبر ، ١٩٩٢م

CHAPTER 1

INTRODUCTION

Water is a key ingredient for agricultural and industrial growth, and adequate supplies of drinking water are essential to support the growing urban populations. Adequate quantities of water and quality are also essential if lasting improvements in health conditions are to be achieved. Today more than 10 million cubic meters of freshwater are produced from seawater every day, as indicated in figure (1.1) [1]. Figure (1.2) [1] demonstrates the accumulated world capacity of desalination plants and the worldwide geographic distribution of desalination plants as of January 1988.

Saudi Arabia is a vast, sparsely populated desert country with no rivers or lakes and the average annual rainfall is less than 10 cm. Only in the southwest may rainfall reach 30 cm [2]. Deprived of such fresh water supplies, Saudi Arabia must depend on its ground and sea water resources. Figure (1.3) [3] shows that the country is surrounded by the Red sea from the west and the Arabian Gulf from the east. The demand for potable water on a vast scale has placed greater concern during the most recent years due to the increasing urbanization of the population, the nature and level of industrial growth, and the type and intensity of agricultural production, in addition to other components of economic and social development.

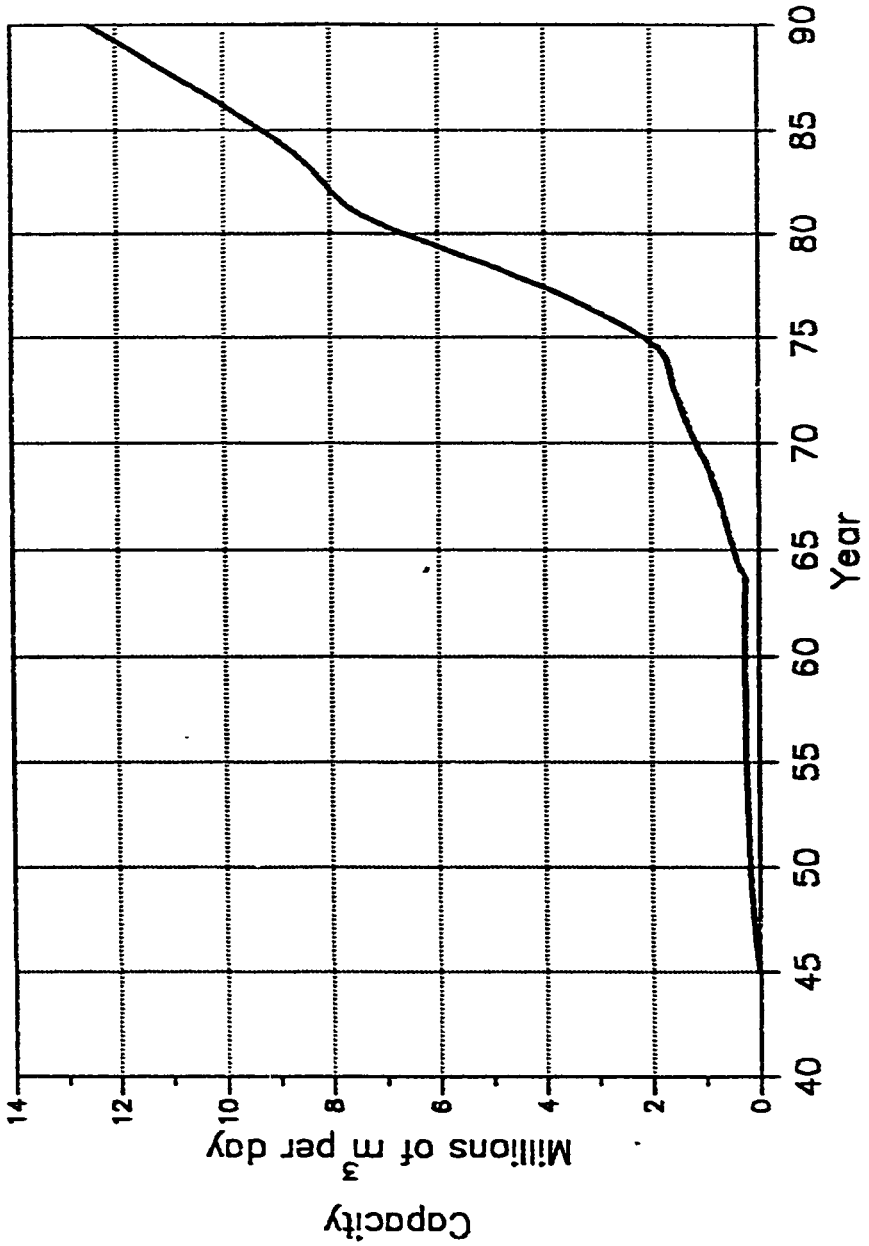

Figure (1.1) Accumulated World Capacity of Desalination Plants [1]

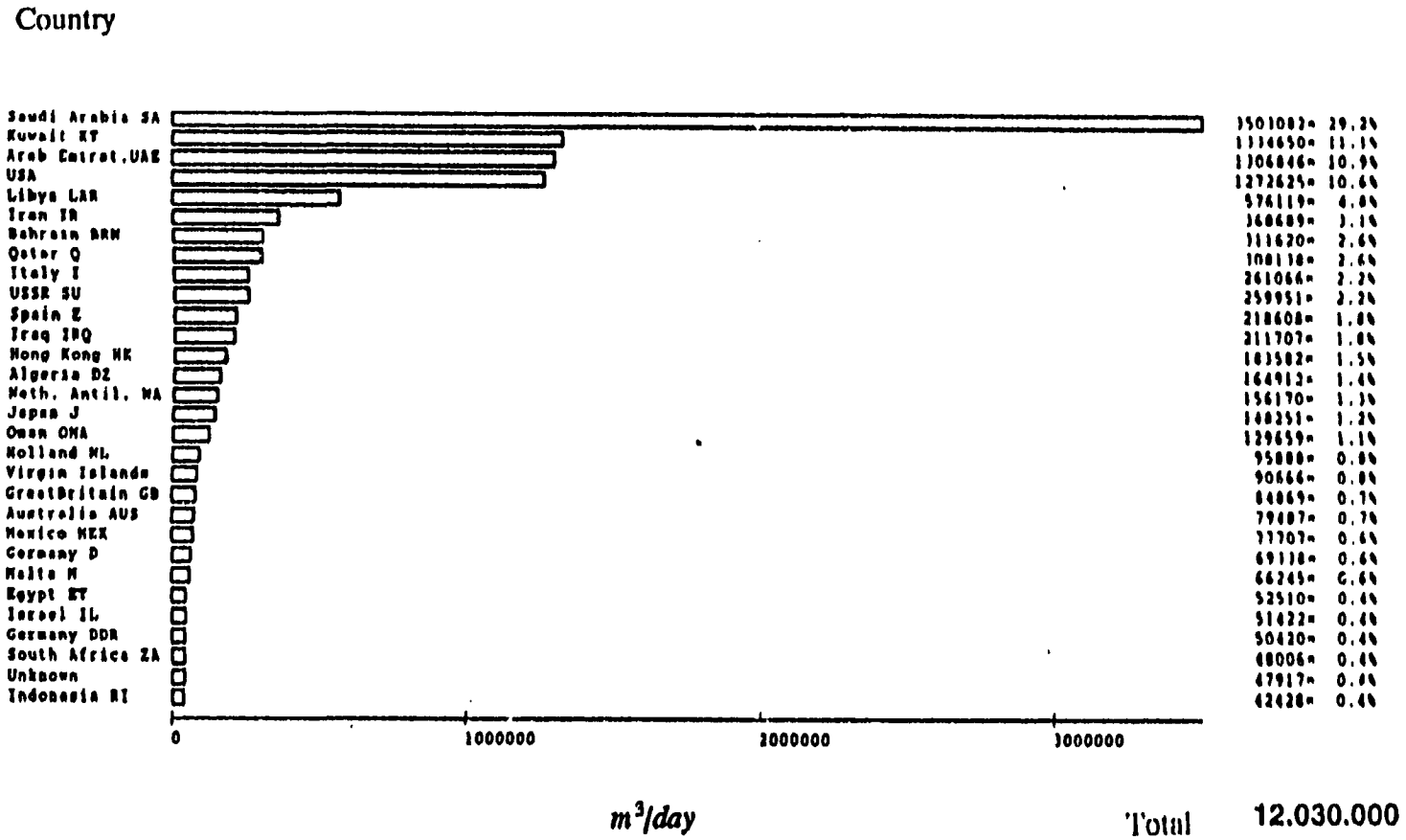

Figure (1.2) Worldwide Distribution of Desalination Plants Production in 1988 [1]

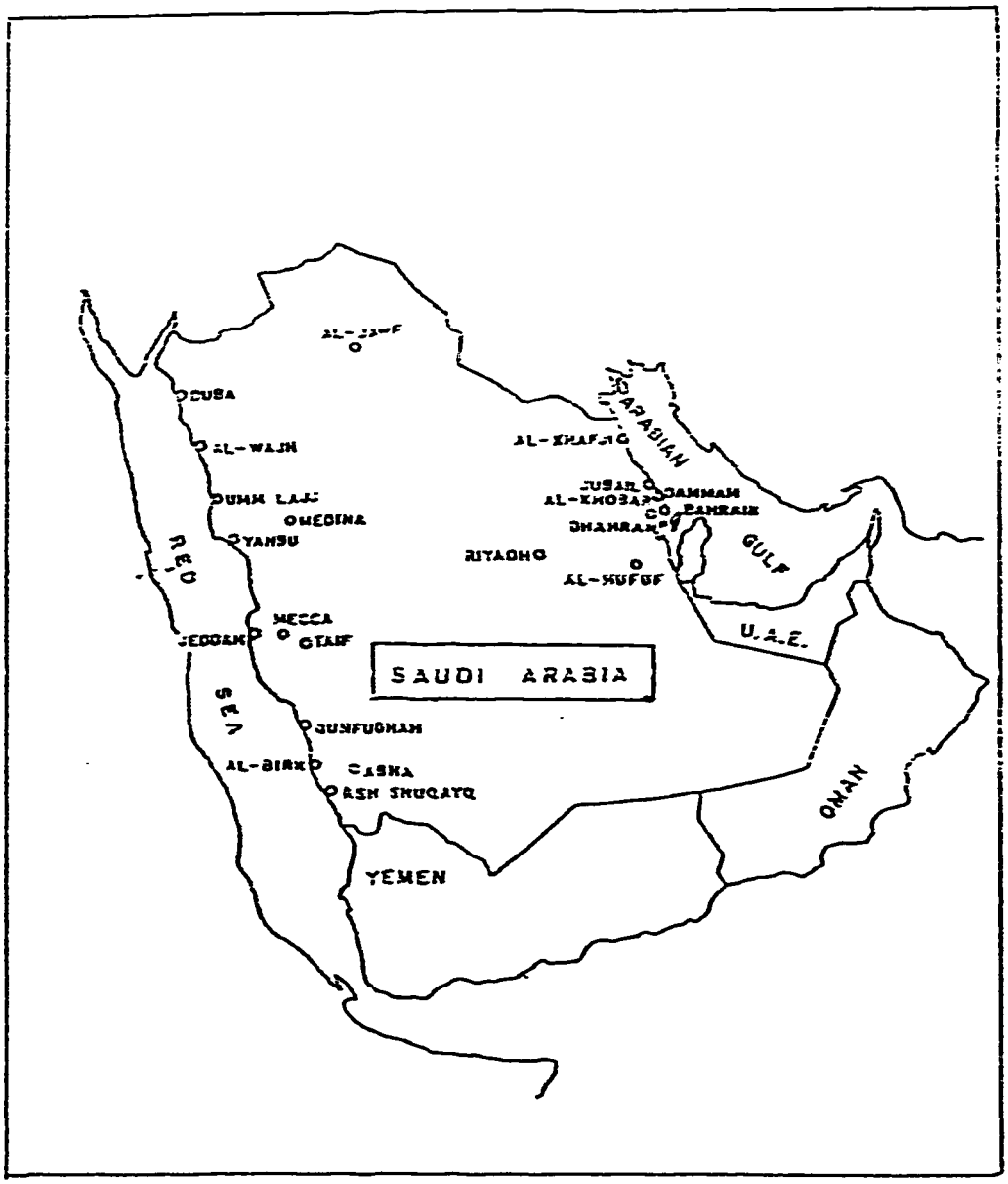

Figure (1.3) Map of Saudi Arabia [3]

To satisfy the growing demands for fresh water, the government of Saudi Arabia, through its agency, the saline water conversion corporation (SWCC) embarked on desalination on a scale never witnessed before anywhere. Desalination has taken great optimistic interest from the government primarily because it has recently shown a great impact on the growth of the country [4]. Figures (1.4) and (1.5) [2] show the projection of water desalination capacity in Saudi Arabia for the time period 1965-1990. Projected annual supply of water in the Kingdom (1980-2000) is depicted in figure (1.6) [2].

Desalination is a separation process needing energy in the form suitable for operation of the selected technique. It has been observed that nearly 50% to 60% of the total cost of desalted water is due to energy cost. The water scarcity is mostly faced in distant places which lack in many basic amenities including supply of the conventional energy sources [5]. This results in a great need to non-conventional sources.

Several desalination methods exist, and for convenience they can be classified by energy consumption or by considering the band of feedwater salinities for which they are applicable. Another useful way to classify desalination methods is to separate the process into those which involve phase change to separate the pure water from the saline water and those which do separation without phase change [6].

The processes which involve phase change are :

- Multistage Flash Distillation (MSF)
- Multiple Effect Distillation (MED)

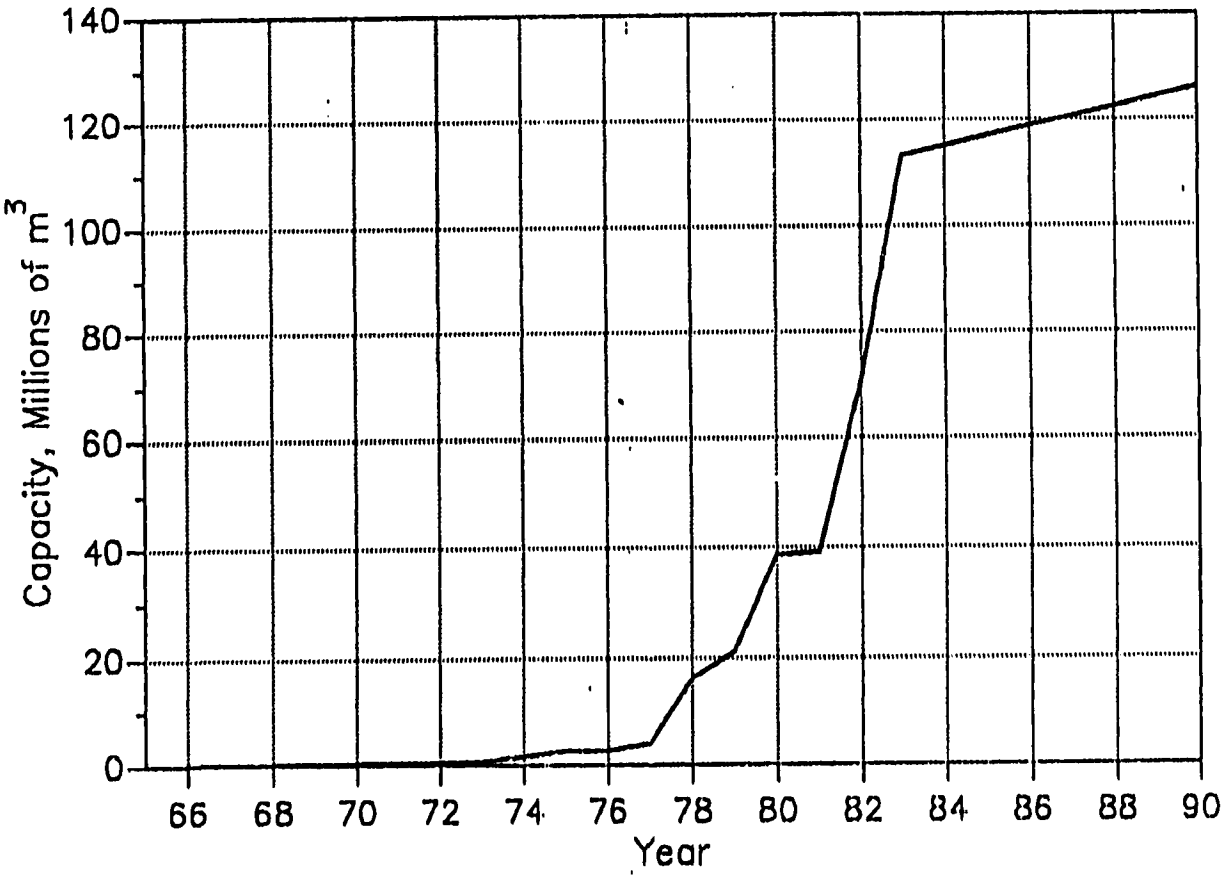

Figure (1.4) Desalination Capacity in Saudi Arabia 1965-1990 (Adapted) [2]

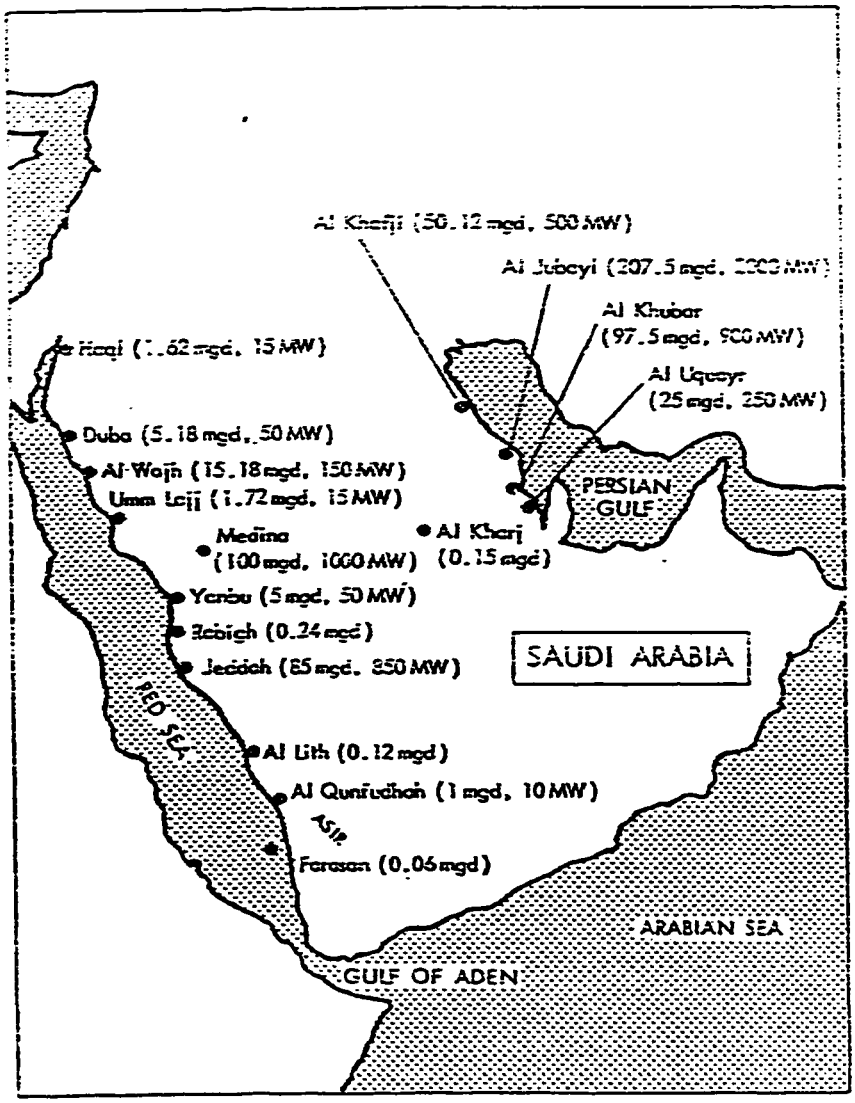

Figure (1.5) Projected Water Desalination Capacity (million gallon per day and megawatts) in Saudi Arabia [2]

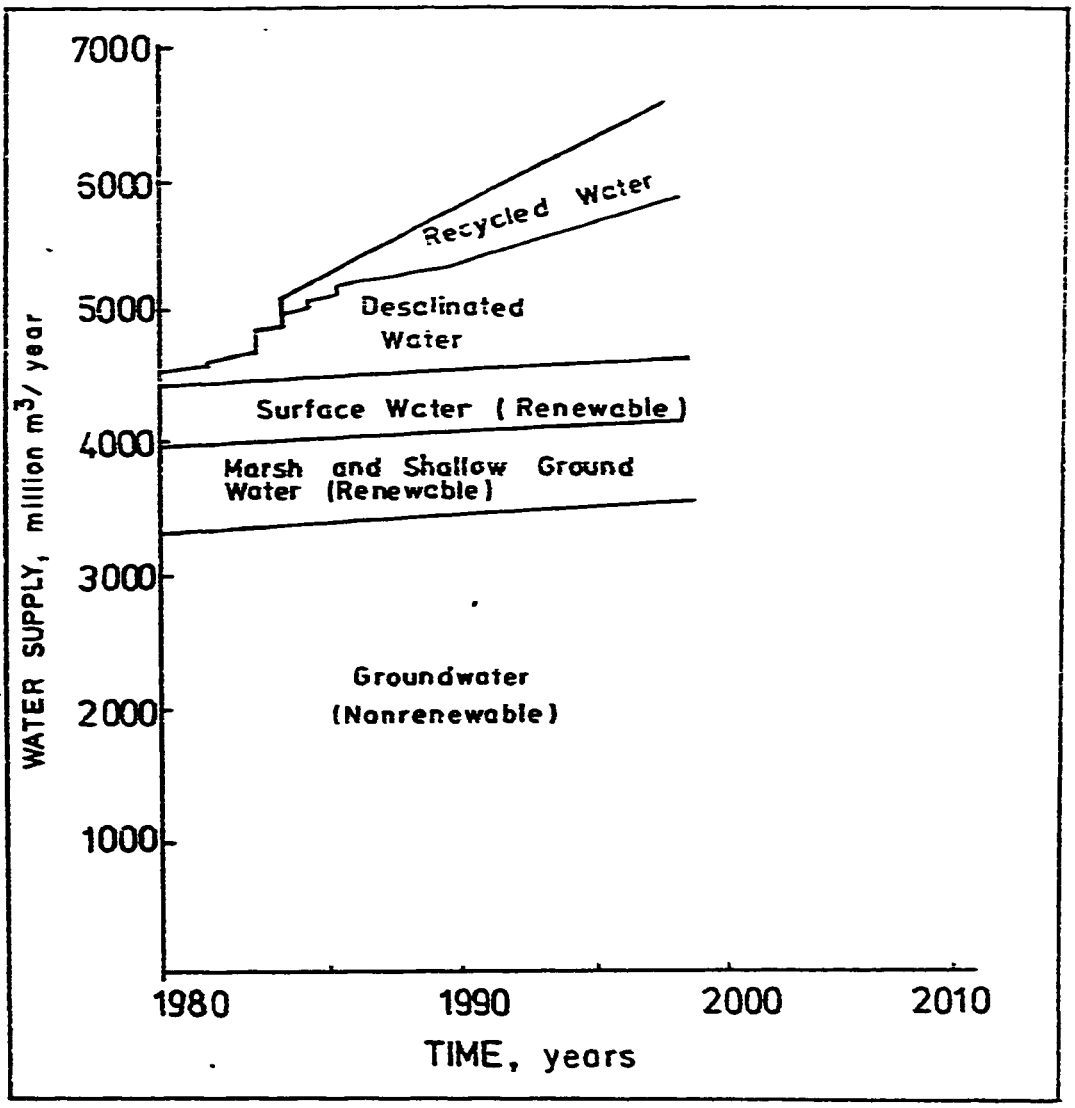

Figure (1.6) Projected Annual Supply of Water in Saudi Arabia 1980-2000 [2]

- Vapor Compression (VC)
- Solar Distillation (Solar Stills)
- Freezing (FR)

Those processes which do not require phase change are :

- Reverse Osmosis (RO)
- Electrodialysis (ED)

The multistage flash (MSF), reverse osmosis (RO), and electrodialysis (ED) are the most commonly used processes for desalination in Saudi Arabia. The MSF process accounts for about two-thirds of production of potable water in Saudi Arabia. It is used exclusively for conversion of seawater. The reverse osmosis and electrodialysis are used for desalination of brackish water, with RO being a strong leader and accounting 80% of conversion of such water.

In recent years, a number of RO plants have been built in the Kingdom for desalination of seawater as well. Their commercial success has still to be demonstrated [7]. Figure(1.7) [7] illustrates the capacity of desalination units installed in Saudi Arabia for the period 1973-1990 .

The use of renewable (non-conventional) energy sources, such as solar and wind to obtain potable water from saline water was known to mankind a long time ago.

During the early 20th century, before rural electrification was widespread throughout North America and Europe, many reliable devices, such as windmills, were developed and sold to be used to pump water and generate

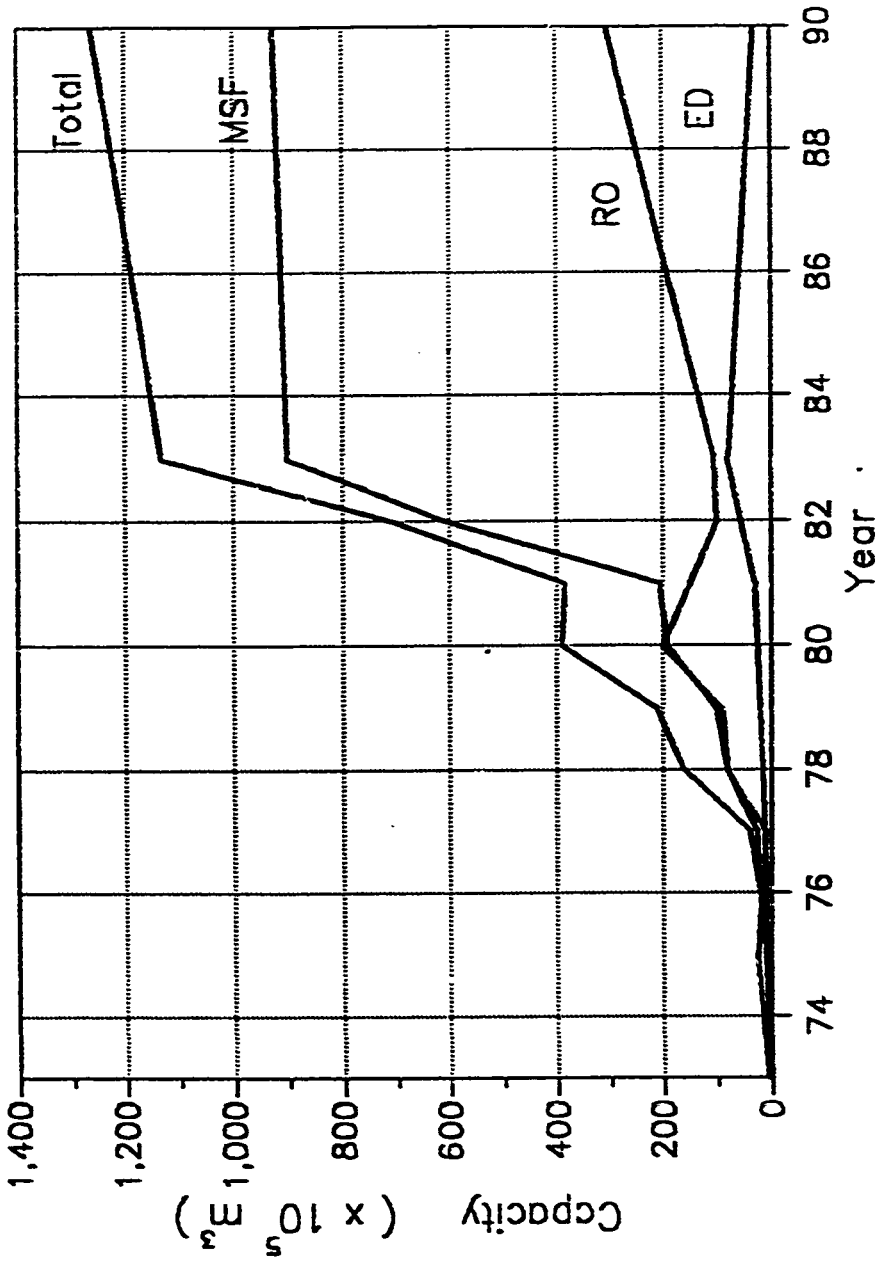

Figure (1.7) Capacity of Desalination Units Installed in Saudi Arabia [7]

small quantities of electricity. In fact many recent developments involve rather sophisticated devices, such as solid state circuity and photovoltaic cells [8].

The solar energy has been used even in earlier days for recovery of salt distillation of perfumes etc. The earliest large capacity conventional glass covered solar distiller for desalination was successfully constructed in 1872 in Chile. Later investigations have resulted in newer designs yielding higher outputs ranging between 2 to 4 litres or more per square meter [5]. Aside from the basic solar still, the development of alternate energy sources for desalination is in its infancy. The need for these sources is recognized by many throughout the world, but their commercial development and large-scale application, especially in developing countries, can be expected to take time to implement. Solar and wind power take a considerable capital investment per unit of power to develop, and their interface with desalination system can be complicated [9].

Solar energy has received the most attention as far as utilization for desalination is concerned. Using solar energy for desalination was mentioned as early as 17th century by the Italian scientist Della Porta. A variety of mechanisms are used to convert solar energy directly to other forms of energy--either heat or electricity. Among the commonly employed devices for energy conversion which are commercially available now are flat plate collectors, focused collectors, solar ponds, and photovoltaic cells [8]. Figure(1.8) [8] illustrates some commonly used solar energy conversion devices .

There is evidence that wind power has been used in windmill-type devices for thousand years. Their major functions have been to grind, pump water, and

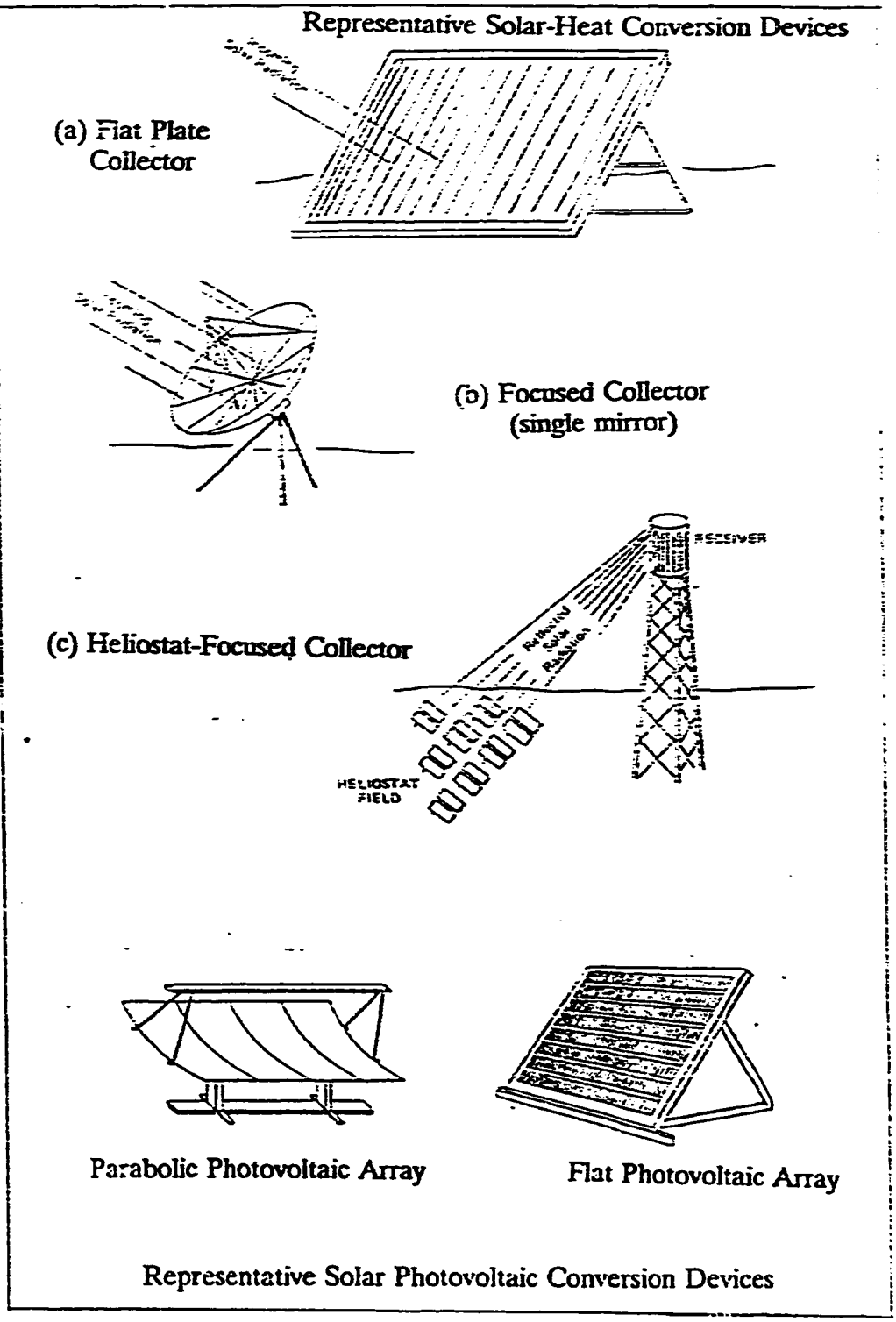

Figure (1.8) Common Solar Conversion System [8]

(most recently) to generate electricity. The application of wind energy systems to desalination processes offers an economical solution. Commercially available wind turbines and those under development appear promising for producing electricity [9]. Figure (1.9) [8] demonstrates some commonly used wind energy conversion systems.

There are, in general, three basic rationals for the use of renewable energy sources for desalination, namely, the high cost of standard fuels, the conservation of fossil fuels, and the lack of conventional power sources in isolated areas. In general, the high, and continually rising, cost of conventional fuels is a dominant factor in directing attention toward the utilization of alternate energy sources. Recently, air pollution is becoming the most dominant factor. The most commonly used renewable "clean" resources are solar and wind power, which require no further investment in power once the proper energy collection system is installed. Table (1.1) [5] demonstrates some worldwide desalination plants operated by solar and wind power.

Desalination is an expensive way of obtaining fresh water. The processes involved are quite complex and the degree of complexity is directly related to the size of the system. Equipment costs are high because suppliers are few and competition is somewhat limited. Besides a large capital investment, operation requires large expenses for fuel, labor, chemicals, maintanence etc. In order to make a decision regarding the most appropriate process for brackish/seawater desalination, both technical and economical characteristics of various desalting processes need to be studied thoroughly [10].

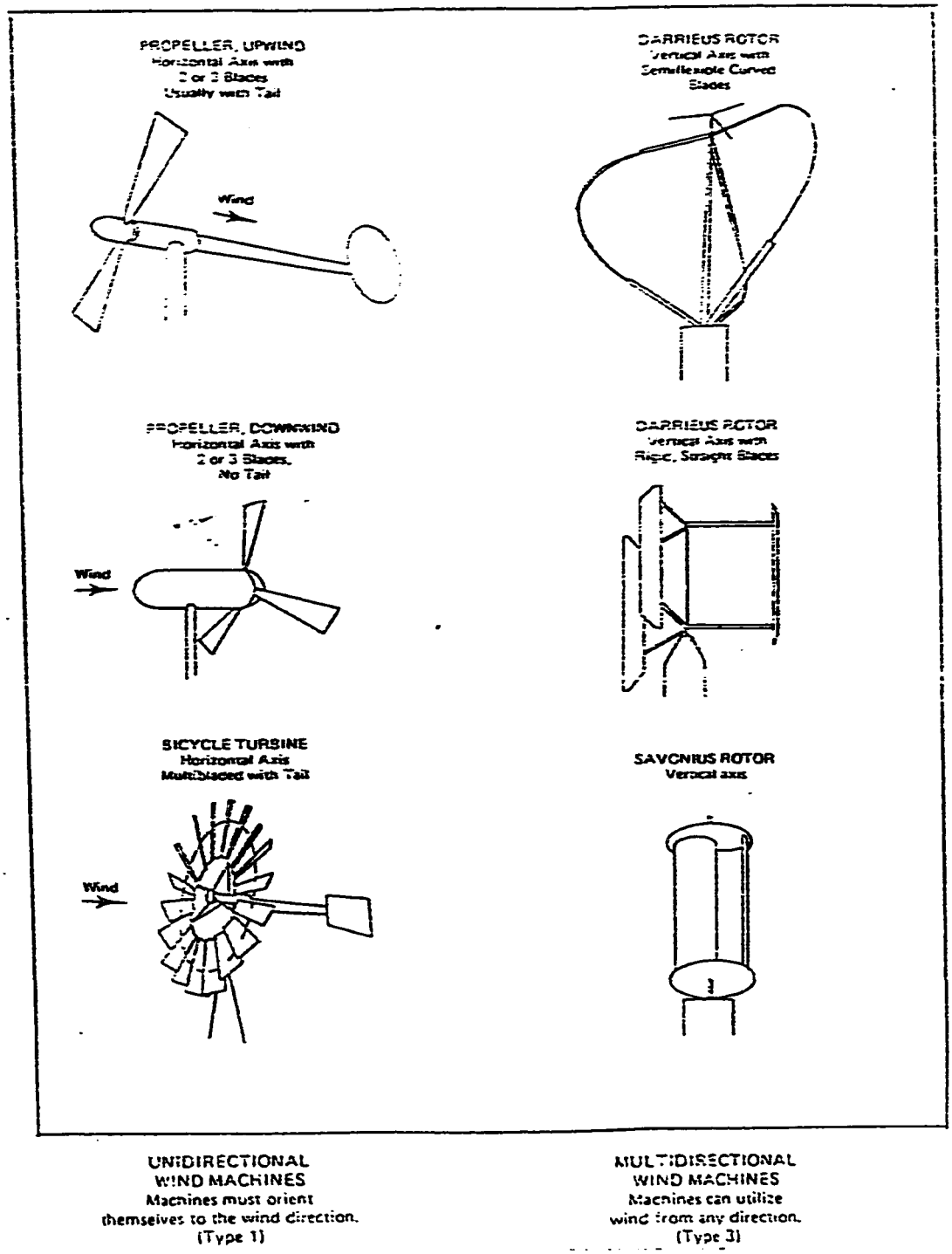

Figure (1.9) Common Types of Wind Machines [8]

Table (1.1) Desalination Plants Operated by Renewable Energy Sources [8]

Sr. No.	Location	Year of installation	Type of saline water	Capacity	Details of desalination plant	Energy system
1	2	3	4	5	6	7
			1.Solar Powered			
A. Distillation Processes						
1.	Helic Lab. Tashkent.USSR		-	1 m^3/day	M.E.E. - 3 effect	Parabolicidal conc. of. dia. 10 m
2.	La Paz, Mexico	1980	Sea water	10 m^3/day	M.S.F. - 10 stages	Flat plate collectors with selective surface (513 m^2)+(160 m^2) concentrator
3.	Takamijara Island (Japan)	1981	/do/	10 m^3/day	Horizontal tube multi-effect stack (16 effects)	
4.	Umm Al Nar, Abu Dabhi, U.A.E.	1984	/do/	80 m^3/day	/do/ (16 effects)	Evacuated glass tube collectors.1382 m^2
5.	La De'sigrade, French Carribean Island		/do/	40 m^3/day	M.E.E.-14 effects operation at 65-70 °C	Tubular vacuum collector, 670 m^2
6.	Bari, Italy		do/	10 m^3/day	MSF - 12 stage	Line focussing collectors - 320 m^2
B.Electrodialysis (ED)						
7.	Colorado school of Mines, USA	1980	Brackish (3200 ppm salinity)	1.8 m^3/day	E-D stack with 2 electrical and 5 hydraulic stages, 55% recovery operation at 48 V	PV solar cells 300 watt
8.	Yuma, USA		Brackish water	3 m^3/day		PV Solar cells and 30 KwH battery back-up
9.	Ohsima Island, Japan	1985	Sea water	10 m^3/day (24 hours)	E.D.stack with 20 membrane pairs, operation at 100 Volts	PV Solar cells of 25 KWp with batteries of 1200 Amphr. capacity

Cont. Table (1.1) Desalination Plants Operated by Renewable Energy Sources

Sr. No.	Location	Year of installation	Type of saline water	Capacity	Details of desalination plant	Energy system
1	2	3	4	5	6	7
			I.Solar Powered			
I.Reverse Osmosis (RO)						
10.	Cadarache, France	1978	Brackish water (3000 ppm)	1.5 m^3/hr	RO-Dupont Permascap module - operating pressure 12 bar	Flat plate collectors with black chrome selective surface with 108 m^2 area.
11.	Conception del Oro, Mexico	1990	Brackish water (3000 ppm)	1.5 m^3/day	GZSS plate type RO module with 8.2 m^2 membrane area, operating pressure 40 bar	PV solar cells with 3.5 KW capacity. Area of array = 30 m^2
12.	Near Jeddah Saudi Arabia	1980	Sea water (42,000 ppm)	1.35 gpm	Two stage unit operating at 850 psi. 22% recovery	PV mirror type array with 5 KW capacity. Battery back-up of 240 V
13.	Cituis village, North coast of Java		Brackish water	12 m^3/day	RO unit operated for 6 hrs a day	PV Solar cells with 25.5 KWp capacity
14.	Doha, Qatar	1983	-do-	1500 gpd	Single stage RO unit operating pressure 700-900 psi	PV Solar Cells with 11.2 KWp capacity. Battery back-up
15.	SERIWA/SECWA test center W.Australia	1982	-do- (5000 ppm)	500-100 lpd	RO unit with DC motor pump (32 volt), salt rejection 85% and recovery 12%	PV Solar Cells with inverter and storage battery back-up. Array capacity 1.2 KW
16.	Billabong Road House, 700 Kms North of Perth W.Australia	1984	Brackish water (11000 ppm salinity)	6.0 m^3/day	Spiral module with thin film polymide membranes, salt rejection 98%, recovery 59%	PV array with 4 KWp capacity Battery back-up with 750 Amph capacity. 48 V DC operation.
17.	Tremiti Island.. Italy	1984	Sea water	10 m^3/day (potential output)		PV Solar array of 65 KWp capacity covering an area of 1600 m^2.

Cont. Table (1.1) Desalination Plants Operated by Renewable Energy Sources

Sr. No.	Location	Year of installation	Type of saline water	Capacity	Details of desalination plant	Energy system
1	2	3	4	5	6	7
			II. Wind Powered			
A. Distillation Processes						
1.	Brace Research Institute Canada	1961	Brackish water	1.2 m^3/day	Vapour Compression	Wind generator
B. Reverse Osmosis (RO)						
2.	Sidcroog island, north Coast of Germany	1981-82	Sea water	6-8 m^3/day	GKSS plate type module. Membrane area = 30 m^2 Operating Pressure = 80 bar	Wind generator with 8 kW capacity at wind vel. of 5m/sec. Rotor dia = 16 m
3.	Napier Island. Near Marseilles, France	1982-83	Sea water	0.5 m^3/hr	RO plant with 25% recovery	Wind generator with 4 kW capacity at - ind speed of 7 m/sec. 2 blade propeller with 9.2 m dia.

The main factors to be studied carefully before a particular desalting process is selected, in general, are :

- product water quality and quantity,
- feedwater quantity,
- feedwater characteristics,
- feedwater temperature,
- feedwater reliability,
- type of energy used,
- availability of energy,
- location of plant,
- suitability,
- process limitations, and
- process economics.

The basic concepts of thermodynamics are two commodities called ***Energy and Available-Energy***. The basic principles are the ***First Law*** , dealing with energy, and the ***Second Law*** , dealing with available-energy. The first law only states that energy is conserved. It does not tell about the type or quality of energy taking place in a real process. In contrast with energy, available-energy (exergy) is not a conserved commodity. The main purpose of the use of available-energy concept, through the second law, is to pinpoint the inefficiencies in and losses from processes, devices and systems [11].

The use of the second law to pinpoint the inefficiencies (irreversibilities) that take place in any desalination process would, therefore, be a great tool.

Overall Objectives of The Study

The scope of using solar and wind power for desalination on the east coast of Saudi Arabia will be examined with the following objectives :

(1) To assess the availability of solar and wind power. for desalination purposes, in Dhahran area (case study).

(2) To select the most suitable desalination process for coupling with solar and wind power in Dhahran area.

(3) To demonstrate the significance of using second-law-based analysis on the process selection.

(4) To evaluate some existing desalination plants based on the second-law concept. Some of which are :

- Al-Jubail MSF plant
- Al-Khobar MSF plant
- Jeddah MSF plant
- Abu Dhabi Solar-MES plant
- Typical RO plant
- Wind-RO plant at Germany

(5) To propose a scheme for coupling both wind and solar power with the selected desalination process.

(6) To provide a cost-effective design of an integrated solar/wind - powered desalination system.

The procedure to achieve such objectives is illustrated in figure (1.10). This figure is considered to be the flow chart of this study.

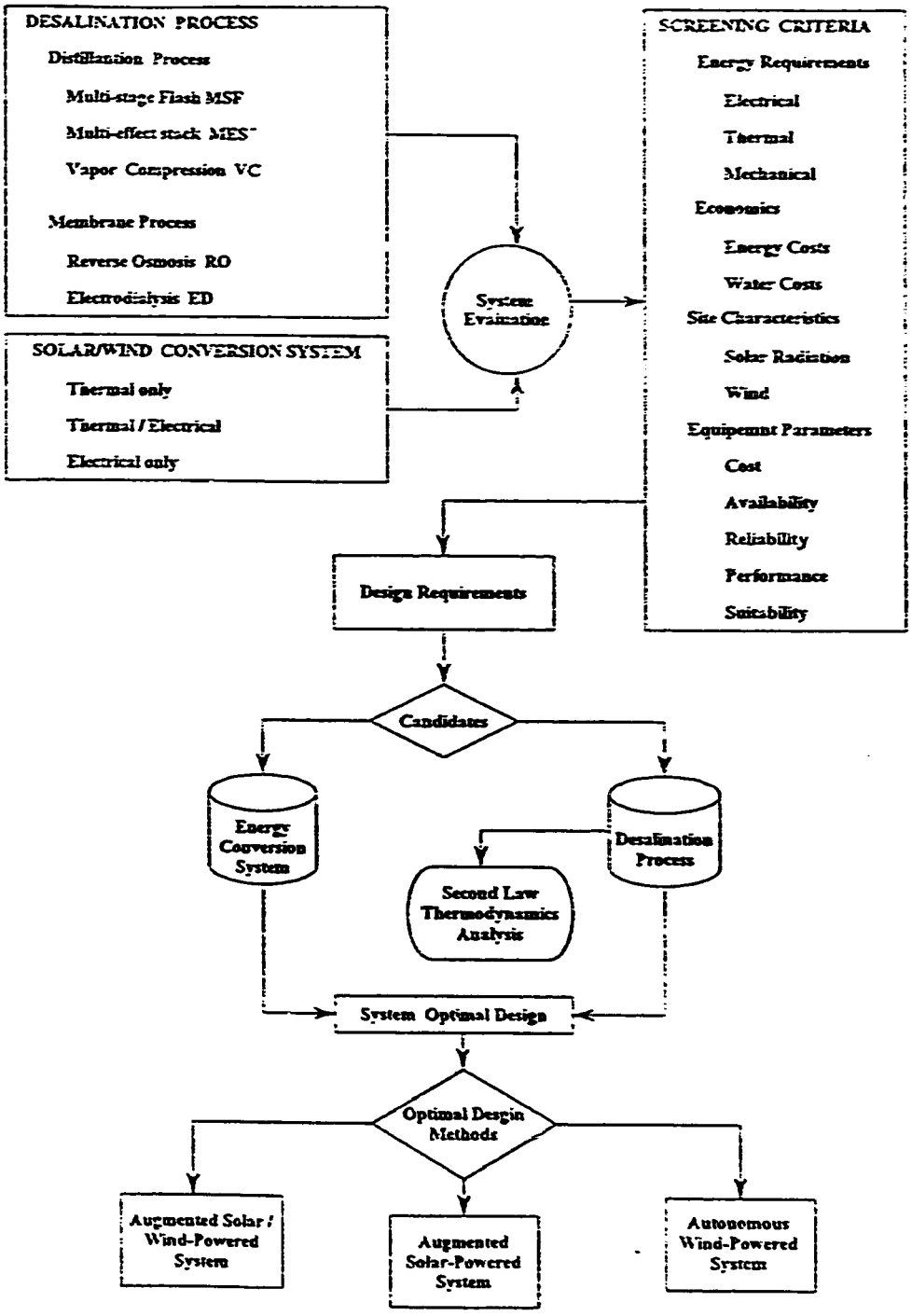

Figure (1.10) Procedure and Flow Diagram of the Method Adapted in this Study

CHAPTER 2

LITERATURE REVIEW

An extensive and thorough literature review was conducted. This endavour failed to produce a single citation on the application of wind and solar power for desalination on the eastern coast of Saudi Arabia. Al-Sulaiman and Jamjoum [12] assessed the wind power on the east coast of Saudi Arabia. The study indicated that the producibility of wind power in this area is similar to that of solar power (using current technologies). It was concluded that using wind power for some applications, such as water pumping for irrigation or desalination purposes, and electrical power generation in remote areas, needs further investigations.

In 1977 the Kingdom of Saudi Arabia and United States signed a project agreement for cooperation in the field of solar energy (SOLERAS). In 1980, the Solar Energy Research Institute (SERI) in Golden, Colorado, which is responsible for implementing the SOLERAS program, accepted proposals concerning studies on the technical and economic feasibility of large-scale desalination of brackish and seawater using solar power exclusively. These proposals were the initial part of a three-phase activity [8].

In 1980, Catalytic Inc., and Scientific Applications, have designed a solar-powered RO brackish water desalination facility. The design contract is part of the SOLERAS program. The city of Brownsville in Texas, was selected as the

site for application of this design concept. This site is typical, in terms of climatic conditions, of many areas in the southwestern United States and the Kingdom of Saudi Arabia. The electric power required to operate the the desalination plant is to be generated by point focus, high temperature collectors to provide thermal energy to a steam turbine generator. The solar energy system has been designed for a solar fraction of 1.0 [13].

In 1978, Abdel-Aal et al [14] proposed some schemes for utilizing solar energy in desalination for Saudi Arabia. Maurel, A. [1] reported on some activities in the field of desalination using renewable energy sources (wind/solar) in some Mediterranean countries. He concluded that it is economically feasible to use wind/solar power for desalination for energy requirements equal or less than 10 to 12 kW-hr per day for plants with production capacities of less than or equal to 10 to 12 m^3 a day using brackish water and in the vicinity of 2 m^3 a day for seawater.

Crutcher et al [15] reported on two installations of photovoltaic powered seawater desalination systems (PV-SWRO). According to the experience gained throughout the years of operation a number of conclusions were made. Some of which are; a PV-RO system is an excellent combination for solar powered desalination, a very high overall system efficiencies can be achieved, and commercial PV-RO systems can be designed that will desalt seawater with smaller collector areas and lower costs than other forms of solar powered desalination.

In order to make a decision regarding the most appropriate process for desalination to be coupled with solar/wind energy conversion systems, some important characteristics of various desalting processes need to be thoroughly studied. A comparison of desalinating processes on the basis of maintenance and operating complexity and capital costs was made by Finnegan et al [16]. The comparison is based primarily on the experience of the authors and the company that they represent. It was concluded that each process has advantages and disadvantages and the final process design should be based on achieving the desired reliability while minimizing the unit water cost. Another comparison was done by Gerofi and Fenton [17]. They compared the unit water cost from 100 m^3 /day solar driven RO plants with that from solar driven distillation plants. It was concluded that distillation is cheaper than RO for water salinities above 6,000 ppm. Ericsson and Hallmans [18] did a comparative study of the economics of RO and MSF in the Middle East. The study concluded that the dominating cost items are energy and capital recovery for both MSF and RO as well as membrane replacement for RO. The yearly average energy consumption of RO is calculated to be 7.4 kWh / m^3 and that for MSF is 16.7 kWh / m^3 (depending on performance ratio), out of which 4.8 kWh / m^3 are electrical power consumption for pumps. Khan [10] proposed some factors to be studied before a particular desalinating process is selected. Some main factors are feed water characteristics, availability of energy, location of plant, and process economics. He also concluded that there is no desalination process which can be called a clear winner and that the most important parameter in selecting a particular process is the verification that it has proven its performance and

reliability in similar commercial installations.

Lawand [19] studied the economics of wind powered desalination systems. According to him it is imperative that simple desalination units be developed which preferably can be maintained or even built and assembled by local craftsmen. This ensures that repairs can be undertaken on the site. In this respect, he concluded, wind powered units with their relatively simple power drivers would appear to be far more adaptable to this type of condition than diesel engines.

Wojcik et al [3] evaluated and compared the water desalination methods that are used most frequently in Saudi Arabia, namely, MSF, RO, and ED. The evaluation was based on actual performance data and done in terms of energy consumption, water recovery, and investment costs. Such evaluations were performed for a number of selected MSF and RO plants in the Kingdom.

According to Petit [20], the second law is a perfectly rational basis for assigning value to a fuel whether that fuel is coal. steam, electricity, water in an elevated reservoir, or any other commodity having the potential to drive a process. Second law efficiency is defined as [20] :

$$\eta_{II} = \frac{available\text{-}energy\ in\ useful\ products}{available\ energy\ supplied}$$

The denominator exceeds the numerator by the amount of available -energy consumed by the transformation :

$$\eta_{II} = \frac{\dot{A}_{products}}{\dot{A}_{products} + \dot{A}_{consumed}} .$$

No citation was noted by the author regarding the use of the second law-based-Thermodynamic analysis (availability analysis) in the process selection of desalination systems, though the combined energy and entropy balance, has long been recognized as the most appropriate method for evaluating losses in, and efficiency of, processes. Availability analysis is the true thermodynamic measure for any process [21]. London [22] proposed a method for calculating the irreversibilities (entropy generation) for a particular process. Gaggioli et al [23] exploited the second law efficiency for costing analysis of a combined power and desalination plant at the Umm Al-Nar in Abu Dhabi. Due to the non-availability of the operating conditions of the plant, a simulation model "DIST" was used for the exergy evaluation of the distillation plant.

In this study, the second-law will be used as a criterion for the selection of a desalination process.

Because of the intermittent nature of solar and wind power and possible mismatches between supply and demand, short-term energy storage is an essential feature of solar/wind-powered desalination systems. For solar-thermal desalination systems, energy storage in the form of sensible-heat has been proven to be viable. One of the most attractive features of sensible-heat storage systems is that charging and discharging can be expected to be completely reversible for the unlimited number of cycles, i.e., over the life-span of storage [24].

Andrews [25] showed in his study that energy-storage requirements can be reduced in coupled wind-solar generating systems which in turn reduces the overall cost of such systems.

Jesch et al [26], experimentally investigated the advantages of using multiple tanks to achieve thermal stratification. It was concluded that for the same total storage volume three equal size tanks gave better performance than two equal size tanks, which in turn were better than one single tank.

For electrical-based solar/wind desalination systems, such as RO and ED, rechargeable electric batteries offer considerable promise in energy storage systems [26].

Pumped hydro (PH) storage has been very successful in terms of safety, reliability, round-trip efficiency, flexibility of operation, and economics [24].

Integrated energy systems often have a wide range of potential design configurations and subsystems parameters. Darlington et al [27], Barra et al [28] proposed analytical methods for optimal sizing of a photovoltaic plant. Duffie and Beckman [29] proposed a method, namely, $\overline{\varphi}-f$ chart method for predicting the performance of solar water heating systems. El-Nashar [30] utilized the $\overline{\varphi}-f$ chart method for predicting the performance of the solar-multieffect plant installed at Abu Dhabi. The method showed reasonable agreement with the computer simulation work.

CHAPTER 3

EVALUATION OF DESALINATION PROCESSES

Before a decision to be made regarding which desalination process is most suitable for coupling with solar/wind power in Dhahran (a representative city located on the eastern coast of Saudi Arabia), a revision for the processes currently available and a number of factors need to be considered.

3.1 Desalination Processes Overview

The methods/processes which are most used in seawater and brackish water desalination are either based on a phase change or on the use of of semi-permeable membranes. Besides this classification, the desalination methods can also be divided into processes which use heat (called distillation processes) and processes which use electrical/ mechanical work (called membrane processes) to perform the separation process. A general configuration for a saline water conversion process is depicted in figure (3.1) [31].

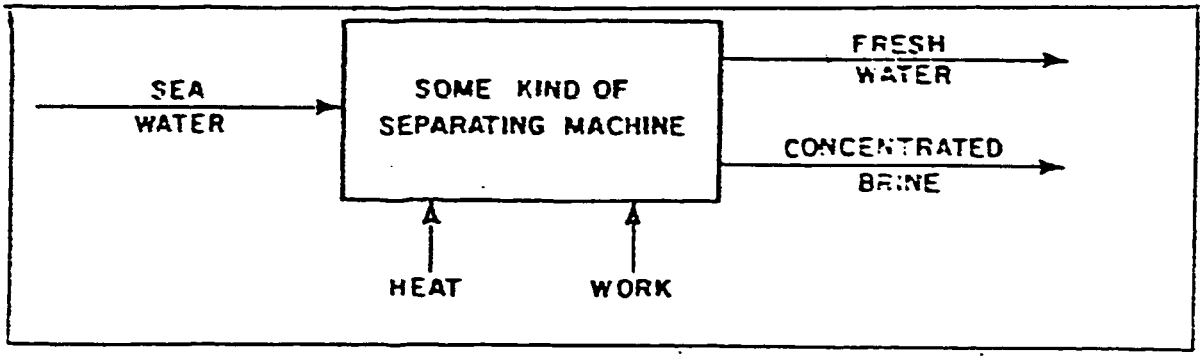

Figure (3.1) Flow Diagram of a Saline Water Conversion Process [31]

These processes which use heat (phase change) are :

- Multistage Flash MSF
- Multiple Effects ME
- Vapor Compression VC
- Solar Stills
- Freezing FR

These processes which use electrical/mechanical work are:

- Reverse Osmosis RO
- Electrodialysis ED

Most commonly used processes, such as, MSF, ME, and RO will be considered in the description. Table (3.1) [32] shows the world desalination production capacity for different types of processes.

Multiple Effects Distillation ME

In the multi-effect distillation process, two or more evaporators are employed as shown in figure (3.2). Each evaporator operates at a successively lower temperature and pressure. The first (highest temperature) effect is heated by low pressure steam. The heat source may be prime steam, turbine exhaust steam. Vapors are generated from feedwater in the first effect tubes. These vapors are directed to the second (lower temperature) effect. Thus, vapors from one effect are used as heat input to the next effect for heating and evaporating the brine.

The most important parameter which indicates the effectiveness of the ME

Table (3.1) World Desalination Production Capacity as of Jan. 1, 1984 [32]

Type of process		Daily production in m^3	%
Distillation processes	Flash	5 980 000	~64
	Miscellaneous	620 000	~ 6
	Total for distillation	6 600 000	~70
Membrane processes	Reverse osmosis . Seawater	140 000	1.5
	Reverse osmosis . Brackish water	2 200 000	23.5
	Electrodialysis	460 000	5
	Total for membrane	2 800 000	~30
Overall total		9 400 000	100

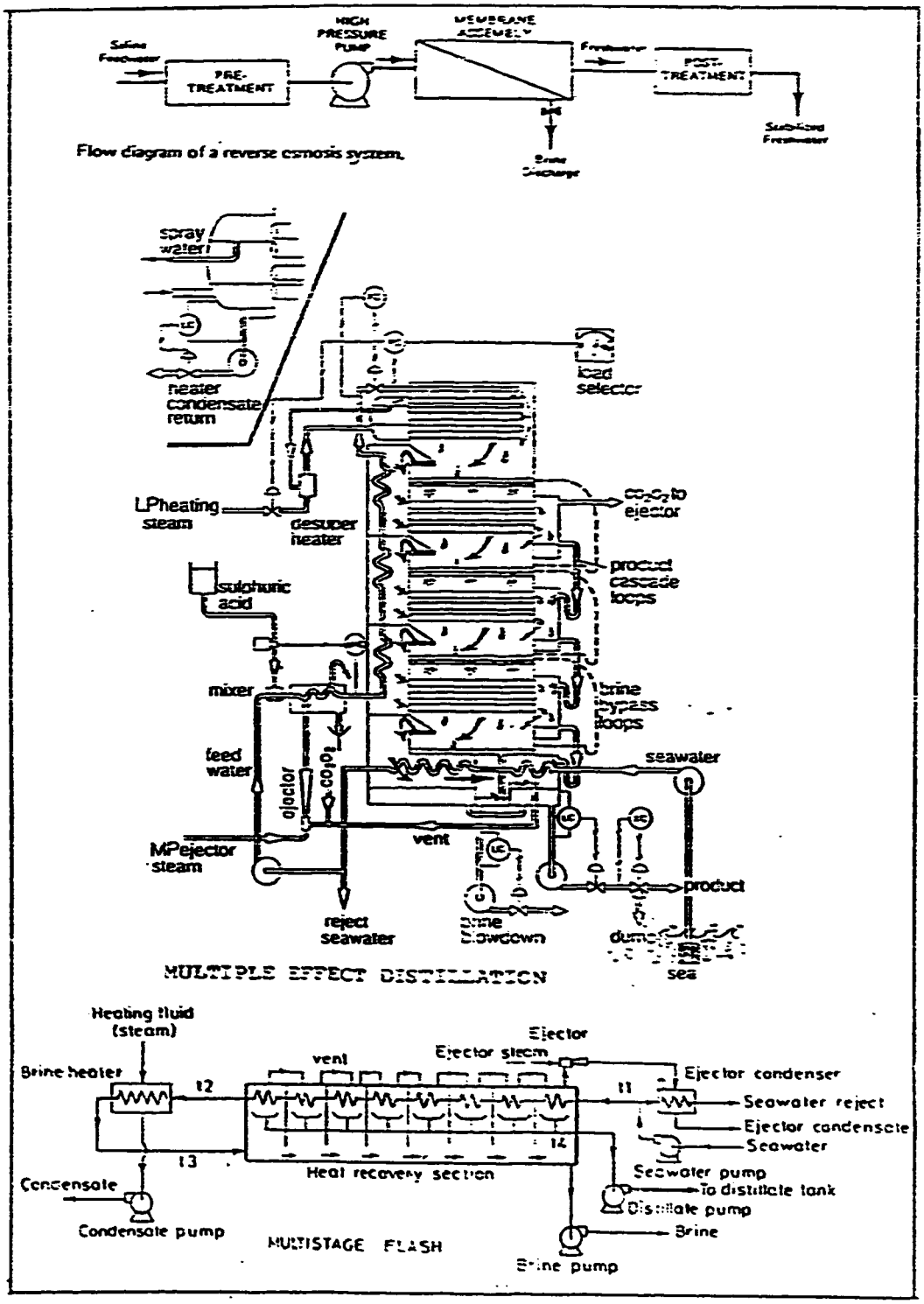

Figure (3.2) Common Types of Desalination Process [10]

plant, is called the performance ratio (PR). It is defined by the equation [10]:

$$\frac{1}{PR} = \frac{1}{n} + \frac{C_p \Delta T}{h_{fg} R_c} \qquad (3.1)$$

Where :

PR - Performance ratio

C_p - Specific heat of brine

n - Number of effects

ΔT - Temperature difference between brine leaving the top preheater and brine in the top effect.

h_{fg} - Latent heat of evaporating brine.

R_c - Recovery ratio of the plant (ratio of productwater produced to brine feedwater).

Multistage Flash MSF

Vapor can be produced from a liquid which is at its boiling point, either by heat addition (boiling) at constant pressure or by pressure reduction at constant temperature (flashing). ME processes use the first concept. Single and multistage flash processes use the second concept. Feedwater is preheated in a condenser. It then flows to a brine heater where low pressure steam is introduced from an external source. Hot feedwater from brine is introduced into the flash chamber, which is maintained under vacuum by an ejector. To increase the heat recovery efficiency of a single stage unit, the number of flash stages is increased.

Heat consumption can be given [10]:

$$Q = \frac{Distillate\ produced\ (kg/s)}{Performance\ ratio} \times 2326 \times 1.04 \quad (kW) \tag{3.2}$$

where the performance ratio is given by :

$$PR = \frac{Distillate\ output\ (kg)}{steam\ input\ (kJ)} \times 1.04 \times 2326 \ . \tag{3.3}$$

Reverse Osmosis RO

Saline water is pretreated, filltered and then pumped with a high pressure feed pump through modules containing semi-permeable membranes. At the membranes, separation of most the salts occurs. The permeate (concentrate) ratio is one of the characteristic features of a module. The recovery ratio (water conversion ratio) is defined as :

$$R_c = \frac{V_p}{V_f} \times 100\ \% \tag{3.4}$$

where :

V_p – $ProductFlow$ (m^3/day)

V_f – $Feedwater\ flow$ (m^3/day) .

ME, MSF, and RO processes are depicted in figure (3.2) [10].

3.2 Factors for Consideration in the Process Selection

In the initial stage of process selection a number of factors need to be considered. These factors are :

(a) Technical Factors, including

- Salinity of feedwater

- Salinity of productwater
- The physical properties of the water (e.g. cloudiness)
- The chemical properties of the water (e.g. sulphate content)
- The workload
- The extent of the automation and control
- Energy source available
- Capacity of plant

(b) Economical Factors, including

- Cost of energy
- Cost of chemicals
- Variation in currency exchange rates
- Cost of manpower
- Financing terms, i.e. interest rate

3.3 Comparison of Desalination Processes

3.3.1 Desalination Energy Requirements

Energy is necessary for converting saline water into fresh water; thermal energy for the distillation methods, electrical energy for electrodialysis, and solely mechanical energy for reverse osmosis. If these processes operated as reversible, each of them would require the same energy for desalination [10].

Using figure (3.3) for seawater, the minimum power requirement is 0.7 kWh/m^3 at a zero conversion ratio where the conversion ratio is given by Eq. (3.4).

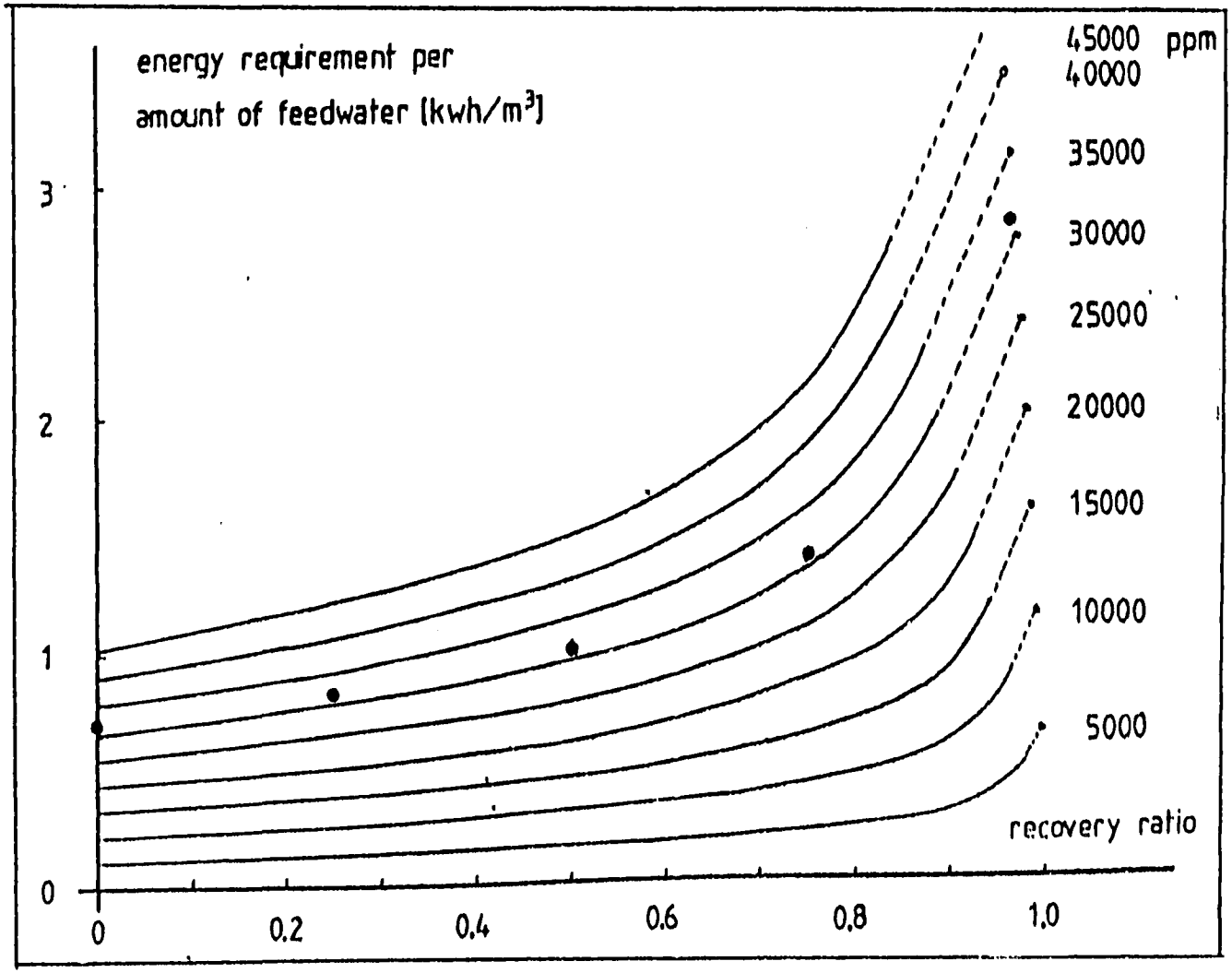

Figure (3.3) Minimum Amount of Energy Required for the Extraction of Pure Water for NaCl Solution [32]

Figure (3.3) [32] shows the variation of the minimum desalination energy requirements with conversion ratio and the salinity of the water being processed. Theoretical minimum energy required for desalination of seawater (salinity 53000 ppm) as a function of recovery ratio is shown in figure (3.4) [33]. In practice the amount of energy required is much greater than the values given in this figure for two main reasons :

(1) Irreversibilities (losses) encountered

(2) Energy required for auxiliary equipments (e.g. pumps)

Table (3.2) [34] shows comparison of thermal seawater (distillation) desalting processes. Energy requirements of various desalting processes (distillation and membrane) for conversion of brackish water are shown in table (3.3) [35]. Table (3.4) [34] shows comparison of multiple effect distillation processes. Comparison of energy consumption for the various seawater desalination processes (with the prime energy source being the fuel oil) is shown in table (3.5) [1]. Table (3.6) [36] gives a survey of the most important desalination techniques together with some typical values of the energy consumption. The same table shows that the heat (distillation) processes have a relatively high energy consumption. Reverse osmosis is the process with the lowest energy consumption, approximately 8-10 times lower than that of the heat processes. If one assumes an energy conversion efficiency of 1/3 for the electricity generation, the primary energy consumption per amount of productwater will be 24-36kWh/m^3, still being considerably less than the energy consumption of heat processes. Electrodialysis is at present mainly used for

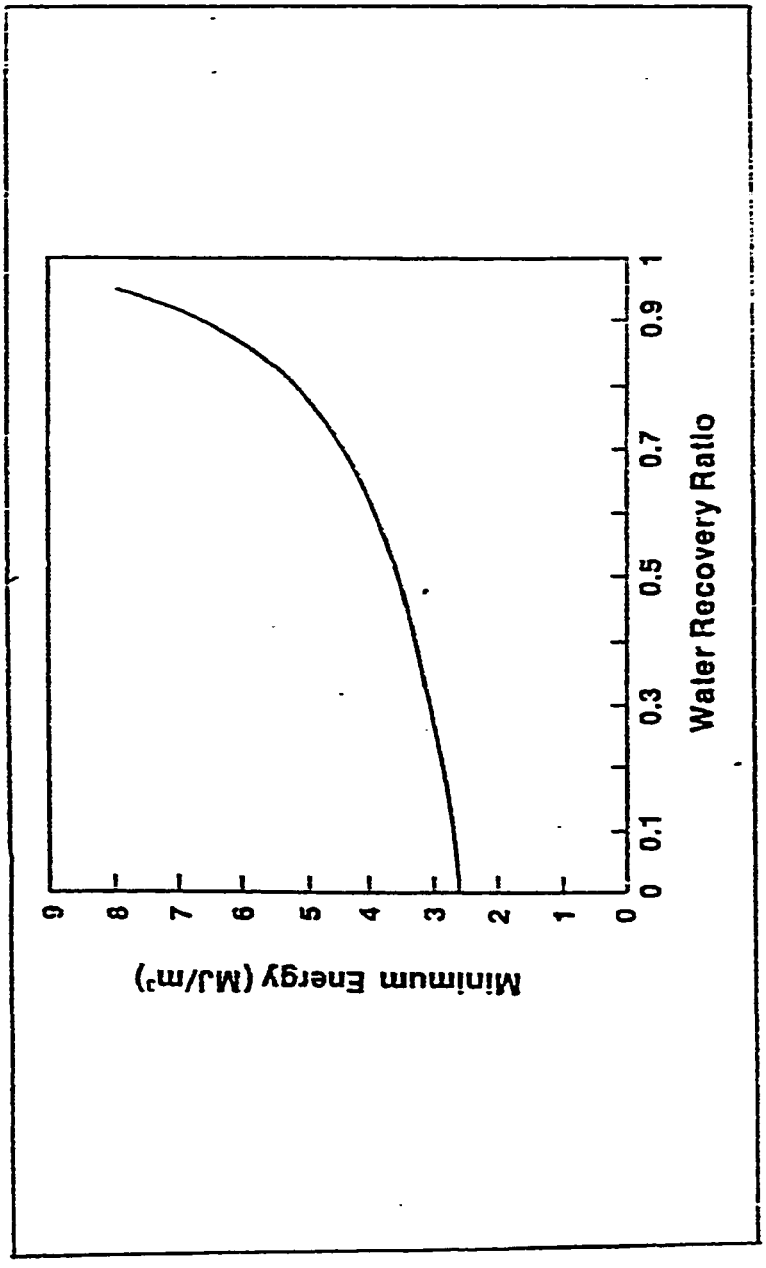

Figure (3.4) Theoretical Minimum Energy Required for Desalination of SeaWater as a Function of Water Recovery Ratio [33]

Table (3.2) Comparison of Thermal Seawater Desalination Process [34]

Process	Energy Consumption kWh_e/m^3	Energy Consumption kWh_t/m^3	Capital Cost $/m³/day	Development
Vapor Compression (Steam Jet)	1	115 @ 117°C	1,100	Commercial
Freezing (Absorption Refrigeration)	2.5	14 @ 454°C 115 @ 55°C	1,700	Experimental
Multistage Flash Evaporation (MSF)	3	48 @ 132°C	2,300	Commercial
Multiple Effect Distillation (MED)	1-2.5	32 @ 132°C	1,850	Commercial

Table (3.3) Energy Requirements and Performance Factors for Desalting Brackish Water [35]

Process	kJ/kg	PF
Reverse osmosis	30	77.0
Electrodialysis	50	46.0
Absorption vacuum freeze	63	37.0
Vacuum freeze/vapor compression	102	25.0
Multieffect, multistage distillation	125	19.0
Multistage flash/vertical tube distillation	175	13.0
Vapor compression distillation	186	12.0
Vertical tube evaporator distillation	204	11.0
Multistage flash distillation	251	9.0
Single-effect solar still	4,350	0.53

Feedwater, 3,500 mg/L; product water, 500 mg/L; recovery ratio, 70%; and thermal-to-electric energy conversion efficiency, 25%.

Table (3.4) Comparison of Multiple Effect Distillation Processes [34]

Process	Energy Requirements kW_e/m^3	Energy Requirements kWh_t/m^3	Capital Cost $/m³/day
Vertical Tube Downflow	2.5	32 @ 132°C	2,150
Vertical Tube Upflow	2.5	32 @ 132°C	2,150
Horizontal Tube Side By Side	1.2	32 @ 132°C	1,850
Horizontal Tube HTMEST	1.0	32 @ 132°C	1,850

Table (3.5) Comparison of Energy Consumption Values for the Various Seawater Desalination Processes with the Prime Energy Source Being Fuel Oil (underlined Values refer to the present state of the technique) [1]

DESALINATION PROCESSES		Energy requirement megacals/m3 + kWh/m3	Fuel quantity kg/m3	
DISTILLATION PROCESSES	MULTIFLASH Ratio 3	70 + 3	8,45	3,5
	MULTIFLASH Ratio 14	40 + 5	5,65	2,8
	MULTIPLE EFFECT - 7 effects	90 + 2	10,4	4
	MULTIPLE EFFECT - 7 actions	50 + 3	6,25	2,7
	Steam compression At // 5°C	0 + 16	4	4
	Steam compression At # 3°C	0 + 12	3	3
MEMBRANES TYPE PROCESSES	RO(1) sea water without recovery 60 bars	0 + 12	3	3
	RO(1) sea water with recovery - 60 bars	0 + 8	2	2
	RO(1) brackish water at 2,5 g/l-40 bars	0 + 3	0,75	0,75
	ED(2) sea water - 1,2 volts/cell	0 + 30	7,50	7,50
	ED(2) brackish water at 2,5 g/l-1,2 volts/cell	0 + 3	0,75	0,75

Table (3.6) Survey of Existing Desalination Methods [36]

	Heat	Work	Phase change	Membranes	Energy consumption (kWh/m^3)
Multiple Effect Distillation	X		X		73-121 + (p)
Multistage Flash Distillation	X		X		66- 98 + (p)
Vapour Compression		X	X		12- 16 + (e)
Freezing Methods		X	X		16 ++ (e)
Electrodialysis		X		X	30- .. + (e)
Reverse Osmosis		X		X	8- 12 + (e)
Minimum requirement energy (0% recovery)					0.71
" " " (50% recovery)					0.99
heat of evaporation					630
heat of fusion					93

p: based on primary energy
e: based on electrical energy
+: right numbers refer to proven energy consumption in existing plants;
left numbers refer to plants which are commercially available but not yet proven in the field.
++: pilot plant

brackish water desalination (< 10000 ppm) where it is competitive with reverse osmosis. Its energy consumption is fairly high in case of seawater desalination. The freezing methods have a low energy consumption but their technological development is still in the pilot plant. Table (3.7) [37] gives typical energy consumption in desalination processes, including pumping energy requirements. Figure(3.5) [38] demonstrates the specific energy consumption for reverse osmosis seawater system at different operating pressures and conversions. As a conclusion based on the observation of the previous tables, Table (3.8) ranks the desalting processes from the least to the most energy-consuming process.

3.3.2 Performance Comparison

Ease of Operation and Startup

Table (3.9) [16] ranks the desalting processes from the easiest to the most difficult from an operation and startup standpoint.

Complexity

Table (3.10) [16] ranks the processes from the least to the most complex based on a comparison of the number of controls, alarms, chemical systems, and pumps as well as the experience with these processes.

Maintenance

It is not possible to quantify the subject of maintenance when comparing the various desalting processes. In table (3.11) [16] desalting processes are ranked, based on experience, from the process requiring the least to the most

Table (3.7) Typical Energy Consumption for Various Desalination Processes [37]

Process	Feature	Performance Factor		Pumping Energy kJ/kg Water
		lb Water/MBtu	kJ/kg Water	
Distillation	Single-effect Waste-heat	0.95	2,443	14-33
Distillation MSF	90°C	8.0	290	8-10
Distillation MSF	120°C	12.0	193	6-8
Distillation MEF	71°C	8.0	290	4-6
Distillation MEF	120°C	15.0	155	4-6
Vapor Compression	65 kWh/kgal	38.0	61	Included
Freezing	50 kWh/kgal	49.0	47	Included
Reverse Osmosis	Seawater feed 45 kWh/kgal	54.0	43	Included
Reverse Osmosis	5,000 ppm feed 12 kWh/1,000 gal	200.0	12	Included
Electrodialysis	5,000 ppm feed 12 kWh/1,000 gal	200.0	12	Included

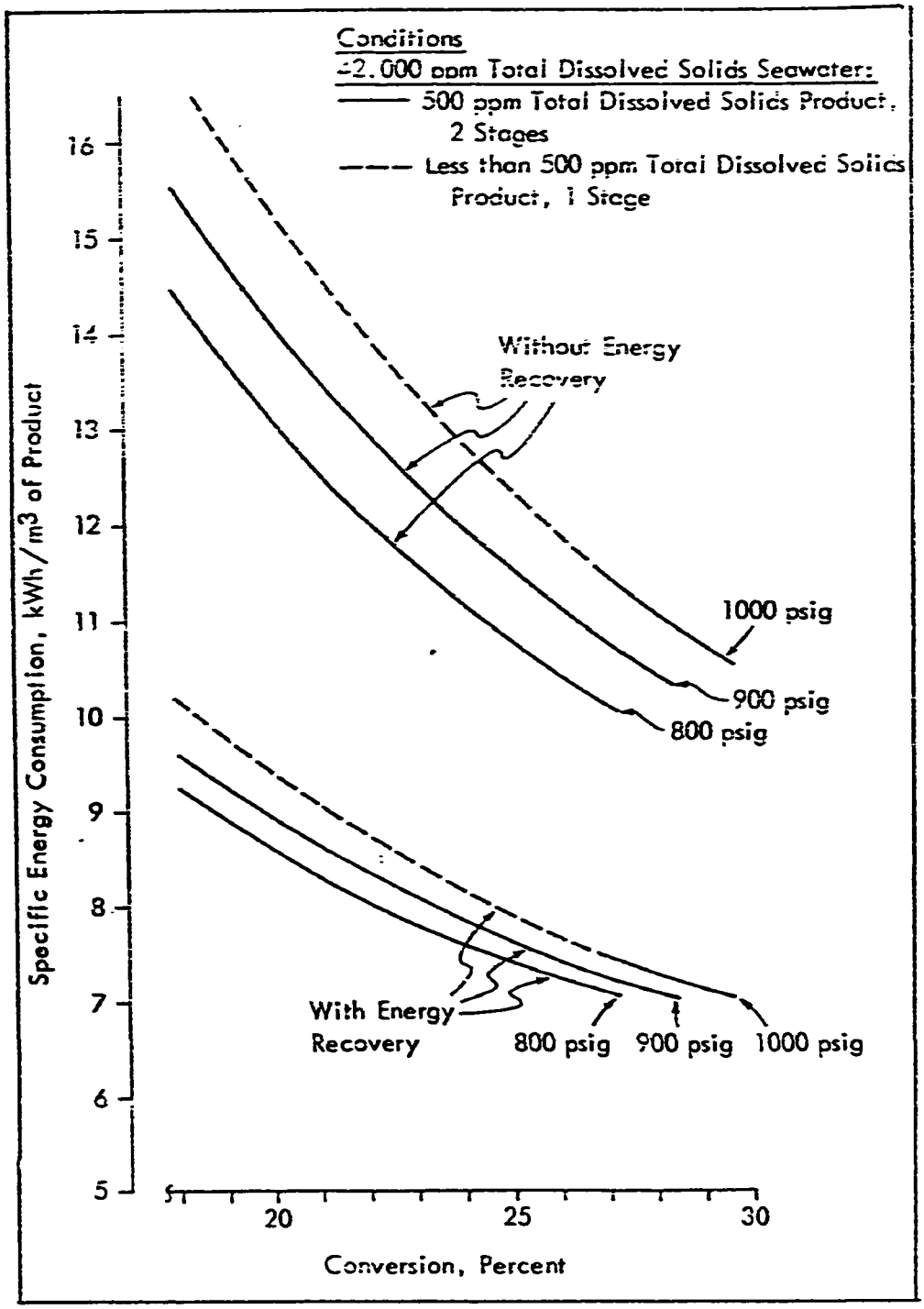

Figure (3.5) Specific Energy consumption for Reverse Osmosis SeaWater System ar Different Operating Pressures and Conversions [38]

Table (3.8) Energy Consumption Comparison

Ranking	Process
1	Reverse Osmosis (RO)
2	Vapor Compession (VC)
3	Freezing (FR)
4	Electrodialysis (ED)
5	Multistage Flash (MSF)
6	Multiple Effects (ME)

Table (3.9) Ease of Operation Comparison [16]

Ranking	Process
1	RO
2	MSF
3	VC
4	ME

Table (3.10) Complexity Comparison [16]

Ranking	Process
1	RO
2	MSF
3	ME
4	VC

Table (3.11) Maintenance Comparison [16]

Ranking	Process
1	MSF
2	RO
3	ME
4	VC

maintenance. Table (3.2), Shown in the preceding section ranks the desalination processes according to their performances from most to least.

3.3.3 Economics and Desalination Costs

The cost of desalting water is made up of two major components. They are the the capital and operating costs. They can be further broken down into :

1. Fixed or capital costs, including
    - Land costs
    - Desalting equipment
    - Structures
    - Water treatment
    - Feedwater
    - Brine disposal
    - Indirect capital costs

2. Operating costs, including
    - Operation manpower
    - Maintenance manpower
    - General and administrative
    - Spares supplies and maintenance materials
    - Chemicals
    - Energy supply costs

Interaction of factors in solar/wind-powered desalination systems is demonstrated in figure (3.6).

In general, energy costs account for more than 50% of the total cost. Operating and capital costs are interdependent. If one is increased, it is usual for the other to be decreased. Figure (3.7) [33] demonstrates the effect of feed water salinity on productwater cost for various desalting processes. It is obvious from this figure that membrane processes are more preferable over the others at lower feedwater salinity, whereas distillation processes are favorable at higher salinity. In other words, for conversion of brackish water, membrane processes are most suitable (from economics standpoint), whereas for seawater conversion, distillation processes lead.

Productwater costs for various conventional (fuel-powered) desalination processes are presented in table (3.12) [33]. It is obvious from this table that reverse osmosis is best suited for brackish water desalination with water cost ranging between 0.25-0.36 ($/m^3$)for*theyear*1981. Whereas, distillation processes are best suited for seawater desalination with productwater cost ranging between 0.57-0.75 ($/m^3$). Direct capital cost and annual costs are compared in figure (3.8) [18] for reverse osmosis and multistage flash methods, and in table (3.13) [17] for reverse osmosis (brackish water). Water costs as a function of salinity for photovoltaic-powered reverse osmosis (PV-RO) systems are presented in figure (3.9) [17]. From figure (3.9) it is obvious that, desalting water using (PV-RO) is much costly as compared to the conventional systems (fuel-powered). General comparison of seawater desalination technologies is shown in table (3.14) [39].

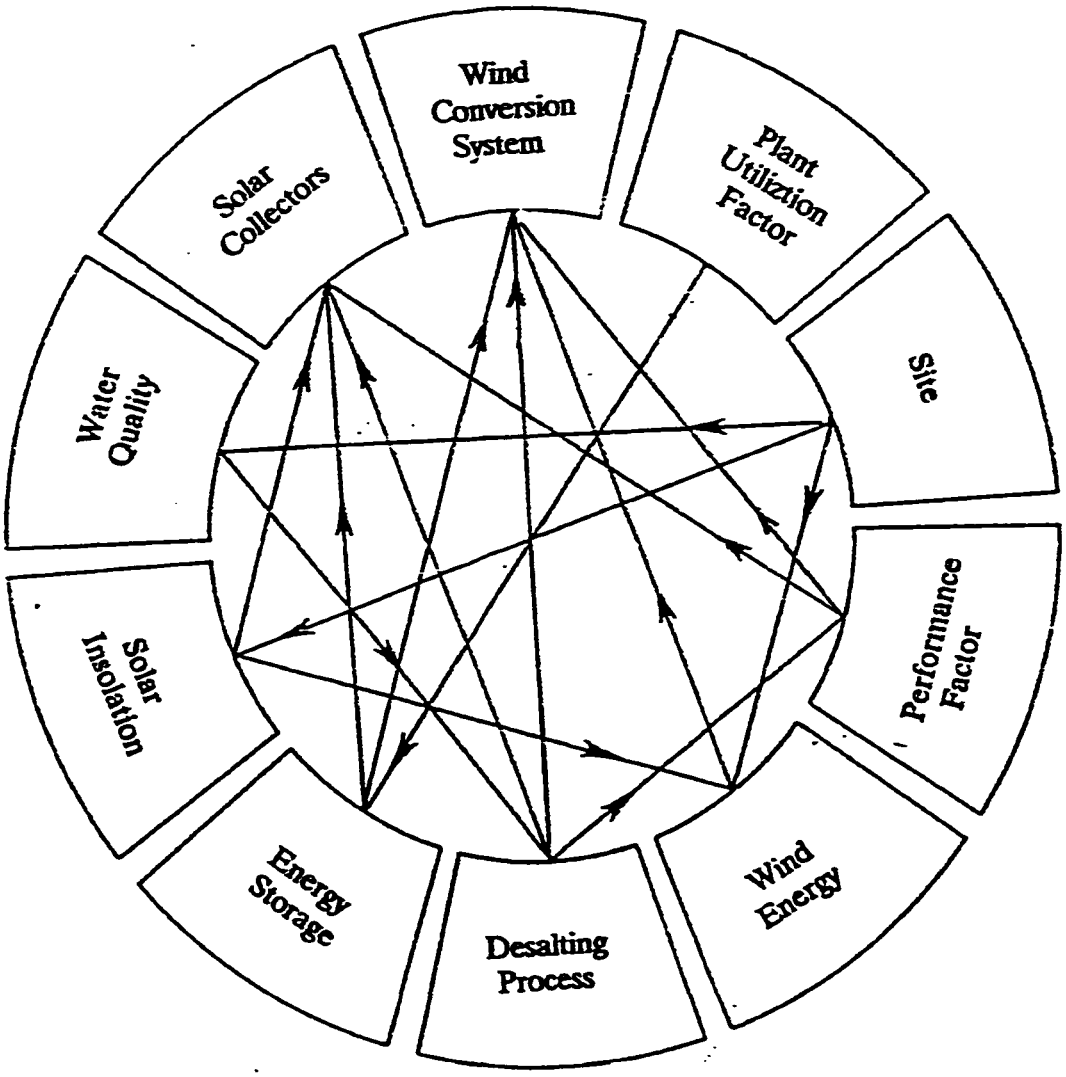

Figure (3.6) Interaction of Factors in Solar/Wind-Powered Desalination Systems

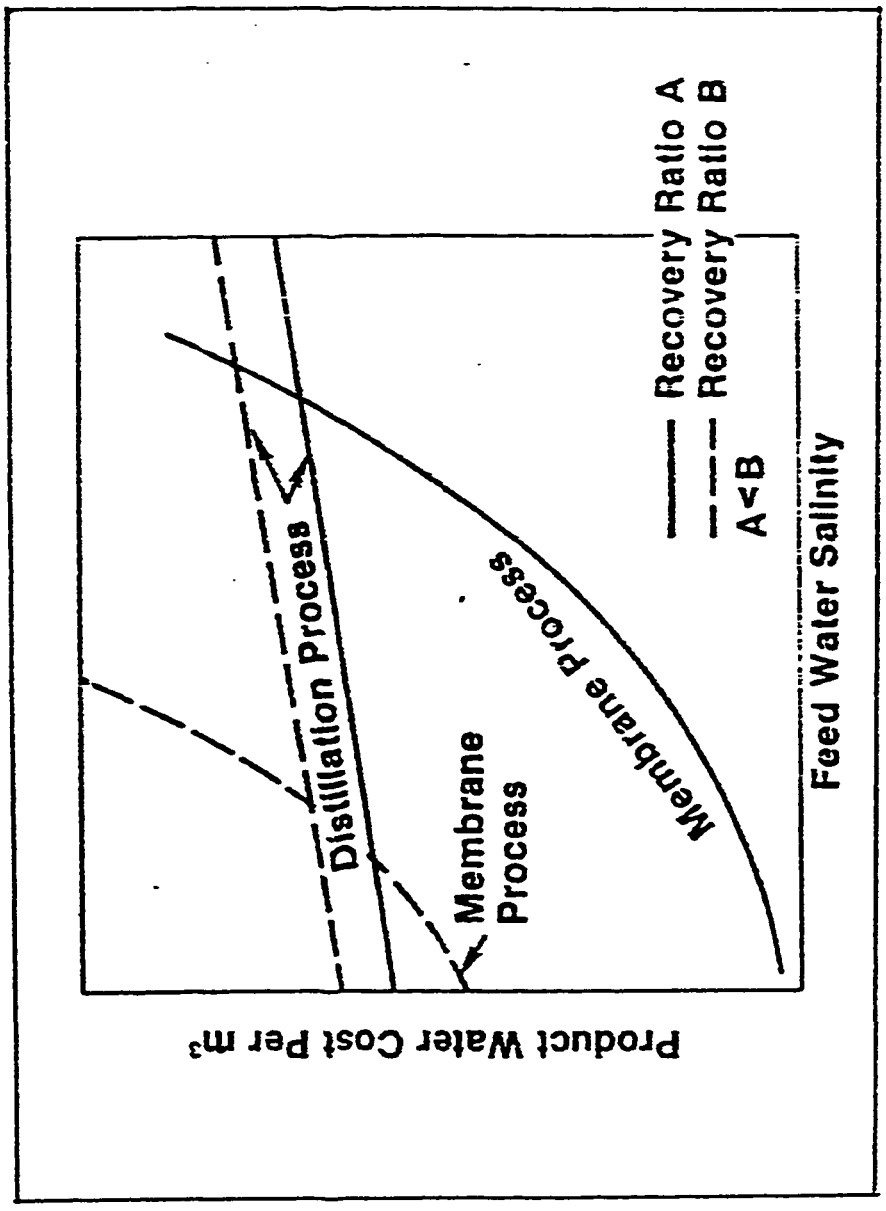

Figure (3.7) Effect of Feed Water Salinity on Product Water Cost [33]

Table (3.12) Product Water Costs for Various Conventional Desalination Process in $/m [33]

Process	Plant Capacity (m^3/day)	Product Water Costs ($/$m^3$)
Distillation	3,800	1.69 - 1.45
	190,000	0.72
	380,000	0.57 - 0.75
Freezing	190,000	0.42
Reverse osmosis	380 - 19,000	1.14 - 1.73
Seawater	190,000	1.00
Reverse osmosis	4,000 - 95,000	0.25 - 0.36
Brackish water (2,000-5,000 mg/L)	190,000	0.26
Electrodialysis	190,000	1.10
Seawater		
Electrodialysis	4,000 - 90,000	0.16 - 0.25
Brackish water	95,000	0.19 - 0.35
(2,000-5,000 mg/L)		

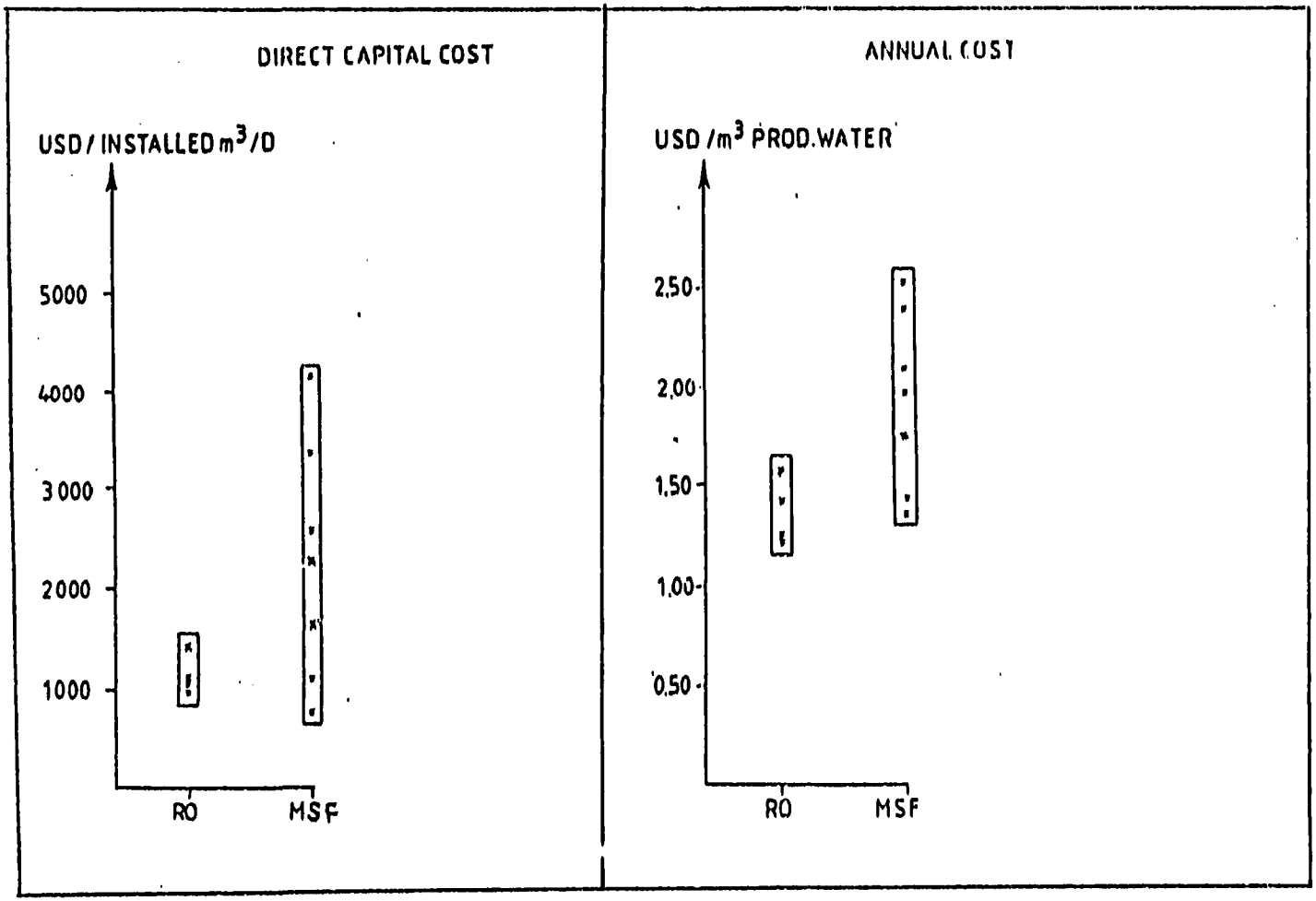

Figure (3.8) Direct Capital and Annual Costs of RO & MSF Desalination Plants [18]

(Capacity 10 *MIGD, Interest Rate* 7%, *Energy Cost* 0.05 *$/kWh)*

Table (3.13) Brackish Water RO Costs [17]

Salinity Recovery Rate Pretreatment	2,000ppm 50% A*	 S*	6,000ppm 70% A	 B	10,000ppm 50% A	 B
Capital Costs : ($x10^3)						
Plant	32	32	35	35	120	120
Pretreatment	11	60	12	70	15	80
Installation	17	32	18	37	48	80
Intake/outfall	20	20	20	20	20	20
Subtotal	80	144	85	162	150	240
Management and Overheads	4	7	5	8	9	15
Contingency	8	14	9	16	18	30
	92	165	99	186	177	285
Annual Costs ($x10^3)						
Capital Charges	12	22	13	25	28	45
Operating Labour	20	20	20	20	20	20
General & Admin.Charges	8	8	8	9	8	8
Chemicals	1	6	2	7	5	8
Maintenance	3	5	4	6	5	8
Membranes	3	3	4	4	8	8
TOTAL	47	64	51	70	74	97

*A = simple pretreatment. *B = difficult pretreatment

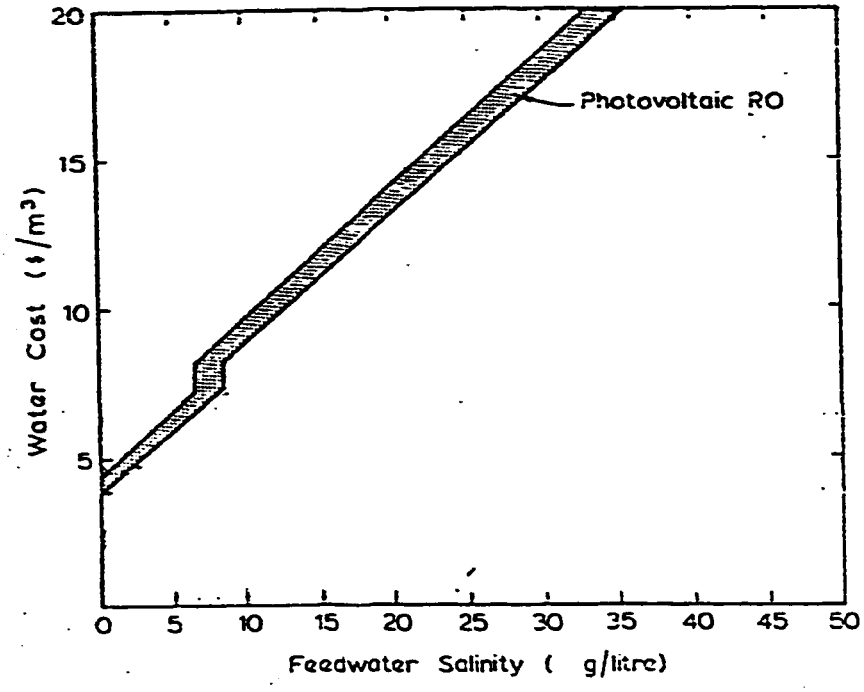

Figure (3.9) Water Costs as a Function of Salinity [17]

Table (3.14) Overall Comparison of Seawater Desalination Technologies [39]

Process	Commercial Availability	Efficiency (Unit Output for Seawater Plants/ Energy)	Capital Cost	Economies of Scale	Flexibility of Operation	Reliability, Availability, and Maintainability	Environmental Acceptability
Distillation							
Multistage Flashing	Yes	Low-Medium	High	High	None	Medium	Medium
Multiple Effect Multistage	Yes	Medium	High	High	Low	Medium	Medium
Vapor Compression	Yes	Low	Medium	High	Low	Low	Medium
Freezing	No	High	Medium	Likely	None	Low	Low-Medium
Membrane							
Reverse Osmosis	Yes	Medium-High	Medium	Low	Low-Medium	Medium	High
Electrodialysis	Yes	Medium	Medium-High	Low	Very High	High	High
RO-ED Hybrid	Yes	Medium-High	Medium	Low	Very High	High	High

3.4 Choice of Desalination Technology Operated By Solar And Wind Power

Availability of renewable energy sources, such as. solar and wind. saline water and other facilities at the selected site has to be completely assessed prior to selection and installation of desalination plant. It is generally felt that solar-powered desalination plants may not be economical for capacities higher than $100\ m^3/day$, and a general selection criteria is given in figure (3.10) [5]. The recent development has shown that RO with its lower energy requirements is a better choice even for seawater desalination than distillation processes (ME,MSF) upto $30m^3/day$ capacity. For wind-power desalination. it is expected that wind energy is liable to supply power at least 55% of the time [12]. Due to the lower power requirement for operation, RO is considered more suitable for coupling with wind energy conversion system. Considering the intermittent availability of wind energy, the most preferable coupling of wind energy conversion system with RO is DC operation with batteries [5].

There are many configurations for coupling solar and wind power conversion systems with desalination systems. Figures (3.11) [10]. (3.12) [40,17], and (3.13) [41] demonstrate some possible combinations.

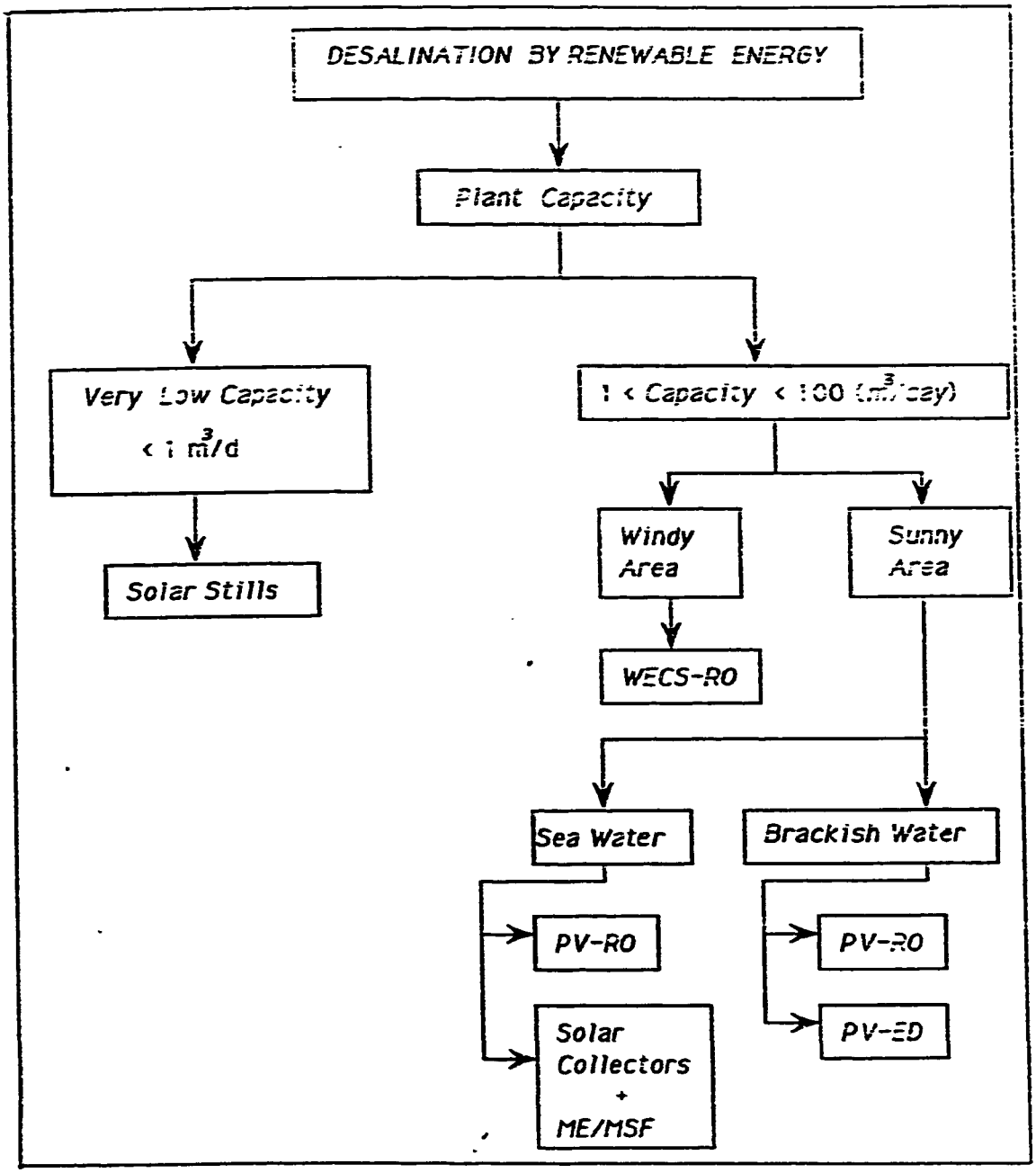

Figure (3.10) General Selection Criteria for the Choice of Desalination Process [5]

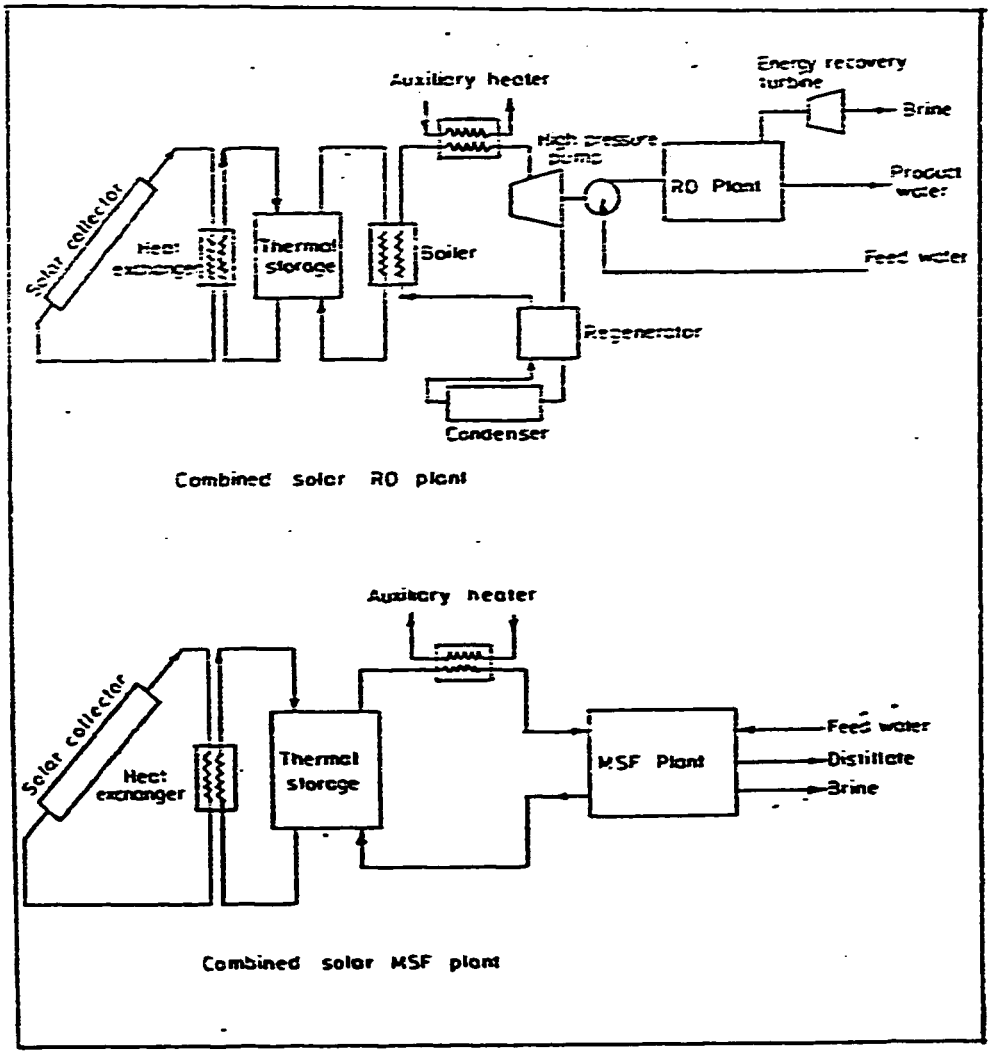

Figure (3.11) Configuration of Solar-Powered Desalination Plants [10]

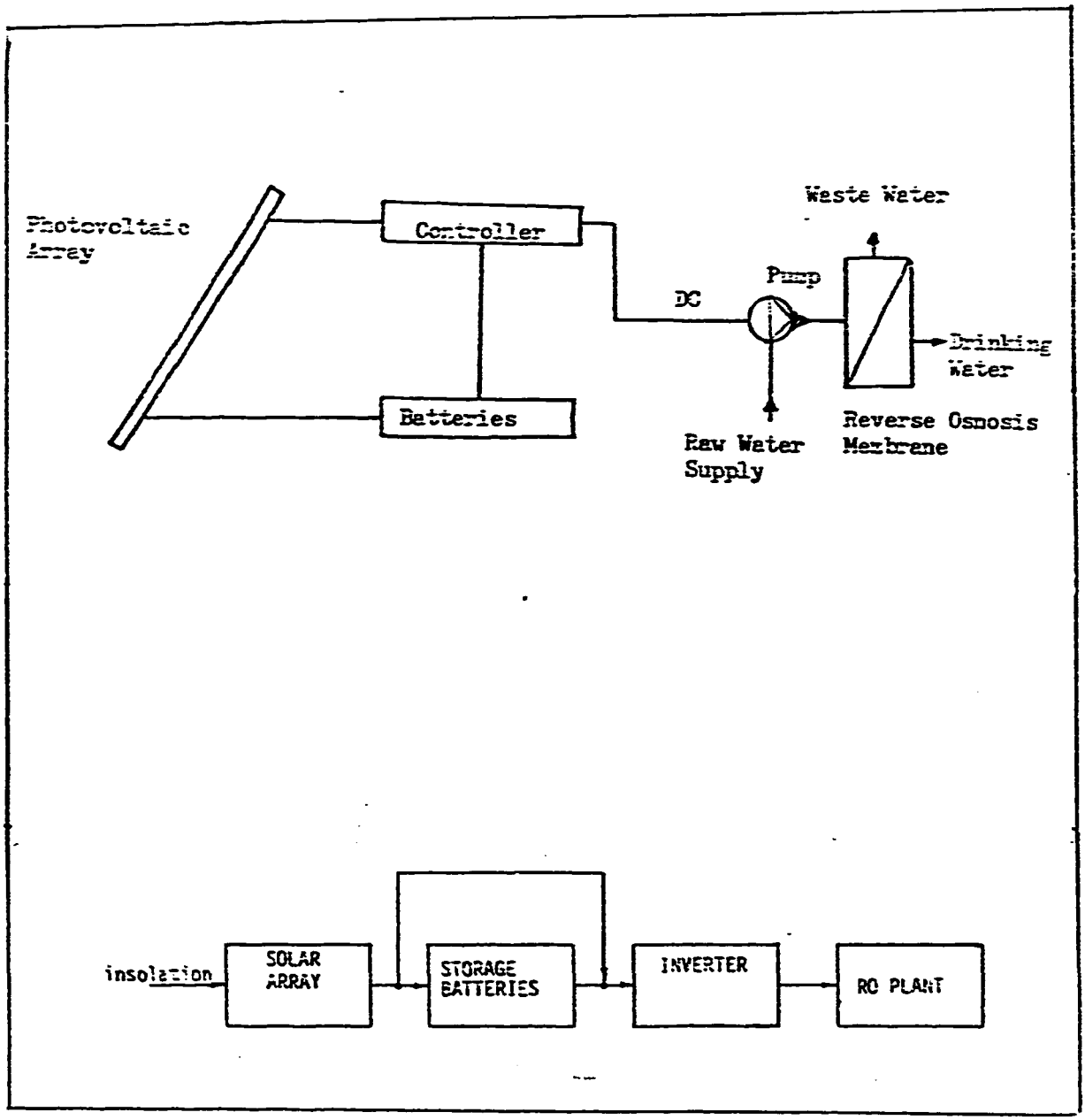

Figure (3.12) Schematic of a Solar-Powered RO Plant [17,40]

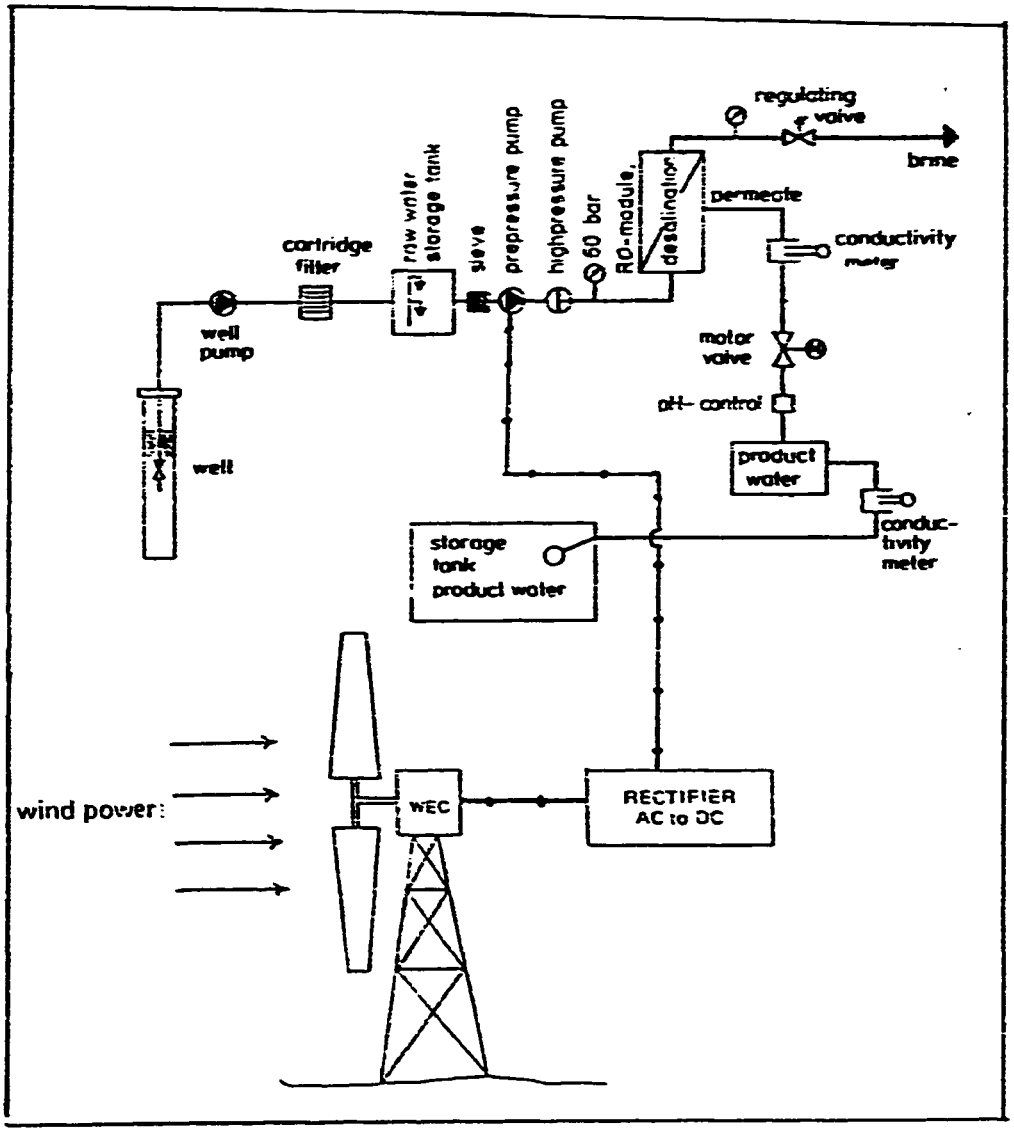

Figure (3.13) Schematic of a Wind-Powered RO Plant [41]

3.5 Selection of A Desalination Process

Several desalination methods have been compared with regard to their complexity, startup procedure, operation, maintenance, and economics. This study favours reverse osmosis (RO) as a representative method for membrane processes since it is the simplest, most reliable, the easiest to operate, the fastest method to startup, and less expensive. Also, multieffect (ME) method (as a representative method for distillation) is favoured for small production capacity (1-500 m^3/day). This is primarily because of certain unique design features inherent in the ME evaporators. They have the advantage of being able to operate under variable operating conditions (like the ones accompanied by the fluctuations in solar energy source) with their distillate production varying from about 40% of the design rated capacity to around 120% of this rated capacity without drastic change in their specific thermal energy consumption. These features make this type of desalination process quite attractive in solar desalination plants employing distillation [42].

Further comparison of desalination processes based on the second law of thermodynamics is presented separately in chapter 4.

General Design Requirements

The final selection of a desalination process is based on the following design requirements:

1. Viability for application under the prevailing climatic conditions of Dhahran city.

2. The selected desalination process is required to produce freshwater with salinity ranging between 200-500 p.p.m.

3. Suitability for operation in remote locations.

4. Production capacity ranging between 10-150 m^3/day.

5. Operational time is 24 h/day.

6. Low investment costs.

3.6 Selection of Solar and Wind Energy Conversion Systems

The following energy conversion systems will be used in the optimal design stage of this study :

1 - Solar-Photovoltaic Conversion System :

for the conversion of solar energy into electrical energy

2 - Evacuated-Tube Solar Collectors :

for the conversion of solar energy into thermal energy

3 - Wind Converter Machines (windmills) :

for the conversion of wind energy into electrical energy

CHAPTER 4

SECOND LAW-BASED THERMODYNAMICS ANALYSIS AS A TOOL FOR THE PROCESS SELECTION

The basic concepts of thermodynamics are two commodities called ***Energy and Available-Energy.*** The basic principles are the ***First Law*** , dealing with energy. and the ***Second Law*** , dealing with available-energy. The first law only states that energy is conserved. It does not tell about the type or quality of energy taking place in a real process. In contrast with energy, available-energy (exergy) is not a conserved commodity. The main purpose of the use of available-energy concept, through the second law, is to pinpoint the inefficiencies in and losses from processes, devices and systems [11].

Desalination processes are real processes and, therefore, the exergy analysis would be perfectly a rational basis for evaluating and comparing them. In this chapter the concept of exergy is used for evaluation of some existing desalination plants (RO,MSF,ME). This exergy evaluation is calculated based on actual operating conditions of such plants, so as to have an actual observation of their performances. Consequently, the virtual comparison of desalination processes from thermodynamics standpoint would be made. In this chapter the second-law efficiency will be the framework of such comparison.

4.1 Availability And Second Law Efficiency

In general, the availability (exergy) of any substance can be expressed as [11]:

$$A = H - T_o S - \Sigma \mu_{oi} N_i \qquad (4.1)$$

where

A - Availability

H - Enthalpy

T_o - Some Reference Temperature

S - Entropy

μ_{oi} - Chemical Potential of an ith Component

N_i - Moles of an ith Component

Since the desalination process is designed for long term steady operation so it can be modeled as a steady-state, steady-flow (SSSF) process. It should be noted also that, the last term in Eq. (4.1) can be cancelled since desalination processes, such as, RO, MSF, and ME, do not involve any chemical reactions.

Thus Eq. (4.1) becomes

$$A = H - T_o S \ . \qquad (4.2)$$

Also, Eq. (4.2) can be expressed in rates form as

$$\dot{A} = \dot{m} \ (h - T_o s) \ . \qquad (4.3)$$

The quantity in the R.H.S. of Eq.(4.3) is also called exergy, which can be expressed as [23] :

$$e = \dot{m}\,(h - T_o\, s) \tag{4.4}$$

where

e - Exergy

h - Enthalpy per unit mass

s - Entropy per unit mass

4.1.1 Available Energy Balance

Writing a steady-state balance for available energy is just like writing a steady-state energy balance except for one major difference. While energy is conserved, available energy can be destroyed (not lost, but actually consumed), and so the balance must contain a destruction term. The equivalent expression for this statement is given by ref. [11] *as*

$$\Sigma \dot{A}_{supply} = \Sigma \dot{A}_{products} + \dot{A}_{\delta} \tag{4.5}$$

where

$\Sigma \dot{A}_{supply}$ - Total available energy supplied into the system

$\Sigma \dot{A}_{products}$ - Total available energy in useful products

$\dot{A}_{\delta}$ - Available energy destroyed within the system (also called the dissipation term)

4.1.2 Second Law Efficiency

From Eq. (4.5), the second law efficiency can be defined as [11]:

$$\eta_{II} = \frac{\Sigma \dot{A}_{products}}{\Sigma \dot{A}_{supply}} \times 100\ \% \quad . \tag{4.6}$$

For any energy conversion process the theoretical upper limit of η_{II} is 100 %, which corresponds to the ideal case with no dissipations (irreversibilities).

4.2 Irreversibility

A measure of an internal irreversible loss, particularly of interest to the system analyst in order to make decisions, is defined as an energy measure of irreversible loss, which is typically described as the irreversibility. It is defined relative to the entropy generation as [22]:

$$\dot{I} = T_{WF}(\dot{S}) \tag{4.7}$$

where T_{WF} is a temperature weighting factor to be specified by the analyst based on a judgement of its relevance to the system being analyzed.

With steady-state, steady-flow process with more than one flow into and out of the system, we can express Eq. (4.7) as

$$\dot{I} = T_{WF}[\Sigma \dot{m}_e s_e - \Sigma \dot{m}_i s_i - \frac{\dot{Q}_{C.V.}}{T}] \quad . \tag{4.8}$$

For adiabatic processes, like most desalting processes, the term $\dot{Q}_{C.V.}$ can be set equal to zero, and Eq. (4.8) can be simplified as

$$\dot{I} = T_{WF}[\Sigma \dot{m}_e s_e - \Sigma \dot{m}_i s_i] \quad . \tag{4.9}$$

4.2.1 Normalized Irreversibility

For the sake of comparing different desalination processes based on the irreversibility measure, it is useful to normalize Eq. (4.7) as

$$i = \frac{\dot{I}}{\dot{m}_p} \tag{4.10}$$

where

i - Normalized irreversibility (kJ/kg)

$\dot{I}$ - Irreversibility (kW)

$\dot{m}_p$ - Productwater flow (kg/s)

Application of Eqs. (4.3) through (4.10) will be illustrated in the following section.

4.3 Working Examples For The Application Of Second Law In The Process Selection

The concept of irreversibility will be applied for the following existing desalination plants :

- Al-Khobar MSF Desalination Plant
- Al-Jubail MSF Desalination Plant
- Jeddah MSF Desalination Plant
- Abu Dhabi Solar-MES Desalination Plant
- Typical RO Desalination Plant
- Wind-Powered RO Desalination Plant at Germany

These desalination plants have been chosen for the application of the second law primarily because of the availability of their operating conditions and design data which will be used extensively in the analysis.

Procedure and Methodology

In order to be able to apply the concept of irreversibility and second-law efficiency by means of Eqs. (4.3) through (4.10), some required information need to be determined prior to that, and this is illustrated in the following procedure.

1- The layout and flow diagram for each plant is obtained.

2- According to some engineering judgements the control volume for each plant is then specified.

3- Some operating conditions (design data), namely: Temperatures, pressures, mass flowrates, and salinities, are obtained for the given flow diagrams and located at the interested points within the specified control volume.

4- Using steam tables [43] for water and seawater tables (thermodynamic properties of aqueous sodium chloride solutions) [44], state variables, such as, enthalpy h, and entropy s, can be determined by knowing their respective inlet and exit states (i.e. temperatures, pressures, and salinities) at their respective locations within the specified control volume.

5- Mass flowrates at unknown locations are to be determined by applying the mass conservation equation.

6- Tables containing all required data are then formulated.

7- The second-law analysis, Eqs. (4.3) through (4.10), is then, performed.

Simplifying Assumptions

Since it is very difficult (and very time consuming) to treat any desalination plant under actual conditions, the following assumptions make the analysis become possible, and the objectives of this study can be accomplished with no significant errors. These assumptions, in general, are :

1- Processes are all assumed steady-state (time-independent).

2- Thermal desalination processes are all assumed to be adiabatic (systems are well insulated).

3- For desalination plants, (e.g. Al-Jubail, Al-Khobar, and Jeddah) in which their design structures consist of identical lines/units (every line is considered as a small desalination plant, and the lines as a total are connected in parallel and form the major plant). It is very reasonable to take only one line as a representative for the entire plant. This is going to be applied only for the MSF plants.

4- Because of the non-availability of thermodynamic tables for seawater (compositions of seawater vary very widely from place to place), thermodynamic properties of seawater are taken as that for sodium chloride solutions, since the latter is the primary salt (80-90 %) in seawater.

5- The ambient temperature (chosen here to be the reference temperature given in Eq. (4.1) as well as Eq. (4.7)) is assumed to remain constant.

4.3.1 Al-Khobar MSF Desalination Plant

General Description

This plant is the second phase (Al-Khobar II), located on the Arabian Gulf coast near the city of Al-Khobar. Al-Khobar II is a dual purpose plant (i.e. generating electricity and desalting seawater), consisting of 10 multistage flash (MSF) distillation units (lines). Each unit is designed to produce 19417 m^3/day fresh water.

Second-Law-Based Thermodynamic Analysis

A flow-diagram of one distillation unit (line) of Al-Khobar II, is shown in figure (4.1) [45]. This unit consists of two main sections (heat recovery section and heat rejection section) with 16 stages. The analysis is to be done mainly for these stages as well as the brine heater. Therefore, a control volume (C.V.) is specified as shown in figure (4.2), indicating that, there are 10 state points (inlets and outlets). The maximum temperature corresponds to the low pressure steam entering the C.V. at state point number 8, and the lowest is that for seawater entering at point number 1. Performance operating conditions at various points of the C.V. are shown clearly in table (4.1). Using steam tables as well as seawater tables (appendix A) the state variables (h,s) are determined at their respective locations in the C.V. as shown in table (4.2). It should be noted that these values of the state variables are strong functions of temperatures and salinities. It should also be noted that these values are given in the appendix as specific values, whereas in table (4.2), they are adjusted by subtracting them

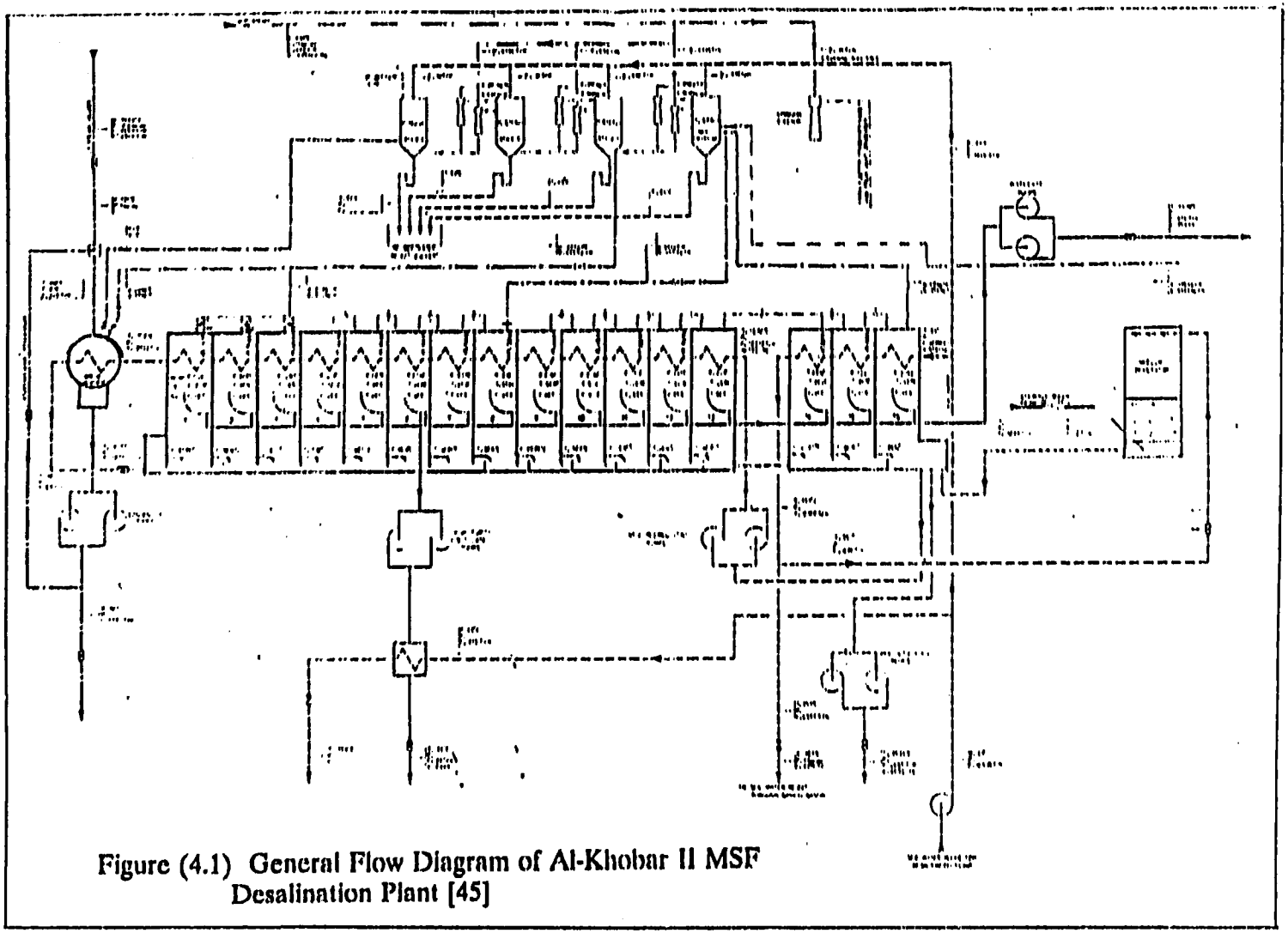

Figure (4.1) General Flow Diagram of Al-Khobar II MSF Desalination Plant [45]

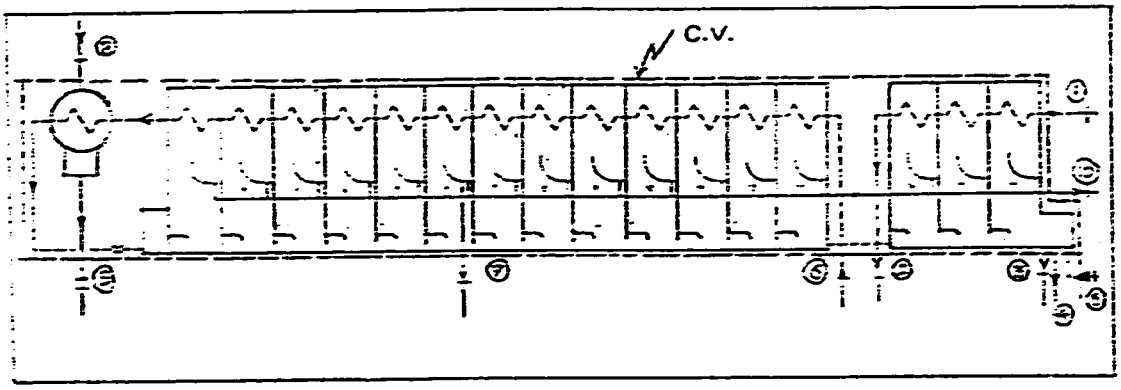

Fig. (4.2) Control Volume for Al-Khobar MSF

Table (4.1) Al-Khobar MSF Distillation Plant
(Performance Operating Conditions)

State Point	T (C°)	P (bar)	$\dot{m}$ (kg/s)
1	35	1	3297.78
2	41.34	1	3297.78
3	41.5	1	3222.22
4	39.84	1	1211.1
5	41.34	1	1445.83
6	41.5	1	3222.2
7	67.55	0.105	9.1667
8	104	0.83	36.58
9	94	0.83	36.58
10	39.84	1	224.73

Table (4.2) Al-Khobar MSF Distillation Plant
(Performace Operating Conditions)

State Point	Stream Type	Salinity s (g/kg)	Enthalpy h (kJ/kg)	Entropy s (kJ/kg·K)
1	Sea Water	57	136.7	0.4705
2	Sea Water	57	161.55	0.5505
3	Sea Water	63	169.84	0.5525
4	Sea Water	68	154.91	0.5291
5	Sea Water	57	161.55	0.5505
6	Sea Water	63	169.84	0.5525
7	Distillate	-	282.52	0.9248
8	LP Steam	-	2682.3	7.3076
9	Condensate	-	393.75	1.2385
10	Distillate	-	167.5	0.5703

from the values at dead-states (i.e. at zero temperature).

With table (4.2), the exergy as given in Eq. (4.4) can be determined at various state points and the results are shown in table (4.3). It should be noted from this table that exergy values at some state points have negative values. This is primarily because the reference at which exergy was calculated has been chosen to be negative.

Second-Law Efficiency, η_{II}

From Eq. (4.6). the second-law efficiency, η_{II} , can be determined as follows,

$$\Sigma \dot{A}_{supplied} = e_8 - e_9$$

$$= 15.786 - 0.450 = 15.336 \ MW$$

and

$$\Sigma \dot{A}_{products} = e_2 - e_1 - e_6 + e_3 + e_4 - e_5 + e_{10} + e_7$$

$$= -26.395 - (-27.088) - (-22.414)$$

$$+(-22.414)+(-9.753)-(-11.572)$$

$$+(-1.832)+(-0.021)= 0.6589 \ MW$$

Thus,

$$\eta_{II} = \frac{0.6589}{15.335} \times 100 = 4.3\ \%$$

Irreversibility, $\dot{I}$

The irreversibility, $\dot{I}$, can be found using Eq. (4.9) as follows,

Table (4.3) Al-Khobar MSF Distillation Plant
Exergy Analysis Results

State Point	Enthalpy h (kJ/kg)	Entropy s ($kJ/kg\text{-}K$)	Exergy e (MW)
1	136.70	0.4705	- 27.088
2	161.55	0.5505	- 26.395
3	169.84	0.5525	- 22.414
4	154.91	0.5291	- 9.753
5	161.55	0.5505	- 11.572
6	169.84	0.5525	- 22.414
7	282.52	0.9248	- 0.021
8	2682.30	7.3076	+ 15.786
9	393.75	1.2385	+ 0.450
10	167.50	0.5703	- 1.832

$$\Sigma \dot{m}_e s_e = \dot{m}_2 s_2 + \dot{m}_3 s_3 + \dot{m}_4 s_4 + \dot{m}_8 s_8 + \dot{m}_9 s_9 + \dot{m}_{10} s_{10}$$

$$= 3297.78\,(0.5505) + 3222.22\,(0.5525) + 1211.1\,(0.5291)$$

$$+ 9.1667\,(0.9248) + 36.58\,(1.2385) + 224.73\,(0.5703)$$

$$= 4418 \quad kJ/s.K$$

and

$$\Sigma \dot{m}_i s_i = \dot{m}_1 s_1 + \dot{m}_5 s_5 + \dot{m}_6 s_6 + \dot{m}_8 s_8$$

$$= 3297.78\,(0.4705) + 1445.83\,(0.5505) + 3222.22\,(0.5525)$$

$$+ 936.58\,(7.3076) = 4395 \quad kJ/s.K \quad .$$

Taking,

$$T_{WF} = T_{ambient} = 35 + 273 = 308K$$

we get,

$$\dot{I} = 308\,[\,4418 - 4395\,] = 7.182 \quad MW$$

Normalized Irreversibility, i

The normalized irreversibility for Al-Khobar MSF plant can be calculated using Eq. (4.10) as follows,

$$i = \frac{\dot{I}}{\dot{m}_p} = \frac{\dot{I}}{\dot{m}_{10}}$$

$$= \frac{7182}{224.73} = 31.96 \quad kJ\ kg\ water$$

Thermal Efficiency and Specific Energy Consumption

Thermal efficiency, η . can be defined as:

$$\eta = \frac{\Sigma \dot{m}_e h_e}{\Sigma \dot{m}_i h_i} \times 100\ \% \qquad (4.11)$$

where.

$\Sigma \dot{m}_e h_e$ = Total energy going out of C.V.

$\Sigma \dot{m}_i h_i$ = Total energy going into C.V.

Also,

$$\Sigma \dot{m}_i h_i = \dot{m}_1 h_1 + \dot{m}_8 h_8 + \dot{m}_6 h_6 + \dot{m}_5 h_5$$

$$= 3297.78\ (136.7) + 36.58\ (2682.3) + 3222.22\ (169.84)$$

$$+ 1445.83\ (161.55) = 1330\ \ MW$$

and

$$\Sigma \dot{m}_e h_e = \dot{m}_9 h_9 + \dot{m}_7 h_7 + \dot{m}_2 h_2 + \dot{m}_3 h_3 + \dot{m}_4 h_4 + \dot{m}_{10} h_{10}$$

$$= 36.58\ (393.75) + 9.1667\ (282.52) + 3297.78\ (161.55)$$

$$+ 3222.22\ (169.84) + 1211.1\ (154.91) + 224.73\ (167.5)$$

$$= 1284\ \ MW\ .$$

Thus,

$$\eta = \frac{1284}{1330} \times 100 = 96.6\ \%$$

Specific energy consumption, SEC, can be calculated from the following equation :

$$SEC = \frac{Net\ Energy\ Supplied\ (kW)}{Plant\ Capacity\ (m^3\ day)} \times 24 \quad (kWh/m^3) \ . \tag{4.12}$$

For our case,

$$Net\ Energy\ Supplied = \dot{m}_8 h_8 - \dot{m}_9 h_9$$

$$= 36.58\ (2682.3 - 393.75) = 83715 \quad kW$$

and

$$Plant\ Capacity = \dot{m}_{10} \times \frac{3600 \times 24}{1000}$$

$$= 224.73 \times \frac{3600 \times 24}{1000} = 19417\ m^3/day \ .$$

Hence,

$$SEC = \frac{83715}{19417} \times 24 = 103.5\ kWh/m^3 \ .$$

Second-Law Efficiency For The Brine Heater

Second-law analysis can also be applied to the brine heater (major part in MSF plant) so as to have more insight into the MSF plant. Flow-diagram and operating conditions of Al-Khobar MSF brine heater are shown in figure (4.3) and table (4.4) respectively. State variables (h,s) are determined from steam and seawater tables, and entered in table (4.5). In a manner similar to the previous analysis, exergy can be determined at various state points and the results are shown in table (4.6). Using Eq. (4.6), we obtain

$$(\eta_{II})_{BH} = \frac{e_2 - e_1}{e_3 - e_4} \times 100$$

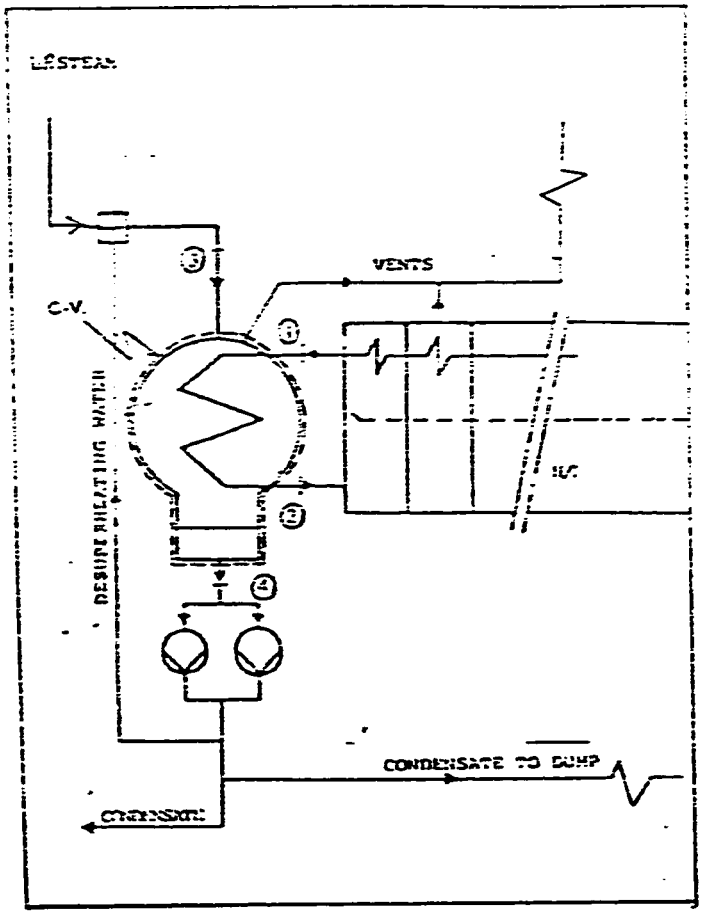

Fig. (4.3) Al-Khobar MSF Brine Heater Flow Diagram

Table (4.4) Al-Khobar Brine Heater
(Operating Conditions)

State Point	T (C°)	P (bar)	$\dot{m}$ (kg/s)
1	80.48	1	3222.22
2	87.0	1	3222.22
3	104	0.83	36.58
4	94	0.83	36.58

Table (4.5) Al-Khobar Brine Heater
(Operating Conditions)

State Point	Stream Type	Salinity a (g/kg)	Enthalpy h (kJ/kg)	Entropy s (kJ/kg·K)
1	Sea Water	63	315.17	0.9960
2	Sea Water	63	341.15	1.0774
3	LP Steam	-	2682.3	7.3076
4	Condensate	-	393.75	1.2385

Table (4.6) Al-Khobar MSF-Brine Heater Exergy Results

State Point	Exergy e (MW)
1	27.073
2	30.163
3	15.786
4	0.450

$$= \frac{30.16 - 27.07}{15.79 - 0.45} \times 100 = 20.14\ \%$$

4.3.2 Al-Jubail MSF Desalination Plant

General Description

This plant is of a dual purpose type. It is the largest in the world [45] with total water production capacity of 230 million gallons per day, and power generating capacity of 1295 *MW*. The plant is located on the Arabian Gulf coast near the city of Al-Jubail. It consists of 40 distillation units each of which produces about 23500 m^3/day distillate.

Second-Law-Based Thermodynamic Analysis

A flow-diagram of one distillation unit (line) of Al-Jubail MSF, is shown in figure (4.4) [45]. This unit consists of 22 stages as well as the brine heater. A control volume (C.V.) is drawn as shown in figure (4.5), indicating that, there are 10 state points (inlets and outlets). The maximum temperature corresponds to the low pressure steam entering the C.V. at state point number 9, and the lowest is that for seawater entering at point number 1. Performance operating conditions at various points of the C.V. are shown clearly in table (4.7).

Using table (4.7), the state variables (h and s) can be determined at various state points and the results are shown in table (4.8). With the help of table (4.8) and Eq. (4.4), the exergy can be calculated at various state points and the results are shown in table (4.9).

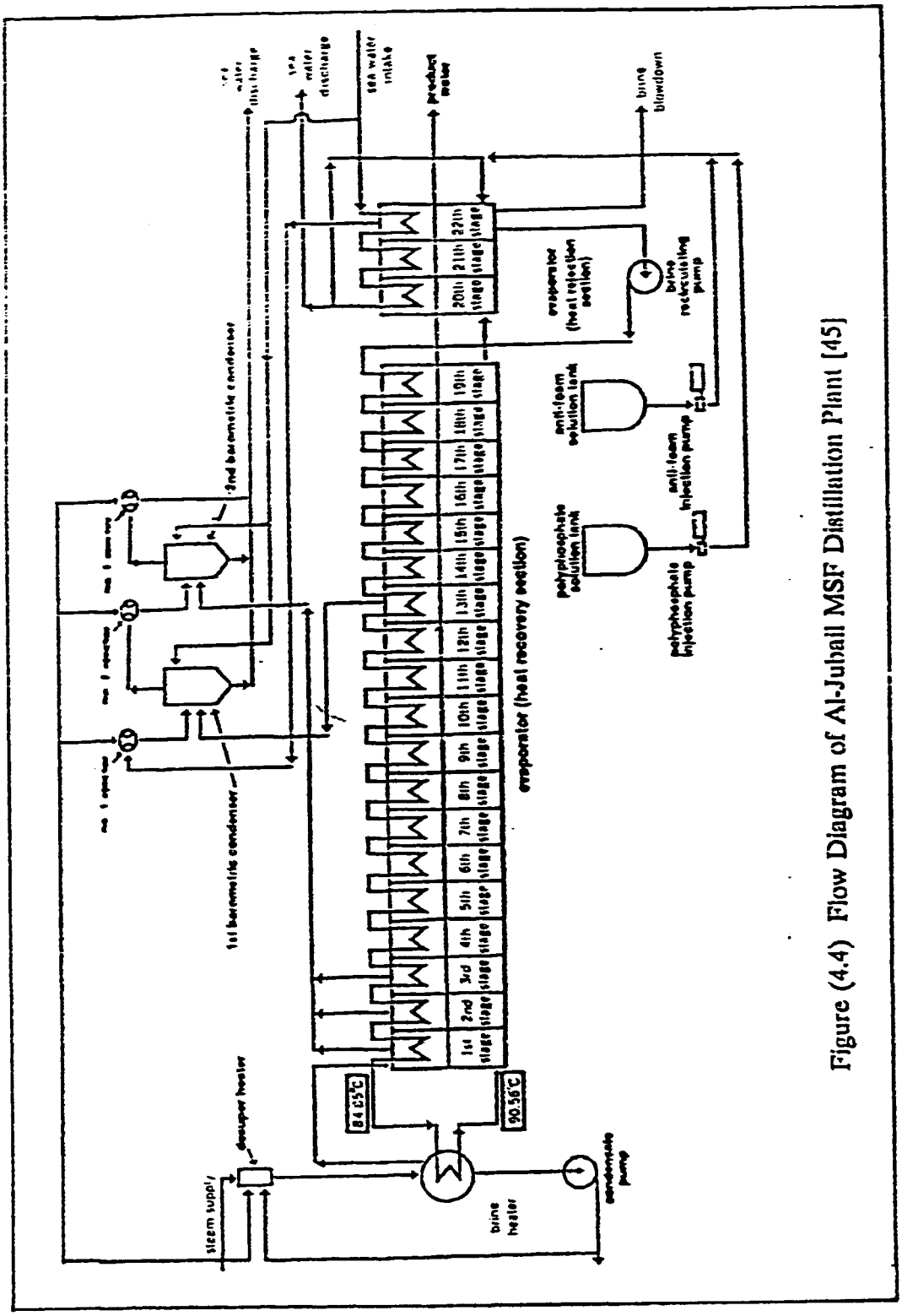

Figure (4.4) Flow Diagram of Al-Jubail MSF Distillation Plant [45]

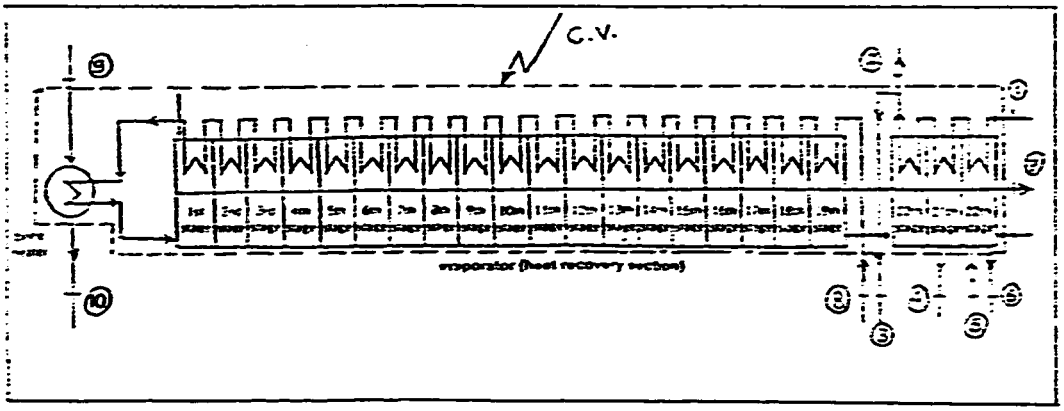

Fig. (4.5) Control Volume for Al-Jubail Plant

Table (4.7) Al-Jubail MSF Distillation Plant
(Performance Operating Conditions)

State Point	T (C°)	P (bar)	$\dot{m}$ (kg/S)
1	35	1.68	2396.94
2	43.3	.55	1589.17
3	43.3	1.15	807.78
4	43.3	.0796	3620.94
5	43.3	-	807.78
6	43.3	2.92	533.49
7	41.5	5.78	271.94
8	43.3	6.35	3620.94
9	98.9	.974	34.93
10	98.9	.974	34.93

Table (4.8) Al-Jubail MSF Distillation Plant: (Performance Operating Conditions)

State Point	Stream Type	Salinity σ (g/kg)	Enthalpy h (kJ/kg)	Entropy s $(kJ/kg \cdot K)$
1	Sea Water	46.5	138.9	0.4780
2	Sea Water	46.5	171.93	0.5842
3	Sea Water	46.5	171.93	0.5842
4	Sea Water	46.5	171.93	0.5842
5	Sea Water	46.5	171.93	0.5842
6	Brine	64.9	169.24	0.5745
7	Distillate	-	173.83	0.5924
8	Sea Water	46.5	171.93	0.5842
9	LP Steam	-	2673.0	7.3683
10	Condensate	-	414.30	1.2890

Table (4.9) Al-Jubail Distillation Plant
Exergy Analysis Results

State Point	Enthalpy h (kJ/kg)	Entropy s ($kJ/kg\cdot K$)	Exergy e (MW)
1	138.90	0.4780	- 19.952
2	171.93	0.5842	- 12.719
3	171.93	0.5842	- 6.465
4	171.93	0.5842	- 28.981
5	171.93	0.5842	- 6.465
6	169.24	0.5745	- 4.111
7	173.83	0.5924	- 2.347
8	171.93	0.5842	- 28.981
9	2673.00	7.3683	+ 14.097
10	414.30	1.2890	+ 0.604

***Second-Law Efficiency*, η_{II}**

From Eq. (4.6), η_{II} can be determined as follows.

$$\Sigma \dot{A}_{supplied} = e_9 - e_{10}$$
$$= 14.097 - 0.604 = 13.493 \ MW$$

and

$$\Sigma \dot{A}_{products} = e_2 + e_3 + e_4 + e_6 + e_7 - e_1 - e_5 - e_8$$
$$= -12.719 + (-6.465) + (-28.981)$$
$$+ (-4.111) + (-2.347) - (-19.952)$$
$$- (-6.465) - (-28.981) = 0.7753 \ MW \ .$$

Thus,

$$\eta_{II} = \frac{0.7753}{13.493} \times 100 = 5.7\ \%$$

***Irreversibility*, $\dot{I}$**

The irreversibility, $\dot{I}$, can be found using Eq. (4.9) as follows,

$$\Sigma \dot{m}_e s_e = \dot{m}_2 s_2 + \dot{m}_3 s_3 + \dot{m}_4 s_4 + \dot{m}_6 s_6 + \dot{m}_7 s_7 + \dot{m}_{10} s_{10}$$
$$= 1589.17\,(0.5842) + 807.78\,(0.5842) + 3620.94\,(0.5842)$$
$$+ 533.49\,(0.5745) + 271.94\,(0.5924) + 34.93\,(1.289)$$
$$= 4028 \ kJ/s.K$$

and

$$\Sigma \dot{m}_i s_i = \dot{m}_1 s_1 + \dot{m}_5 s_5 + \dot{m}_8 s_8 + \dot{m}_9 s_9$$
$$= 2396.94\,(0.4780) + 807.78\,(0.5842) + 3620.94\,(0.5842)$$

$$+ 34.93\,(7.3683) = 3990 \quad kJ/s.K \quad .$$

Taking,

$$T_{WF} = T_{ambient} = 35 + 273 = 308K$$

we get,

$$\dot{I} = 308\,[\,4028 - 3990\,] = 11.671 \quad MW .$$

Normalized Irreversibility, i

The normalized irreversibility for Al-Jubail MSF plant can be calculated using Eq. (4.10) as follows,

$$i = \frac{\dot{I}}{\dot{m}_7}$$

$$= \frac{11671}{271.94} = 42.92 \quad kJ/kg\ water$$

Thermal Efficiency and Specific Energy Consumption

Using Eq. (4.11), we obtain

$$\Sigma \dot{m}_i h_i = \dot{m}_1 h_1 + \dot{m}_5 h_5 + \dot{m}_8 h_8 + \dot{m}_9 h_9$$

$$= 2396.94\,(138.9) + 807.78\,(171.93) + 3620.94\,(171.93)$$

$$+ 34.93\,(2673.0) = 1187 \quad MW$$

and

$$\Sigma \dot{m}_e h_e = \dot{m}_2 h_2 + \dot{m}_3 h_3 + \dot{m}_4 h_4 + \dot{m}_6 h_6 + \dot{m}_7 h_7 + \dot{m}_{10} h_{10}$$

$$= 1589.17\,(171.93) + 807.78\,(171.93) + 3620.94\,(171.93)$$

$$+ 533.49\,(169.24) + 271.94\,(173.83) + 34.93\,(414.3)$$

$$= 1186 \ MW \ .$$

Thus,

$$\eta = \frac{1186}{1187} \times 100 = 99.9 \ \% \ .$$

Using Eq. (4.12) to calculate SEC, we get

$$Net\ Energy\ Supplied = \dot{m}_9 h_9 - \dot{m}_{10} h_{10}$$

$$= 34.93\ (2673.0 - 414.3) = 78896 \ \ kW$$

and

$$Plant\ Capacity = \dot{m}_7 \times \frac{3600 \times 24}{1000}$$

$$= 271.94 \times \frac{3600 \times 24}{1000} = 23496 \ m^3/day \ .$$

Thus,

$$SEC = \frac{78896}{23496} \times 24 = 80.6 \ kWh/m^3 \ \ .$$

Second-Law Efficiency For The Brine Heater

Flow-diagram and operating conditions of the brine heater are given in figure (4.6) and table (4.10) respectively. State variables (s and h) are determined at their respective locations, and the results are presented in table (4.11). With the help of table (4.11) and Eq. (4.4), exergy (at the specified state points) is calculated, and the results are shown in table (4.12).

With the help of table (4.12) and using Eq. (4.6), we obtain

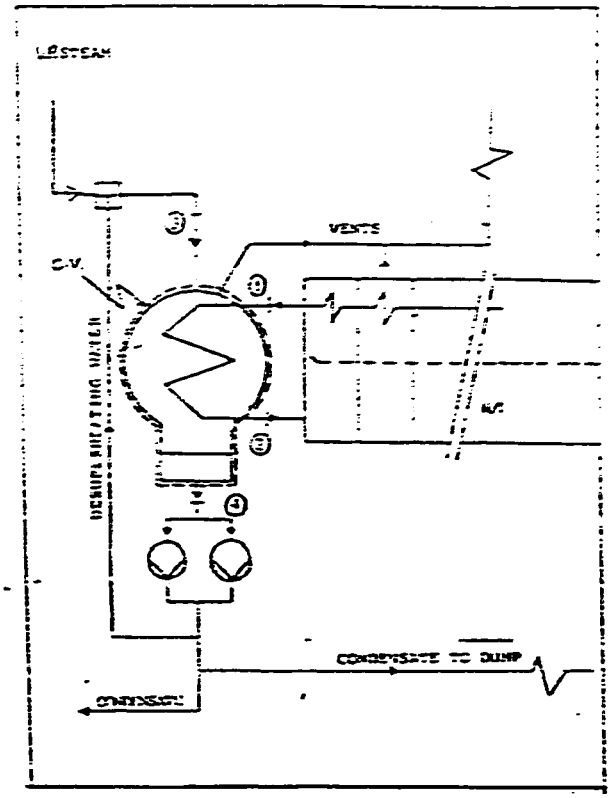

Fig. (4.6) Al-Jubail MSF Brine Heater Flow Diagram

Table (4.10) Al-Jubail Brine Heater (Operating Conditions)

State Point	T (C°)	P (bar)	$\dot{m}$ (kg/s)
1	85	6.35	3620.94
2	90.8	6.35	3620.94
3	98.9	0.974	34.93
4	98.9	0.974	34.93

Table (4.11) Al-Jubail Brine Heater (Operating Conditions)

State Point	Stream Type	Salinity σ (g/kg)	Enthalpy h (kJ/kg)	Entropy s $(kJ/kg \cdot K)$
1	Sea Water	46.5	338.3	1.078
2	Sea Water	46.5	358.3	1.134
3	LP Steam	-	2673	7.3683
4	Condensate	-	414.3	1.289

Table (4.12) Al-Jubail MSF-Brine Heater Exergy Results

State Point	Exergy e (MW)
1	22.725
2	32.690
3	14.097
4	0.604

$$(\eta_{II})_{BH} = \frac{e_2 - e_1}{e_3 - e_4} \times 100$$

$$= \frac{30.69 - 22.73}{14.10 - 0.60} \times 100 = 73.83\ \% \ .$$

4.3.3 Jeddah MSF Desalination Plant

General Description

This plant (Jeddah-III) is located on the coast of Red Sea near the city of Jeddah. It consists of 4 distillation units each designed to produce 22000 m^3/day of distillate and four steam turbines, each with power generating capacity of 50 MW [3].

Second-Law-Based Thermodynamic Analysis

A flow-diagram of one distillation unit (line) of Jeddah-III MSF, is shown in figure (4.7) [45]. This unit consists of 16 flashing stages as well as a brine heater. A control volume (C.V.) is drawn as shown in figure (4.8), indicating that, there are 10 state points (inlets and outlets). The maximum temperature corresponds to the low pressure steam entering the C.V. at state point number 8, and the lowest is that for seawater entering at point number 1. Performance operating conditions at various points of the C.V. are shown clearly in table (4.13).

Using table (4.13), the state variables (h and s) can be determined at various state points and the results are shown in table (4.14). With the help of table (4.14) and Eq. (4.4), the exergy can be calculated at various state points and the results are shown in table (4.15).

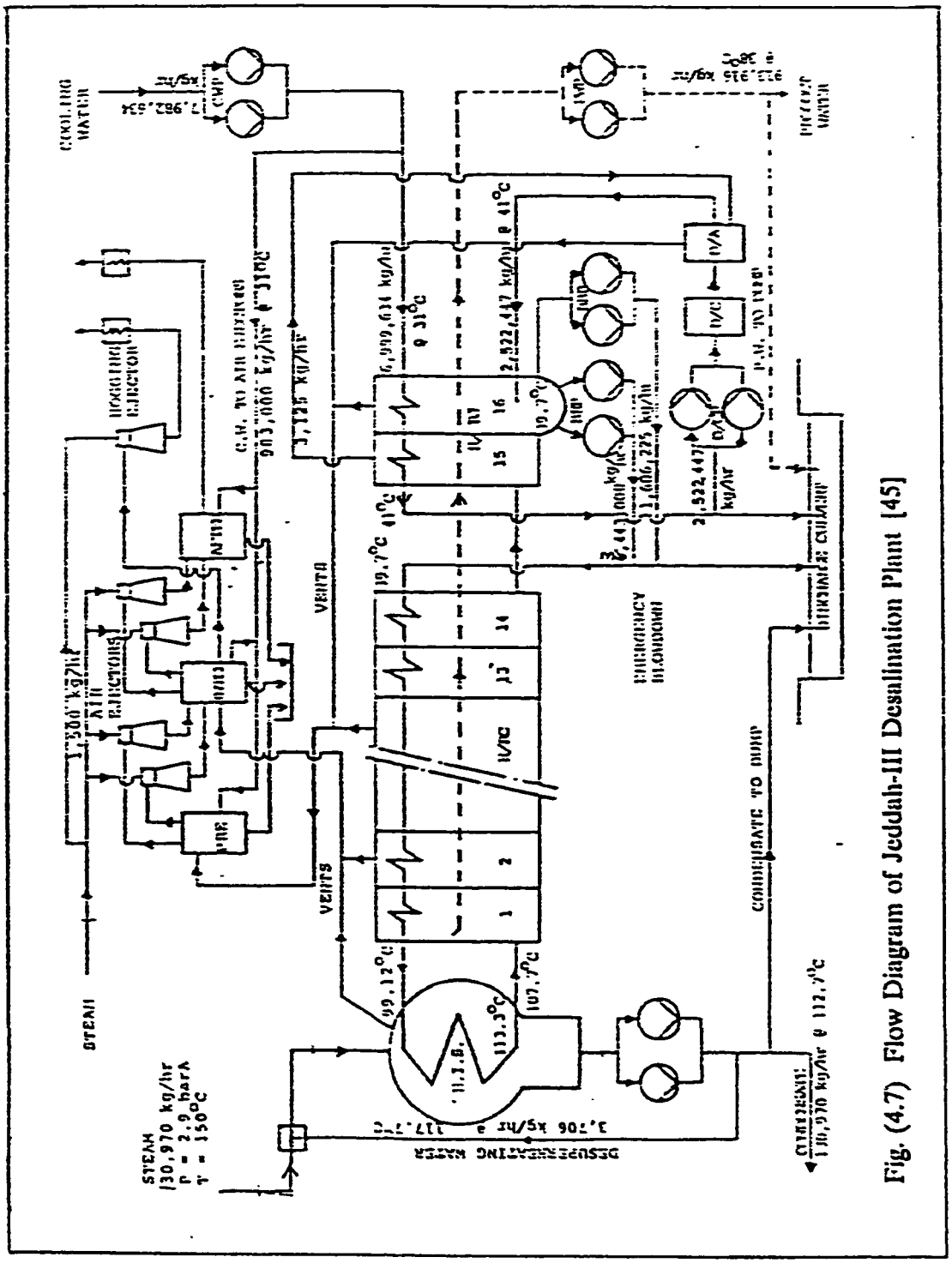

Fig. (4.7) Flow Diagram of Jeddah-III Desalination Plant [45]

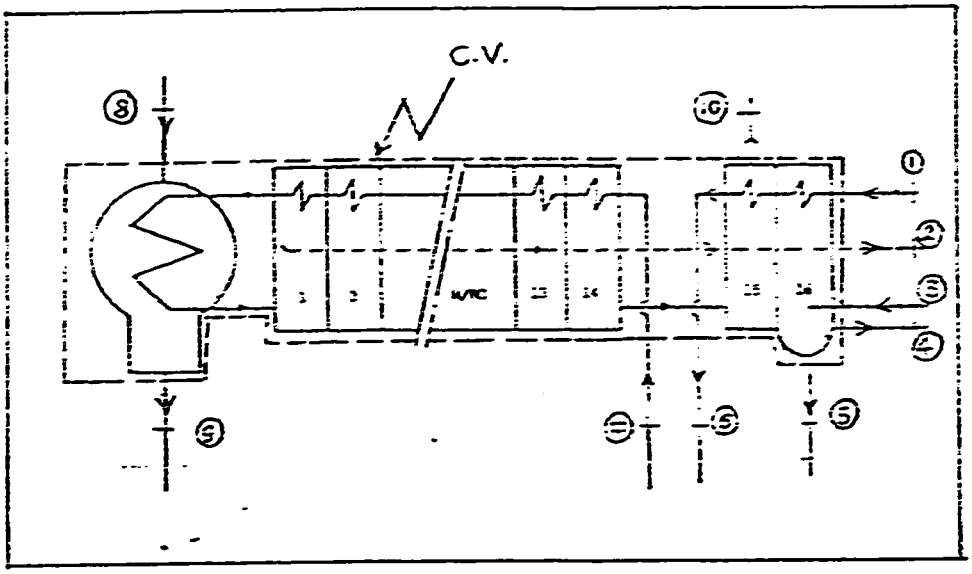

Fig. (4.8) Control Volume for Jeddah-III Plant

Table (4.13) Jeddah MSF Distillation Plant (Performance Operating Conditions)

State Point	T (C°)	P (bar)	$\dot{m}$ (kg/s)
1	31	1	1944.34
2	38	1	253.87
3	41	1	700.68
4	39.7	1	446.17
5	39.7	1	956.39
6	41.0	1	1944.34
7	39.7	1	956.62
8	134.0	2.9	37.41
9	117.7	2.9	37.41
10	41.0	1	0.868

Table (4.14) Jeddah MSF Distillation Plant
(Performance Operating Conditions)

State Point	Stream Type	Salinity σ (g/kg)	Enthalpy h (kJ/kg)	Entropy s $(kJ/kg \cdot K)$
1	Sea Water	41.4	122.98	0.4260
2	Distillate	-	157.125	0.5389
3	Sea Water	41.4	162.78	0.5555
4	Sea Water	41.4	157.61	0.5391
5	Sea Water	47	157.61	0.5391
6	Sea Water	41.4	162.78	0.5555
7	Sea Water	47	157.61	0.5391
8	LP Steam	-	2725.94	6.9875
9	Condensate	-	493.94	1.5027
10	Sea Water	41.4	162.78	0.5555

Table (4.15) Jeddah MSF Distillation Plant
Exergy Analysis Results

State Point	Enthalpy h (kJ/kg)	Entropy s ($kJ/kg\text{-}K$)	Exergy e (MW)
1	122.98	0.4260	- 15.988
2	157.13	0.5389	- 2.248
3	162.78	0.5555	- 5.826
4	157.61	0.5391	- 3.763
5	157.61	0.5391	- 8.065
6	162.78	0.5555	- 16.165
7	157.61	0.5391	- 8.067
8	2725.94	6.9875	+ 21.465
9	493.94	1.5027	+ 1.164
10	162.78	0.5555	- 0.007

Second-Law Efficiency, η_{II}

From Eq. (4.6), η_{II} , can be determined as follows,

$$\Sigma \dot{A}_{supplied} = e_8 - e_9$$

$$= 21.465 - 1.164 = 20.301 \ MW$$

and

$$\Sigma \dot{A}_{products} = e_6 + e_5 + e_4 + e_2 + e_{10} - e_1 - e_3 - e_7$$

$$= -16.165 + (-8.065) + (-3.763)$$

$$+ (-2.248) + (-0.007) - (-15.988)$$

$$- (-5.826) - (-8.067) = 0.368 \ MW$$

Thus,

$$\eta_{II} = \frac{0.3680}{20.308} \times 100 = 1.7\ \%$$

Irreversibility, $\dot{I}$

The irreversibility, $\dot{I}$, can be found using Eq. (4.9) as follows,

$$\Sigma \dot{m}_e s_e = \dot{m}_2 s_2 + \dot{m}_4 s_4 + \dot{m}_5 s_5 + \dot{m}_6 s_6 + \dot{m}_9 s_9 + \dot{m}_{10} s_{10}$$

$$= 253.87\ (0.5389) + 446.17\ (0.5391) + 956.39\ (0.5391)$$

$$+ 1944.34\ (0.5555) + 37.41\ (1.5027) + 8.68\ (0.5555)$$

$$= 2030 \ kJ/s.K$$

and

$$\Sigma \dot{m}_i s_i = \dot{m}_1 s_1 + \dot{m}_3 s_3 + \dot{m}_7 s_7 + \dot{m}_8 s_8$$

$$= 1944.34\ (0.4260) + 700.68\ (0.5555) + 956.62\ (0.5391)$$

$$+ 37.41\ (6.9875) = 1995 \quad kJ/s.K \quad .$$

Taking.

$$T_{WF} = T_{ambient} = 35 + 273 = 308K$$

we get.

$$\dot{I} = 308\ [\ 2030 - 1995\ ] = 10.804 \quad MW$$

Normalized Irreversibility, i

The normalized irreversibility for Jeddah MSF plant can be calculated using Eq. (4.10) as follows,

$$i = \frac{\dot{I}}{\dot{m}_2}$$

$$= \frac{10804}{253.87} = 42.56 \quad kJ/kg\ water$$

Thermal Efficiency and Specific Energy Consumption

Using Eq. (4.11), we obtain

$$\Sigma \dot{m}_i h_i = \dot{m}_1 h_1 + \dot{m}_3 h_3 + \dot{m}_7 h_7 + \dot{m}_8 h_8$$

$$= 1994.34\ (122.98 + 700.68\ (162.78) + 956.62\ (157.61)$$

$$+ 37.41\ (2725.94) = 606 \quad MW$$

and

$$\Sigma \dot{m}_e h_e = \dot{m}_2 h_2 + \dot{m}_4 h_4 + \dot{m}_5 h_5 + \dot{m}_6 h_6 + \dot{m}_9 h_9 + \dot{m}_{10} h_{10}$$

$$= 253.87\ (157.13) + 446.17\ (157.61) + 956.39\ (157.61)$$

$$+ 1944.34\ (162.78) + 37.41\ (493.94) + 0.868\ (162.78)$$

$$= 596 \ MW \ .$$

Thus,

$$\eta = \frac{596}{606} \times 100 = 98.37 \ \% \ .$$

Using Eq. (4.12) to calculate SEC, we get

$$Net\ Energy\ Supplied = \dot{m}_s h_s - \dot{m}_c h_9$$

$$= 37.41\ (2725.94 - 493.94) = 83499 \ \ kW$$

and

$$Plant\ Capacity = \dot{m}_2 \times \frac{3600 \times 24}{1000}$$

$$= 254.0 \times \frac{3600 \times 24}{1000} = 22000\ m^3/day \ .$$

Thus,

$$SEC = \frac{83499}{22000} \times 24 = 91.1\ kWh/m^3 \ \ .$$

4.3.4 Abu Dhabi Solar-Multieffect Distillation Plant

General Description

The solar desalination plant is built on a plot measuring 1382 m^2 within the Umm Al Nar power and desalination complex located near Abu Dhabi. Seawater is drawn from a near by channel connected to the Arabian Gulf. A schematic flow diagram is given in figure (4.9). The plant basically consists of three systems: a solar energy collection system, a hot water storage system (heat accumulator), and a seawater evaporator. The energy collection system uses evacuated glass tube solar collectors to convert the incident solar radiation into thermal energy. The water storage system (heat accumulator) consists of three vertical vessels with a total capacity of 300 m^3, connected in series and thermally stratified. The evaporator is a horizontal tube, thin-film, multi-effect-stack (MES) distiller with a design capacity ranging between 80-120 m^3/day [46].

Second-Law-Based Thermodynamic Analysis

A schematic for the control volume of this plant is shown in figure (4.10), indicating that, there are 7 state points (inlets and outlets). Hot water (low pressure steam) is entering at point no. 1 and leaving at point no. 2. Performance operating conditions at various points of the C.V. are shown clearly in table (4.16).

Using table (4.16), the state variables (h and s) can be determined at various

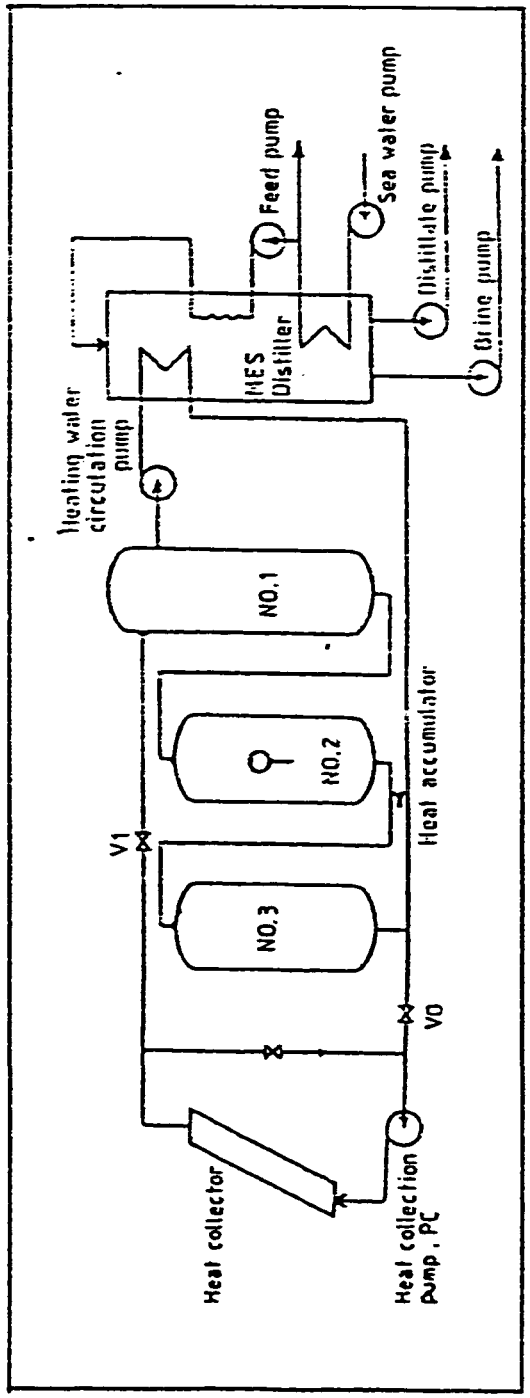

Figure (4.9) Schematic Flow Diagram of the Solar-Powered Multi-effect Distillation Plant [46]

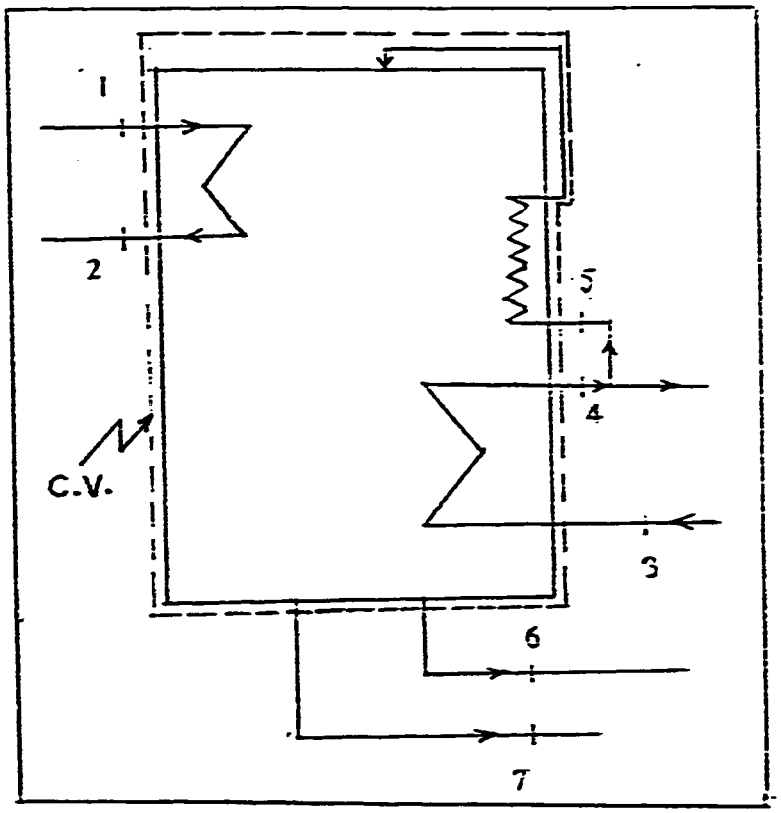

Fig. (4.10) Control Volume for Abu Dhabi Solar-MES Plant

Table (4.16) Abu Dhabi Solar-MES Distillation Plant (Performance Operating Conditions)

State Point	T (C°)	Stream Type	$\dot{m}$ (kg/s)
1	99	LP Steam	5.111
2	87	Hot Water	5.111
3	35	Sea Water	12.255
4	40	Sea Water	12.255
5	40	Sea Water	11.0
6	40	Brine	10.07
7	40	Distillate	0.9259

state points and the results are shown in table (4.17). With the help of table (4.17) and Eq. (4.4). the exergy can be calculated at various state points and the results are shown in table (4.18).

Second-Law Efficiency, η_{II}

From Eq. (4.6). η_{II} , can be determined as follows,

$$\Sigma \dot{A}_{supplied} = e_1 - e_2$$

$$= 149.04 - 69.29 = 79.75 \quad kW$$

and

$$\Sigma \dot{A}_{products} = e_4 + e_6 + e_7 - e_3 - e_5$$

$$= -67.43 + (-55.41) + (-5.46)$$

$$- (-71.83) - (-60.52)$$

$$= 4.063 \quad kW \ .$$

Thus,

$$\eta_{II} = \frac{4.063}{79.75} \times 100 = 5.09\ \%$$

Irreversibility, $\dot{I}$

The irreversibility. $\dot{I}$, can be found using Eq. (4.9) as follows,

$$\Sigma \dot{m}_e s_e = \dot{m}_2 s_2 + \dot{m}_4 s_4 + \dot{m}_6 s_6 + \dot{m}_7 s_7$$

$$= 5.111\ (1.1576) + 12.255\ (0.5340) + 10.07\ (0.5340)$$

$$+ 0.9259\ (0.5725)$$

$$= 18.368 \quad kJ/s.K$$

Table (4.17) Abu Dhabi Solar-MES Distillation Plant
(Performance Operating Conditions)

State Point	Salinity σ (g/kg)	Enthalpy h (kJ/kg)	Entropy s (kJ/kg-K)
1	-	414.82	1.2728
2	-	364.31	1.1576
3	55	136.70	0.4705
4	55	156.30	0.5340
5	55	156.30	0.5340
6	58	156.30	0.5340
7	-	167.57	0.5725

Table (4.18) Abu Dhabi Solar-MES Plant
Exergy Analysis Results

State Point	Enthalpy h (kJ/kg)	Entropy s (kJ/kg-K)	Exergy e (kW)
1	414.82	1.2728	+ 149.04
2	364.31	1.1576	+ 69.29
3	136.70	0.4705	- 71.83
4	156.30	0.5340	- 67.43
5	156.30	0.5340	- 60.52
6	156.30	0.5340	- 55.41
7	167.57	0.5725	- 5.46

and

$$\Sigma \dot{m}_i s_i = \dot{m}_1 s_1 + \dot{m}_3 s_3 + \dot{m}_5 s_5$$

$$= 5.111\ (1.2728) + 12.255\ (0.4705) + 11.00\ (0.5340)$$

$$= 18.145\ \ kJ/s.K \quad .$$

Taking,

$$T_{WF} = T_{ambient} = 35 + 273 = 308K$$

we get,

$$\dot{I} = 308\ [\ 18.368 - 18.145\ ] = 67.57\ kW$$

Normalized Irreversibility, i

The normalized irreversibility for Abu Dhabi MES plant can be calculated using Eq. (4.10) as follows,

$$i = \frac{\dot{I}}{\dot{m}_7}$$

$$= \frac{67.57}{0.9259} = 72.98\ \ kJ/kg\ water$$

Thermal Efficiency and Specific Energy Consumption

Using Eq. (4.11), we obtain

$$\Sigma \dot{m}_i h_i = \dot{m}_1 h_1 + \dot{m}_3 h_3 + \dot{m}_5 h_5$$

$$= 5.111\ (414.82) + 12.255\ (136.70) + 11.00\ (156.30)$$

$$= 5514.7\ \ kW$$

and

$$\Sigma \dot{m}_e h_e = \dot{m}_2 h_2 + \dot{m}_4 h_4 + \dot{m}_6 h_6 + \dot{m}_7 h_7$$

$$= 5.111\,(364.31) + 12.255\,(156.30) + 10.07\,(156.30)$$

$$+ 0.9254\,(167.57)$$

$$= 5506.4 \quad kW \ .$$

Thus,

$$\eta = \frac{5506}{5515} \times 100 = 99.8\ \% \ .$$

Using Eq. (4.12) to calculate SEC, we get

$$\textit{Net Energy Supplied} = \dot{m}_1 h_1 - \dot{m}_2 h_2$$

$$= 5.111\,(414.82 - 364.31) = 258.2 \quad kW$$

and

$$\textit{Plant Capacity} = \dot{m}_7 \times \frac{3600 \times 24}{1000}$$

$$= 0.9259 \times \frac{3600 \times 24}{1000} = 80 \ \ m^3/day \ .$$

Thus,

$$SEC = \frac{258.2}{80} \times 24 = 72.45 \ \ kWh/m^3 \ .$$

4.3.5 Typical 100 m^3/Day RO Plant

General Description

A schematic of the flow diagram of this plant is depicted in figure (4.11) [47].

Second-Law-Based Thermodynamic Analysis

A schematic for the control volume of this plant is shown in figure (4.12), indicating that, there are 3 state points (inlets and outlets). High pressure feedwater is entering at point no. 1 and leaving as a product water at point 2 and as a brine at point 3. Performance operating conditions at various points of the C.V. are shown clearly in table (4.19).

The state variables (h and s) are also determined at various state points and the results are shown in table (4.19). Based on this table (4.19) and with the help of Eq. (4.4), the exergy can be calculated at various state points and the results are shown in table (4.20).

Second-Law Efficiency, η_{II}

For this type of process, electrical energy is needed, and the rate of exergy supplied is nothing but the rate of electrical energy (high quality form of energy) input to the RO system. Therefore, the analysis would be different ,in some way, than previously. The following equations to be used for the analysis.

$$W_{act.} = W - W_t + W_{aux.} \quad (kWh/m^3) \ . \tag{4.13}$$

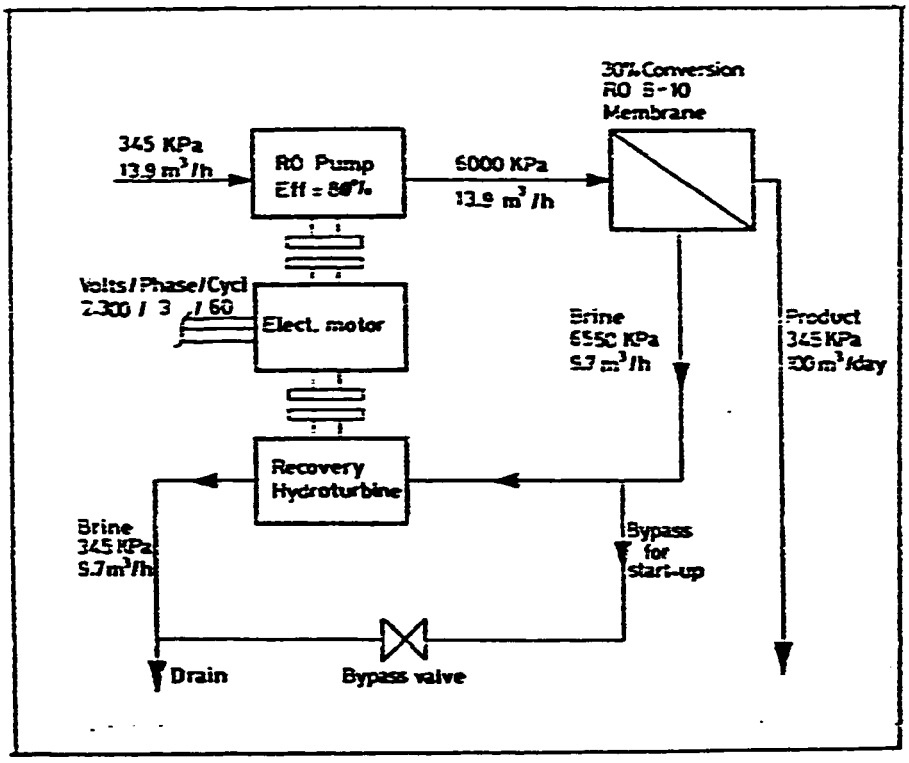

Figure (4.11) Typical RO Plant [47]

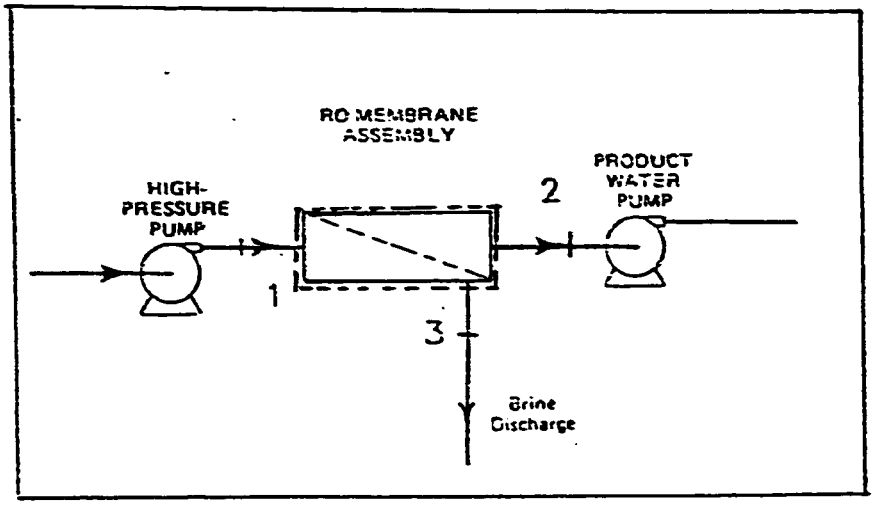

Fig. (4.12) Control Volume for the RO Plant

Table (4.19) Typical 100 m^3/day RO Desalination Plant (Performance Operating Conditions)

State Point	T (C°)	P (bar)	$\dot{m}$ (kg/s)
1	30	60.0	3.9579
2	30	3.45	1.1574
3	30	65.5	2.8568

State Point	Stream Type	Salinity σ (g/kg)	Enthalpy h (kJ/kg)	Entropy s ($kJ/kg\cdot K$)
1	Sea Water	42.0	118.00	0.4090
2	Permeate	-	125.79	0.4369
3	Brine	83.58	112.95	0.3930

Table (4.20) Typical 100 m^3/d RO Plant Exergy Analysis Results

State Point	Enthalpy h (kJ/kg)	Entropy s ($kJ/kg\cdot K$)	Exergy e (kW)
1	118.00	0.4090	- 30.365
2	125.79	0.4369	- 10.156
3	112.95	0.3930	- 23.123

Rewriting this Eq. in rate form, we obtain

$$\dot{W}_{act.} = \dot{W} - \dot{W}_t + \dot{W}_{aux.} \quad (kW) \tag{4.14}$$

where

$\dot{W}_{act.}$ = Actual energy consumption of RO

$\dot{W}$ = Energy cons. of RO without recovery

$\dot{W}_t$ = Energy recovery by the turbine

$\dot{W}_{aux.}$ = Actual energy cons. of auxiliary pumps .

In order to determine $\dot{W}_{act.}$, the terms on the R.H.S. of Eq. (4.13) need to be evaluated. From ref. [32], W can be calculated using the following equation:

$$W = \frac{\Delta P}{36.7 \times R_c \times \eta_p} \tag{4.15}$$

where

ΔP = Pressure across RO membrane

R_c = Recovery ratio

η_p = Pump efficiency .

For our case, we have

$$\Delta P = P_1 - P_2$$

$$= 69 - 3.45 = 65.55 \ bars$$

$$R_c = \frac{\dot{m}_2}{\dot{m}_1}$$

$$= \frac{1.1574}{3.9579} = 0.2924 \quad (i.e. 29\ \%)$$

and

$$\eta_p = 0.8 \ .$$

Thus, Eq. (4.15) becomes

$$W = \frac{65.55}{36.7 \times 0.2924 \times 0.8} = 7.64 \ kwh/m^3 \ .$$

Since the production capacity of the RO unit is equal to

$$PC = 100 \ m^3/day$$

and

$$\dot{W} = W \times PC \times \frac{1}{24} \quad (kW) \ . \tag{4.16}$$

Substituting, we get

$$\dot{W} = 7.64 \times 100 \times \frac{1}{24} = 31.83 \ kW \ .$$

W_t is defined as [32]:

$$W_t = \frac{1}{36.7} \times P_3 \times \eta_t \times (\frac{1}{R_c} - 1)$$

where

P_3 = Pressure of brine leaving membrane

η_t = Efficiency of energy recovery turbine .

Substituting, we get

$$W_t = \frac{1}{36.7} \times (65.5) \times 0.75 \times (\frac{1}{0.2924} - 1)$$

$$= 3.24 \ \ kWh/m^3$$

and in rate form Eq. (4.16), we get

$$\dot{W}_t = 3.24 \times 100 \times \frac{1}{24} = 13.50 \ kW \ .$$

$W_{max.}$ is given in ref. [47] as

$$W_{max.} = 0.764 \ \ kWh/m^3$$

or in rate form as

$$\dot{W}_{max.} = 0.764 \times 100 \times \frac{1}{24} = 3.183 \ kW \ .$$

Substituting these values of $\dot{W}$, $\dot{W}_t$, and $\dot{W}_{max.}$ in Eq. (4.14), we obtain

$$\dot{W}_{act.} = 31.83 - 13.50 + 3.18 = 21.51 \ kW \ .$$

Since,

$$\Sigma \dot{A}_{supply} = \dot{W}_{act.} \qquad (4.17)$$

thus,

$$\Sigma \dot{A}_{supplies} = 21.51 \ kW \ .$$

Exergy can be found in a manner similar to previous analysis, i.e.

$$\Sigma \dot{A}_{products} = e_1 - e_2 - e_3$$
$$= -30.365 - (-10.156) - (-23.123) = 2.914 \ kW \ .$$

Thus,

$$\eta_{II} = \frac{2.914}{21.51} \times 100 = 13.26 \ \%$$

Irrerersibility, $\dot{I}$

The irreversibility, $\dot{I}$, can be found using Eq. (4.9) as follows,

$$\Sigma \dot{m}_e s_e = \dot{m}_2 s_2 + \dot{m}_3 s_3$$
$$= 1.1574(0.4369) + 2.8568(0.393)$$
$$= 1.6284 \ \ kJ/s.K$$

and

$$\Sigma \dot{m}_i s_i = \dot{m}_1 s_1$$
$$= 3.9579(0.4090) = 1.6188 \ \ kJ/s.K \ .$$

Taking,

$$T_{WF} = T_{ambient} = 35 + 273 = 308K$$

we get,

$$\dot{I} = 308 \, [\, 1.6284 - 1.6188 \,] = 2.957 \ kW$$

Normalized Irreversibility, i

The normalized irreversibility for this plant can be calculated using Eq. (4.10) as follows,

$$i = \frac{\dot{I}}{\dot{m}_2}$$

$$= \frac{2.957}{1.1574} = 2.555 \quad kJ/kg\ water$$

Thermal Efficiency and Specific Energy Consumption

SEC is nothing but,

$$SEC = W_{act.} \tag{4.18}$$

where SEC can be calculated using Eq. (4.13) as

$$W_{act.} = 7.64 - 3.24 + 0.764$$

$$= 5.164 \quad kWh/m^3$$

thus,

$$SEC = 5.164 \quad kWh/m^3$$

It should be noted that, the values of enthalpy (given in appendix A) have been found not to be sensitive to pressure changes, in the contrary they are very sensitive to temperature and salinity variations. Also, the temperature variation during the operation of RO unit (across the membrane) is not appreciable. This fact is a general one and because of it the use of Eq. (4.11) would give no sound meaning. Despite this fact, energy has to be conserved and it is the case here :

$$\eta = \frac{\dot{m}_2 h_2 + \dot{m}_3 h_3}{\dot{m}_1 h_1} \times 100$$

$$= \frac{(1.1574 \times 125.79) + (2.8568 \times 112.95)}{(3.9579 \times 118)} \times 100 = 99.7\ \% \quad .$$

4.3.6 Wind-Powered RO Plant At Germany

General Description

This plant is located on the coast of the North Sea in Germany and is powered solely by wind energy converter as shown in figure (4.13) [41].

Second-Law-Based Thermodynamic Analysis

A schematic for the control volume of this plant is shown in figure (4.14), indicating that, there are 3 state points (inlets and outlets). High pressure feedwater is entering at point no. 1 and leaving as a product water at point 3 and as a brine at point 2. Performance operating conditions at various points of the C.V. are shown clearly in table (4.21).

The state variables (h and s) are also determined at various state points and the results are shown in the same table (4.21). Based on this table (4.21) and with the help of Eq. (4.4), the exergy can be calculated at various state points and the results are shown in table (4.22).

Second-Law Efficiency, η_{II}

For this type of process, electrical energy is needed, and the rate of exergy supplied is nothing but the rate of electrical energy (high quality form of energy) input to the RO system as in the previous section. Since this plant has no energy recovery turbine, Eq. (4.13) would be modified as

$$W_{act.} = W + W_{aux.} \quad (kW/h/m^3) \ . \tag{4.19}$$

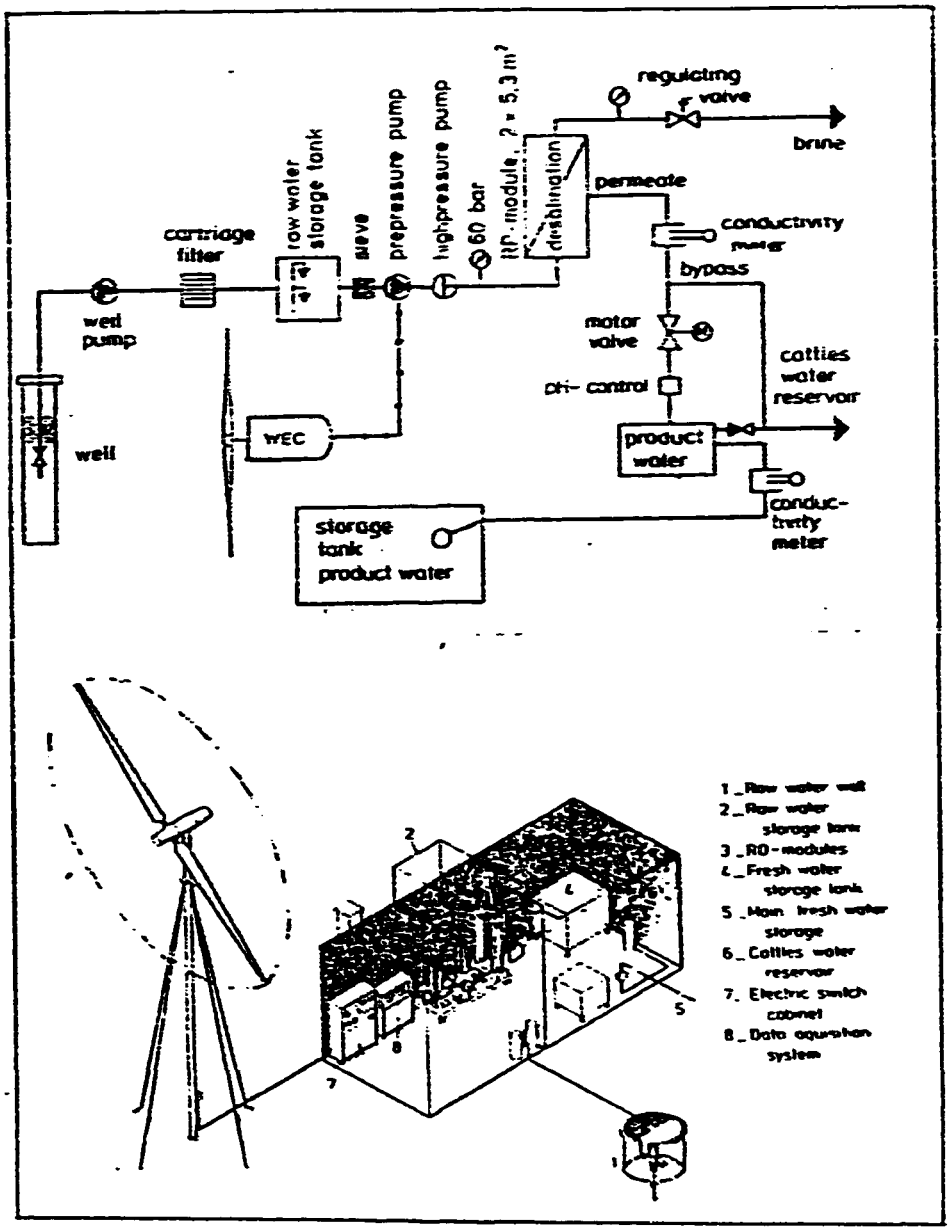

Figure (4.13) Schematic Flow Diagram of Wind-Powered RO Plant at Germany [41]

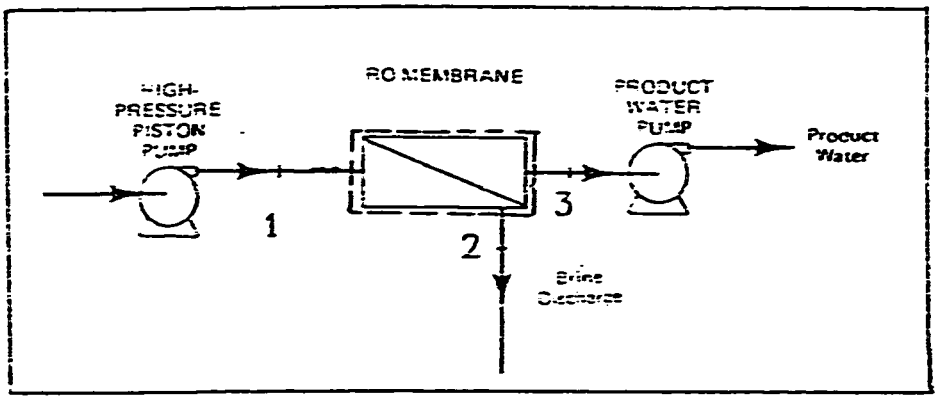

Fig. (4.14) Control Volume for Wind-Powered RO Plant

Table (4.21) Wind-Powered RO Desalination Plant at Germany (Performance Operating Conditions)

State Point	T ($C°$)	p (bar)	$\dot{m}$ (kg/s)
1	20	60	0.2282
2	20	59	0.1744
3	20	1	0.0552

State Point	Stream Type	Salinity σ (g/kg)	Enthalpy h (kJ/kg)	Entropy s ($kJ/kg\cdot K$)
1	Brackish Water	28	80.61	0.2849
2	Brine	100	77.873	0.2800
3	Distillate	-	83.96	0.2966

Table (4.22) Wind-Powered RO Plant at Germany
Exergy Analysis Results

State Point	Enthalpy h (kJ/kg)	Entropy s $(kJ/kg \cdot K)$	Exergy e (kW)
1	80.61	0.2849	- 0.654
2	77.87	0.2800	- 0.727
3	83.96	0.2966	- 0.163

Rewriting this Eq. in rate form, we obtain

$$\dot{W}_{act.} = \dot{W} + \dot{W}_{aux.} \quad (kW) . \tag{4.20}$$

where $\dot{W}$ can be calculated using Eq. (4.15), as follows

$$\Delta P = P_1 - P_2 = 59 \ bars$$

$$R_c = \frac{\dot{m}_3}{\dot{m}_1} = \frac{0.0552}{0.2282} = 0.2419$$

$$\eta_p = 0.80$$

and

$$PC = 4.77 \ m^3/day \ .$$

Thus,

$$W = \frac{59}{36.7 \times 0.2419 \times 0.8} = 8.3 \ kWh/m^3 \ .$$

And from Eq. (4.16),

$$\dot{W} = 8.3 \times 4.77 \times \frac{1}{24} = 1.66 \ kW$$

$\dot{W}_{aux.}$ is given in ref. [41] as

$$\dot{W}_{aux.} = 0.166 \ kW$$

Substituting these values in Eq. (4.19), we get

$$\dot{W}_{act.} = 1.66 + 0.166 = 1.862 \ kW$$

or

$$W_{act.} = 9.13 \ \ kWh/m^3 \ .$$

Thus,

$$\Sigma \dot{A}_{supply} = 1.826\, kW \ .$$

Exergy can be found in a manner similar to previous analysis, i.e.

$$\Sigma \dot{A}_{products} = e_1 - e_2 - e_3$$
$$= -0.654 - (-0.727) - (-0.163) = 0.2352\, kW \ .$$

Hence,

$$\eta_{II} = \frac{0.2352}{1.828} \times 100 = 12.88\ \%$$

Irreversibility, $\dot{I}$

The irreversibility, $\dot{I}$, can be found using Eq. (4.9) as follows,

$$\Sigma \dot{m}_e s_e = \dot{m}_2 s_2 + \dot{m}_3 s_3$$
$$= 1.1744(0.2809) + 0.552(0.2966)$$
$$= 0.0652 \ \ kJ/s.K$$

and

$$\Sigma \dot{m}_i s_i = \dot{m}_1 s_1$$
$$= 0.2282(0.2849) = 0.0650 \ \ kJ/s.K \ .$$

Taking,

$$T_{WF} = T_{ambient} = 35 + 273 = 308K$$

we get,

$$\dot{I} = 308\,[\,0.0652 - 0.0650\,] = 0.05571\ kW\ .$$

Normalized Irreversibility, i

The normalized irreversibility for this plant can be calculated using Eq. (4.10) as follows.

$$i = \frac{\dot{I}}{\dot{m}_3}$$

$$= \frac{0.05571}{0.0552} = 1.01\ \ kJ/kg\ water$$

Thermal Efficiency and Specific Energy Consumption

Using Eq. (4.18), we obtain

$$SEC = 9.13\ kWh/m^3$$

and

$$\eta = \frac{\dot{m}_2 h_2 + \dot{m}_3 h_3}{\dot{m}_1 h_1} \times 100$$

$$= \frac{(0.1744 \times 77.873) + (0.0552 \times 83.96)}{(0.2282 \times 80.61)} \times 100 = 99\ \%\ .$$

4.4 Comparisons And Concluding Remarks

In the preceding sections of this chapter, three types of desalting processes have been analyzed. These processes are :

1. Multistage Flash Distillation (MSF)
2. Multieffect Distillation (ME)
3. Reverse Osmosis (RO)

The analysis made in this chapter was entirely based on thermodynamics criteria (first and second laws of thermodynamics). The final objective sought from such analysis, is to compare the previously mentioned desalting processes. Based on this comparison as well as the results obtained in chapter 3, a decision regarding which process is most suited for coupling with solar and wind energy conversion systems will be made.

4.4.1 Thermal Efficiency-Based Comparison

Table (4.23) lists the desalting processes along with their specific energy consumption results. It can be noted from this table that the reverse osmosis (RO) process against other processes, requires the least amount of energy, approximately 8-10 times lower than that of the heat processes, to produce the same amount of distilled water. However, the type of energy used in this process is electrical whereas the other processes require thermal type of energy. If one assumes an energy conversion efficiency of 1/3 for the electricity generation, the primary energy consumption per amount of productwater will be 15-27 kWh/m^3, still being considerably less than the energy consumption of heat processes. This

Table (4.23) Comparison of the Specific Energy Consumption (SEC), for the Selected Desalination Plants

Plant	Production Capacity (m^3/d)	Type of Energy	SEC (kWh/m^3)
Al-Khobar MSF	19417	Thermal	103.50
Al-Jubail MSF	23496	Thermal	80.60
Jeddah MSF	21934	Thermal	91.10
Abu Dhabi MES	80	Thermal	77.45
Typical RO	100	Electrical	5.164
Wind-RO	4.8	Electrical	9.13

result coincides with the previous results obtained in chapter 3.

4.4.2 Second-Law-Based Comparison

Fortunately, it is considered to be the first time that the desalting processes are compared from the second-law standpoint. Three types of comparison are dealt with. These types are :

1- Comparison based on irreversibility (entropy generation)

2- Comparison based on normalized irreversibility

3- Comparison based on the second-law efficiency

Comparison of processes based on irreversibility (entropy generation) is presented in table (4.24). It is clearly shown that thermal processes (MSF and ME) are associated with tremendous amount of irreversibility (ranging between 68-11671 kW), whereas membrane process (RO) is associated with relatively very low irreversibility (maximum of 3 kW). This result is anticipated since thermal processes require heat for their operation, and heat in turn is the main source for irreversibility (entropy) creation. In contrast to heat processes, membrane processes require electrical energy which is considered as a high quality form of energy.

The second type of comparison (normalized irreversibility comparison) is related to the first type, but the former has more logical meaning since it normalizes the basis on which the processes need to be compared. Results of this comparison is given in table (4.25). Such comparison favours reverse osmosis as the one with the minimum normalized irreversibility. The unit used is

Table (4.24) Comparison of Irreversibility

Plant	Plant Capacity (m^3/day)	Irreversibility $\dot{I}$ (MW)
Al-Khobar MSF	19417	7.182
Al-Jubail MSF	23496	11.671
Jeddah MSF	21934	10.804
Abu Dhabi Solar-MES	80	0.0676
Typical RO	100	0.00296
Wind-RO	4.8	0.0000557

Table (4.25)

Comparison of the Normalized Irreversibility , i , for the Selected Desalination Plants

Desalination Plant	Type of Energy	i $kJ/(kg\ water)$
Al-Khobar MSF	Thermal	31.96
Al-Jubail MSF	Thermal	42.92
Jeddah MSF	Thermal	42.56
Abu Dhabi Solar-MES	Thermal	72.98
Wind-RO	Electrical	1.01
Typical RO	Electrical	2.56

kJ/kgwater which indicates how much irreversibility (*kJ*) is created to produce one *kg* of productwater.

Comparison of desalting processes based on the second-law efficiency is presented in table (4.26). Despite the fact that the efficiency values are, in general, quite low it is interesting to note that reverse osmosis processes have relatively higher values of efficiency. This result reflects the fact that processes which require electrical energy for their operation tend to be more efficient as compared to those requiring less quality forms of energy, such as heat processes.

Efficiency of MSF plants ranges between 1.7-5.7%. This result is compared with the result of a detailed analysis (computer based simulation model) performed for Umm Al Nar West MSF desalination plant in Abu Dhabi [23]. This detailed analysis showed that such plant has a second-law efficiency varying between 5.1% in winter time and 5.5% in summer time. These values coincide with the results found in this study. The reasons for such plants (high-volume desalination plants) in having low second-law efficiency values should not be surprising. It should be recognized that a distillation process is a refining operation, seeking small changes in the exergy of large quantities of materials.

The thermal efficiency and the second-law efficiency for the MSF plants are compared in table (4.27). This table shows that, although Al-Khobar plant has a lower η as compared to Jeddah plant, the former is more efficient than the latter as far as η_{II} is concerned.

Table (4.26) Comparison of Various Desalting Processes Based on The Second Law Efficiency

Plant	η_{II}[8]
Al-Khobar MSF	4.30
Al-Jubail MSF	5.70
Jeddah MSF	1.70
Abu Dhabi Solar-MES	5.09
Typical RO	13.26
Wind-RO	12.88

Table (4.27) Efficiency Comparison

Plant	η %	η_{II}%
Al-Khobar MSF	96.6	4.3
Al-Jubail MSF	99.S	5.7
Jeddah MSF	98.4	1.7

Table (4.28) Specific Energy Consumption (SEC) and Irreversibility Comparisons

Plant	SEC (kWh/m^3)	Irreversibility $\dot{I}$ (MW)
Al-Khobar MSF	103.50	7.182
Al-Jubail MSF	80.60	11.671
Jeddah MSF	91.10	10.804
Abu Dhabi Solar-MES	77.45	0.0676
Typical RO	5.16	0.00296
Wind-RO	9.13	0.0000557

Table (4.29) Comparison of the Second-Law Efficiency for the Brine Heaters

Plant	η_{II}%
Al-Khobar MSF	20.17
Al-Jubail MSF	73.85

4.4.3 Concluding Remarks

Based on the previous analysis, the following remarks can be made:

1- Concerning the two laws of efficiency, the results obtained in this chapter favours reverse osmosis as the most efficient process.

2- Thermal efficiency is not a true measure for comparing energy driven processes. However, the second-law is a rational and powerful tool for such purpose.

3- MSF process is the most irreversible (entropic) and energy consuming process as shown in table (4.28).

4- Al-Jubail MSF brine heater is found to have a higher second-law efficiency (74 %) as compared to that for Al-Khobar (20 %) as given in table (4.29). These values of efficiency are compared with Umm Al Nar MSF brine heater's efficiency (54 %) [23].

5- Reverse Osmosis is turned out to be a very promising process for coupling with solar and wind energy conversion system.

CHAPTER 5

ASSESSMENT OF SOLAR AND WIND POWER AVAILABILITY AND THEIR APPLICATION TO DESALINATION

In this chapter, an assessment of solar and wind power on Dhahran city (representative city located on the eastern coast of Saudi Arabia) will be made. This assessment will be based on actual as well as computed solar radiation and wind data. Using such data, profiles of solar and wind power on hourly and monthly basis of a typical year will be obtained. These profiles will be examined and compared for desalination purposes.

5.1 Solar Radiation

Dhahran city is characterized by a very hot weather in summer season which extends from March to November. The temperature peaks in May to about 50 °C, and drops in January to about 4 °C [12].

5.1.1 Measured Solar Radiation Data

Monthly average daily values of solar radiation, $(\overline{H}_H)$ received on a horizontal surface, located in Dhahran area, for a typical year (1986) [48] are presented in figure (5.1). From this figure it can be noticed that the maximum amount of falling radiation is occurring in the month of June (26.83 MJ/m^2) while the lowest is that on the month of December.

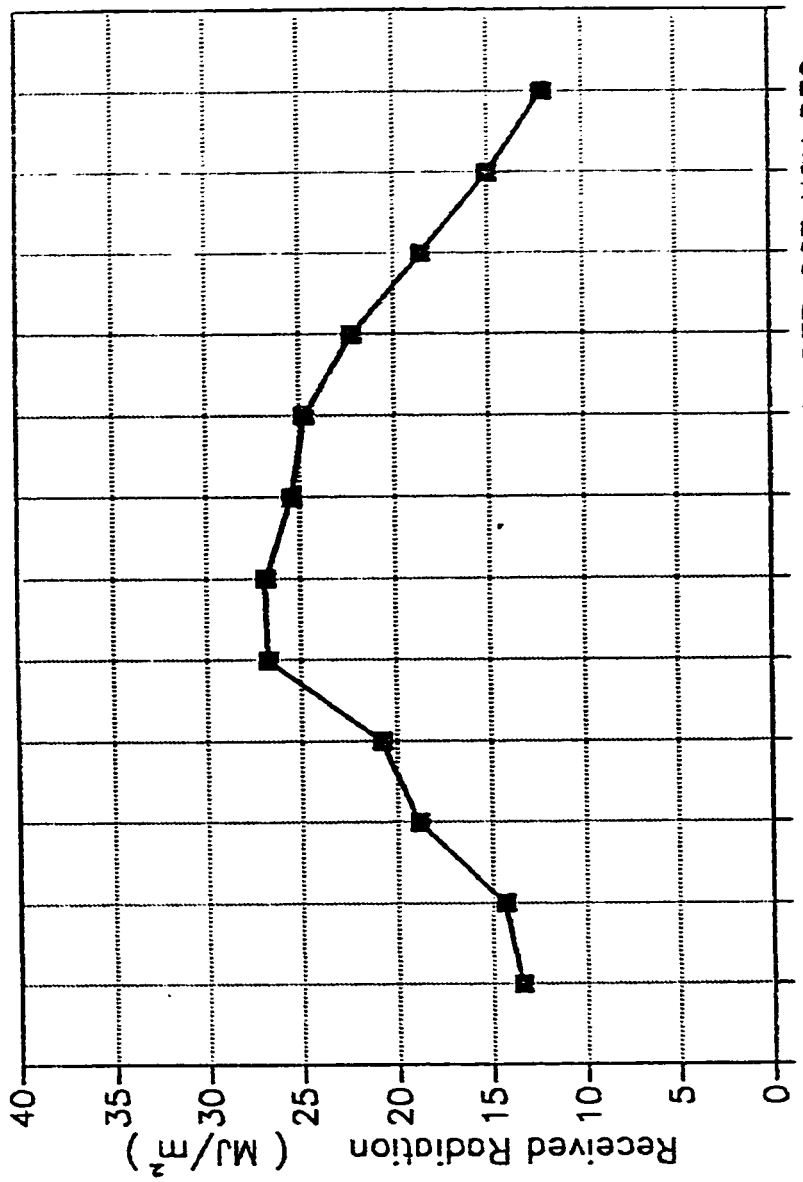

Figure (5.1) Measured Values of Monthly Average Daily Radiation, $\bar{H}_H$ [48]

5.1.2 Calculation of Solar Radiation Received on a Tilted Surface

Monthly Average Daily Radiation, $\overline{H}_T$

Solar radiation received on a surface can be maximized by tilting the surface with an angle β, equal to the latitude φ, of the surface location, and by orienting it so that it is facing south (*i.e. Azimuth angle*, $\gamma = 0$) [29]. For Dhahran city (latitude, $\varphi = 26.13\ ^{\circ}N$), the tilt (slope) angle β, would be equal to φ. Since it is unusual procedure to measure solar radiation on sloped surfaces, the method described by Duffie and Beckman [29] is used to calculate (estimate) the monthly average daily radiation ($\overline{H}_T$) incident on a tilted surface ($\beta = 26.13^{\circ}$) located in Dhahran. Since the procedure for such calculations is very lengthy, general guidelines and main results will be presented in this chapter.

General Procedure

1- Monthly average daily extraterrestrial radiation , $\overline{H}_{OH}$, is calculated (using a computer program, appendix B), and the results are presented in table (5.1).

2- The monthly average clearness index, $\overline{K}_T$, is obtained for each month in the year using the relationship:

$$\overline{K}_T = \frac{\overline{H}_H}{H_{OH}} \qquad (5.1)$$

Table (5.1) Computed Monthly Average Daily Extraterrestrial Radiation (Dhahran)

Month	Average Day n	$\bar{H}_{oz}$ (MJ/m^2)
January	17	23.2
February	15	27.4
March	16	32.6
April	15	37.0
May	15	39.4
June	9	40.1
July	18	39.7
August	17	37.7
September	16	34.0
October	16	28.8
November	15	24.1
December	11	22.0

3- The ratio of monthly average diffuse radiation to total radiation (i.e. $\frac{\overline{H}_{dH}}{\overline{H}_H}$)is obtained for each month (average day of the month) with the help of $\overline{K}_T$ obtained in step no.1 and figures in [29].

4- The geometric factor of beam radiation $\overline{R}_b$ for each average day of the month is calculated as given in [29].

5- The isotropic sky model which is given as [29]:

$$\overline{H}_T = \overline{H}_H \left(1 - \frac{\overline{H}_{dH}}{\overline{H}_H}\right) \overline{R}_b + \overline{H}_{dH} \frac{(1 + \cos\beta)}{2} + \overline{H}_H \rho_g \frac{(1 - \cos\beta)}{2} \qquad (5.2)$$

is used to obtain $\overline{H}_T$ for each month.

The results of this procedure are shown in table (5.2). It should be noted that the values for the monthly mean daily ambient temperatures, $\overline{T}_a$, are those measured values for a typical year (1986) [48], as shown in figure (5.2). Comparison between $\overline{H}_T$ and $\overline{H}_H$ is made in table (5.3). Also, comparison between $\overline{H}_T$, $\overline{H}_H$, and $\overline{H}_{OH}$ is illustrated in figure (5.3). It is interesting to note from this figure that the maximum radiation is obtained in the month of June while the lowest value corresponds to the month of December.

Table (5.2) Solar Radiation Data for Dhahran

(ϕ=26.13°N, L=50.1°E, z=β)

Month	Avg. Day n	$\overline{T}_a$ (C°)	$\overline{\delta}$ (deg.)	$\overline{\omega}_s$ (deg.)	$\overline{H}_{oh}$ (MJ/m²)	$\overline{H}_h$ (MJ/m²)
Jan.	17	17.4	-20.9	79.2	23.28	13.40
Feb.	15	15.5	-13.3	83.3	27.44	14.30
Mar.	16	19.8	-2.4	88.8	32.59	18.79
Apr.	15	25.7	9.4	94.7	36.99	20.72
May	15	31.6	18.8	99.6	39.45	26.72
June	9	33.8	22.9	102.0	40.19	26.83
July	18	35.5	21.0	100.8	39.67	25.42
Aug.	17	35.6	13.1	96.6	37.70	24.72
Sept.	16	32.7	1.8	90.9	33.93	22.19
Oct.	16	28.3	-10.0	85.0	28.81	18.49
Nov.	15	23.9	-19.1	80.2	24.12	15.04
Dec.	11	17.4	-23.1	77.9	21.98	12.08

Month	$\overline{K}_T$	ρ_g	$\overline{R}_b$	$\overline{H}_{d_h}/\overline{H}_h$	$\overline{H}_{d_h}$ (MJ/m²)	$\overline{R}$	$\overline{H}_T$ (MJ/m²)
Jan.	0.58	0.35	1.50	0.32	4.29	1.34	17.98
Feb.	0.52	0.35	1.30	0.41	5.86	1.17	16.78
Mar.	0.58	0.35	1.15	0.36	6.76	1.09	20.58
Apr.	0.56	0.35	1.00	0.37	7.67	1.00	20.70
May	0.68	0.35	0.88	0.27	7.21	0.92	24.48
June	0.67	0.35	0.84	0.28	7.51	0.89	23.83
July	0.64	0.35	0.84	0.30	7.63	0.89	22.64
Aug.	0.66	0.35	0.94	0.29	7.17	0.96	23.74
Sept.	0.65	0.35	1.08	0.29	6.44	1.06	23.52
Oct.	0.64	0.35	1.28	0.30	5.55	1.20	22.16
Nov.	0.62	0.35	1.46	0.28	4.21	1.33	20.07
Dec.	0.55	0.35	1.56	0.34	4.11	1.37	16.55

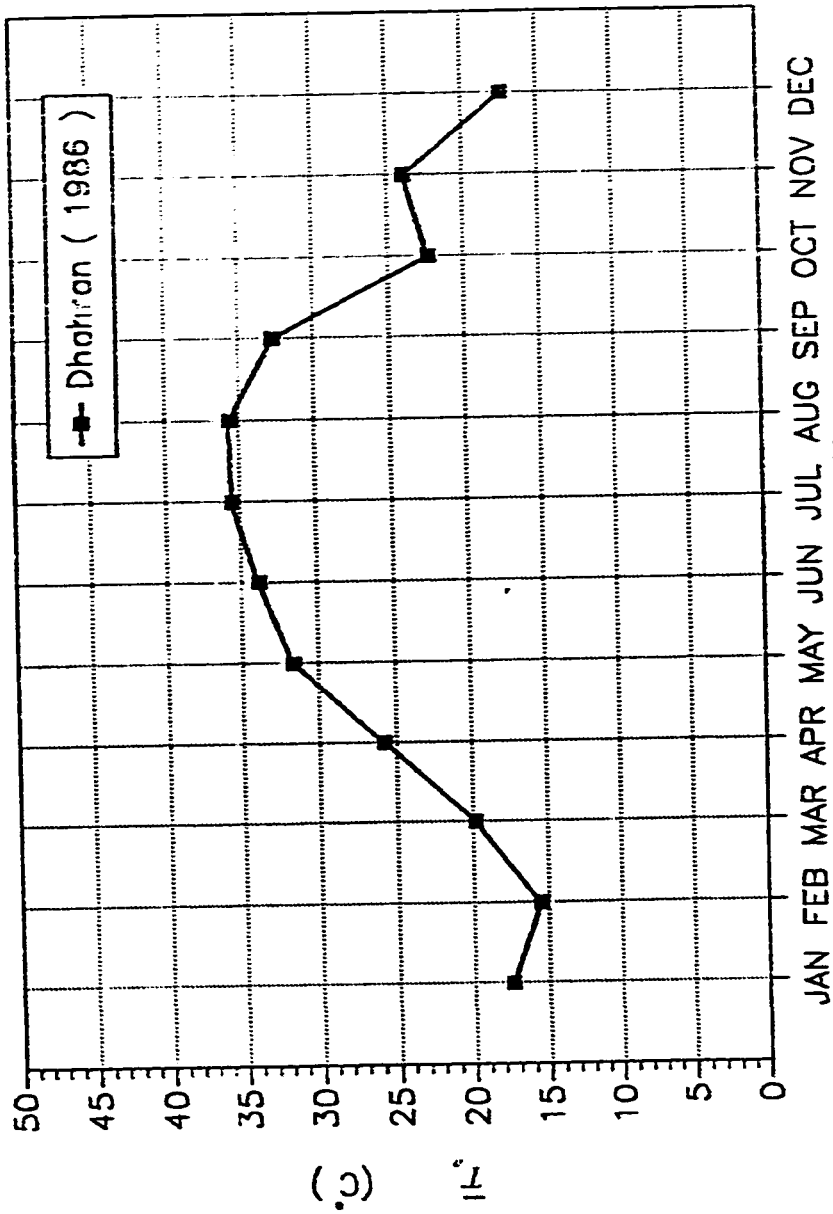

Figure (5.2) Monthly Average Daily Ambient Temperature [48]

Table (5.3) Solar Radiation at Dhahran (1986)

Month	Total Horz. Radn. Monthly Avg. Daily $\overline{H}_g$ (MJ/m^2)	Total Tilted Radn. Monthly Avg. Daily $\overline{H}_T$ (MJ/m^2)
Jan.	13.40	17.98
Feb.	14.30	16.78
Mar.	18.79	20.58
Apr.	20.72	20.70
May	26.72	24.48
June	26.83	23.83
July	25.42	22.64
Aug.	24.72	23.74
Sept.	22.19	23.52
Oct.	18.49	22.16
Nov.	15.04	20.07
Dec.	12.08	16.55

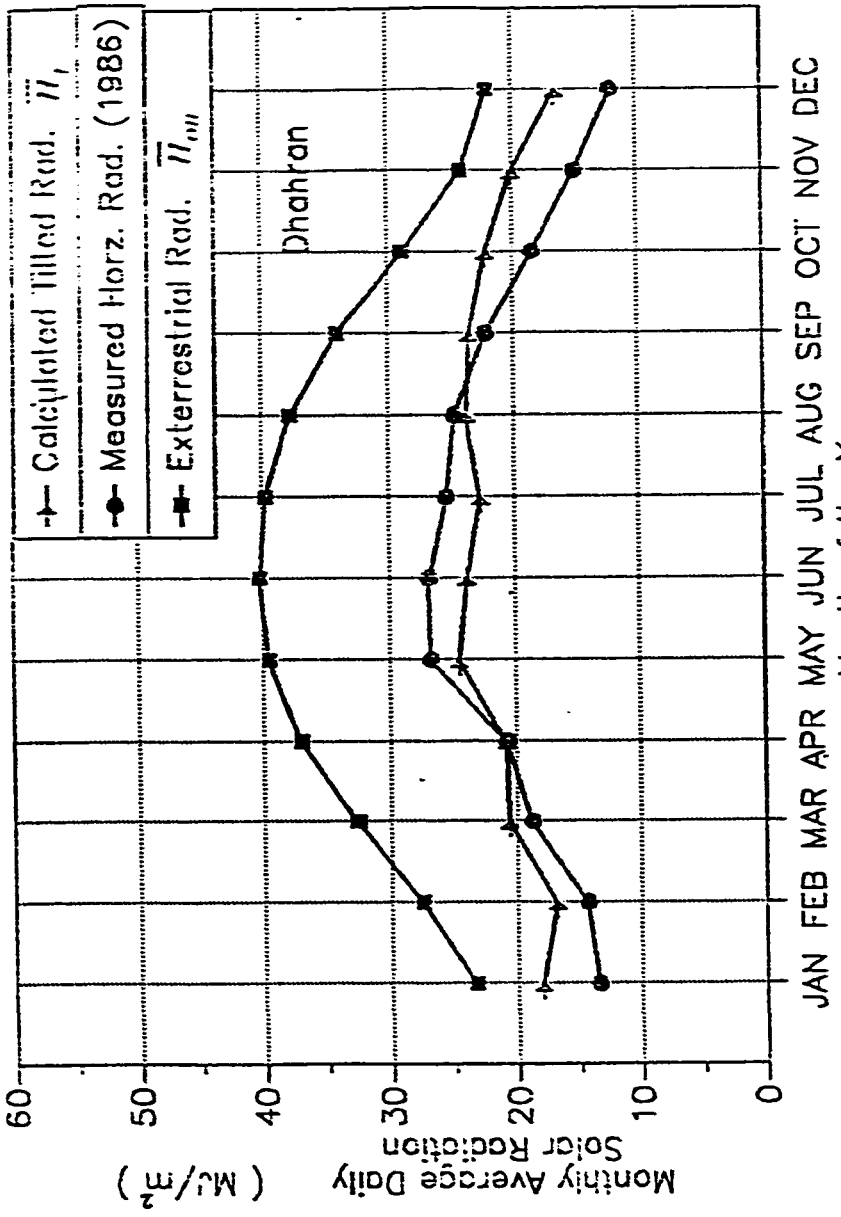

Figure (5.3) Monthly Average Daily Radiation

Calculation of the Monthly Average Hourly Radiation, $\bar{I}_T$

Values of $\bar{I}_T$ indicate the amount of radiation received on a tilted surface for the representative hours of the month (taken as that for average days of the months). These values can be averaged for the entire year so as to give a general idea of the solar radiation pattern on hourly basis.

General Procedure

1- Geometric factor of beam radiation, R_b for each hour of the average day is obtained as described in [29]. Then this step is repeated for each month.

2- The fractions r_t (hourly total radiation/daily total radiation) and r_d (hourly diffuse radiation/daily diffuse radiation) are obtained for each hour of the average day from figures in [29].

3- The values of $\bar{K}_T$, $\bar{H}_{OH}$, and $\frac{\bar{H}_{dH}}{H_H}$ are taken as those of daily data.

4- $\bar{I}_T$ is calculated for each hour using the relationship of the isotropic sky model [29]:

$$\bar{I}_T = \bar{K}_T \bar{H}_{OH} [(r_t - \frac{\bar{H}_{dH}}{H_H} r_d) \bar{R}_b + \bar{H}_{dh} r_d \frac{(1 + \cos\beta)}{2} + r_t \rho_g \frac{(1 - \cos\beta}{2})] \quad . \tag{5.3}$$

This procedure is performed and the results are shown in table (5.4). It should be noted from this table that the day is taken to be symmetrical around noon time. These values of $\bar{I}_T$ have been checked with some actual data and the result was found to be satisfactory (maximum difference was found to be 8%). Also, these calculated values can be averaged over the entire year. The result of this averaging is shown in table (5.5). It is interesting to note that the availability of solar power in Dhahran area is about 42% of the time.

Table (5.4) Monthly Average Hourly Solar Radiation Incident on a Tilted Surface

(*Dhahran*, $\phi = \beta = 26.13°N$)

January

Hour (Solar Time)	Hours From Noon	R_b	r_t	r_d	$\bar{I}_T$ (MJ/m^2)
12-1 P.M. [11-12 A.M.]	0.5	1.37	0.154	0.146	2.620
1-2 P.M. [10-11 A.M.]	1.5	1.40	0.138	0.132	2.385
2-3 P.M. [9-10 A.M.]	2.5	1.46	0.108	0.109	1.914
3-4 P.M. [8-9 A.M.]	3.5	1.60	0.068	0.078	1.266
4-5 P.M. [7-8 A.M.]	4.5	2.18	0.027	0.038	0.599

February

Hour (Solar Time)	Hours From Noon	R_b	r_t	r_d	$\bar{I}_T$ (MJ/m^2)
12-1 P.M. [11-12 A.M.]	0.5	1.26	0.152	0.139	2.519
1-2 P.M. [10-11 A.M.]	1.5	1.27	0.135	0.130	2.237
2-3 P.M. [9-10 A.M.]	2.5	1.30	0.107	0.108	1.790
3-4 P.M. [8-9 A.M.]	3.5	1.37	0.070	0.078	1.194
4-5 P.M. [7-8 A.M.]	4.5	1.59	0.033	0.042	0.600

Cont. Table (5.4) Monthly Average Hourly Solar Radiation Incident on a Tilted Surface

(*Dhahran*, $\phi = \beta = 26.13°N$)

March

Hour (Solar Time)	Hours From Noon	R_b	r_t	r_d	$\bar{I}_T$ (MJ/m^2)
12-1 P.M. [11-12 A.M.]	0.5	1.140	0.143	0.130	2.960
1-2 P.M. [10-11 A.M.]	1.5	1.140	0.130	0.122	2.687
2-3 P.M. [9-10 A.M.]	2.5	1.143	0.106	0.106	2.186
3-4 P.M. [8-9 A.M.]	3.5	1.153	0.073	0.080	1.505
4-5 P.M. [7-8 A.M.]	4.5	1.180	0.039	0.050	0.805

April

Hour (Solar Time)	Hours From Noon	R_b	r_t	r_d	$\bar{I}_T$ (MJ/m^2)
12-1 P.M. [11-12 A.M.]	0.5	1.03	0.134	0.124	2.832
1-2 P.M. [10-11 A.M.]	1.5	1.02	0.124	0.118	2.6017
2-3 P.M. [9-10 A.M.]	2.5	1.01	0.102	0.102	2.1241
3-4 P.M. [8-9 A.M.]	3.5	0.98	0.075	0.080	1.5313
4-5 P.M. [7-8 A.M.]	4.5	0.92	0.045	0.052	0.8858
5-6 P.M. [6-7 A.M.]	5.5	0.69	0.018	0.024	0.31159

Cont. Table (5.4) Monthly Average Hourly Solar Radiation Incident on a Tilted Surface

(Dhahran, $\phi = \beta = 26.13°N$)

May

Hour (Solar Time)	Hours From Noon	R_b	r_t	r_d	$\bar{I}_T$ (MJ/m^2)
12-1 P.M. [11-12 A.M.]	0.5	0.95	0.129	0.118	3.3486
1-2 P.M. [10-11 A.M.]	1.5	0.94	0.119	0.112	3.0652
2-3 P.M. [9-10 A.M.]	2.5	0.92	0.100	0.099	2.5368
3-4 P.M. [8-9 A.M.]	3.5	0.87	0.076	0.079	1.8554
4-5 P.M. [7-8 A.M.]	4.5	0.78	0.049	0.057	1.1186
5-6 P.M. [6-7 A.M.]	5.5	0.49	0.023	0.030	0.4131

June

Hour (Solar Time)	Hours From Noon	R_b	r_t	r_d	$\bar{I}_T$ (MJ/m^2)
12-1 P.M. [11-12 A.M.]	0.5	0.92	0.127	0.117	3.2330
1-2 P.M. [10-11 A.M.]	1.5	0.91	0.117	0.111	2.9560
2-3 P.M. [9-10 A.M.]	2.5	0.88	0.099	0.098	2.4446
3-4 P.M. [8-9 A.M.]	3.5	0.83	0.077	0.079	1.8289
4-5 P.M. [7-8 A.M.]	4.5	0.72	0.050	0.058	1.0936
5-6 P.M. [6-7 A.M.]	5.5	0.43	0.026	0.032	0.4388

Cont. Table (5.4) Monthly Average Hourly Solar Radiation Incident on a Tilted Surface

(Dhahran, $\phi = \beta = 26.13°N$)

July

Hour (Solar Time)	Hours From Noon	R_b	r_t	r_d	$\bar{I}_T$ (MJ/m^2)
12-1 P.M. [11-12 A.M.]	0.5	0.94	0.128	0.118	3.1210
1-2 P.M. [10-11 A.M.]	1.5	0.92	0.118	0.112	2.8346
2-3 P.M. [9-10 A.M.]	2.5	0.90	0.100	0.099	2.3674
3-4 P.M. [8-9 A.M.]	3.5	0.85	0.076	0.079	1.7342
4-5 P.M. [7-8 A.M.]	4.5	0.75	0.049	0.057	1.6277
5-6 P.M. [6-7 A.M.]	5.5	0.46	0.025	0.030	0.4151

August

Hour (Solar Time)	Hours From Noon	R_b	r_t	r_d	$\bar{I}_T$ (MJ/m^2)
12-1 P.M. [11-12 A.M.]	0.5	1.00	0.132	0.121	3.2987
1-2 P.M. [10-11 A.M.]	1.5	0.99	0.122	0.113	2.9371
2-3 P.M. [9-10 A.M.]	2.5	0.97	0.102	0.100	2.4921
3-4 P.M. [8-9 A.M.]	3.5	0.94	0.075	0.080	1.7928
4-5 P.M. [7-8 A.M.]	4.5	0.86	0.048	0.056	1.0845
5-6 P.M. [6-7 A.M.]	5.5	0.59	0.020	0.028	0.3750

Cont. Table (5.4)Monthly Average Hourly Solar Radiation Incident on a Tilted Surface

(Dhahran, $\phi = \beta = 26.13°N$)

September

Hour (Solar Time)	Hours From Noon	R_b	r_t	r_d	$\bar{I}_T$ (MJ/m^2)
12-1 P.M. [11-12 A.M.]	0.5	1.10	0.139	0.130	3.3014
1-2 P.M. [10-11 A.M.]	1.5	1.09	0.127	0.121	2.9940
2-3 P.M. [9-10 A.M.]	2.5	1.09	0.105	0.103	2.4727
3-4 P.M. [8-9 A.M.]	3.5	1.09	0.074	0.080	1.7360
4-5 P.M. [7-8 A.M.]	4.5	1.07	0.042	0.052	0.9675
5-6 P.M. [6-7 A.M.]	5.5	0.99	0.013	0.018	0.2842

October

Hour (Solar Time)	Hours From Noon	R_b	r_t	r_d	$\bar{I}_T$ (MJ/m^2)
12-1 P.M. [11-12 A.M.]	0.5	1.22	0.147	0.136	3.1514
1-2 P.M. [10-11 A.M.]	1.5	1.23	0.132	0.128	2.8383
2-3 P.M. [9-10 A.M.]	2.5	1.25	0.106	0.108	2.2982
3-4 P.M. [8-9 A.M.]	3.5	1.30	0.071	0.079	1.5719
4-5 P.M. [7-8 A.M.]	4.5	1.44	0.035	0.045	0.8186

Cont. Table (5.4) Monthly Average Hourly Solar Radiation Incident on a Tilted Surface

(*Dhahran*, $\phi = \beta = 26.13°N$)

November

Hour (Solar Time)	Hours From Noon	R_b	r_c	r_d	$\bar{I}_T$ (MJ/m^2)
12-1 P.M. [11-12 A.M.]	0.5	1.34	0.155	0.145	2.9101
1-2 P.M. [10-11 A.M.]	1.5	1.36	0.138	0.132	2.6164
2-3 P.M. [9-10 A.M.]	2.5	1.42	0.108	0.109	2.1073
3-4 P.M. [8-9 A.M.]	3.5	1.54	0.068	0.078	1.3912
4-5 P.M. [7-8 A.M.]	4.5	2.00	0.028	0.038	0.6777

December

Hour (Solar Time)	Hours From Noon	R_b	r_c	r_d	$\bar{I}_T$ (MJ/m^2)
12-1 P.M. [11-12 A.M.]	0.5	1.41	0.159	0.148	2.4642
1-2 P.M. [10-11 A.M.]	1.5	1.44	0.139	0.134	2.1794
2-3 P.M. [9-10 A.M.]	2.5	1.51	0.108	0.110	1.7412
3-4 P.M. [8-9 A.M.]	3.5	1.70	0.068	0.077	1.1745
4-5 P.M. [7-8 A.M.]	4.5	2.46	0.028	0.033	0.6338

Table (5.5) Yearly Average Hourly Solar Radiation Incident on a Tilted Surface (Typical Year 1986)

Mid-Hour (Solar Time)	$\overline{I}_T$ (W/m^2)
6:30 A.M.	103.6
7:30	252.6
8:30	430.1
9:30	612.8
10:30	748.4
11:30	827.8
12:30 P.M.	827.8
1:30	748.4
2:30	612.8
3:30	430.1
4:30	252.6
5:30	103.6

5.2 Wind Energy

5.2.1 Wind Speed

Monthly average values of wind speed (1986) for Dhahran area are shown in table (5.6) [48]. This table shows that the maximum wind speed is 6.97 *m/s* in the month of June, whereas the minimum value is 4.31 *m/s* in the month of October. the annual mean value is calculated to be 5.70 *m/s* (year 1986). According to [12,49] detailed investigation of wind data has been done, it was found that the annual mean wind speed is 4.50 *m/s* (Dhahran,1970-1984).

5.2.2 Wind Power

The mean attainable wind power for Dhahran area is 70.6W/m^2. The availability of wind power in this area is 55% of the time (this piece of information is based on a fourteen-year metrological data) [12,49].

Table (5.6) Meteorological Data , Dhahran (1986) [48]

Month	Wind Speed $\overline{V_w}$ (m/s)
Jan.	5.69
Feb.	5.47
Mar.	6.861
Apr.	5.28
May.	6.750
June	6.972
July	5.611
Aug.	5.611
Sept.	4.833
Oct.	4.306
Nov.	5.67
Dec.	5.44

5.3 Comparison Between Solar and Wind Power for Desalination purposes

Based on previous analysis of estimating the solar and wind power in Dhahran, it is very useful to compare them from different prospective.

5.3.1 Hourly Basis Comparison

Profiles of solar and wind power in Dhahran are compared on hourly basis as shown in figure (5.4). As can be noticed from this figure that the maximum amounts of solar and wind power are available between 12-2 p.m. The availability of wind power in this area is 55% while the availability of solar power is 42% [12].

5.3.2 Monthly Basis Comparison

Figure (5.5) shows that the falling solar power in Dhahran is much higher than the available wind power (maximum difference is 225 W/m^2 in the month of September). The maximum available solar power is occurring in the month of July while the one for wind power is occurring in the month of June.

5.3.3 Comparison Between Producible Solar and Wind Power

Several devices are used to convert solar and wind power into useful heat and electrical power. For the sake of comparison the following devices are selected:

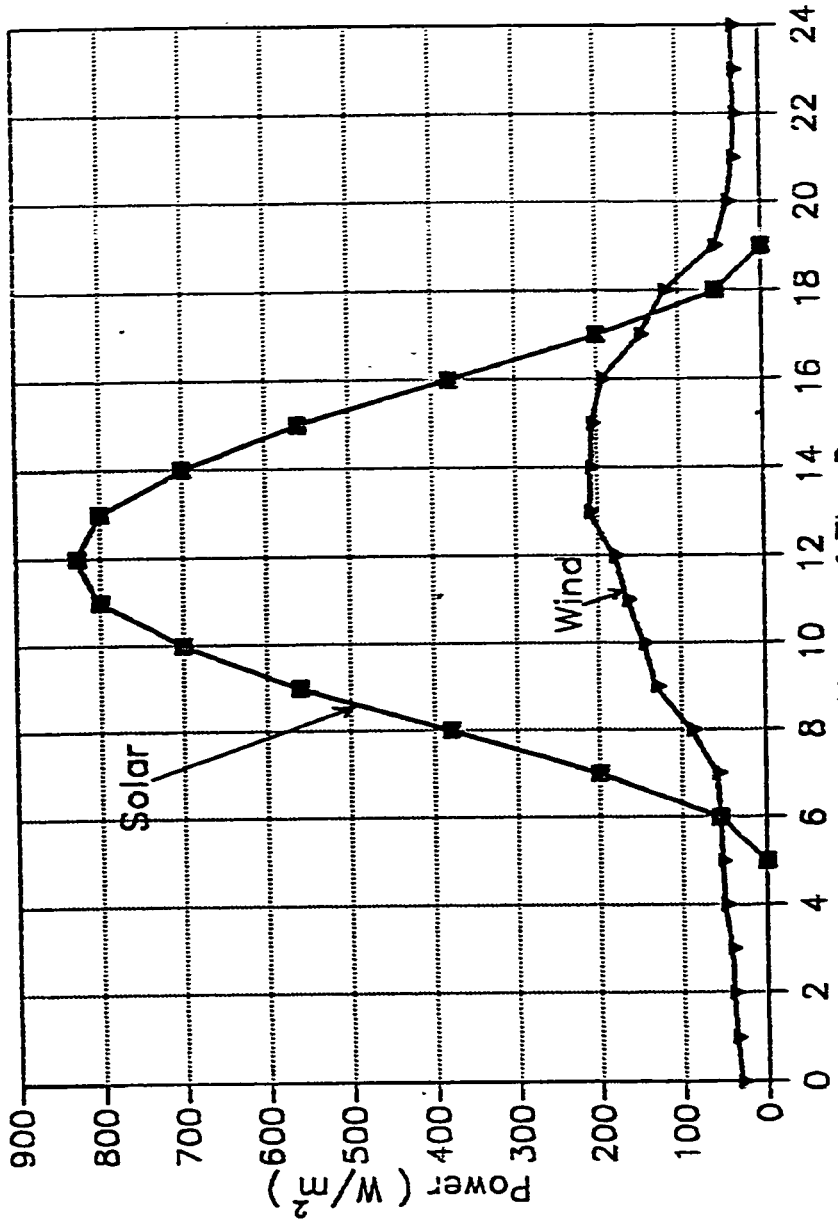

Figure (5.4) Diurnal Solar and Wind Power Profiles

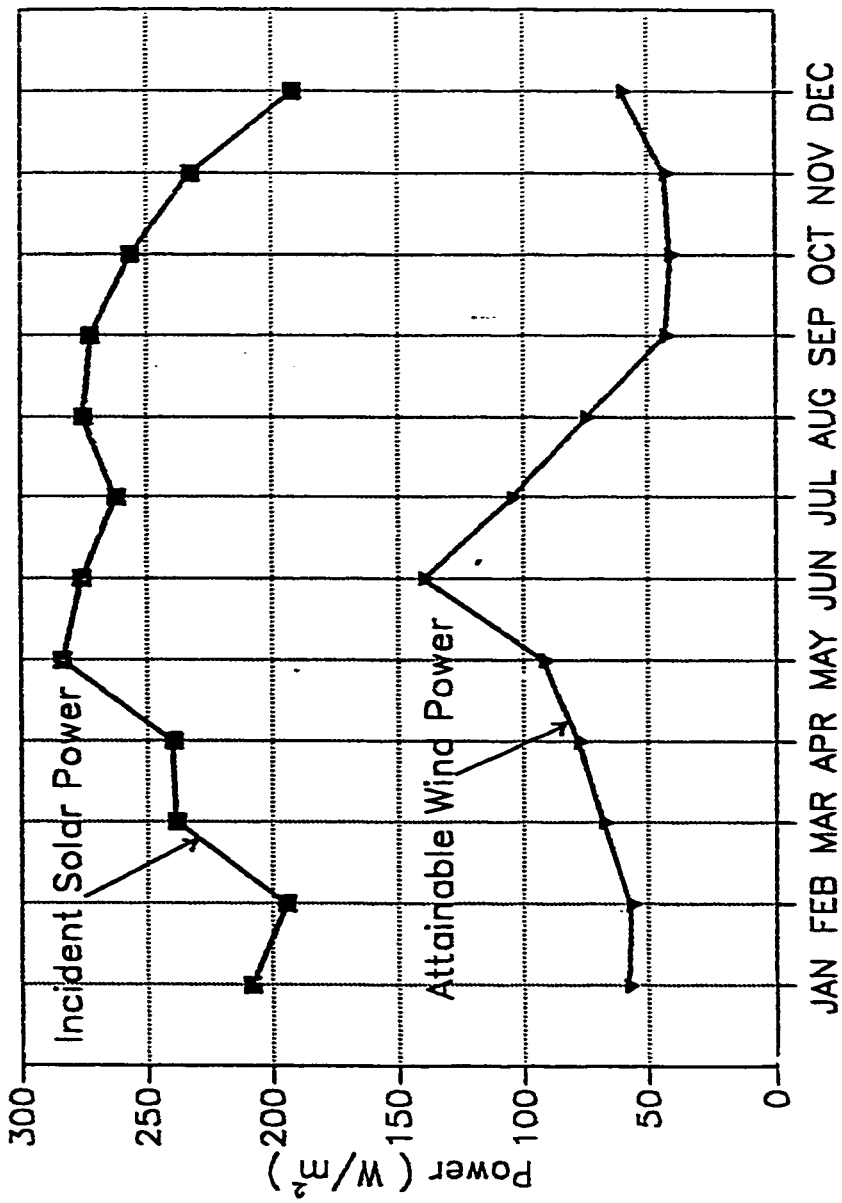

Figure (5.5) Monthly Average Daily Solar and Wind Power

1- Flat plate solar collector. FPSC (average conversion efficiency, η_{FP} = 25 %). This device is used to convert solar energy into heat.

2- Evacuated tube solar collector, ESC (average efficiency, η_{ESC} = 60 %). This device is used to convert solar energy into heat.

3- Photovoltaic solar collector, PV (average efficiency, η_{PV} = 9 %). This device is used to convert solar energy into electrical power.

4- Wind energy convertor, WEC (average coefficient power, C_p = 0.4). This device is used to convert wind power into electrical power.

5- Photovoltaic -water pumping system. PV-Pump (average efficiency, $\eta_{PV\text{-}Pump}$ = 7.2 %). This system is used to convert solar energy into electrical power by means of PV and then to mechanical pumping power by means of a pump having average efficiency = η_{pump} = 80 %.

6- WEC-water pumping system, WEC-Pump ($\eta_{WEC\text{-}Pump}$ = 52 %). This system is used to convert wind power into electrical power by means of WEC and then to mechanical pumping power by means of a pump having efficiency = η_{pump} = 80 %.

Using these average energy-convertors efficiency values, the associated power (either heat or electrical) for each of such devices is calculated. For the sake of illustration suppose that the falling solar power on the PV system is 800 W/m^2, this gives producible power equals 800 times 0.09, thus equals 72 W/m^2.

Similarly, for attainable wind power equals to 120 W/m^2, the resulting producible power by the WEC would be 48 W/m^2. Comparison of various power conversion systems (on monthly basis) is made as illustrated in figure (5.6). Comparison of various energy conversion systems and the resulting power profiles on monthly and hourly basis is shown in figures (5.7) and (5.8) respectively. The power produced from WEC on monthly and hourly basis is illustrated in figures (5.9) and (5.10).

Electrical power produced by WEC is much higher than that produced by the PV as illustrated in figures (5.11), (5.12), and (5.13).

5.3.4 Solar/Wind-Powered Reverse Osmosis

As discussed in previous chapters that reverse osmosis process requires electrical/mechanical (pumping) power for its operation. Figures (4.14) and (5.15) illustrate and compare the useful available electrical power (Dhahran climatic conditions) produced by WEC and that produced by PV required to operate a reverse osmosis unit.

5.3.5 Solar/Wind-Powered Electrodialysis

Electrodialysis (ED) is another desalination process requiring electrical power for its operation. It is based on the principle that salts dissolved in water are ionic in nature and saline solutions are mild electrolytes. Suppose these ions are subjected to an electrical field by means of two electrodes, with a continuous DC potential difference applied between them. The cations (positive ions) will

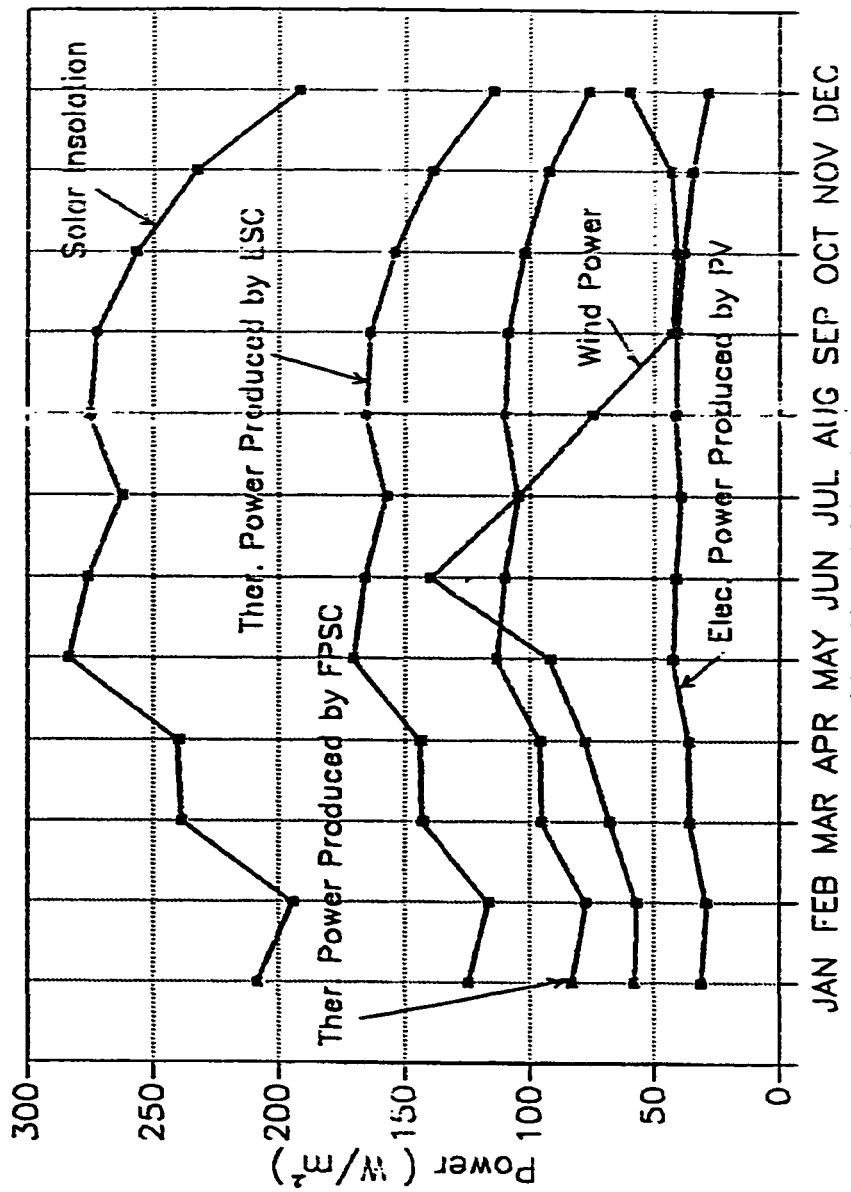

Figure (5.6) Power Profiles of Various Power Conversion Systems

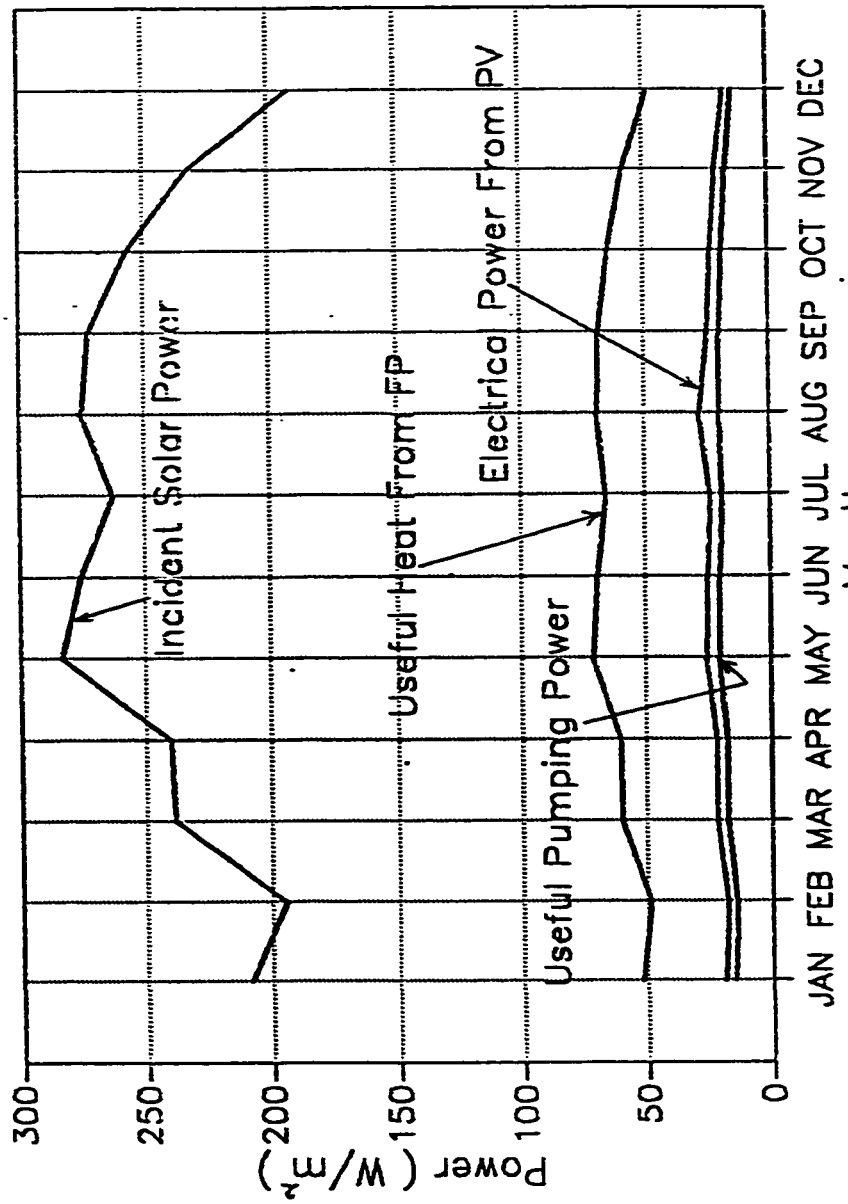

Figure (5.7) Monthly Average Daily Solar Power Profiles

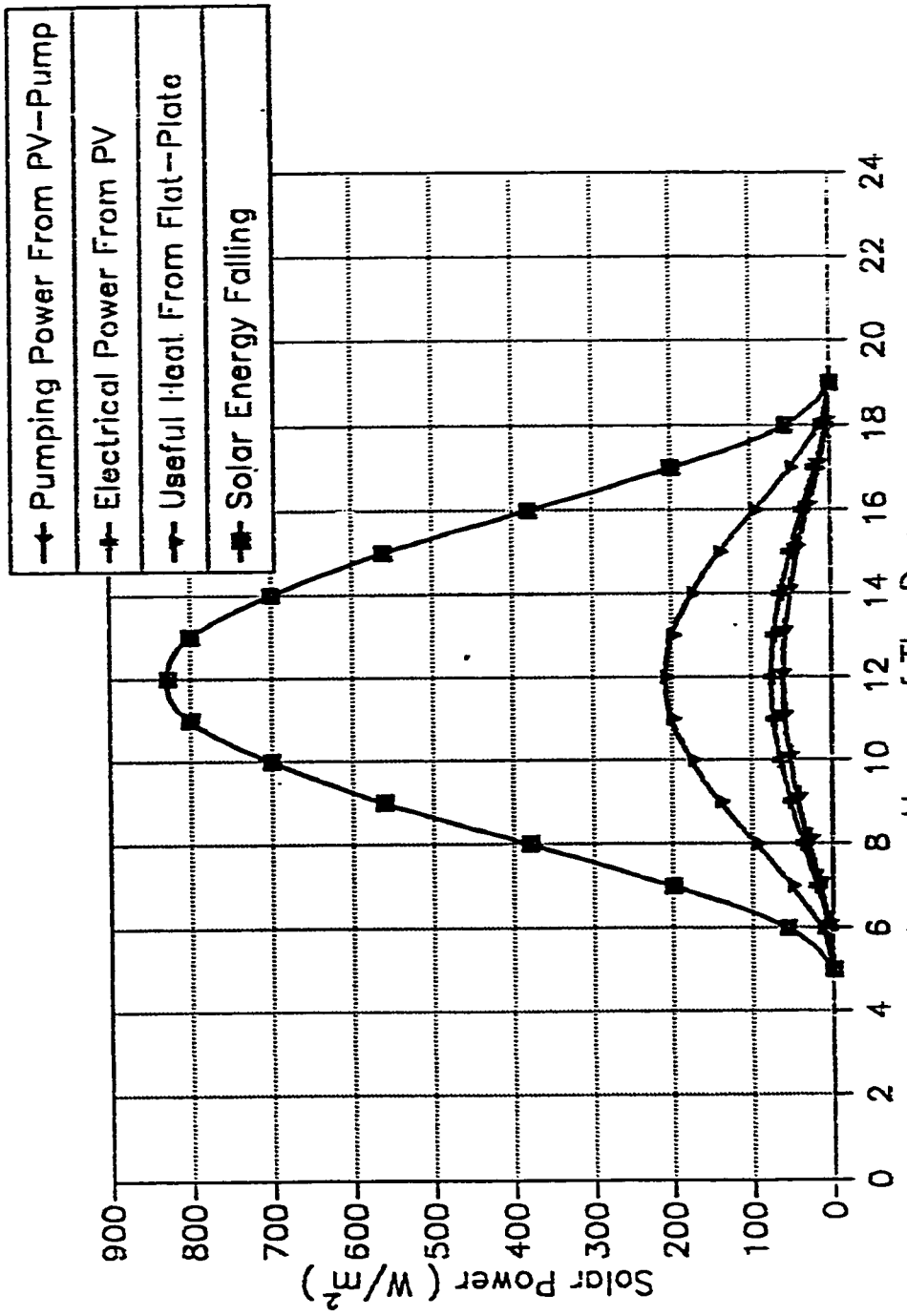

Figure (5.8) Diurnal Solar Power Profiles

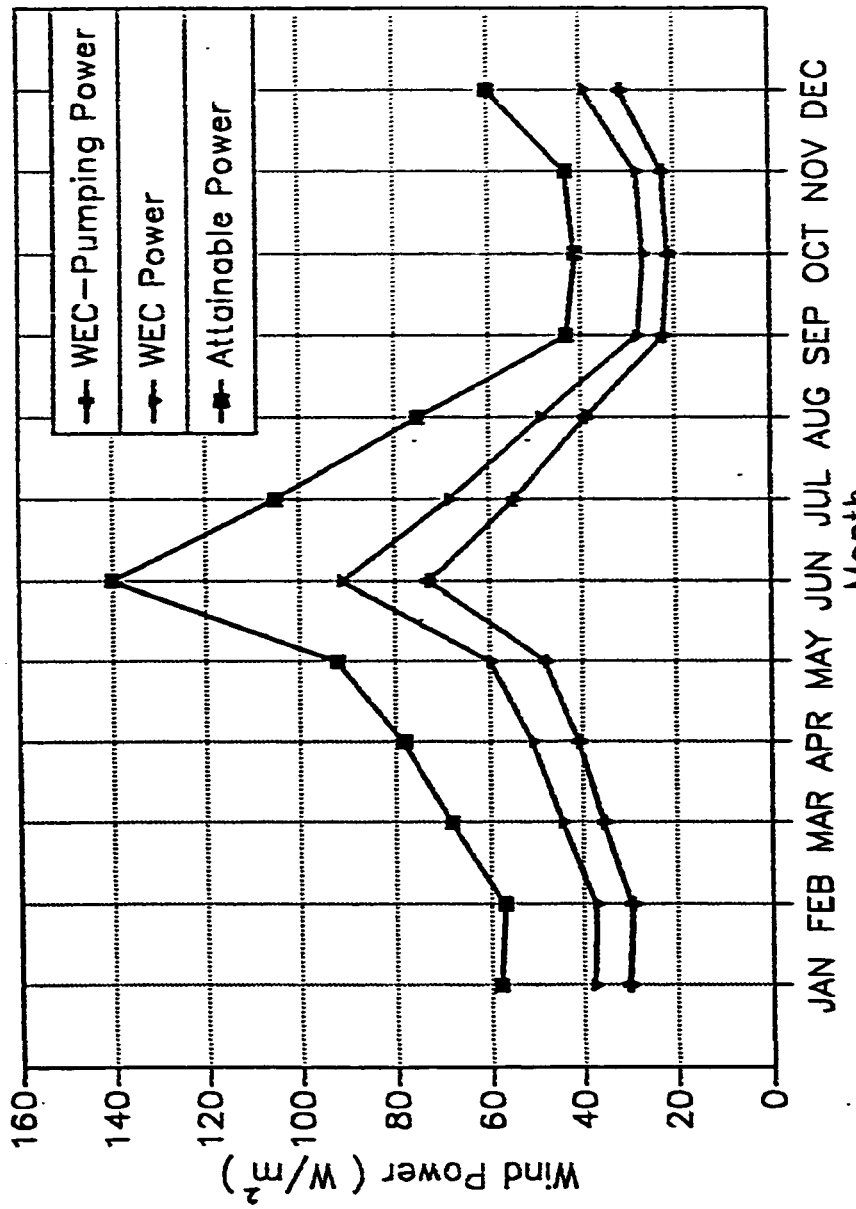

Figure (5.9) Monthly Average Daily Wind Power Profiles

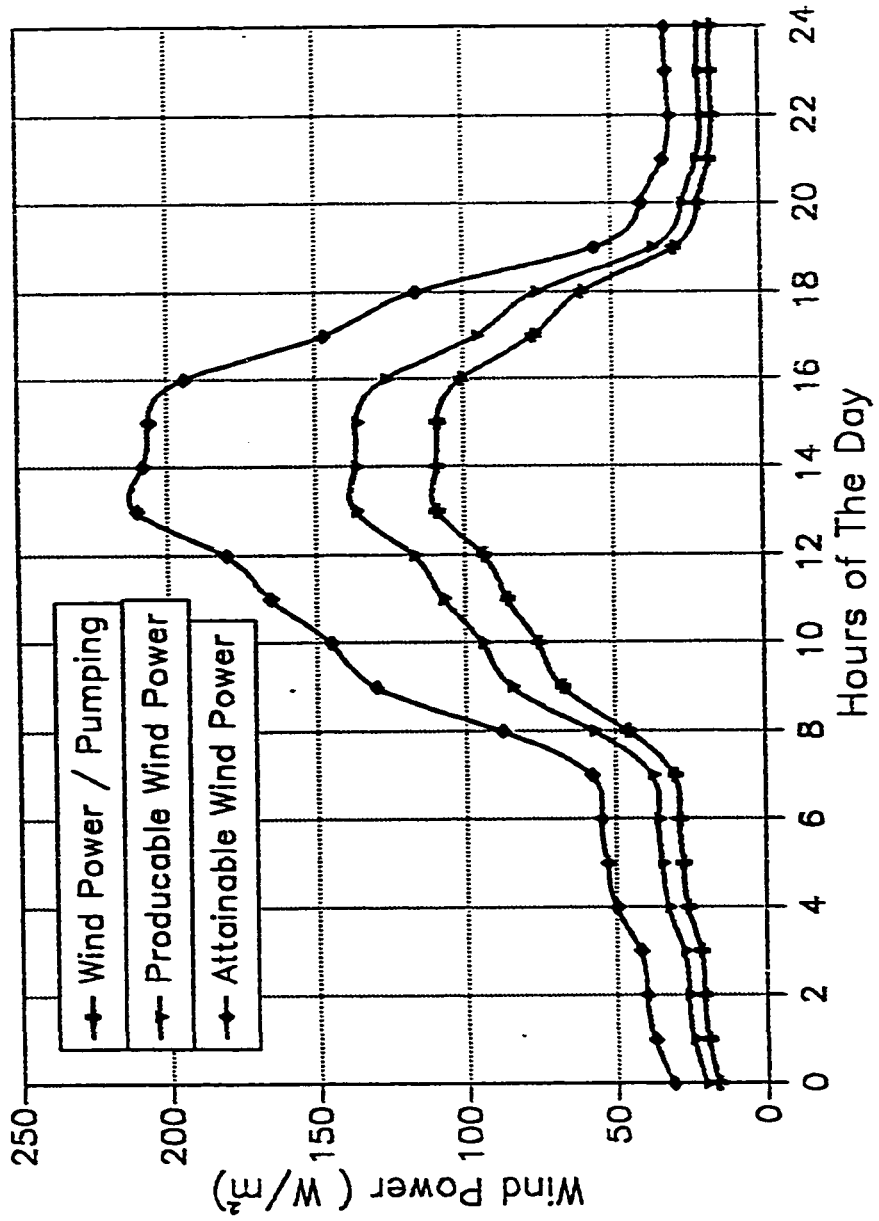

Figure (5.10) Diurnal Wind Power Profiles

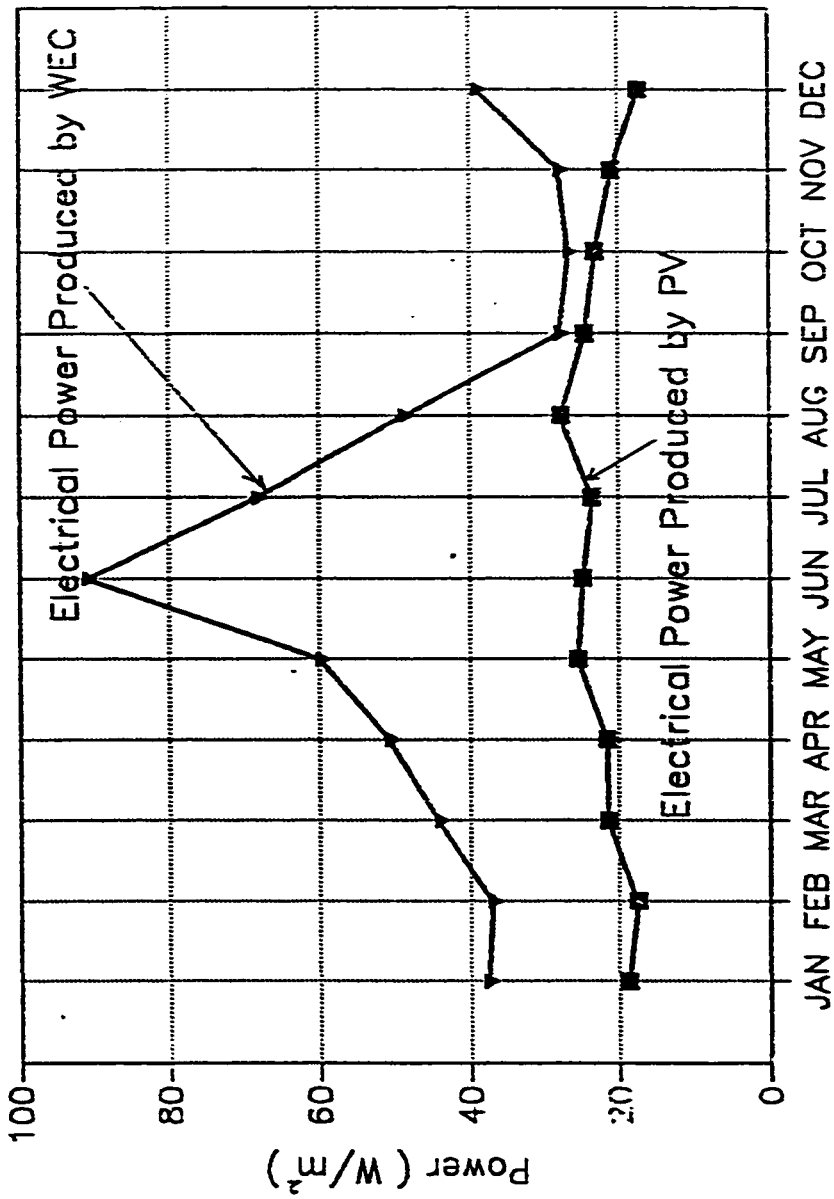

Figure (5.11) Monthly Average Daily Convertable Electrical Power

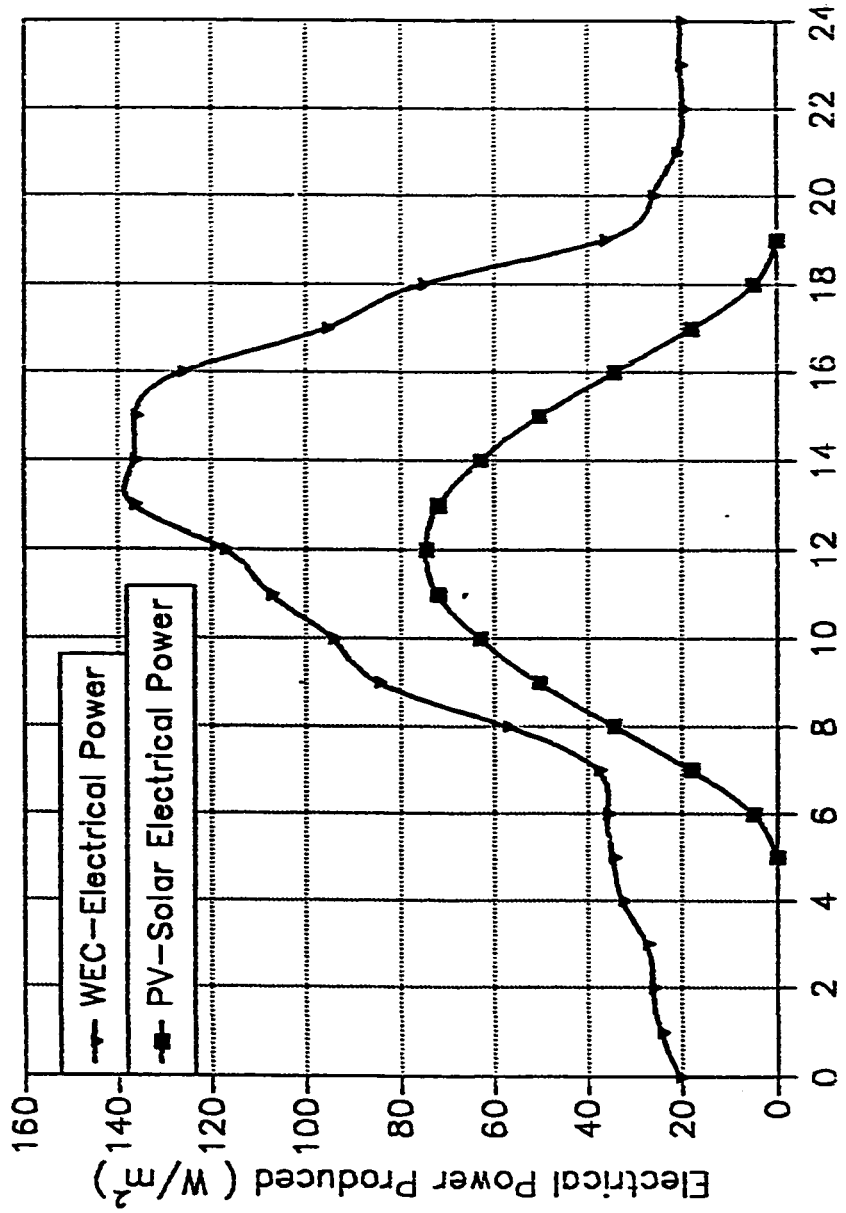

Figure (5.12) Electrical Power Produced by Typical PV and WEC

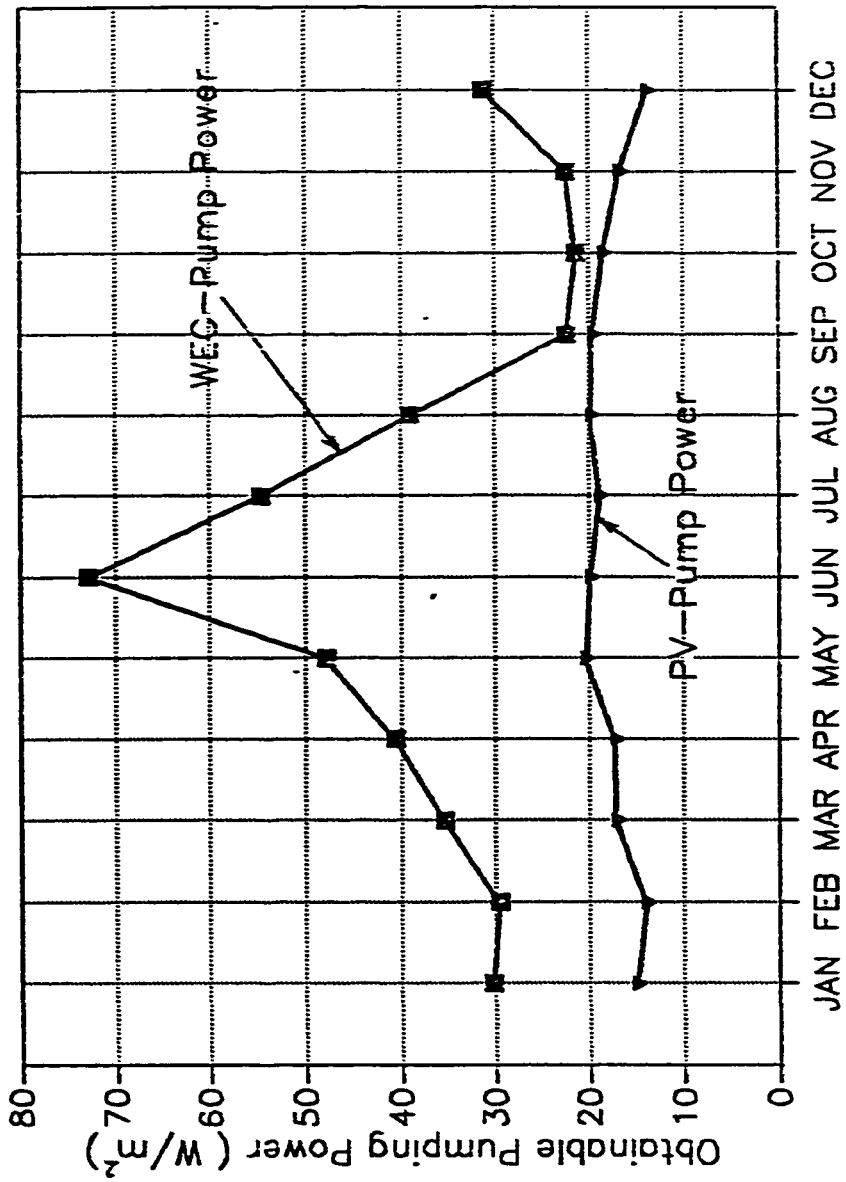

Figure (5.13) Monthly Average Daily Obtainable Pumping Power

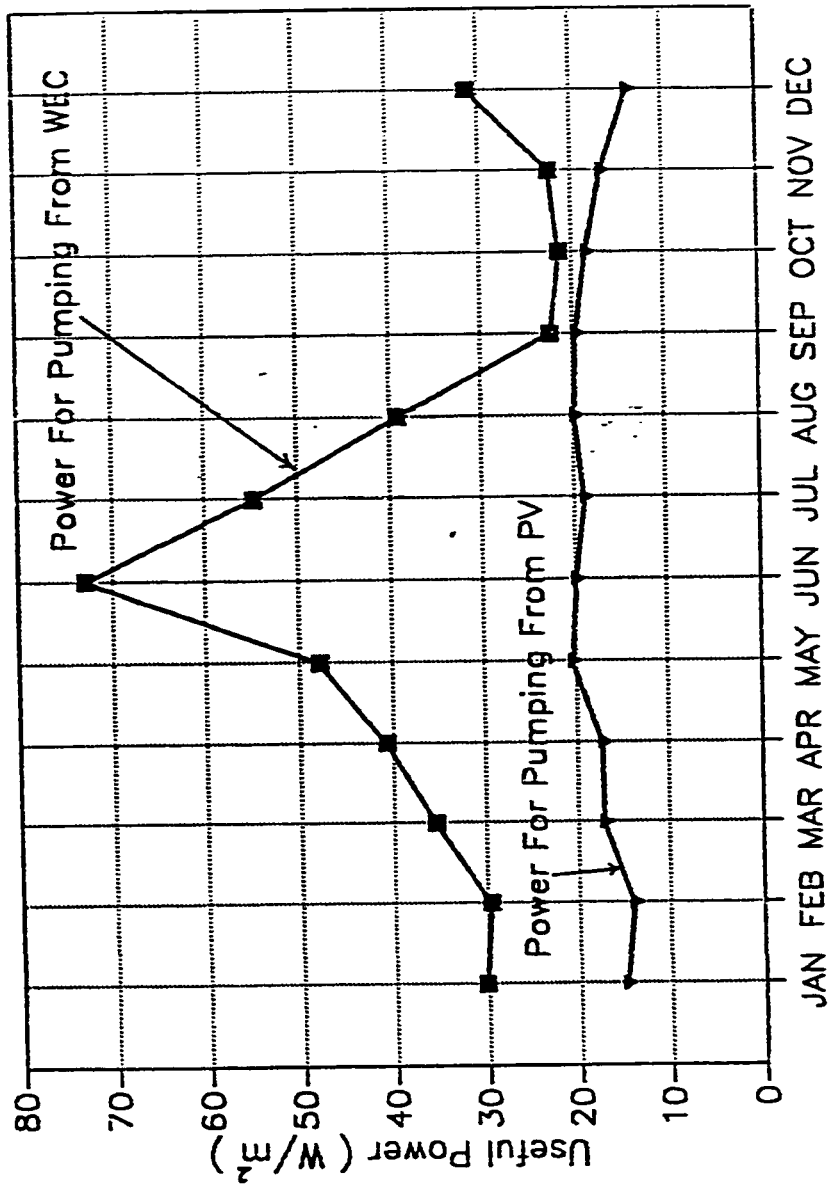

Figure (5.14) Useful Available Power Required for RO Desalination Unit

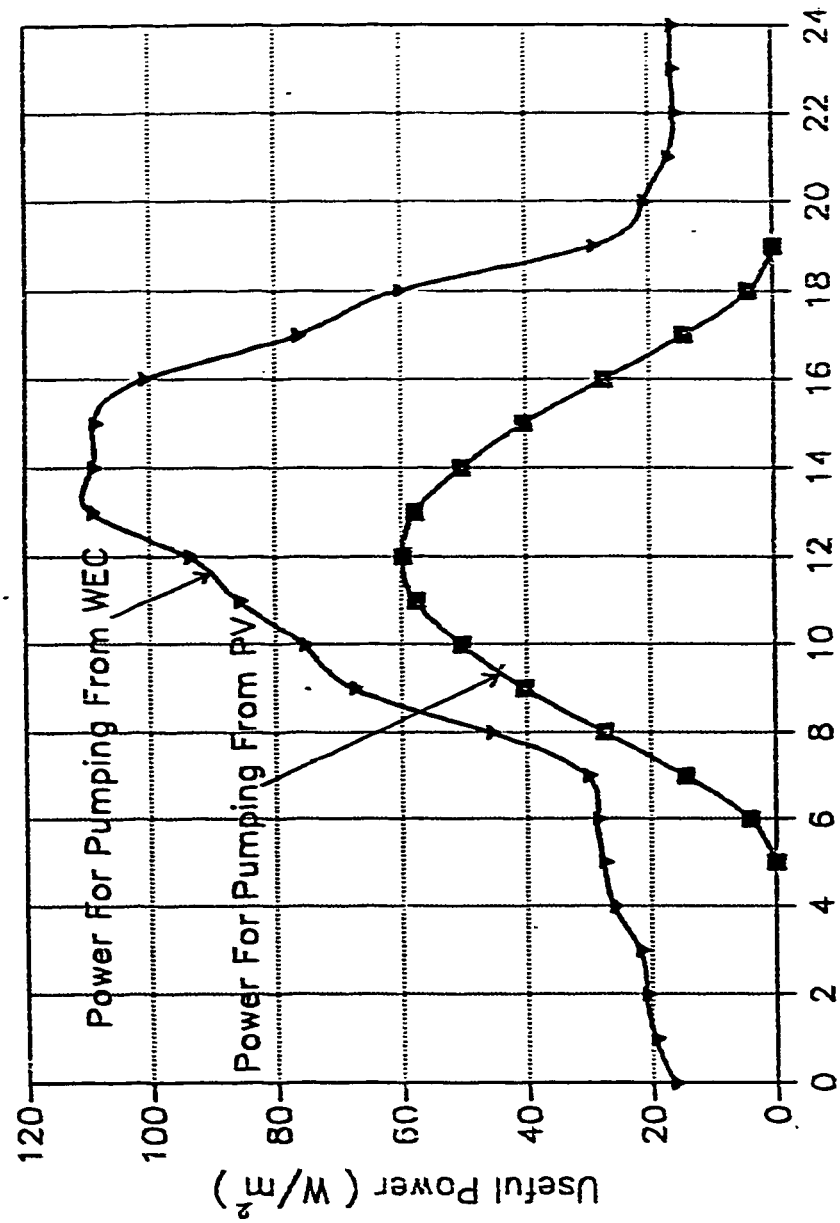

Figure (5.15) Useful Available Power Required for RO Desalination Unit

migrate to the cathode (negative electrode) and anions (negative ions) will migrate to the anode (positive electrode).

The useful available electrical power produced by WEC and that produced by PV are compared in figures (5.16) and (5.17) for the operation of an ED unit.

5.3.6 Solar/Wind-Powered MSF and MES

Multistage flash (MSF) and multieffect stack (MES) are two distillation processes requiring thermal energy (for heating purpose) and electrical power (for pumping purpose). Producible available power needed for such processes is shown in figures (5.18) and (5.19).

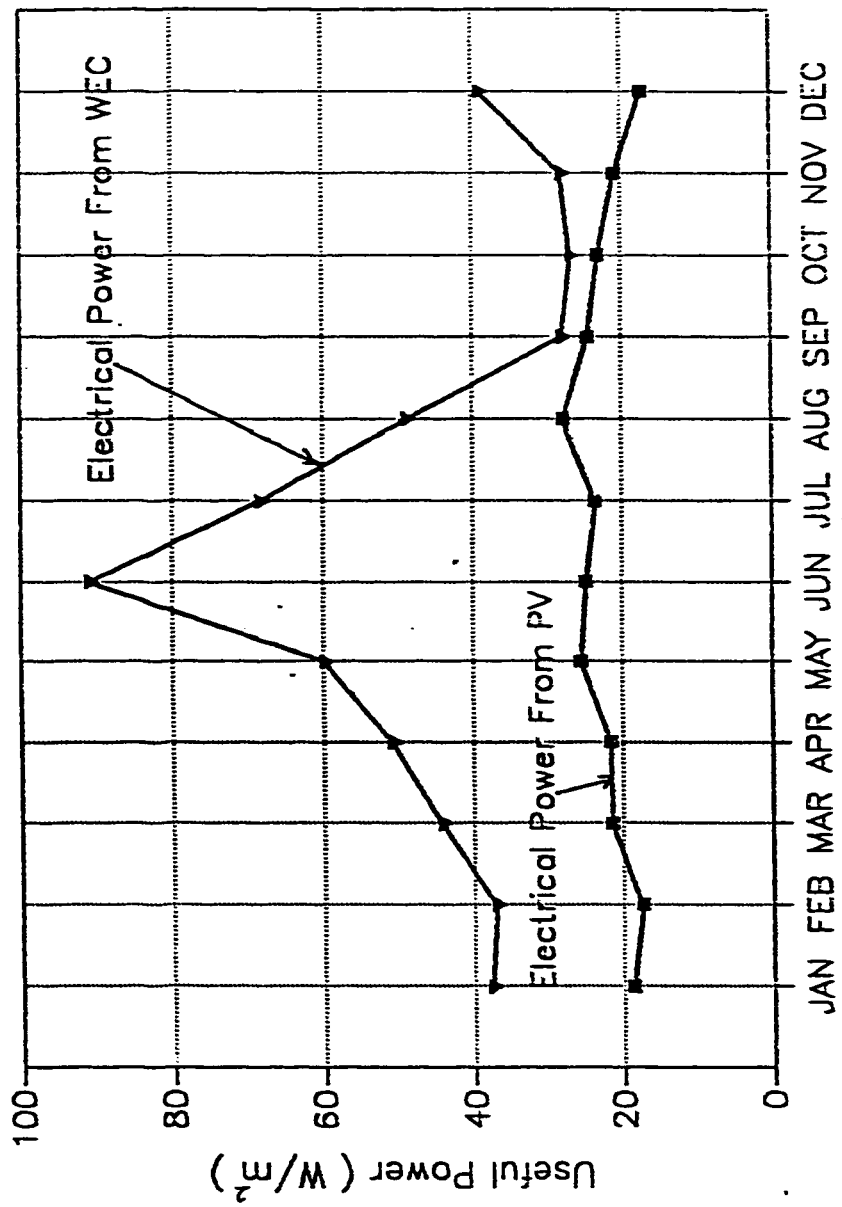

Figure (5.16) Useful Available Power Required for ED Desalination Unit

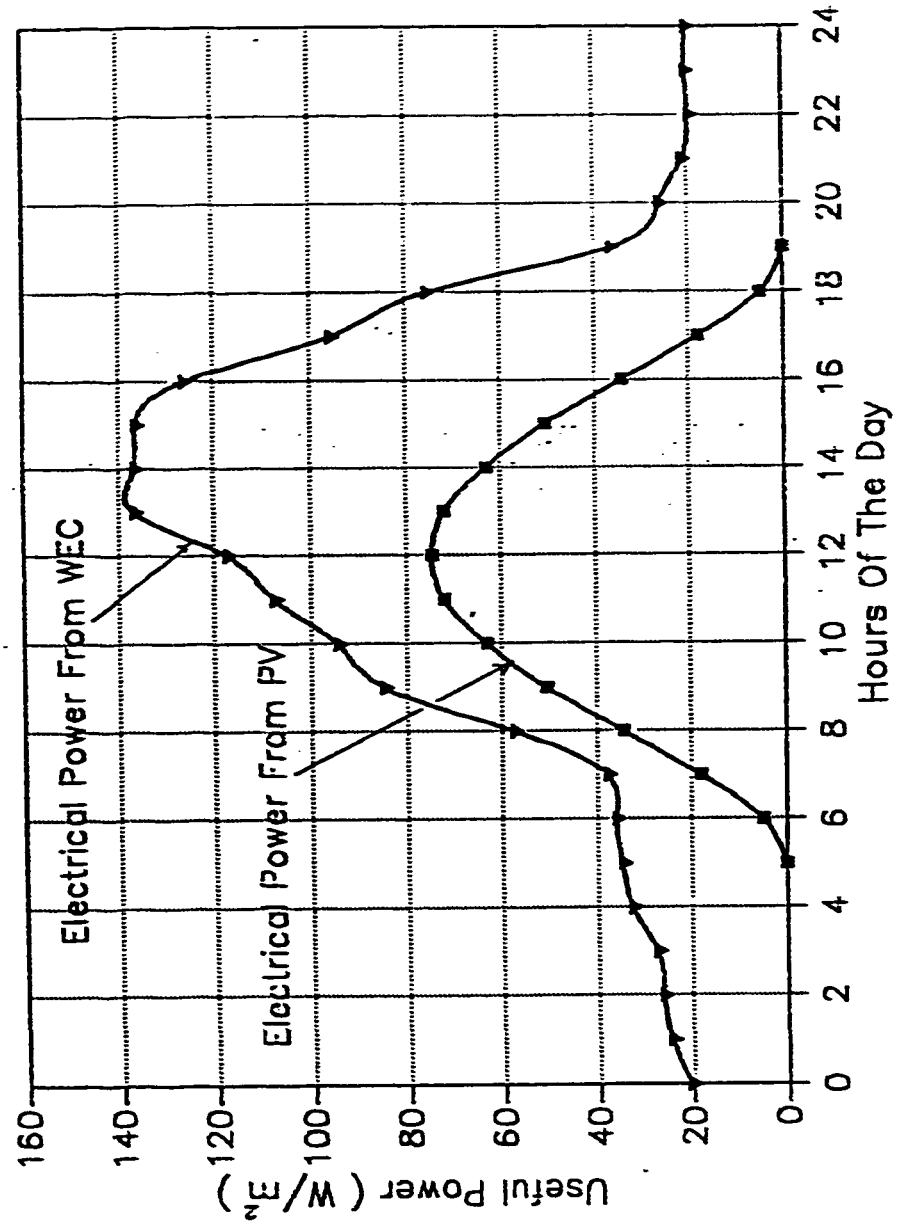

Figure (5.17) Useful Available Power Required for ED Desalination Unit

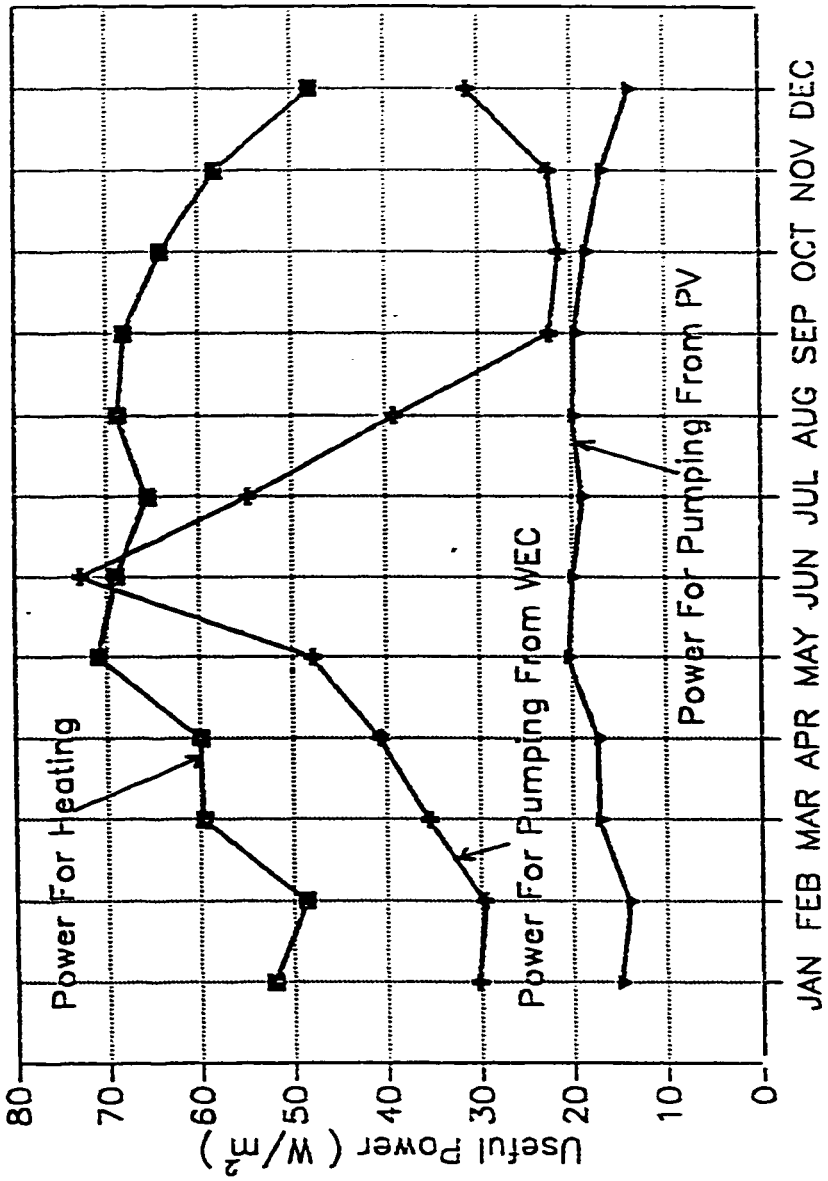

Figure (5.18) Useful Power Required for MSF and MES Distillation Unit

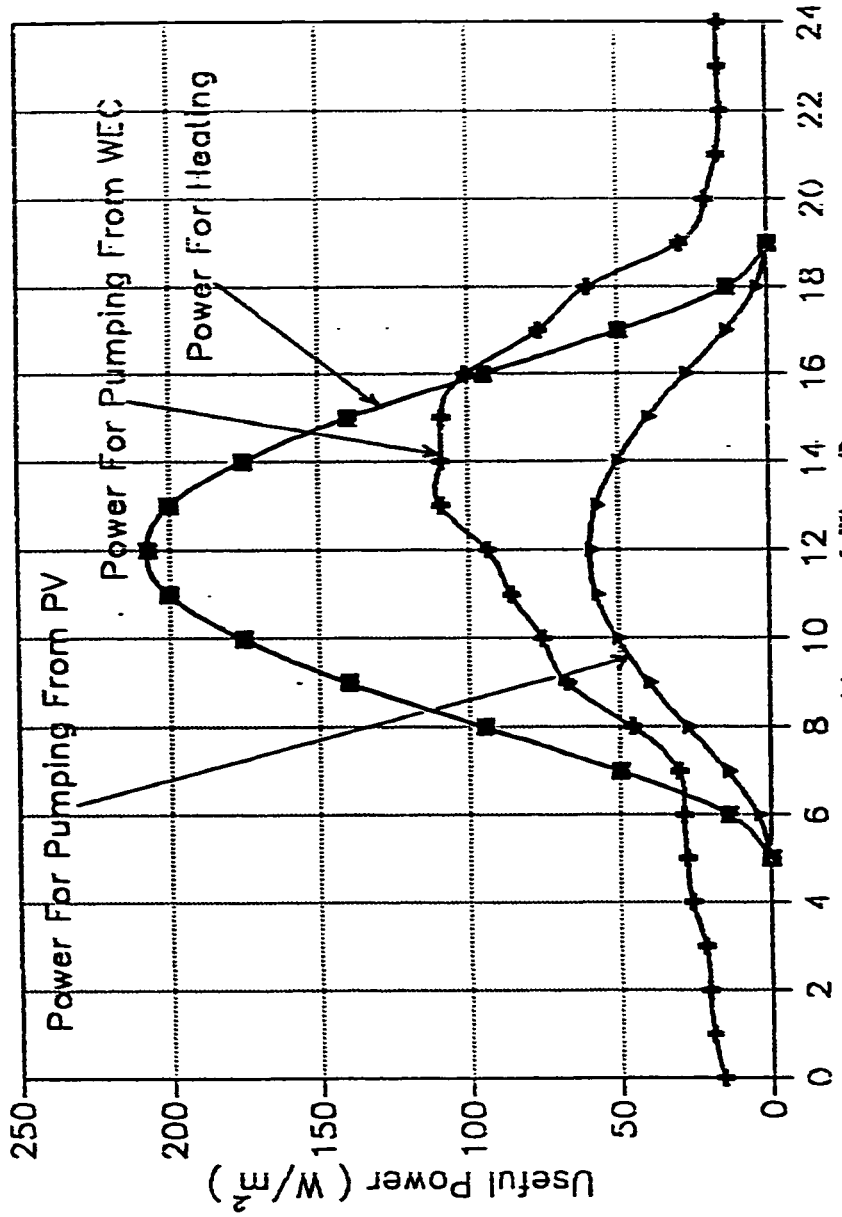

Figure (5.19) Useful Power Required for MSF and MES Distillation Unit

5.4 Discussion and Concluding Remarks

Based on the previous comparisons the following remarks can be made:

1- Dhahran city is abundant of Wind and solar power.

2- The Availability of wind power is 55% of the time while the availability of solar power is about 42%. This means that it is advantegous to operate a desalination unit using combined solar_ wind energy conversion system. In other wards, for the times in which there is no sun, wind energy is an excellent alternative.

3- It is more feasible to use a wind energy convertor to obtain the required electrical power than to use a photovoltaic solar collector. This is because of the fact that electrical power obtained by WEC is, in general, much higher (in terms of W/m^2) than that obtained by PV.

4- It is more viable (with respect to the amount of power produced) to obtain the required thermal power from evacuated solar collector than that produced from flat plate collectors.

5- The highest values of solar and wind power are obtained in the month of June while the lowest exist in the month of December.

CHAPTER 6

PROPOSED COST-EFFECTIVE DESIGN OF SOLAR/WIND POWERED DESALINATION SYSTEMS

In previous chapters, the decision regarding which desalination process is best suited for coupling with solar and/or wind power conversion systems under the prevailing design requirements mentioned in chapter 3 and the climatic conditions of Dhahran, has been made. It has been found that the reverse osmosis process is an excellent choice. In this chapter some optimal (cost-effective) designs of solar/wind powered desalination systems (SWPDS) will be proposed. Those designs will be based on actual climatic (solar and wind) conditions of Dhahran city. Some economics analysis of the proposed SWPDS will be performed as well. Consequently, comparison between these designs will be made. In the light of this comparison one would finally decide on the best combination of SWPDS that would result in optimum cost.

Two desalination processes will be selected for such analysis, namely; the reverse osmosis (RO) process (as a representative of membrane processes) and multieffect-stack distillation (MES) process (as a representative of heat processes). MES process is selected primarily due to its withstandability to fluctuations in the supplied solar/wind power source and its economic consumption of electrical power.

Three different designs of solar wind powered desalination systems will be proposed. These designs are

1. Solar/wind-powered MES (SW)
2. Solar/wind-powered RO (BW)
3. Solar/wind-powered RO (SW)

SW and BW stand for seawater and brackish water respectively.

6.1 Solar/Wind-Powered MES Desalination System

Multieffect-stack is a desalination process requiring thermal energy for heating (main load) and electrical power for pumping.

General Design Considerations

The design of the solar/wind-powered desalination plant is based on the following:

1. Climatic conditions in Dhahran.
2. High performance ratio of evaporator (i.e. MES)
3. High efficiency collector.
4. Continuous, stable operation (24 h/day).
5. Arabian Gulf seawater (50000-65000 P.P.M) is used as a feedwater for desalination.

6.1.1 System Design Concept

The system basically consists of four subsystems.

1. The solar energy collection subsystem which uses evacuated glass tube

solar collectors to convert the incident solar radiation into thermal energy.

2. The water storage subsystem (also called heat accumulator) which is assumed to have a low thermal stratification and a storage capacity of 300 m^3.

3. The evaporator subsystem is a horizontal tube, thin-film, multieffect-stack (MES) distiller with a design capacity of 120 m^3/day.

4. The wind energy convertor subsystem (WECS) is used to convert wind power into electrical power. The type of WECS is taken the same as that used in Australia (WECS has never been tested in Dhahran). Battery subsystem is used together with WECS for electrical power storage.

The first three subsystems are those with the identical specifications as to the solar desalination plant at Abu Dhabi. Each of these subsystems will be considered individually in the course of the analysis.

In this study, three design configurations are considered. These are:

1. The solar collector subsystem is used to provide the required full thermal load (100%) to the MES and the WECS is used to provide the required full electrical load.

2. The WECS subsystem is used to provide the full (100%) thermal/ electrical load.

3. The combined solar collector-WECS subsystems are used to provide

thermal/electrical load with different proportions.

6.1.2 Analysis For The Configuration No.1

The design concept of this configuration is illustrated very clearly in figure (6.1).

Design Data

(1) Solar collection subsystem :

evacuated tube collector type with the following characteristics:

- overall heat loss coefficient, $U_L = 3.0\ W/m^2.C^\circ$.
- heat removal factor, $F_R = 0.90$.
- $F_R U_L = 2.7\ W/m^2.C^\circ$.
- monthly average transmittance-absorptance product, $\overline{\tau\alpha} = 0.87$.
- $F_R(\overline{\tau\alpha}) = 0.79$.
- collector face area, A_c is taken as a variable design parameter.

(2) water storage subsystem, with the following specifications:

- total storage volume, $V = 300\ m^3$.
- fiber glass type of insulation.
- design mean temperature, $\overline{T}_s = 99\ C^\circ$.
- heat loss coefficient-area product, $(UA)_s = 195\ W/C^\circ$.

(3) Evaporator (MES)

- design maximum production capacity, $PC = 120\ m^3/day$.

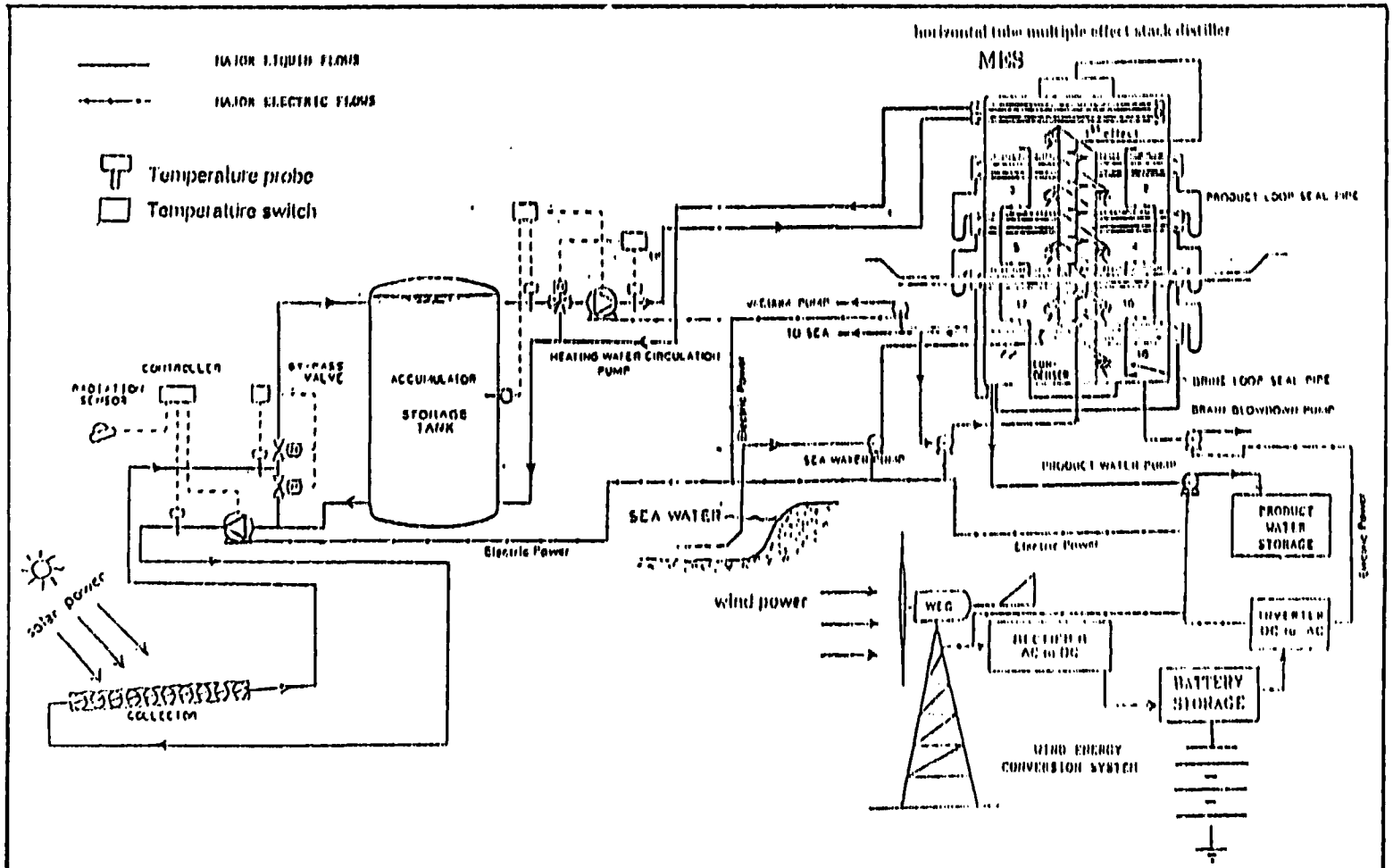

Figure (6.1) Design Concept of the Proposed Solar/Wind-Powered MES Desalination Plant (Config. no.1)

- number of effects, $N = 18$ plus the condenser.
- required minimum water temperature, $\overline{T}_{min} = 99\ C^{\circ}$.

Thermal Calculations by the $\overline{\varphi}$-f Chart Method

The purpose of these calculations is to estimate the monthly solar fraction, f (defined as the ratio of the load met by solar to the total load) at certain collector face area, A_c, which helps in optimizing the whole solar system. The method to be used is the $\overline{\varphi}$-f chart method developed by Duffie and Beckman [29]. Since this method is very detailed and well presented in [29], samples of calculations will be performed. The calculations for January (and sometimes December) will be illustrated. Results for intermediate calculations for all months will be tabulated.

The radiation incident on the tilted surface ($\beta = \varphi = 26.13^{\circ}$) located in Dhahran is calculated by the method given in chapter 5. $\overline{H}_{OH}$ is 23.2 MJ/m^2, $\overline{R}$ is 1.34 and $\overline{T}_a$ is 17.4 C°. $r_{t,n}$ is 0.160, and $r_{d,n}$ is 0.148. The beam radiation conversion factor at noon, $R_{b,n}$, is 1.37 and the noon ratio of radiation on a tilted surface to that on a horizontal surface, R_n, for the average day of January is 1.26. The ratio $\frac{R_n}{\overline{R}}$ is then 0.94. The critical radiation level at the minimum useful temperature for January is found from the Eq. given by [29] as:

$$\overline{X}_{c,min} = \frac{F_R U_L (\overline{T}_{min} - \overline{T}_a)/F_R(\overline{\tau\alpha})}{r_{t,n} R_n H_H} \qquad (6.1)$$

substituting, we get

$$\bar{X}_{c,min} = \frac{2.7 \times (99 - 17.4)/0.97}{0.16 \times 1.26 \times 13.4 \times 10^6/3600} = 0.375$$

The value of maximum utilizability factor, $\bar{\varphi}_{max}$, is found from figures available in [29]. $\bar{\varphi}_{max}$ is found to be 0.50. The dimensionless group, Y, is found from the Eq. given by [29] as:

$$Y = \frac{A_C F_R (\overline{\tau\alpha}) \bar{H}_T N}{L} \tag{6.2}$$

where

L = monthly average load required by MES

Using the specific energy consumption of MES as 183 kJ/kg and the water production capacity, PC, as 120 m^3/day, we obtain

$$L = 183 \times 120 \times 31 \times 10^{-3} = 680\ GJ\ .$$

Taking the value of A_c as 2500 m^2, and substituting in Eq. (6.2), we obtain

$$Y = \frac{2500 \times 0.79 \times 17.98 \times 10^6 \times 31}{680 \times 10^9} = 1.61$$

The product of $\bar{\varphi}_{max} Y$ is, then, 0.81. The dimensionless group X′ is calculated using the eq. given by [29] as:

$$X' = \frac{A_C F_R (100)\, \Delta t}{L} \tag{6.3}$$

where

Δt = total number of seconds in the month

substituting, we get

$$X' = \frac{2500 \times 2.70 \times 100 \times 3600 \times 31 \times 24}{680 \times 10^9} = 2.66$$

The storage capacity of the accumulator per unit collector area, $\frac{mC_p}{A_c}$ (m and C_p represent the mass of the stored water in kg and its associated specific heat respectively) is

$$\frac{mC_p}{A_c} = \frac{300 \times 1000 \times 4.19}{2500} = 503\ kJ/C^\circ m^2 .$$

The solar fraction, f, is then can be calculated from the Eq. given by [29] as:

$$f = \bar{\varphi}_{max} Y - 0.015\,(e^{3.85f} - 1)(1 - e^{-0.15X})\,(R_s)^{0.76} \qquad (6.4)$$

where R_s is the ratio of the standard storage heat capacity per unit of collector area of 350 $kJ/C^\circ m^2$ to the actual storage capacity. Thus

$$R_s = \frac{350}{503} = 0.696 .$$

Substituting the values of X', $(\bar{\varphi}_{max} Y)$, and R_s in Eq. (6.4) and performing trial-and-error solution for f which is expressed implicitly in Eq. (6.4), we get

$$f = 0.74 .$$

This value of f indicates that, with the given design configuration ($A_c = 2500\,m^2$), the solar system is capable of providing 74% of the given load requirement (689 GJ) in the month of January without including the storage tank heat losses (NISTL) to the environment. And the amount of energy provided by the solar system for this month is

$$fL = 0.74 \times 680 = 503\,GJ\ .$$

This procedure for calculating the monthly solar fraction, f, is repeated for the other months and the result is tabulated in table (6.1). It should be noted from this table that the minimum amount of energy provided by solar system (i.e. the lowest value of f) is 456 GJ (f=0.67) in the month of December while the highest value is 748 GJ (f=1.10) in the months of May and August. This means that the proposed solar system is capable of providing the required full thermal load (and slightly more) in the months of May and August and this is anticipated since the solar insolation in those months is relatively high.

The effect of including the heat losses from the storage tank to the surroundings should be considered since the main supply of thermal energy is provided by the storage tank which is storing the thermal energy day and night while being exposed to the environment. In order to include such effect in the calculations, some corrections in the previous analysis are to be made. This is illustrated for the month of December and for the other months the results are tabulated.

For December the the average tank temperature will be assumed to be

Table (6.1) Monthly Solar Fractions

A_c=2500 m^2

(Not Including Storage Tank Losses)

Month	$r_{c,n}$	$r_{d,n}$	$R_{b,n}$	R_n	$\frac{R_n}{\bar{R}}$	$\overline{\tau\alpha}$	$\bar{X}_{C_{min}}$
Jan.	0.160	0.148	1.37	1.26	0.94	0.87	0.375
Feb.	0.153	0.142	1.26	1.16	0.99	0.87	0.408
Mar.	0.144	0.134	1.14	1.09	1.00	0.87	0.333
Apr.	0.138	0.124	1.03	1.02	1.02	0.87	0.312
May	0.132	0.120	0.95	0.97	1.05	0.87	0.244
June	0.130	0.120	0.92	0.95	1.07	0.87	0.244
July	0.131	0.119	0.94	0.96	1.08	0.87	0.247
Aug.	0.135	0.122	1.00	1.00	1.04	0.87	0.236*
Sept.	0.141	0.131	1.10	1.08	1.02	0.87	0.243
Oct.	0.149	0.140	1.22	1.16	0.97	0.87	0.274
Nov.	0.158	0.147	1.34	1.26	0.95	0.87	0.312
Dec.	0.160	0.150	1.41	1.28	0.93	0.87	0.409

Month	$\bar{\alpha}_{max}$	Y	$(\bar{\alpha}_{max}Y)$	$\acute{X}$	f	L (GJ)	fL (GJ)
Jan.	0.50	1.61	0.81	2.66	0.74	680	503
Feb.	0.48	1.50	0.73	2.66	0.69	614	424
Mar.	0.55	1.84	1.01	2.66	0.89	680	605
Apr.	0.57	1.85	1.06	2.66	0.93	658	612
May	0.64	2.19	1.40	2.66	1.10	680	748
June	0.64	2.12	1.35	2.66	1.08	658	711
July	0.64	2.02	1.29	2.66	1.05	680	714
Aug.	0.65	2.11	1.38	2.66	1.10	680	748
Sept.	0.64	2.10	1.35	2.66	1.08	658	711
Oct.	0.61	1.98	1.20	2.66	1.02	680	694
Nov.	0.56	1.79	1.01	2.66	0.89	658	586
Dec.	0.48	1.48	0.71	2.66	0.67	680	456

99 C°. The tank losses can be calculated by the equation given by [29] *as*:

$$Q_{SL} = (UA)_s (\overline{T}_s - \overline{T}_a)\,\Delta t \tag{6.5}$$

where $\overline{T}_s$ and $\overline{T}_a$ are the monthly average tank and ambient temperatures respectively, which are taken to be constant for a month. $(UA)_s$ is the heat transfer loss coefficient-surface area product for the given storage tank. According to [46] this $(UA)_s$ is taken to be 195 W/C° and this value is assumed to be constant for a month. Substituting these values of $(UA)_s$, $\overline{T}_s$, and $\overline{T}_a$ in Eq. (6.5), we get

$$Q_{SL} = 195\,(99 - 17.4) \times 3600 \times 24 \times 3 = 42.6\ GJ\ .$$

The total load is then

$$\begin{aligned} L_{TL} &= Q_{SL} + L \\ &= 42.6 + 680 = 723\ GJ\ . \end{aligned} \tag{6.6}$$

The values of $(\overline{\varphi}_{max}Y)$ and X' are then 680/723 times the values from table (6.1). Thus

$$(\overline{\varphi}_{max}Y)_c = 0.71 \times \frac{680}{723} = 0.67$$

$$(X')_c = 2.66 \times \frac{680}{723} = 2.5\ .$$

The subscript c refers to the corrected value. From Eq. (6.4), we obtain

$$f_{TL} = 0.63 .$$

The average utilizability in this case is

$$\bar{\varphi} = \frac{f_{TL}}{Y} \qquad (6.7)$$

$$= \frac{0.63}{1.39} = 0.45 .$$

With this value of $\bar{\varphi}$, $\bar{X}_c$ is found to be 0.401 [46]. Since the original value of $\bar{X}_{c,min}$ was 0.409, the temperature difference of (99 − 17.4) must be decreased by the ratio 0.401/0.409. The estimate of $\bar{T}_{min}$ is then

$$\bar{T}_{min} = (99 - 17.4) \times \frac{0.401}{0.409} + 17.4 = 97.4\ C^{\circ}$$

and the average tank temperature, $\bar{T}_s$, is estimated to be

$$\bar{T}_s = \frac{97.4 + 99}{2} = 98.2\ ^{\circ}C$$

which is close to the initial guess so no iterations are necessary. The corrected solar fraction, as a result of including storage tank losses (ISTL), is then found [29]:

$$f_c = f_{TL}\left(1 + \frac{Q_{sL}}{L}\right) - \frac{Q_{sL}}{L} \qquad (6.8)$$

$$= 0.63\left(1 + \frac{42.6}{680}\right) - \frac{42.6}{680} = 0.61 .$$

This procedure is repeated for the other months and the detailed results are presented in table (6.2). It should be noted from this table that the load met by solar is decreased from 8 to 9% of the initial value due to the inclusion of the heat losses for the storage tank. Also, we note that the lowest solar fraction still corresponds to the month of December.

It is interesting to study the effect of changing the collector face area, A_c, on the solar fraction. When A_c changes one has to correct the parameters Y, X', R_s, and consequently f. This concept is performed for the month of December (with lowest solar insolation) for A_c varying between $500-3000\,m^2$ and the detailed results are presented in table (6.3) and illustrated in figure (6.2). Table (6.4) shows some results on the variation of A_c ranging between $500-8000\,m^2$. These two tables are valid under two main assumptions, namely; the effect of including the storage tank losses is not considered and the load (required by the MES distiller) is fixed at $680\,GJ$ ($PC = 120\,m^3/day$). When the effect of including the storage tank losses is considered, monthly solar fractions are affected. The procedure is done while including such effect and the results are presented in table (6.5). This table compares between the two cases of including and not including storage tank losses at variable collector areas. As expected, one can note from this table that as the collector face area, A_c, increases the monthly solar fraction increases as well. This is true because of the fact that the more collector area we have, the more thermal energy which can be collected, and consequently the more the solar fraction. Also, from table (6.4) one can notice that the solar system is capable in meeting the required full thermal load

Table (6.2) Monthly Solar Fractions

A_c=2500m^2

(Including Storage Tank Losses)

Month	$r_{t,n}$	$r_{d,n}$	$R_{b,n}$	R_n	$\frac{R_n}{\overline{R}}$	$\overline{\tau\alpha}$	$\overline{X}_{C_{a,n}}$
Jan.	0.160	0.148	1.37	1.26	0.94	0.87	0.40
Feb.	0.153	0.142	1.26	1.16	0.99	0.87	0.40
Mar.	0.144	0.134	1.14	1.09	1.00	0.87	0.38
Apr.	0.138	0.124	1.03	1.02	1.02	0.87	0.36
May	0.132	0.120	0.95	0.97	1.05	0.87	0.35
June	0.130	0.120	0.92	0.95	1.07	0.87	0.28
July	0.131	0.119	0.94	0.96	1.08	0.87	0.30
Aug.	0.135	0.122	1.00	1.00	1.04	0.87	0.30
Sept.	0.141	0.131	1.10	1.08	1.02	0.87	0.32
Oct.	0.149	0.140	1.22	1.16	0.97	0.87	0.33
Nov.	0.158	0.147	1.34	1.26	0.95	0.87	0.38
Dec.	0.160	0.150	1.41	1.28	0.93	0.87	0.44

Month	$\overline{o}_{max}$	Y	$(\overline{o}_{max}Y)_c$	$\acute{X}_c$	f_c	L (GJ)	fL (GJ)
Jan.	0.45	1.52	0.76	2.5	0.66	680	449
Feb.	0.44	1.42	0.69	2.5	0.61	614	374
Mar.	0.47	1.75	0.96	2.5	0.82	680	558
Apr.	0.50	1.77	1.01	2.5	0.87	658	572
May	0.45	2.09	1.34	2.5	0.95	680	646
June	0.53	2.03	1.29	2.5	1.02	658	671
July	0.54	1.93	1.23	2.5	1.00	680	680
Aug.	0.54	2.02	1.32	2.5	1.04	680	707
Sept.	0.54	2.00	1.29	2.5	1.02	658	671
Oct.	0.53	1.88	1.14	2.5	0.98	680	666
Nov.	0.48	1.69	0.95	2.5	0.81	658	533
Dec.	0.44	1.39	0.67	2.5	0.61	680	415

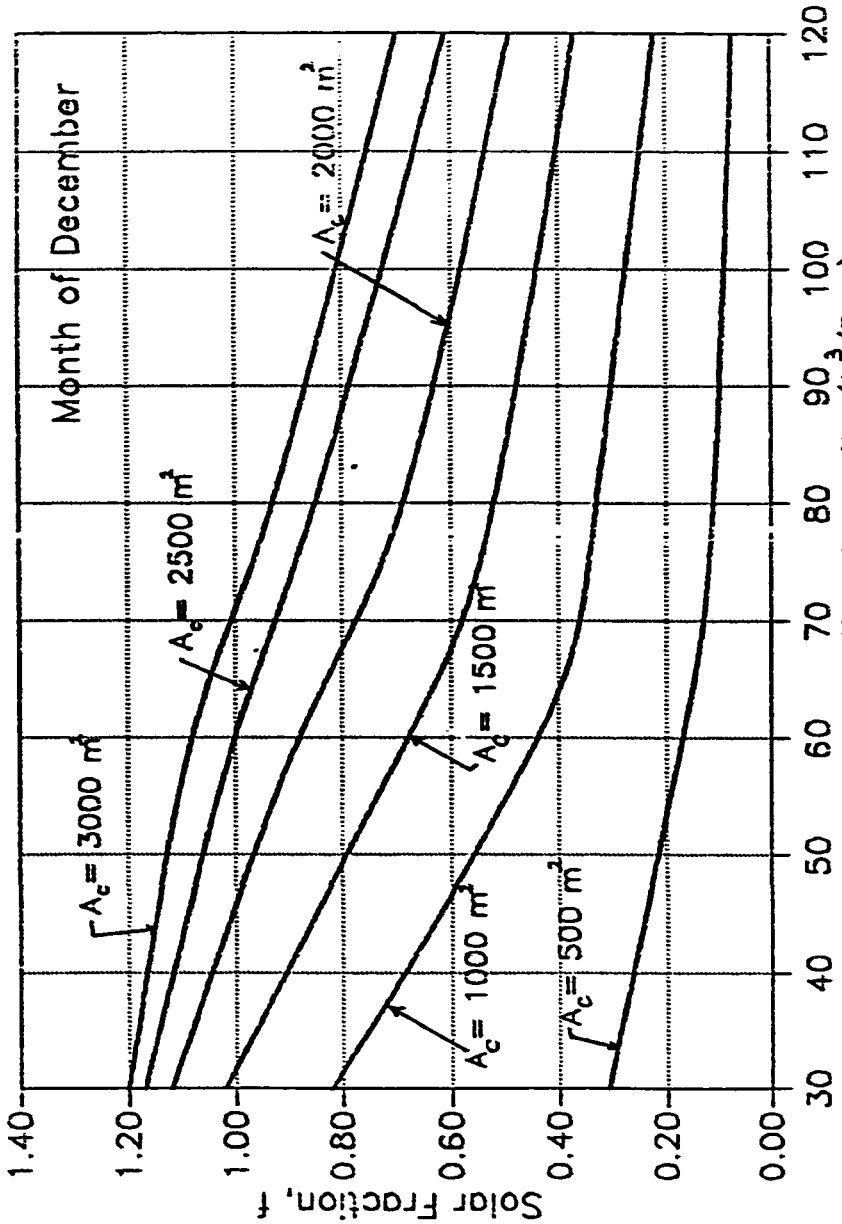

Figure (6.2) Water Production Load Met by Solar for Various Collector

Table (6.3) Results for the calcualtion of Solar Fraction at Various Collector Face Area for the Month of December (L = 680 GJ)

A_c (m^2)	Y	$(\theta_{max}Y)$	$\acute{X}$	$(MC_p)_s / A_c$	R_s	f (NISTL)
500	0.296	0.142	0.532	2512	0.139	0.14
1000	0.592	0.285	1.060	1256	0.279	0.28
1500	0.888	0.427	1.596	837	0.418	0.42
2000	1.184	0.570	2.128	628	0.557	0.56
2500	1.480	0.710	2.660	503	0.696	0.67
3000	1.776	0.854	3.192	419	0.835	0.76

Table (6.4) Solar Fraction as a Function of Collector Face Area for the Month of December (Not Including Storage Tank Losses)

A_c (m^2)	f
500	0.14
1000	0.28
1500	0.42
2000	0.56
2500	0.67
3000	0.76
4000	0.90
5000	0.98
6000	1.02
6250	1.03
6500	1.04
8000	1.07

Table (6.5) Solar Fraction as a Function of Collector Face Area for the Month of December (L = 680 GJ)

A_c (m^2)	f (NISTL)	f_c (TSTL)
500	0.14	0.07
1000	0.28	0.22
1500	0.42	0.37
2000	0.56	0.49
2500	0.67	0.61
3000	0.76	0.70

(at $PC = 120\ m^3/day$) at collector areas more than or equal to 6000 m^2.

Another interesting fact which can be considered is the effect of changing the load requirements (L or PC) on the solar fraction f. For this case one has to (linearly) correct for $(\overline{\varphi}_{max}Y)$, X', and consequently f. Taking into account the effects of variable load requirements, the inclusion of tank losses, and the variable collector area, the analysis is performed and the results are shown in table (6.6). This table is based on the month of December. From this table one can observe that when the load is decreased from 680 GJ (equivalent to 120 m^3/day) to 170 GJ (equivalent to 30 m^3/day) the solar fraction is increased from 0.37 to 1.02, about three times as much, at a fixed collector area 1500 m^2. Also, the storage tank loss Q_{st} is kept constant throughout the month of December at even variable loads and collector areas. In practice this is not true, since the three subsystems (collector, storage tank, and MES distiller) are interacted. However, if one is interested in knowing the exact behavior, one has to develop a detailed hourly-basis computer simulation model. In this study there is no need to go through this head-ache and monthly-based analysis is quite sufficient.

The annual solar fraction, F, can be calculated as [29]:

$$F = \frac{\sum_{i=1}^{12} f_i L_i}{\sum_{i=1}^{12} L_i} \tag{6.9}$$

where

Table (6.6)

Results for the Correction of Solar Fraction as a Result of Including Storage Tank Losses at Different Loads (Month of December)

A_c (m^2)	$Q_{st.}$ (GJ)	L_m (GJ)	(R_s)	$(\phi_{max} Y)_c$	$(\bar{X})_c$	f_m	f_c
L = 680 GJ							
500	42.6	723	0.139	0.133	0.500	0.128	0.07
1000	42.6	723	0.279	0.268	0.996	0.270	0.22
1500	42.6	723	0.418	0.401	1.500	0.405	0.37
2000	42.6	723	0.557	0.536	2.000	0.520	0.49
2500	42.6	723	0.696	0.667	2.510	0.630	0.61
3000	42.6	723	0.835	0.803	3.000	0.720	0.70
L = 453 GJ							
500	42.6	496	0.139	0.194	0.726	0.19	0.11
1000	42.6	496	0.279	0.389	1.447	0.39	0.33
1500	42.6	496	0.418	0.583	2.178	0.56	0.52
2000	42.6	496	0.557	0.778	2.905	0.72	0.69
2500	42.6	496	0.696	0.969	3.180	0.86	0.85
3000	42.6	496	0.835	1.166	4.357	0.94	0.93

cont. Table (6.6) Results for the Correction of Solar Fraction as a Result of Including Storage Tank Losses (Month of December)

A_c (m^2)	$Q_{st.}$ (GJ)	L_m (GJ)	(R_s)	$(\epsilon_{max}Y)_c$	$(\bar{X})_c$	f_m	f_c
L = 340 GJ							
500	42.6	383	0.139	0.252	0.940	0.26	0.17
1000	42.6	383	0.279	0.507	1.880	0.50	0.44
1500	42.6	383	0.418	0.759	2.840	0.72	0.68
2000	42.6	383	0.557	1.010	3.790	0.89	0.88
2500	42.6	383	0.696	1.260	4.730	1.01	1.00
3000	42.6	383	0.835	1.520	5.670	1.07	1.06
L = 170 GJ							
500	42.6	213	0.139	0.454	1.702	0.45	0.31
1000	42.6	213	0.279	0.912	3.392	0.86	0.82
1500	42.6	213	0.418	1.366	5.107	1.09	1.02
2000	42.6	213	0.557	1.824	6.810	1.20	1.12
2500	42.6	213	0.696	2.272	8.512	1.25	1.17
3000	42.6	213	0.835	2.733	10.21	1.29	1.20

$\sum_{i=1}^{12} f_i L_i$ = Sum of monthly loads met by solar in a year

$\sum_{i=1}^{12} L_i$ = Sum of monthly loads in a year .

For the case when A_c is 2500 m^2, the annual solar fraction, F, is found to be 0.87 for the month of December, at MES production capacity equals to 120 m^3/day, and including the tank heat losses. However, when A_c is 8000 m^2, F is found to be 1.17 as illustrated in figure (6.3).

Electrical power provided by WECS

The electrical power required for pumping water as well as for creating vacuum in the MES subsystem is calculated using the empirical relationship given by [50] as:

$$P_e = -(1.25)(10^{-5})\,PC^2 + 0.41\,PC + 6.06 \qquad (6.10)$$

where

P_e = Electrical power consumption of the MES plant, in kW

PC = Water production capacity of the MES plant, in m^3/day

this equation is valid for $PC < 500$.

In order to calculate how much electrical power is needed for pumping, we need to determine the required water production capacity of the plant since

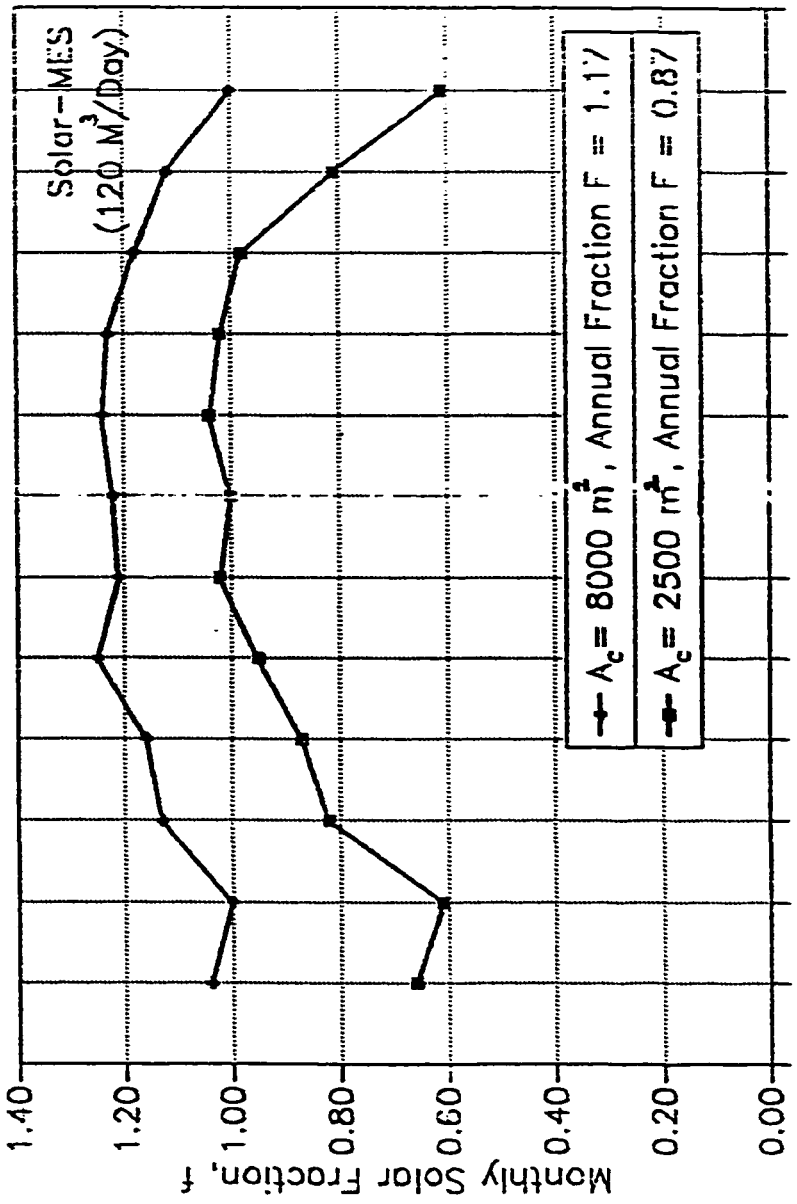

Figure (6.3) Monthly Load Fraction Met by Solar

these two are related by Eq. (6.9). In this analysis, four cases are considered. Procedure of calculation is same for all these cases. Therefore, illustration of calculations is done for one case study and results are tabulated for the remaining cases.

Case Study

This case assumes PC to be 120 m^3/day. Thus Eq. (6.9) gives

$$P_e = -(1.25)(10^{-5})(120^2) + 0.14(120) + 6.06 = 23\,kW$$

This amount of electrical power is provided by the wind energy converter subsystem. The WECS subsystem is taken to be identical to the one used and tested at Woomera in Australia, since WECS has never been tested in Dhahran area. The WECS performance at Woomera as indicated in [51], is based on the annual wind speed of Woomera which is 4.4 m/s. Dhahran has an annual wind speed equal to 4.5 m/s which is very close to that in Woomera. Therefore, it is reasonable in our case to use the performance curve of the WECS at Woomera which would help in performing the analysis.

Analysis For WECS Size Prediction

Figure (6.4) [51] represents the performance prediction of a WECS, with different combinations of WECS size and battery storage capacity, DS, at Dhahran (or Woomera) for a given load. The ordinate of figure (6.4) indicates the fraction of the electrical load, f_w , that can be supplied by WEC (wind energy convertor), while the absica represents a dimensionless parameter, α , is

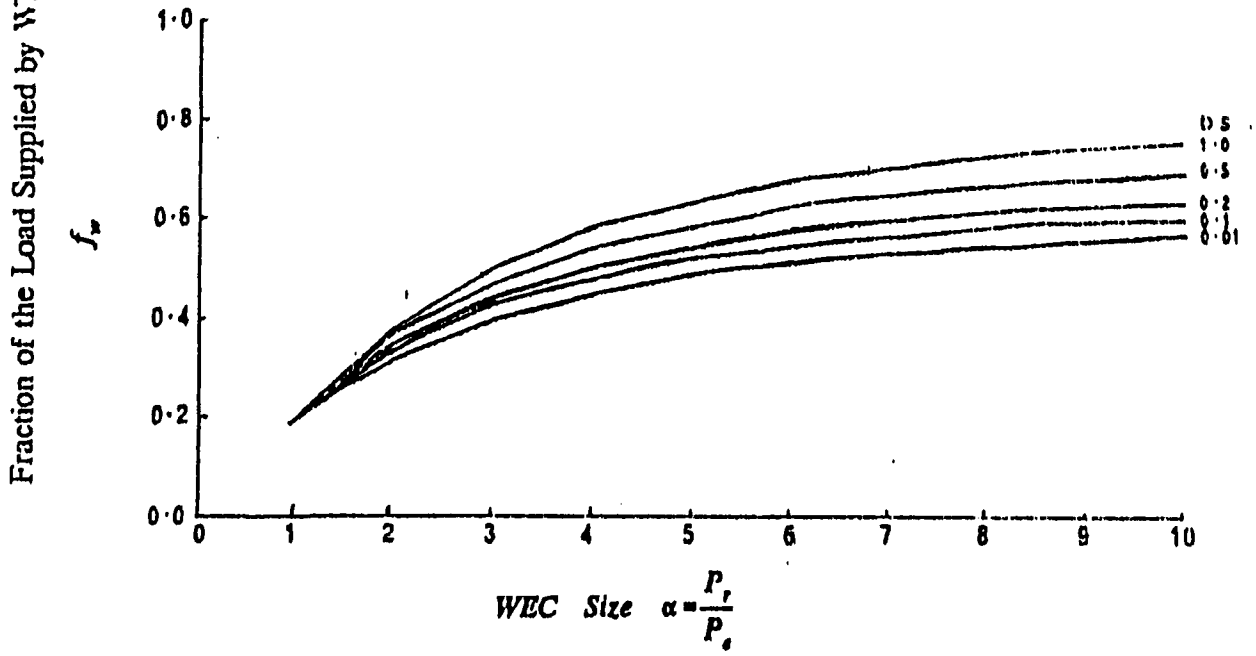

Figure (6.4) WECS Performance at Dhahran (Assumed to be Similar to that at Woomera) [51]

given as a ratio between the WEC rated power, P_r (taken to be less than 20 kW), to the required electrical load, P_e. The parameter DS indicates the number of days storage to supply P_e. Thus, for our system P_e is about 25 kW. and P_e can be divided so as to allow the use of figure (6.4). Thus,

$$P_e' = \frac{P_e}{2} = \frac{25}{2} = 12.5\,kW$$

and from figure(6.4), this gives

$$\alpha = \frac{18}{12.5} = 1.44$$

and

$$f_w = 0.24,\ at\ DS = 1.00\ .$$

The value of f_w indicates that the size of WEC is capable of providing 24% of the assumed P_e' at storage capacity, DS, equivalent to one day. In this case, we need at least four WEC machines to provide P_e' and eight machines to meet our load P_e.

Present Value Method for the Economics Analysis

After we have defined the thermal and electrical requirements and their corresponding sizes of the solar collector and WEC, it is very interesting at this stage to evaluate the case we have from economics standpoint. The method to

be used is called the present value method. This method is represented by the Eq. given by [51] as:

$$pv = CC\left(1 + \frac{MC[(1+IR)^y - 1]}{IR(1+IR)^y}\right) \tag{6.11}$$

where

pv = present value, $

CC = Capital cost of the subsystem, $

IR = Interest rate

y = Number of years in the period of analysis

MC = Maintenance coefficient given as a percentage of CC .

The total present value for our case is:

$$(pv)_{tot} = (pv)_{coll} + (pv)_{WECS} + (pv)_{st} + (pv)_{MES} \tag{6.12}$$

where

$(pv)_{coll}$ = Present value of the collector subsystem, $

$(pv)_{WECS}$ = Present value of the WECS subsystem, $

$(pv)_{st}$ = Present value of the storage tank, $

$(pv)_{MES}$ = Present value of the MES subsystem, $.

$(pv)_{coll}$ and $(pv)_{st}$ can be calculated using some typical unit costs presented in table (6.7) [52]. For the case we have the unit costs are

$$(UC)_{coll} = 300 + 95 + 150 + 30 + 45$$

$$= 620\ \$/m^2$$

and

$$(UC)_{st} = 0.53\ \$/\text{liter}.$$

Thus the capital costs can be calculated using the equation:

$$(CC)_{coll} = A_c \times 620 \tag{6.13}$$

The parameter A_c, here, dictates the size of the collector subsystem. For our case, PC is 120 m^3/day and the collector is supplying the full (100%) thermal load which means that the solar fraction has to be equal or more than 1.0. From figure (6.3) and based on the month of December (with the lowest solar insolation). A_c is found to be 8000 m^2 which gives f equal 1.0. Thus from Eq. (6.12) we get

$$(CC)_{coll} = 8000 \times 620 = 4.96 \times 10^6\ \$$$

For the storage tank, we have

$$(CC)_{st} = 0.53 \times V \tag{6.14}$$

Table (6.7) Typical Unit Costs of the Collector Subsystem

Subsystem	Category	Cost Range	Typical Cost	Units
Collector Array	Evacuated Tubes	260-325	300	$/m^2$ Collector Area
Support Structure	Single Function	30-160	95	$/m^2$ Collector Area
Energy Transport	Hot Water	85-185	150	$/m^2$ Collector Area
Storage (Liquid)	Fiberglass Tank	0.45-0.66	0.53	$/liter
Electrical& Controls	Hot Water	20-55	30	$/m^2$ Collector Area
General Construction	N/A	0-160	45	$/m^2$ Collector Area

where

V = Volume of storage tank in liters.

Thus,

$$(CC)_H = 0.53 \times 300000 = 159000\ \$$$

For MES, with a unit cost of 500 $\frac{\$}{(m^3/day)}$ (obtained from chapter 3), we obtain

$$(CC)_{MES} = 500 \times 120 = = 60000\ \$.$$

The term $(pv)_{WECS}$ can be determined using the Eq. given by [51] (For that WECS used at Woomera) as:

$$(pv)_{WECS} = N_{WEC}\,[2.72636\,\alpha + 5.21688\,(DS)]\,P_e^{'} . \qquad (6.15)$$

The parameter N_{WEC} in this equation refers to the number of WECS used. For our case, this gives

$$(pv)_{WECS} = 8\,[2.72636\,(1.44) + 5.21688\,(1.0)\,] \times 12.5 \times 10^3$$

$$= 8 \times 114286 = 914288\ \$.$$

Assuming

IR = 2 %

y = 20 years

MC = 5 % .

It should be noted that IR, and MC could have different values. For the sake of comparing the various proposed designs, the assumed values are taken to be fixed throughout the analysis. Using Eq. (6.10), we obtain

$$(pv)_{coll} = 9.03 \times 10^6 \$$$

$$(pv)_{st} = 0.29 \times 10^6 \$$$

$$(pv)_{MES} = 0.11 \times 10^6 \$$$

Substituting these values in Eq.(6.12), we get

$$(pv)_{tot} = (9.03 + 0.915 + 0.29 + 0.11) \times 10^6$$

$$= 10.35 \times 10^6 \$.$$

This total present value represents the cost of the entire system which is used to produce 120 m^3/day freshwater. It is beneficial to normalize this value in terms of a unit water cost as

$$Unit\ water\ cost = \frac{Plant\ cost\ in\ service,\ \$}{total\ production\ of\ water,\ m^3} . \qquad (6.16)$$

Thus, for our case we obtain

$$Unit\ water\ cost = \frac{10.35 \times 10^6}{365 \times 20 \times 120}$$

$$= 11.8\ \$/m^3 .$$

In a manner similar to the previous analysis we can obtain the water unit costs at different water production capacities as illustrated in figure (6.5). It is interesting to note that. the minimum cost is obtained when the production capacity is 70 m^3/day. It should be noted that at lower production capacities the unit cost goes up as given in Eq. (6.16) and figure (6.5).

6.1.3 Analysis for the Wind-Powered MES Configuration No.2

The design concept of this configuration is illustrated in figure (6.6). The system shown in this figure assumes that the WECS subsystem has to provide the full (100%) electrical/thermal power required to operate the MES subsystem. The thermal energy (hot water) provided is created by means of an electrical heater powered by the WECS and placed in the water heater (storage tank) subsystem. Thus in this case wind is solely used to operate the desalination unit.

Assumptions

1. Electrical heater efficiency, η_H , is assumed to be 85% .
2. Specifications of the storage tank are the same as those taken before.

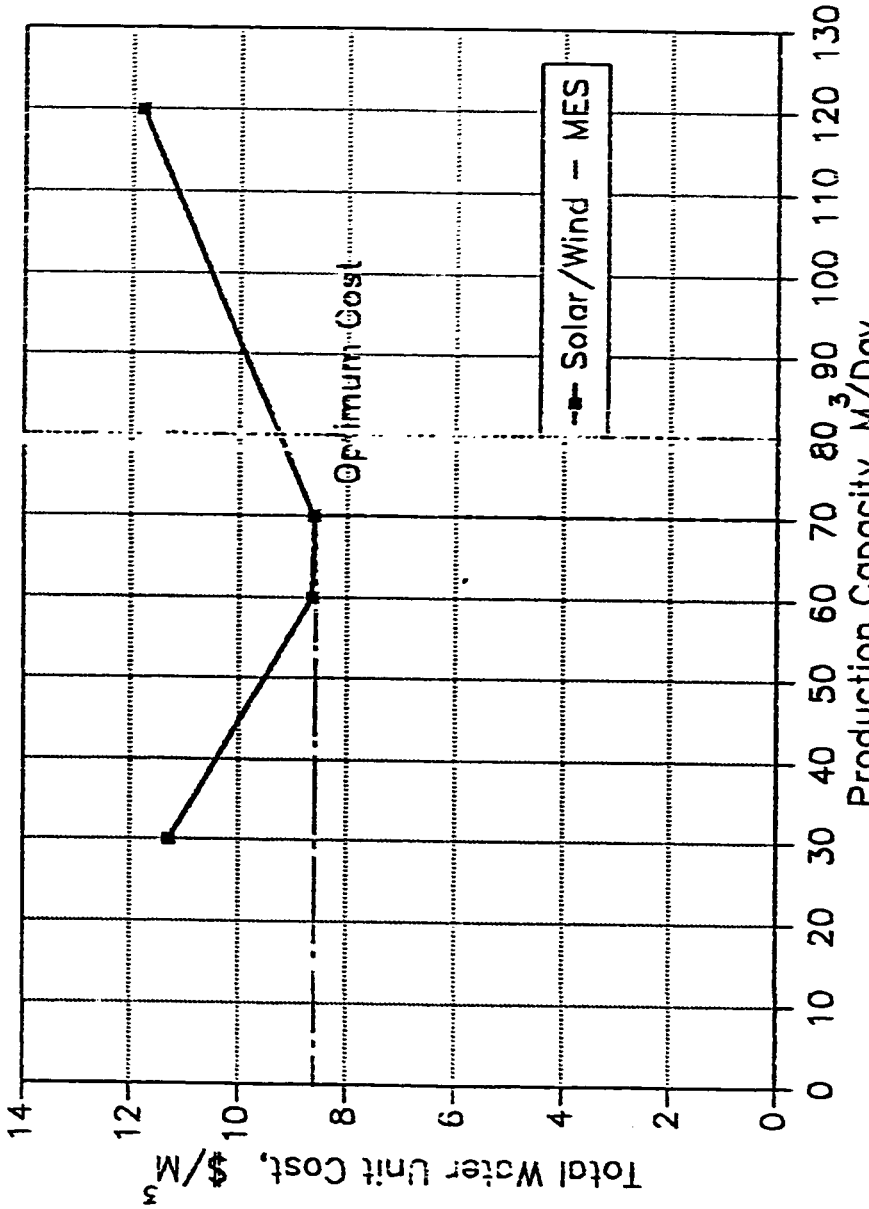

Figure (6.5) Water Unit Cost for Solar/Wind-MES Plan

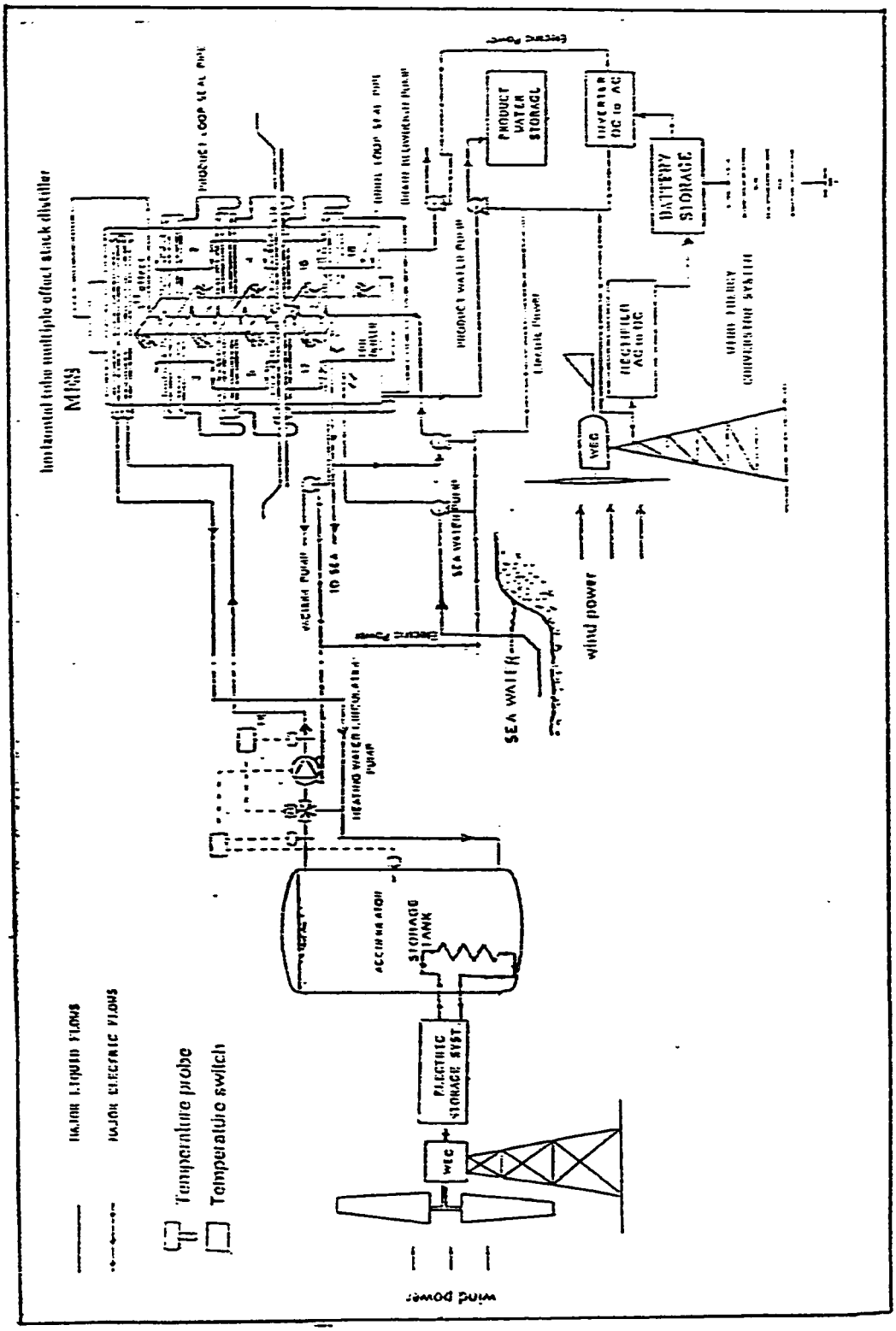

Figure (6.6) Design Concept of the Proposed Wind-powered MES Desalination Plant (Config. no.2)

Thermal and Electrical Power Calculations

The specific thermal energy consumption of the MES subsystem is 183 kJ/kg as defined earlier in this chapter. Thus the thermal power of MES can be calculated as

$$P_t = 183\,(PC) \times \frac{1000}{24} \times 3600 \tag{6.17}$$

where

P_t = Thermal power in kW.

For PC equals to 70 m^3/day, the value of p_t is 149 kW of thermal power. The electrical power, p_e , is calculated, using Eq. (6.10) to be 15.8 kW. Thus, the total electrical power can be calculated using the equation given as:

$$(P_e)_{tot} = \frac{P_t}{\eta_H} + P_e \tag{6.18}$$

and substituting the values of P_t, P_e, and η_H in this equation, we obtain

$(P_e)_{tot}$ = 191 kW.

This is the total amount of electrical power required to operate the desalination plant by the WECS. Using the value of P_e equals to 191 kW in figure (6.4). we can determine the required size of WEC in a manner similar to the previous analysis. In doing so, the number of WEC machines is found to be 75 (WEC

machines having identical characteristics) and the water unit cost is found to be 17 S/m^3. This analysis is repeated for different water production capacities and the results are shown in figure (6.7). It should be noted from this figure that, it is relatively more economical to operate the system at production capacity equals to 120 m^3/day (i.e. more water production at relatively lower cost).

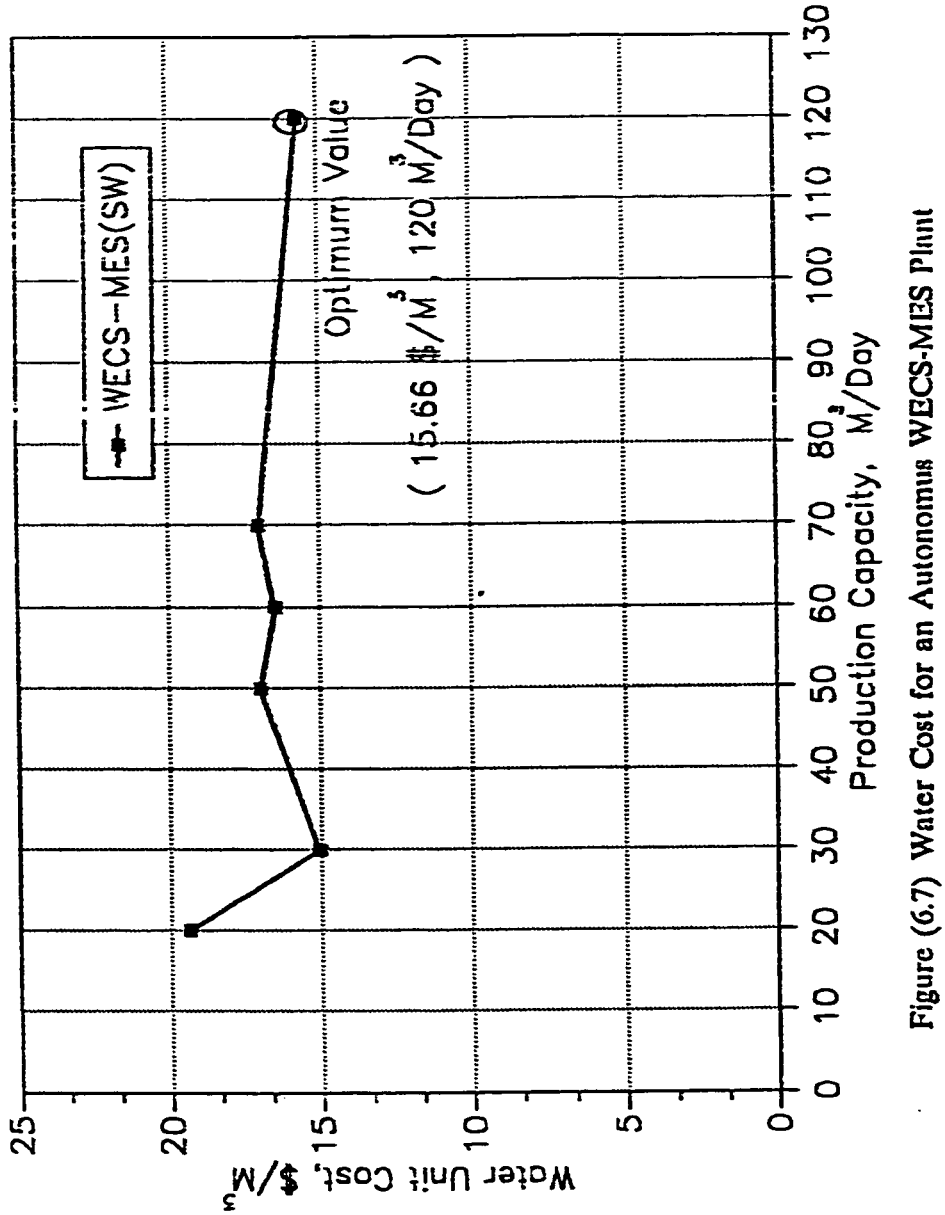

Figure (6.7) Water Cost for an Autonomus WECS-MES Plant

(6.1.4) Analysis for the Combined Solar/Wind-MES System Configuration No.3

The design concept of this configuration is depicted in figure (6.8). In this figure, the solar collector and WECS subsystems are both contributing to provide the required thermal load (electrical power for pumping is solely provided by the WECS). In this part we will try to answer the question of what is the best combination (in terms of solar and wind fractions) of WECS and collector sizes that would result in optimum water cost. By observing Eq. (6.12) one should note that the two dominant variables affecting the water cost are $(pv)_{coll}$ and $(pv)_{WECS}$.

Sizing Procedure

The results to be followed are based on the following summarized procedure:

1. The values of wind and solar fractions and the required water production capacity of the MES are set.
2. The amount of power (either thermal or electrical) that will be shared by the WECS and collector according to the specified solar-wind fractions is determined.
3. According to step 2, the collector area, A_c, needed is estimated from figure (6.2).
4. The number of WEC machines is specified according to the specified wind fraction.

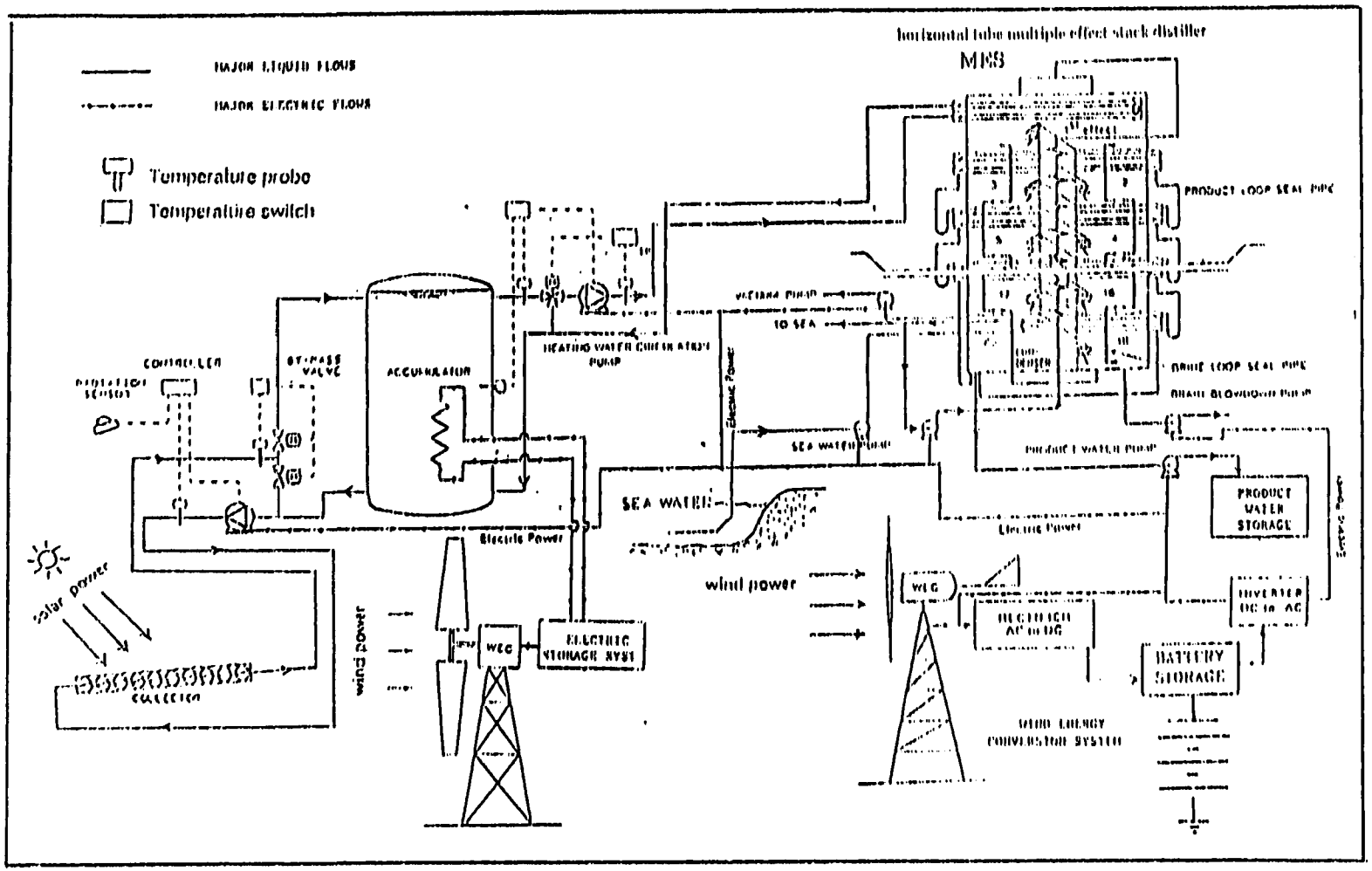

Figure (6.8) Design Concept of the proposed Solar/Wind-powered MES Desalination Plant (Config. no.3)

5. $(pr)_{tot}$ is calculated based on the results of the previous steps and the use of Eqs. (6.10-16).

6. Consequently, the corresponding water unit cost is calculated using Eq. (6.16).

This procedure is implemented for PC equals to $120\,m^3/day$ and (solar,wind) fractions of (1.0,0.0), (0.7,0.3), (0.5,0.5), (0.22,0.78), and (0.0,1.0). The results of this procedure are presented in figure (6.9). It can be noted from this figure that the minimum water cost is achieved using solar-wind fractions of 0.7 and 0.3 respectively with water cost equals to $9.5\,\$/m^3$. The number of WECS machines as a function of wind fraction is shown in figure (6.10). This figure shows that, as one might expect, as the wind fraction increases (wind is contributing more to meet the required load) the required number of WECS machines increases as well.

The final conclusion which can be made based on the previous three configurations is that, for the given types of collector and WECS and their associated unit costs, the choice to go for the augmented wind/solar-powered MES system is promising from energy availability and economical point of views. The energy availability viewpoint says that when there is no sun (or the time of cloudy days) wind can do the job and visa versa. Also, the technical standpoint (e.g. maintenance level, operational problems, and etc) has to be investigated. This is beyond the scope of this study.

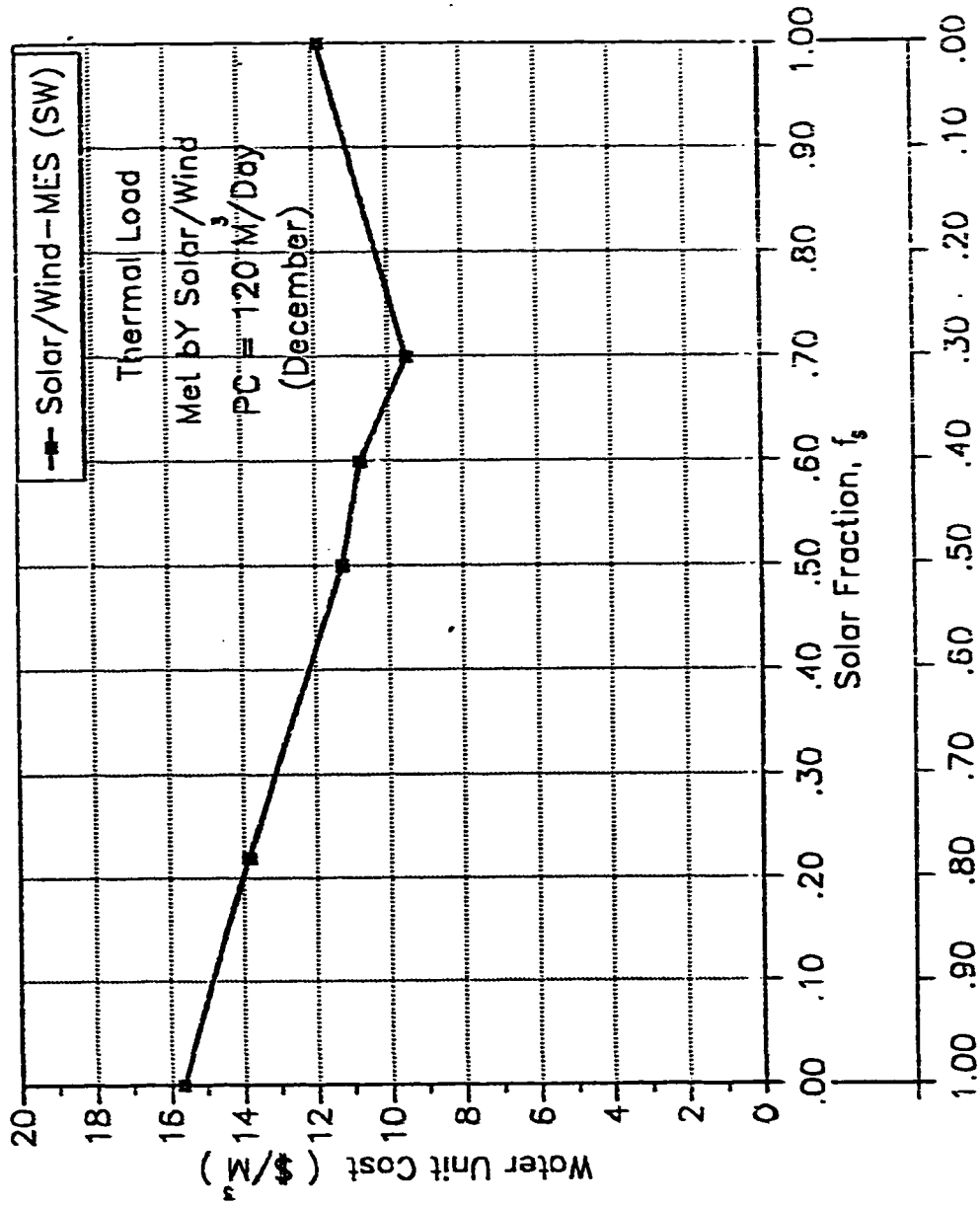

Figure (6.9) Water Cost at Different Solar/Wind Fractions

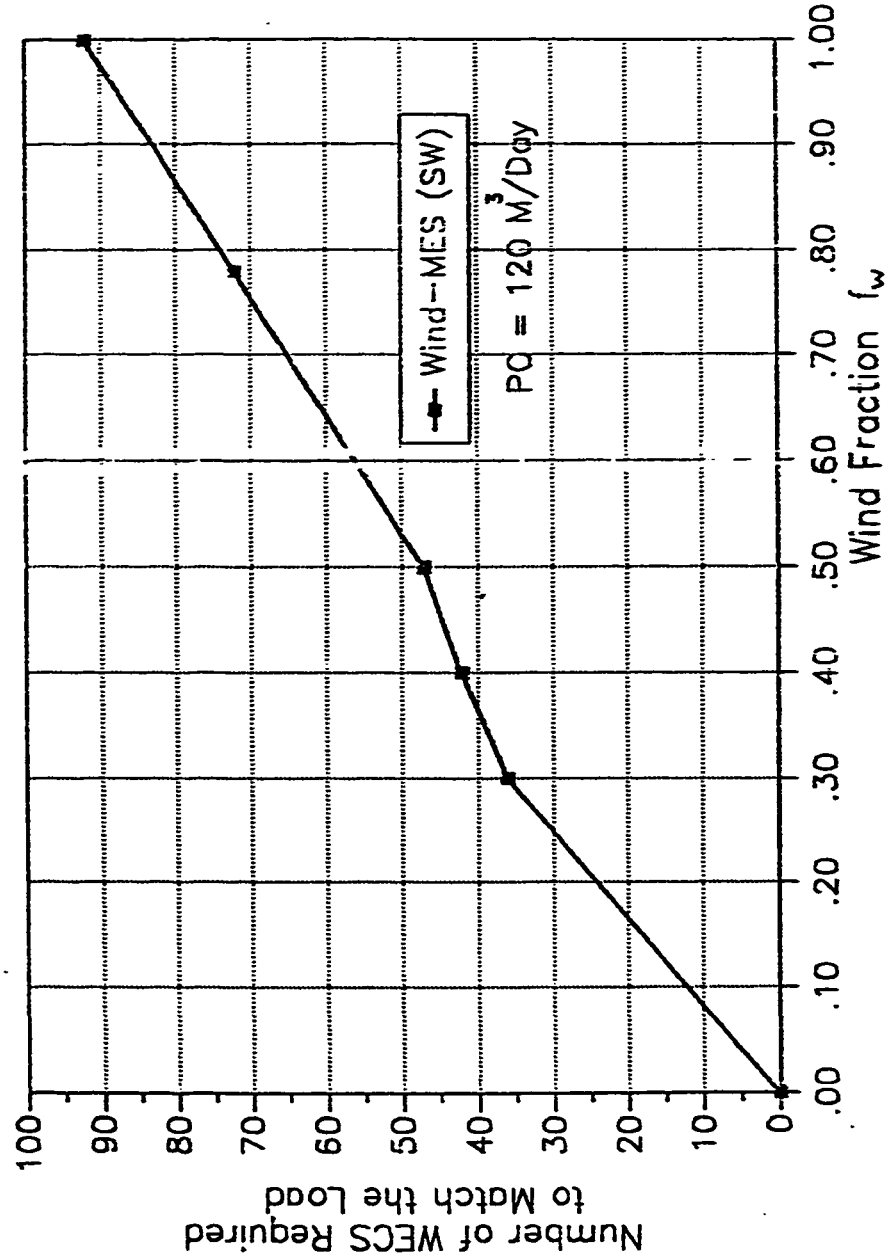

Figure (6.10) Wind-Operated MES Desalination Plant

6.2 Solar/Wind-Powered RO (BW) Desalination System

Reverse osmosis requires electrical mechanical power for its application. Solar and wind power can be converted into electrical power using WECS and Photovoltaic subsystems. Therefore, the design is based on sizing these subsystems in a way to meet the required electrical load.

General Design Considerations

1. Climatic conditions in Dhahran.

2. Continuous, stable operation (24 h/day).

3. Brackish water (2500 p.p.m.) is used as feedwater for desalination.

6.2.1 System Design Concept

The system basically consists of four subsystems.

1. The solar energy collection subsystem which uses the Photovoltaic-cell arrays (PV) converts the incident solar radiation into electrical power. The battery subsystem is used together with PV for electrical power storage.

2. The reverse osmosis subsystem.

3. The wind energy convertor subsystem (WECS) is similar to that used before.

Using these subsystems, three design configurations are considered. These are:

1. The PV- array subsystem is used to provide the required full (100%) electrical load to the RO subsystem.

2. The WECS subsystem is used to provide the full (100%) electrical load to the RO system.

3. The combined PV-WECS subsystems are used to provide the required electrical load with varying proportions.

6.2.2 Analysis for the Autonomous PV-RO System

The design concept of this configuration is illustrated very clearly in figure (6.11).

Design Data

(1) Solar collection subsystem:

Photovoltaic collector type with the following characteristics:

- PV electrical conversion efficiency, η_{PV}, is taken to be equal to 0.11.

- Collector area, A_c, is taken to be a variable parameter.

- Unitary cost of the photovoltaic field, $(UC)_{PV}$, is taken to be 1000 $/m^2 [28].

(2) The battery storage subsystem, with the following characteristics:

- Battery storage efficiency, η_B, is taken to be 0.81.

- Unitary cost of this subsystem is taken to be 60 $/kWh.

- Life service is 10 years.

- Maintenance coefficient, MC, is 5% .

- Interest rate, IR, is 2%.

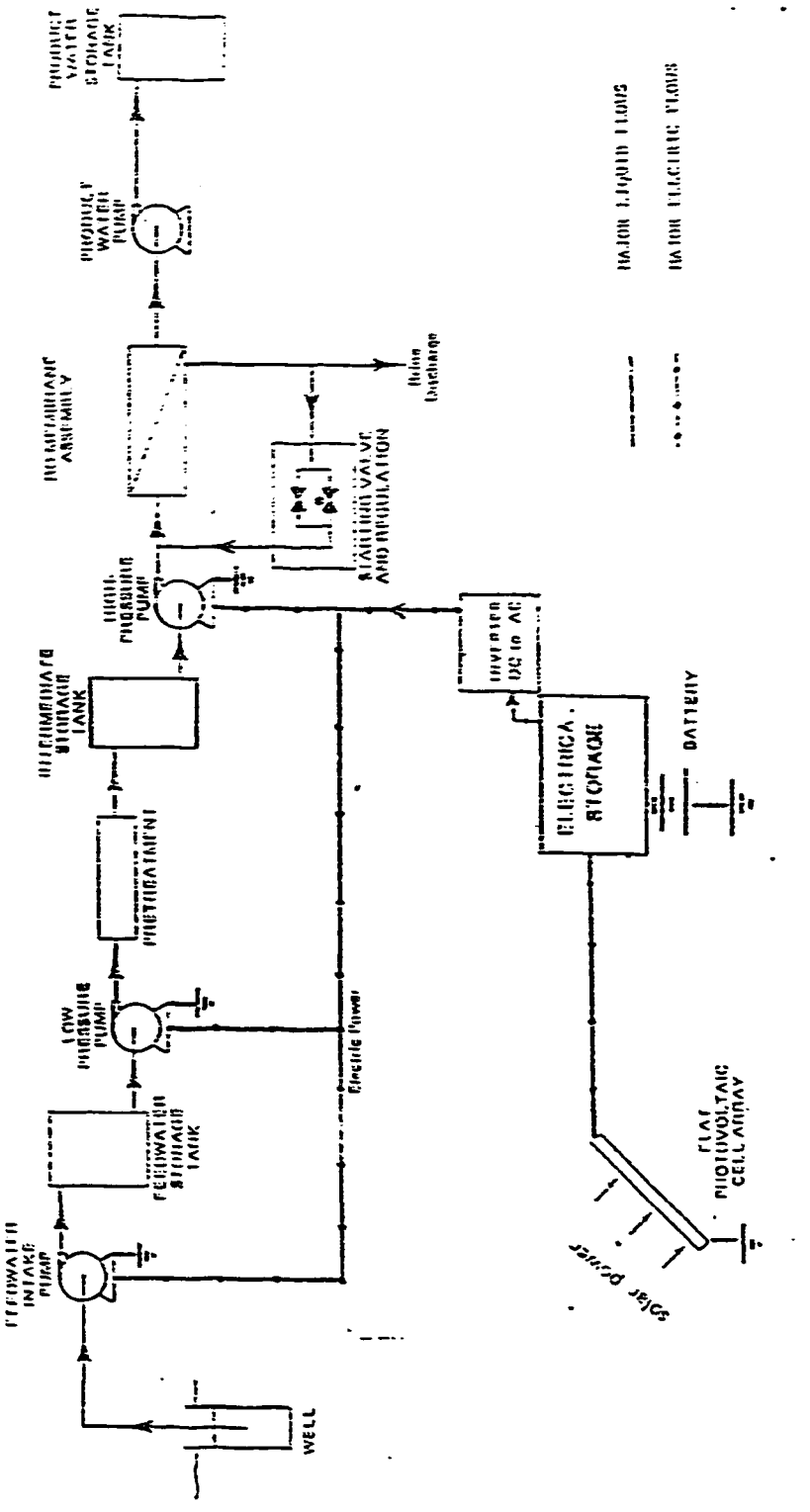

Figure (6.11) Design Concept of the Proposed PV-RO (BW) System

(3) The reverse osmosis, R.O. subsystem, with the following characteristics:

- Membrane modules life service is assumed to be 5 years.
- Capital cost, CC_{RO}, is taken to be 150 $/($m^3$/day) [53].
- Operating pressure is 40 bar suitable for desalting brackish water.
- Operational time is 24 h/day.
- Gross energy consumption is 3.0 kWh/m^3.
- RO subsystem life service is taken to be 15 years.
- Interest rate, IR, is 0.02.

PV Optimal Sizing Analysis

Sizing requirements of the PV subsystem (i.e. sizing of the collector face area, A_c, and battery storage capacity) are to be based on the month of December (with the lowest solar insolation value). The size of the PV has to meet the electrical load required by the RO subsystem. The following Eqs. [28] are used to find the optimal PV-array area, battery storage capacity, and PV-RO system's total cost. These Eqs. are :

$$(A_c)_{opt} = \frac{f_s}{I_m} + \frac{\xi j_m^{-\lambda}}{I_m(1-f_s)} \left[J_m^{-\lambda} \frac{(UC)_{PV}}{(UC)_B} \frac{\xi \lambda}{I_m(1-f_s)} \right]^{\frac{-\lambda}{1+\lambda}} \quad (6.19)$$

$$(C_B)_{opt} = \left[J_m^{-\lambda} \frac{(UC)_{PV}}{(UC)_B} \frac{\xi \lambda}{I_m(1-f_s)} \right]^{\frac{1}{1+\lambda}} \quad (6.20)$$

$$(STL)_{opt} = (UC)_{PV}(A_c)_{opt} + (UC)_B(C_B)_{opt} + (CC)_{RO} \quad (6.21)$$

where

$(A_c)_{opt}$ is the optimum collector area

f_s is the monthly solar fraction

I_m = normalized variable and equals to

$$= \frac{\overline{H}_T \eta_{PV} \eta_B}{L_m}$$

L_m is the electrical load need to be met by PV in Watts

$\overline{H}_T$ is the monthly average incident radiation on a tilted surface (W/m^2) defined in chapter 5.

ξ is constant and equals to 2.41×10^{-2}

λ is constant and equals to 2.29

J_m = normalized variable and equals to

$$= \frac{\overline{K}_T d_m}{L_m}$$

d_m is the fractional length of the sunshine hours in a day

$\overline{K}_T$ is the monthly average clearness index

$(C_B)_{opt}$ is the battery optimum storage capacity in kWh

$(STL)_{opt}$ is the system's optimum total cost in $

and

$(UC)_B$ and $(UC)_{PV}$ are as defined before.

Economics Analysis

The parameter I_m and J_m can be determined from Eqs. (6.20) and (6.21) respectively. Table (6.8) is obtained by using the specified values of η_{PV} and η_B and obtaining the values of $\overline{H}_T$ and d_m (chapter 5) for every month in a year, and implementing them in Eqs. (6.20) and (6.21). From this table we note that the lowest values of I_m and J_m are occurring in the month of December. Thus, the analysis will be based on this month (as anticipated earlier in this chapter). Eqs. (6.19) through (6.21) can be simplified if we use the values of I_m and J_m for December and ξ, λ, $(UC)_{PV}$ and $(UC)_B$ in this Eqs. In doing so we

Table (6.8) Data Used for the Optimal Analysis of The RO-PV Plant

Month	$\overline{K}_T$	d_m	$\overline{H}_T$ (W/m^2)	L_m (kW)	I_m ($\times 10^{-3}$)	J_m ($\times 10^{-3}$)
Jan.	0.58	0.417	208	12.5	1.50	1.57
Feb.	0.52	0.417	194	12.5	1.40	1.41
Mar.	0.58	0.417	238	12.5	1.72	1.57
Apr.	0.56	0.500	240	12.5	1.72	1.81
May	0.68	0.500	283	12.5	2.04	2.20
June	0.67	0.500	276	12.5	1.99	2.17
July	0.64	0.500	262	12.5	1.89	2.07
Aug.	0.66	0.500	275	12.5	1.98	2.14
Sep.	0.65	0.500	272	12.5	1.96	2.11
Oct.	0.64	0.417	257	12.5	1.85	1.73
Nov.	0.62	0.417	232	12.5	1.67	1.68
Dec.	0.55	0.417	192	12.5	1.38	1.49

obtain

$$(STL)_{opt} = 53.37\, L_m f_s + 134.1\, L_m (1 - f_s)^{-0.304} \div (CC)_{RO} \qquad (6.22)$$

The capital cost of the RO subsystem can be determined as follows

$$(CC)_{RO} = (UC)_{RO} \times PC \qquad (6.23)$$

where

$(CC)_{RO}$ = capital cost of RO in S

PC = production capacity in m^3/day

$(UC)_{RO}$ = unit cost of RO taken as 150 $S/(m^3/day)$.

Thus, Eq. (6.23) becomes

$$(CC)_{RO} = 150\, PC \qquad (6.24)$$

and using the present value method Eq. (6.11) with IR is 2%, y is 15 , and MC is 2%, we get

$$(pv)_{RO} = 178.79\, PC\,. \qquad (6.25)$$

The term on the R.H.S of Eq. (6.22) is nothing but the capital cost of the PV (including battery) subsystem, i.e.

$$(CC)_{PV} = 53.37\, L_m f_s + 134.1\, L_m (1 - f_s)^{-0.304}\,. \qquad (6.26)$$

Applying the present value method for PV, with IR is 2%, y is 15, and MC is

2%. we get

$$(pv)_{PV} = 1.257\,(CC)_{PV}. \tag{6.27}$$

Thus, Eq. (6.22) becomes

$$(pv)_{opt} = (pv)_{PV} + (pv)_{RO} \tag{6.28}$$

Eq. (6.28) gives the optimum total present value (in S) for the autonomous PV-RO system. Substituting Eq. (6.26) in (6.27) we get

$$(pv)_{PV} = 1.2570\,[\,53.37\,L_m f_s + 134.1\,L_m\,(1 - f_s)^{-0.304}\,]. \tag{6.29}$$

The parameter L_m can be expressed in terms of PC as:

$$L_m = 3 \times PC \times \frac{1}{24} \tag{6.30}$$

where

L_m = load in kW

PC = production in m^3/day.

the numbers 3 and 24 refer to the specific electrical consumption (i.e. $3\,kWh/m^3$) and the number of hours in a day respectively. Simplifying Eq. (6.30) , we get

$$L_m = 0.125\,PC. \tag{6.31}$$

So for PC equals to $100\,m^3/day$, the corresponding electrical power

consumption, L_m, is 12.5 kW. Substituting Eqs. (6.25) and (6.29) in Eq. (6.28), we obtain

$$(pv)_{opt} = 1.257\,[\,53.37\,L_m f_s + 134.1\,L_m (1 - f_s)^{-0.304}] + 178.79\,PC\ . \tag{6.32}$$

It should be noted that the unit of L_m in this equation is Watt. Also, as the solar fraction, f_s, approaches the value of 1.0 (i.e. Solar is providing 100% of the require load), the present value of the system goes to infinity. This means that Eq. (6.32) is feasible to be used at lower f_s. For f_s equals to 0.99 and production capacity equals to 100 m^3/day, we obtain

$$(pv)_{opt} = 9.93 \times 10^6\ \$\ .$$

In order to get the optimum value of the unit water cost, we substitute this vlue in Eq. (6.16). Thus,

$$(Unit\ water\ cost)_{opt} = \frac{9.39 \times 10^6}{365 \times 15 \times 100} = 17.2\ \$/m^3\ .$$

6.2.3 The Autonomous WECS-RO System (Configuration No.2)

The design concept of this configuration is shown in figure (6.12). In this system the WECS subsystem is supposed to provide the full (100%) electrical power required to operate the RO subsystem.

Design Data

(1) The reverse osmosis subsystem has the same characteristics as those in the first configuration.

(2) The WECS subsystem is the same as that taken previously in part (6.1.2).

WECS Sizing Analysis

Fig. (6.4) is used to determine the wind fraction, f_w, as before. For example, if PC is $100\ m^3/day$ (equivalent to $L_m = P_e^{'} = 12.5\ kW$), the corresponding f_w from figure (6.4) is found to be 0.24 (i.e. 24% of the load is supplied by WEC) at DS equals 1.0 and α equals 1.44. Thus, four WEC machines are needed to meet the load.

Economics Analysis

Using the present value method in a manner similar to the previous analysis we are able to determine the unit water cost at different production capacities. The equation to be used is:

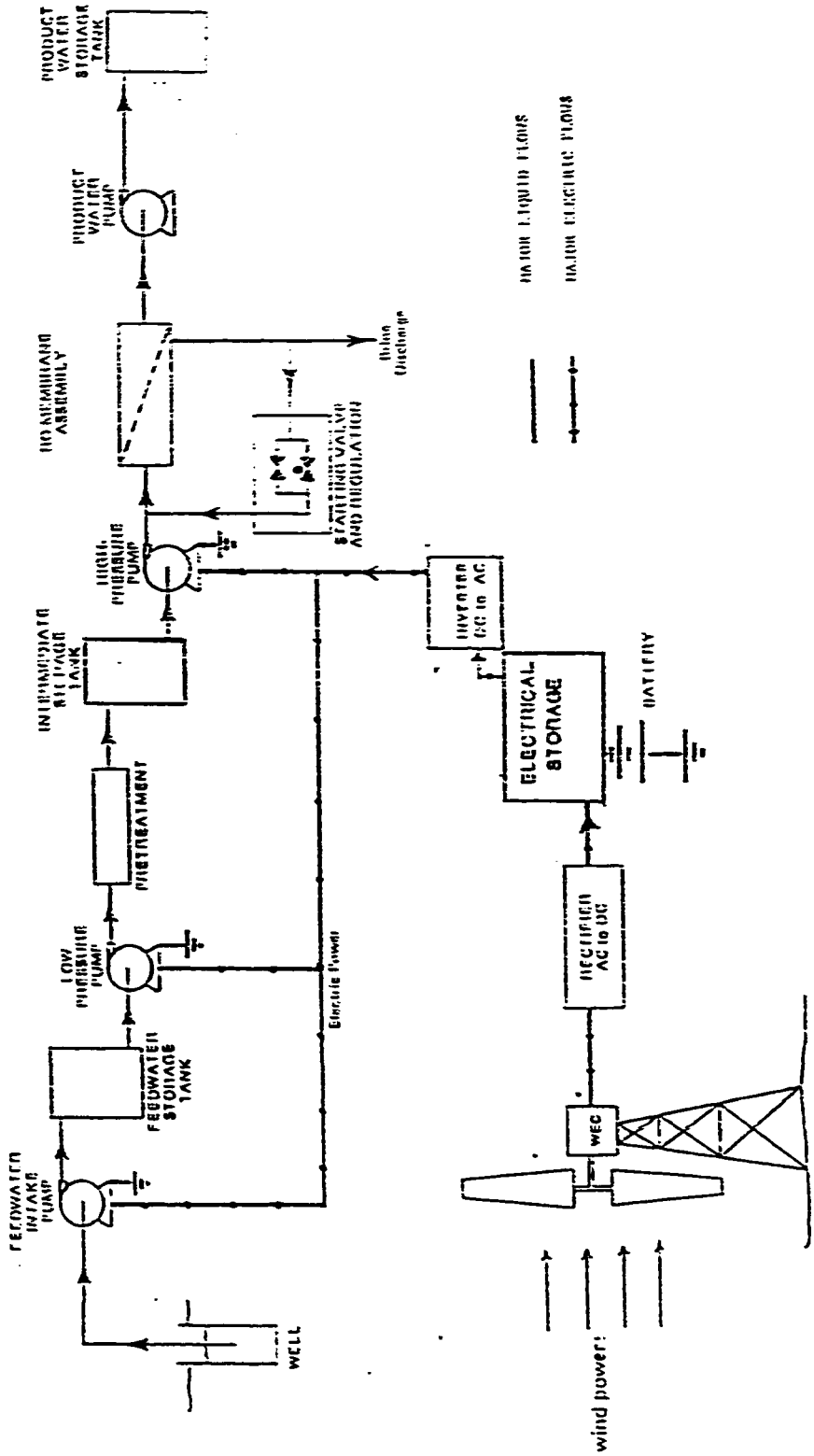

Figure (6.12) Design Concept for the Proposed WECS-RO (BW) System

$$(pv)_{tot} = (pv)_{WECS} + (pv)_{RO} \tag{6.33}$$

and substituting Eqs. (6.15) and (6.25) in Eq. (6.33), we get

$$(pv)_{tot} = N_{WEC}[2.72636\,\alpha + 5.21688\,(DS)]\,P_e^{'} + 178.79\,PC\,. \tag{6.34}$$

Substituting

$N_{WEC} = 4$

$\alpha = 1.44$

$DS = 1.0$

$P_e^{'} = 12.5 \times 10^3$

$PC = 100$

in Eq. (6.34), we get

$$(pv)_{tot} = 0.4575 \times 10^6\ \text{S}\,.$$

Thus, the unit water cost from Eq. (6.16) is 0.87 S/m^3.

It is interesting to compare between the two proposed configurations in terms of the unit water cost. It is found that, it costs 0.87 S to produce one cubic meter of fresh water using the WECS-RO system (configur. 2), while it costs 17.2 S to produce the same amount of fresh water using the PV-RO system (configure1), which means twenty times as much. The main reason behind this high cost of producing water by the latter method is due to the high cost of the photovoltaic cells combined with the battery cost. This fact suggests that using wind power to operate the RO plant is more favourable (from

economics viewpoint) than using solar power. The case when these two solar-wind are combined is discussed next.

6.2.4 The Combined Solar/Wind-Powered RO System

The design concept of this part is shown in figure (6.13). In this figure we notice that the WECS and PV subsystems are used to operate the RO subsystem. This part is considered to be more general as compared to the previous parts. The basic concept of combining the two subsystems is illustrated in figure (6.14).

Design Data

The design data for this part is taken identical to the previous two parts.

System Economics Analysis

The equation to be used for the analysis is

$$(pv)_{tot} = (pv)_{WECS} + (pv)_{PV} + (pv)_{RO} \tag{6.35}$$

where $(pv)_{PV}$ and $(pv)_{WECS}$ are obtained from Eqs. (6.29) and (6.34) respectively. The monthly solar fraction, f_s, is imbedded in Eq. (6.29), while the monthly wind fraction, f_w, is imbedded in Eq. (6.34). The utilization of solar or wind is dependent on the choice of these two fractions.

The analysis for this part is similar in nature to the previous two parts and the procedure is straight forward. According to the choice of f_w, and f_s, the unit water cost is calculated by means of Eqs. (6.29), (6.34), and (6.35). For water production capacity ranging between 10-30 m^3/day, the unit water cost is

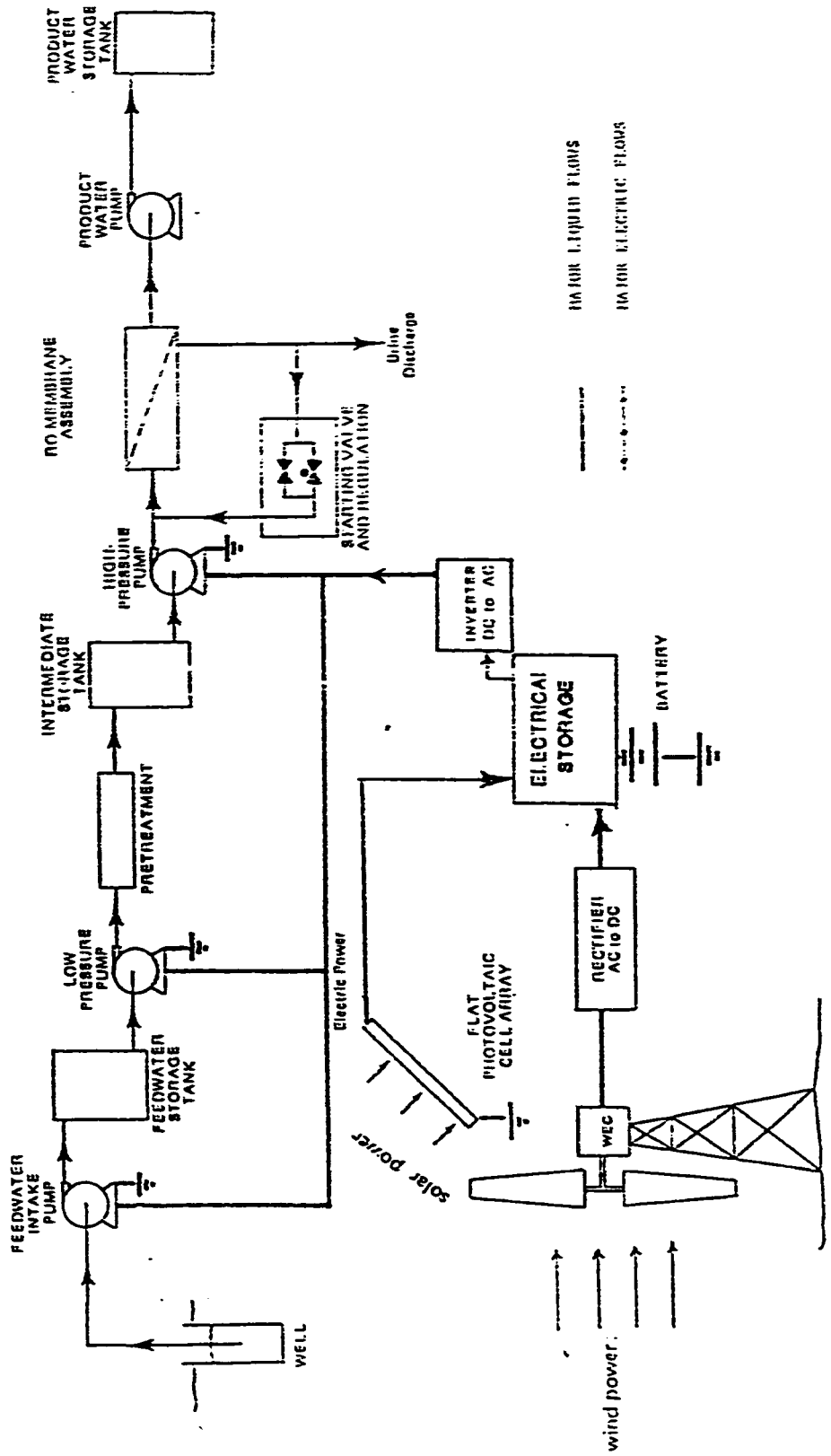

Figure (6.13) Design Concept for the Proposed Solar/Wind-Powered RO System

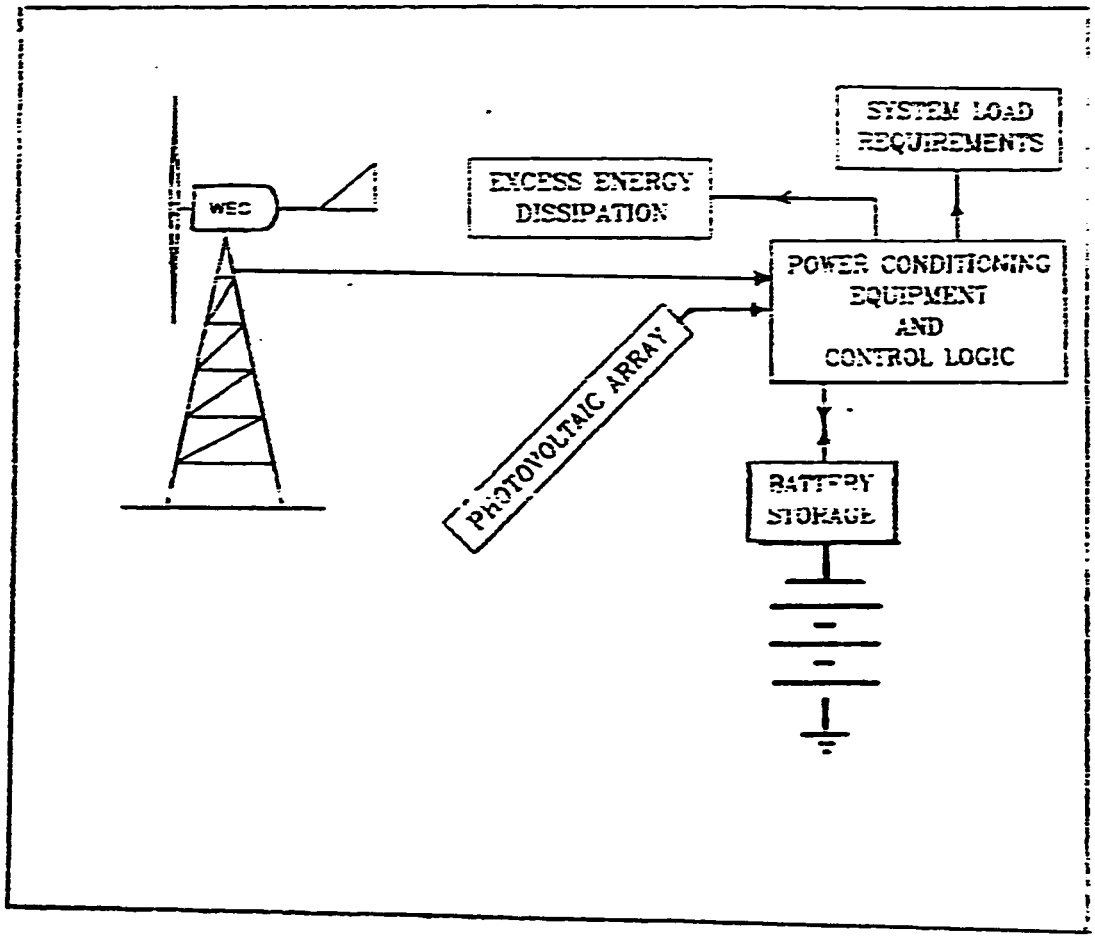

Figure (6.14) Block Diagram for the Combined WECS-PV System

calculated at different values of f_s, and f_w, and the result is shown in figure (6.15). It should be noted from this figure that only one WEC machine is used. This explains the reason why the fraction f_w ranges between 0.1-0.7 which means that the WEC machine can at maximum provide 70 % of the load requirement. The unit water cost is also calculated at different values of f_w, and f_s, for production capacity maintained at 120 m^3 day as demonstrated in figure (6.16). It is obvious from this figure that it is more economically feasible to use the WECS subsystem to provide the full (100%) electrical load demand.

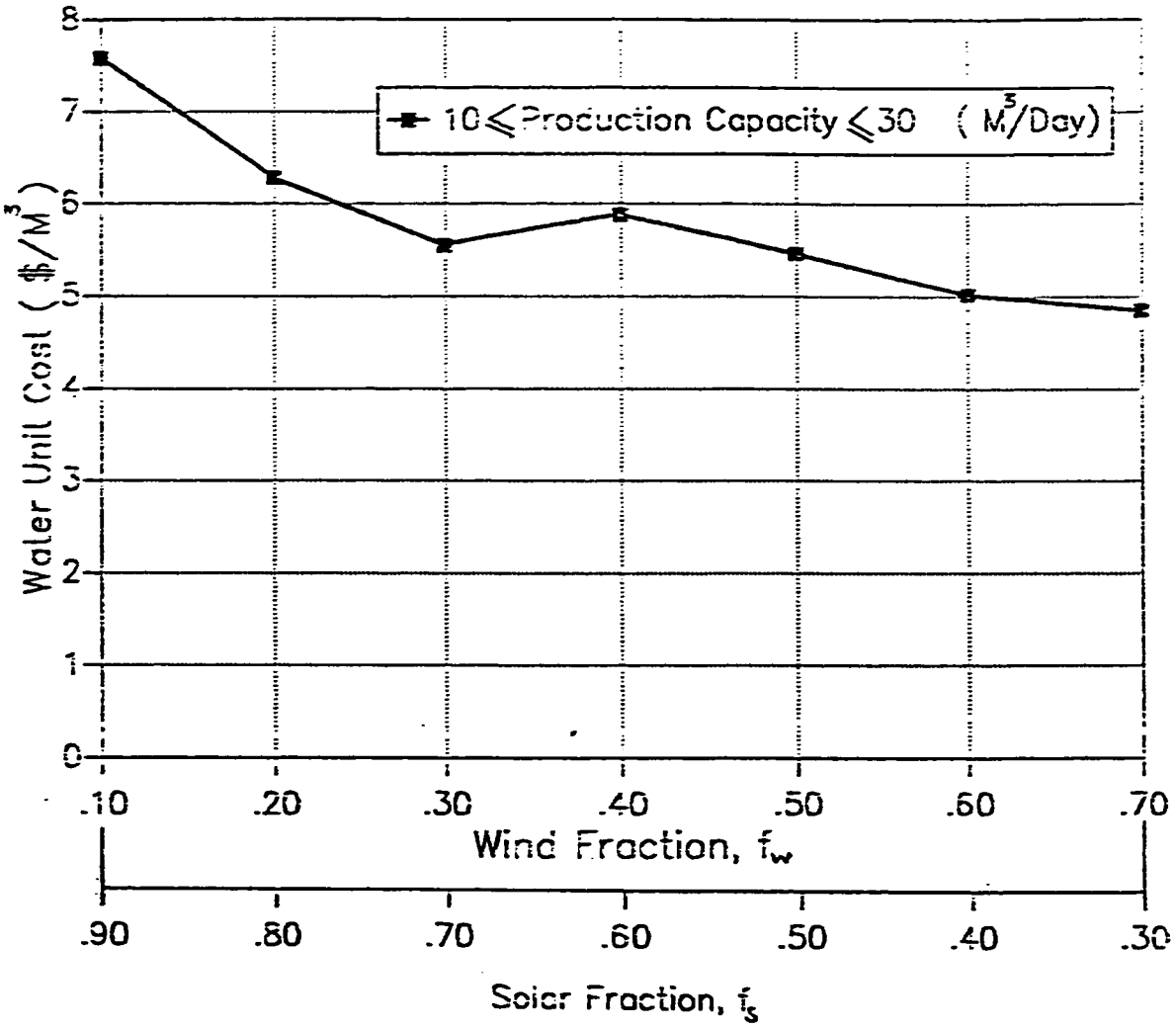

Figure (6.15) Water Unit Cost of a Typical Solar/Wind RO (BW) Plant

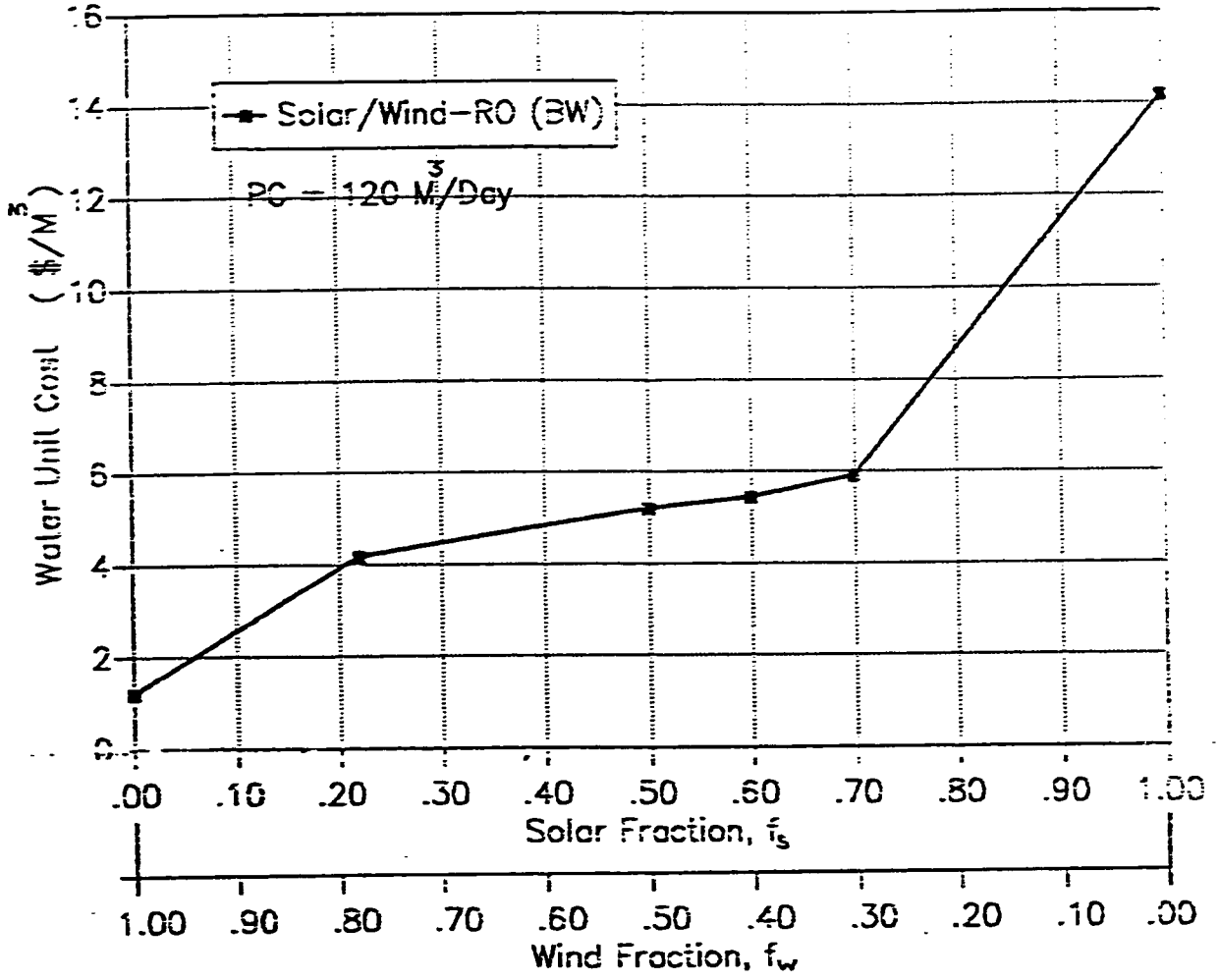

Figure (6.16) Water Cost for a Typical Solar/Wind-RO (BW) Plant

6.3 Solar/Wind-Powered RO (SW) System

6.3.1 Autonomous PV-Powered RO (SW) System

The design concept for this system is almost identical to that used for PV-powered RO (BW) system. The basic difference between these two is that the latter is used to desalinate seawater, whereas the former is designed to desalinate brackish water. This implies that the electrical consumption is different for each case. Seawater desalination by an RO process consumes more electrical power than that of brackish water as discussed earlier in chapter 3. This idea is reflected from the fact that it takes more pumping requirements for RO processes to desalinate high saline water (e.g. seawater) than that to desalinate low saline water (e.g. brackish water). the design concept for the proposed stand-alone PV-RO (SW) system is depicted in figure (6.17).

Economics Analysis

The sizing and economics analysis for this case is identical to that case presented in section (6.2.2). The equations to be used for this case are (6.28) and (6.29). However, Eq. (6.24) and consequently Eqs. (6.25), (6.30), (6.31), and (6.32) have to be slightly modified so as to account for the change in the electrical power consumption load and the capital cost of the RO subsystem. Hence, assuming a specific electrical consumption for this case equals to $8\ kWh/m^3$ and the unit capital cost equals to $1500\ \$/(m^3/day)$, and implementing these two Eqs. in Eqs. (6.24) through (6.32), we get

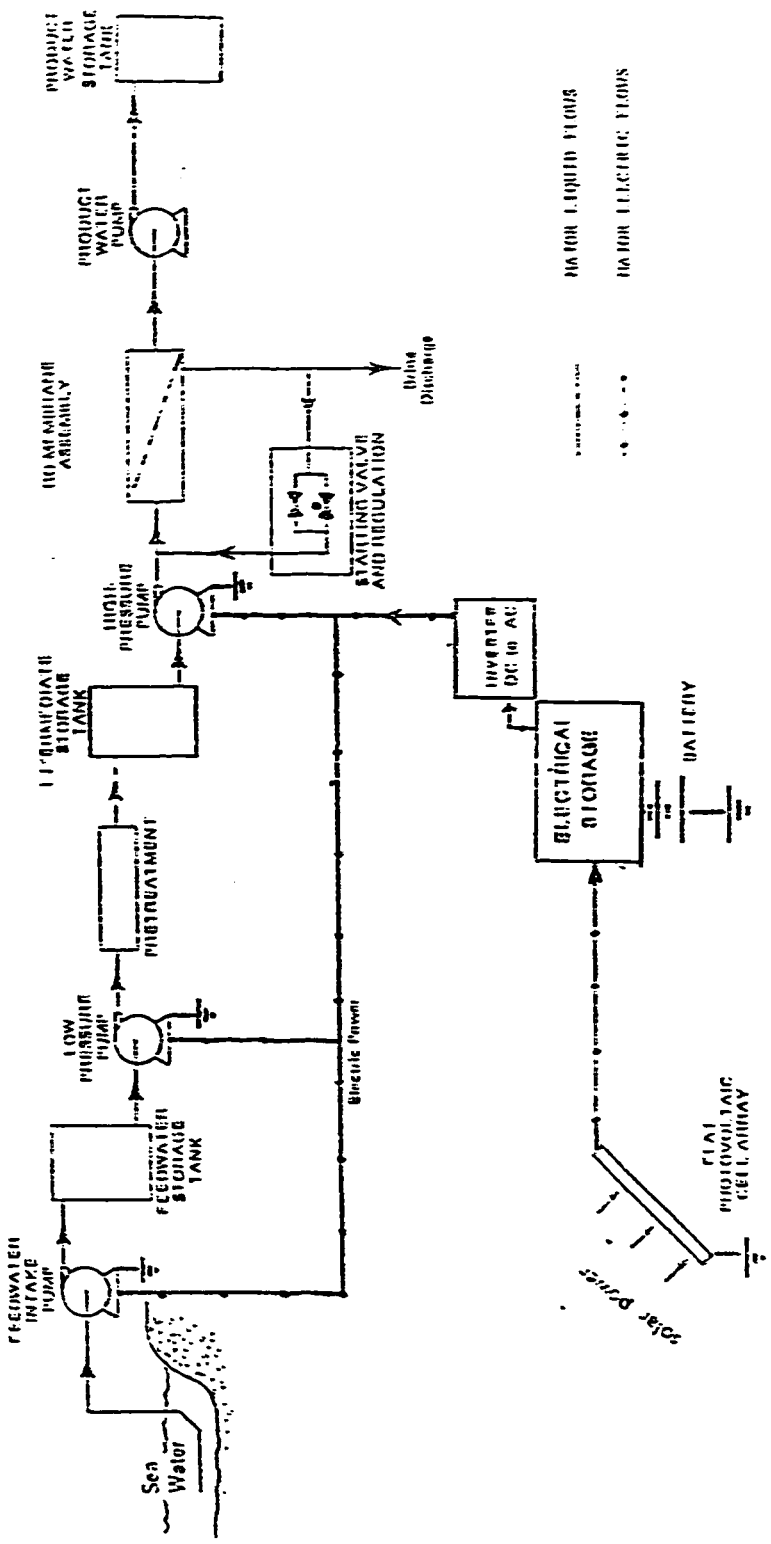

Figure (6.17) Design Concept for the Proposed Stand-Alone PV-RO (SW) System

$$(CC)_{RO} = 1500\ PC \tag{6.36}$$

$$(pv)_{RO} = 1787.9\ PC \tag{6.37}$$

$$L_m = 334\ PC\ ,\ W \tag{6.38}$$

and

$$(pv)_{opt} = 1.257\,[\,53.37\ L_m f_s \div 134.1\ L_m (1 - f_s)^{-0.304}] + 1787.9\ PC\ . \tag{6.39}$$

As an example, if we assume that the required PC to be $100\ m^3/day$ and the solar fraction is assumed to be roughly equals to 1.0 (e.g. 0.99) and implementing these values in the last four equations, we obtain

$$(CC)_{RO} = 150000\ \$$$

$$(pv)_{RO} = 178790\ \$$$

$$L_m = 33400\ W$$

$$(pv)_{tot} = 25.23 \times 10^6\ \$$$

and substituting this value of $(pv)_{tot}$ in Eq. (6.16), we get

$$unit\ water\ cost = 46.1\ \$/m^3.$$

Comparing this value of 46.1 $\$/m^3$ with that 17.2 $\$/m^3$ (obtained previously for the PV-RO/BW system), we conclude that it is highly expensive to desalinate seawater using PV-RO system (the cost is about three times of that for brackish water).

6.3.2 Autonomous WECS-Powered RO (SW) System

The design concept of this system is identical to that of section (6.2.3) as illustrated in figure (6.18).

Economics Analysis

Modifying the last term in Eq. (6.34), we obtain

$$(pv)_{tot} = N_{WEC}[2.72636\,\alpha + 5.21688\,(DS)]\,P_e' + 1787.9\,PC\,. \qquad (6.40)$$

This equation is to be used in coordination with Eq. (6.37) and (6.38). As an example to illustrate the use of this equation, we assume the production capacity of this system to be $100\,m^3/day$ which is equivalent to $33.4\,kW$ electrical load. Taking 1/4 of this total load which gives p'_e equals to $8.35\,kW$ and α equals to 2.16, and using figure (6.4), we get f_w equals to 0.38 at DS equals to 1. This means that we need at least three WEC machines to meet the partial load p'_e and a total of 12 machines to meet the total load. Substituting these values in Eqs. (6.16) and (6.40), we obtain

$$(pv)_{tot} = 1.292 \times 10^6\ \$$$

and

$$unit\ water\ cost = 2.36\ \$/m^3\,.$$

This cost is much cheaper than that obtained for solar-PV ($46.1\ \$/m^3$), but more expensive than that obtained from the WECS-RO (BW) system

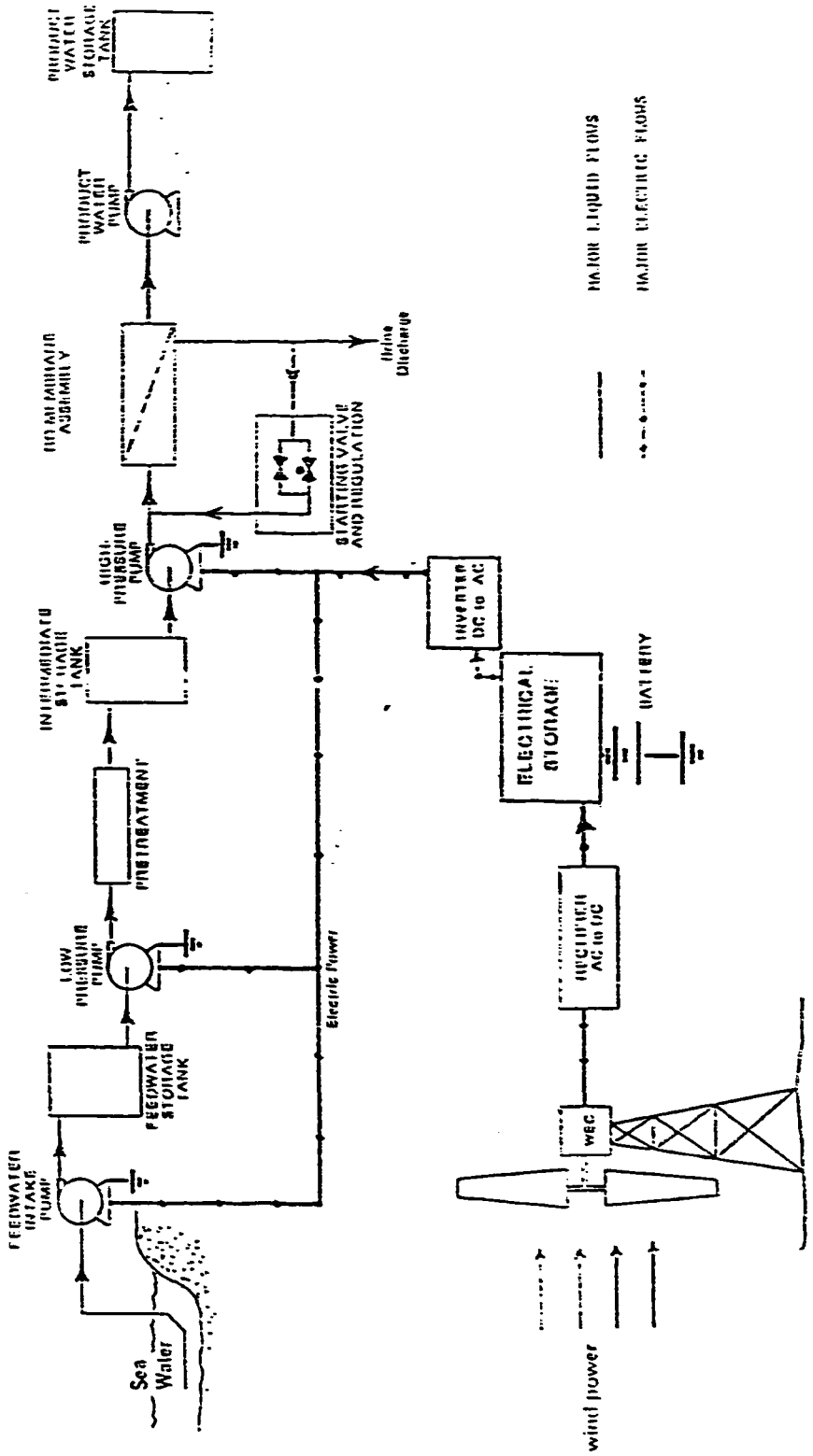

Figure (6.18) Desgin Concept for the Proposed WECS-RO (BW) System

(0.87 $/m^3$).

In conclusion, it is more economically feasible to desalinate brackish water using wind power as a source to fully operate the RO system than that for seawater and than that using solar power. The production capacity as a function of water cost is shown in figure (6.19).

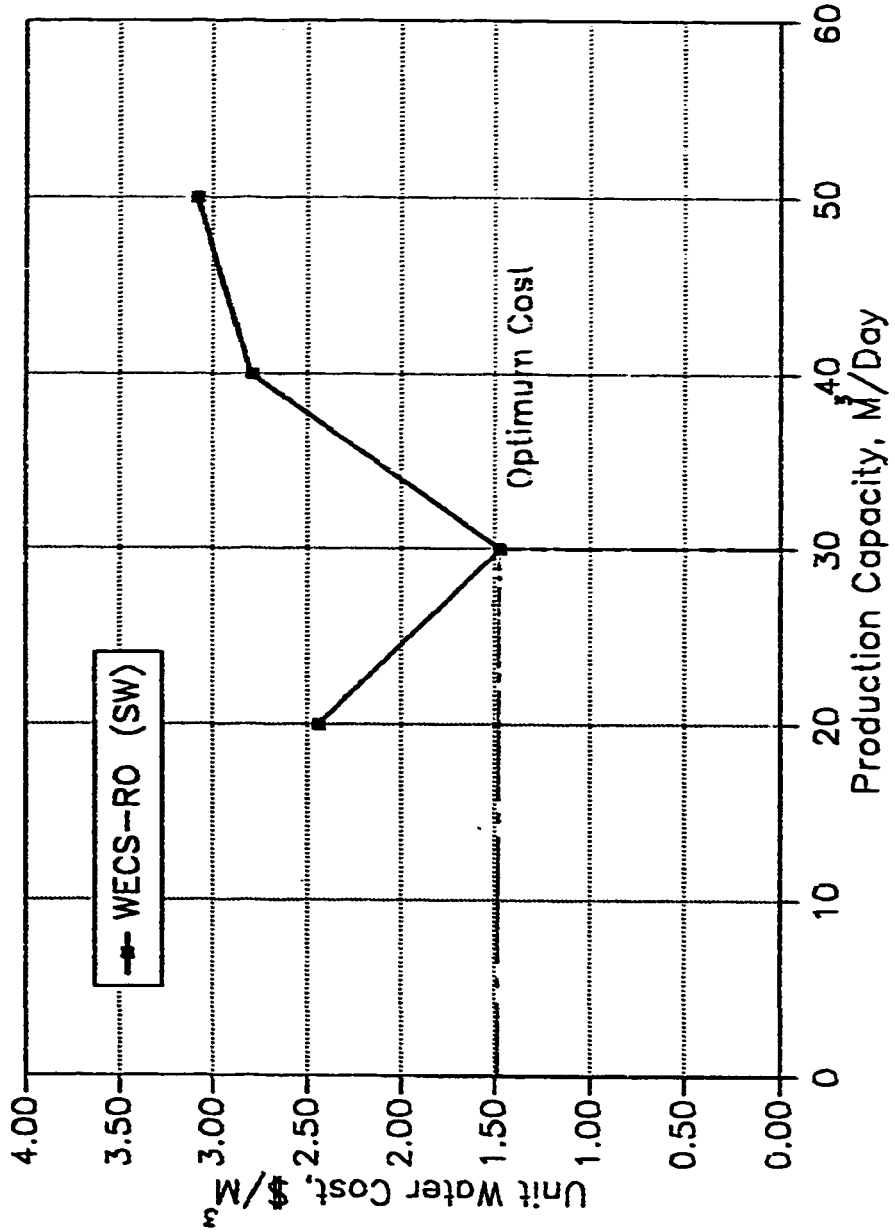

Figure (6.19) Water Cost for Seawater WECS-RO Plant

6.3.3 Combined Solar/Wind-Powered RO (SW) System

The design concept of this system is shown in figure (6.20).

Economics Analysis

Combining Eqs. (6.39) and (6.40), we obtain

$$(pv)_{tot} = N_{WEC}^{*}\,[2.72636\,\alpha + 5.21688\,(DS)]\,P_e' + 1.257\,[\,53.37\,L_m f_s + 134.1\,L_m\,(1 - f_s)^{-0.304}] + 1787.9\,PC\,. \qquad (6.41)$$

Using this equation we can determine the cost of the produced water at different solar-wind fractions. Fig. (6.21) illustrates the relation between the water cost and the solar-wind fractions at a fixed production load (120 m^3/day). From this figure, we conclude that it is much cheaper to produce fresh water using the WECS-RO system.

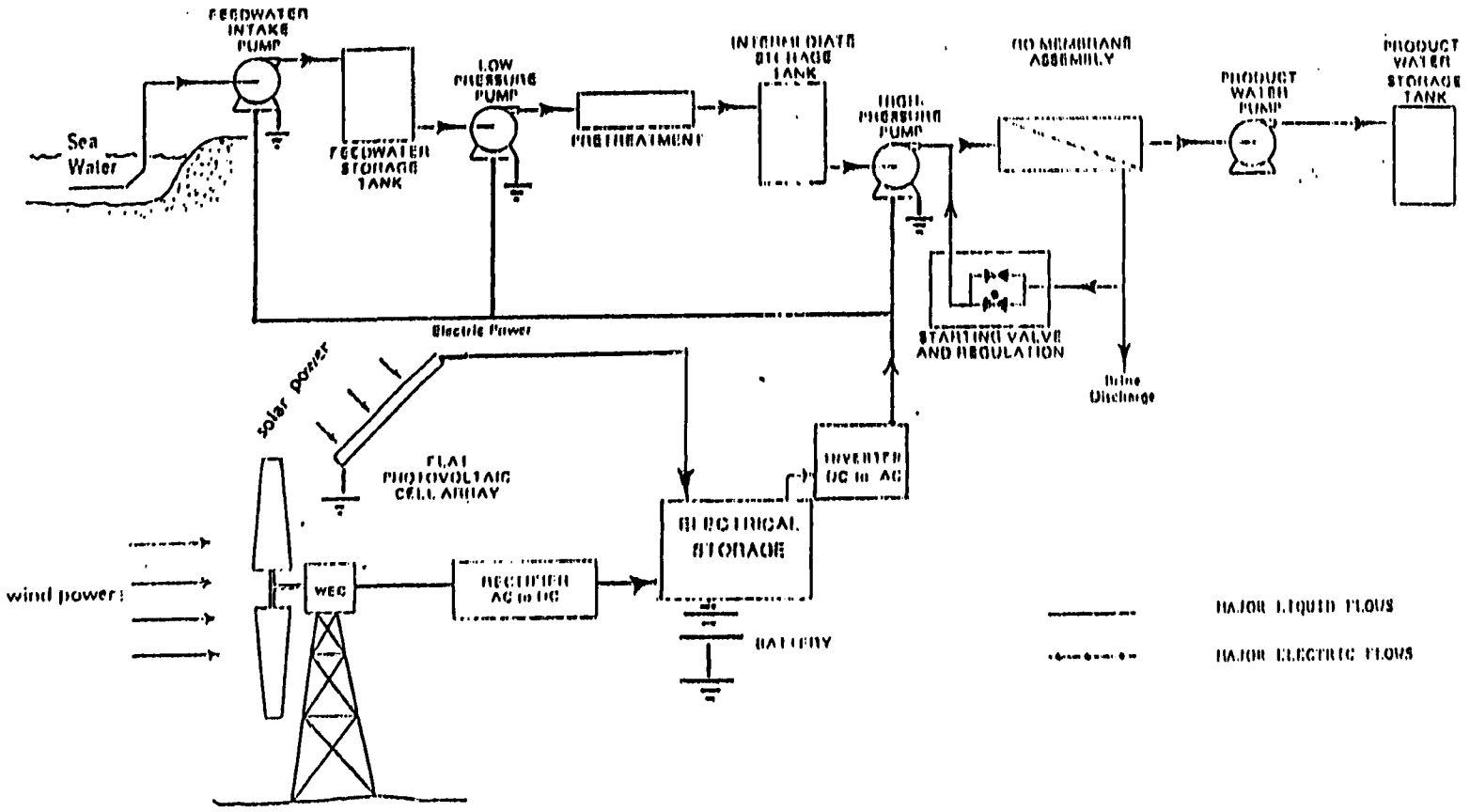

Figure (6.20) Desgin Concept for the Proposed Solar/Wind-Powered RO System

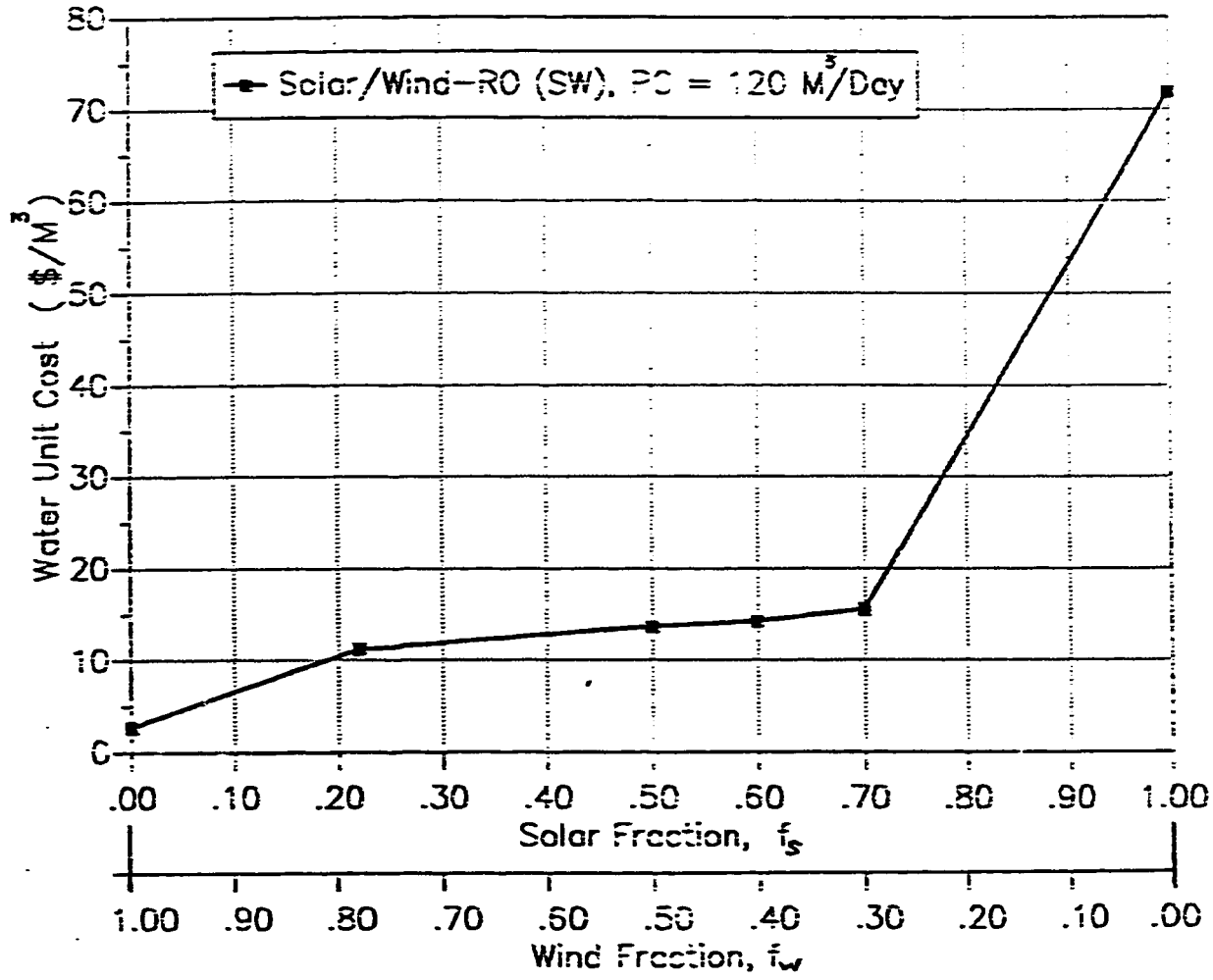

Figure (6.21) Water Cost for a Typical Solar/Wind-RO (SW) Plant

6.4 Conclusions And Recommendations

In this chapter, several designs are proposed for the desalination of saline water. These designs are basically based on the following requirements:

1. Viability for application under the prevailing climatic conditions of Dhahran city.

2. The selected desalination process is required to produce freshwater with salinity ranging between 200-500 p.p.m.

3. Suitability for operation in remote locations.

4. Production capacity ranging between 10-150 m^3/day.

5. Operational time is 24 h/day.

6. Low investment costs.

Basically, two desalination processes have been chosen for coupling with solar and wind power. These two processes are the reverse osmosis process which requires solely electrical power and multieffect-stack process which requires mainly thermal energy.

Systems Comparison

Three reverse osmosis subsystems are compared on the basis of their electrical power consumption in figure (6.22). From this figure we conclude that seawater-RO consumes much more electrical power than that of brackish-RO. This

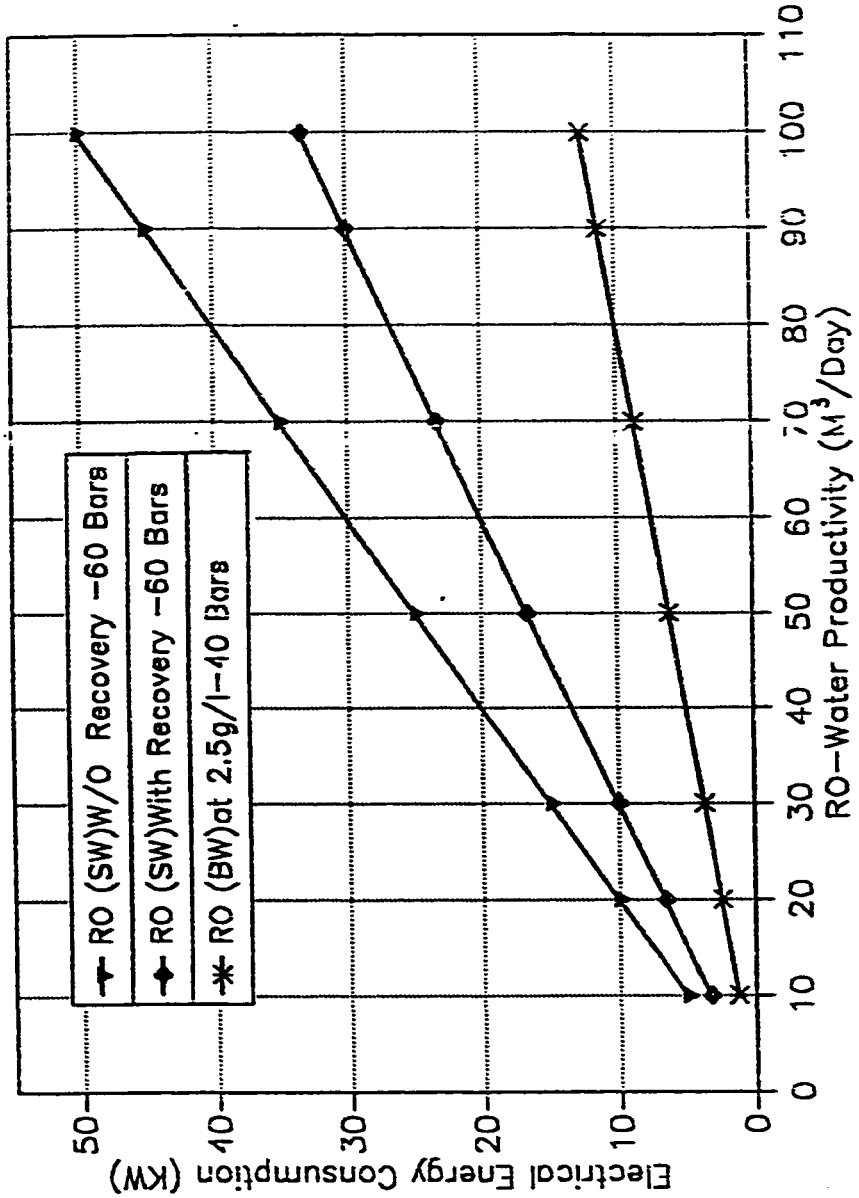

Figure (6.22) Energy Consumption for Various RO Units

difference in the power consumption increases drastically as the water production increases. The optimal sizing method has been used to optimize the PV-collector areas at specific load requirements as shown in figure (6.23).

It was found that it is much cheaper to desalinate brackish water using the WECS-RO system than to desalinate seawater as illustrated in figure (6.24). Comparison between these two as a function of solar-wind fractions is shown in figure (6.25). Desalting brackish water using wind-powered RO system is much cheaper than desalting seawater using wind-powered MES. However, it is relatively cheaper to desalinate seawater using solar-powered MES than to desalinate brackish water using solar-powered RO as shown in figure (6.26). Comparison of water cost for the two (MES and RO) processes operated by wind is illustrated in figure (6.27). From this figure, we note that it is relatively very expensive to desalinate seawater using the autonomous wind-powered MES system even at lower production capacities. Comparison of these two processes in relation to variable solar-wind fractions is demonstrated in figure (6.28). It can be concluded that the incident solar power is an economically feasible choice to be converted into thermal energy which can be used to operate the MES process, while the wind power (but not the solar) is to be converted into electrical power to run the RO process. The choice of using solar for conversion into electrical power becomes economically feasible when the investment of photovoltaic cells becomes attractive.

The relation between the number of WEC machines and the wind fraction, f_w, for the MES and RO processes is shown in figure (6.29). It can be noted

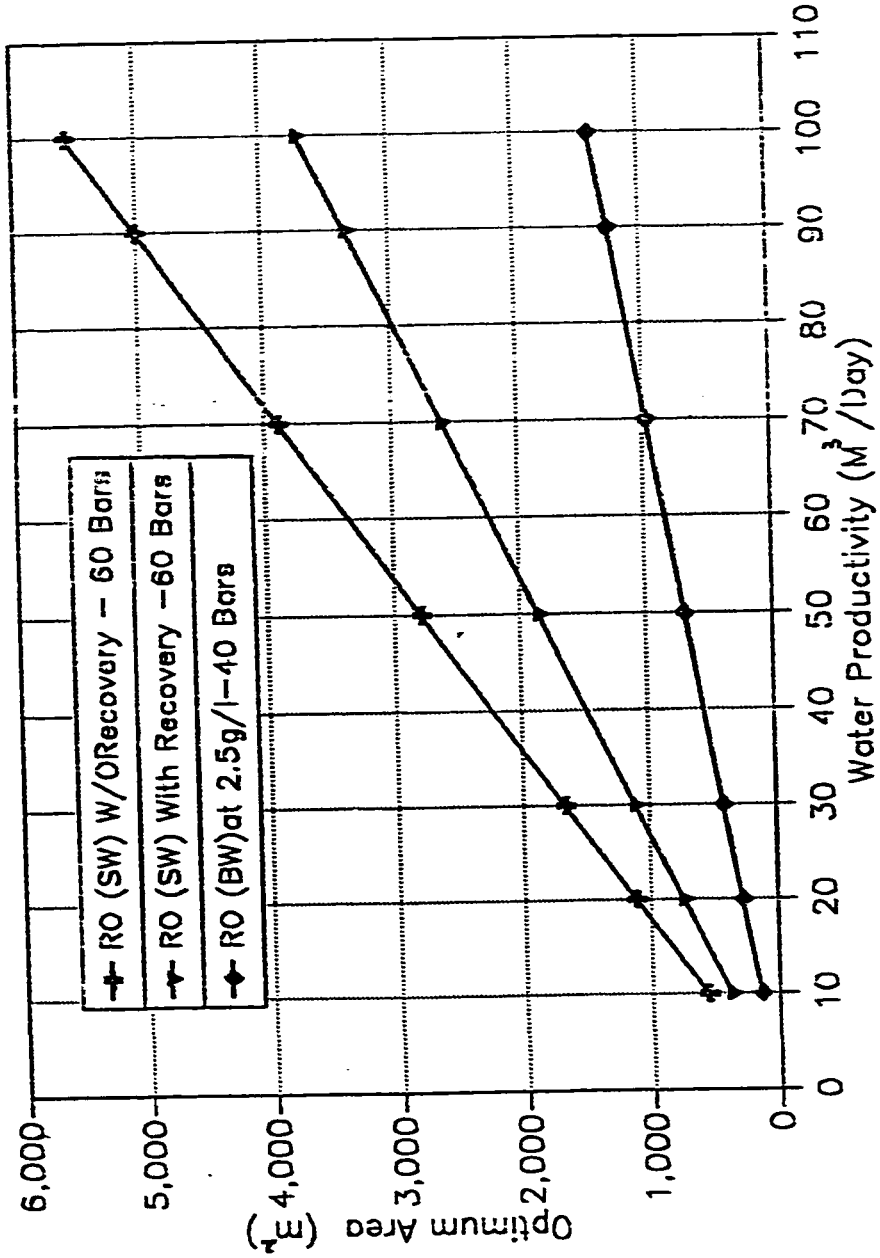

Figure (6.23) Optimal Areas of PV-Array for Various RO-Units

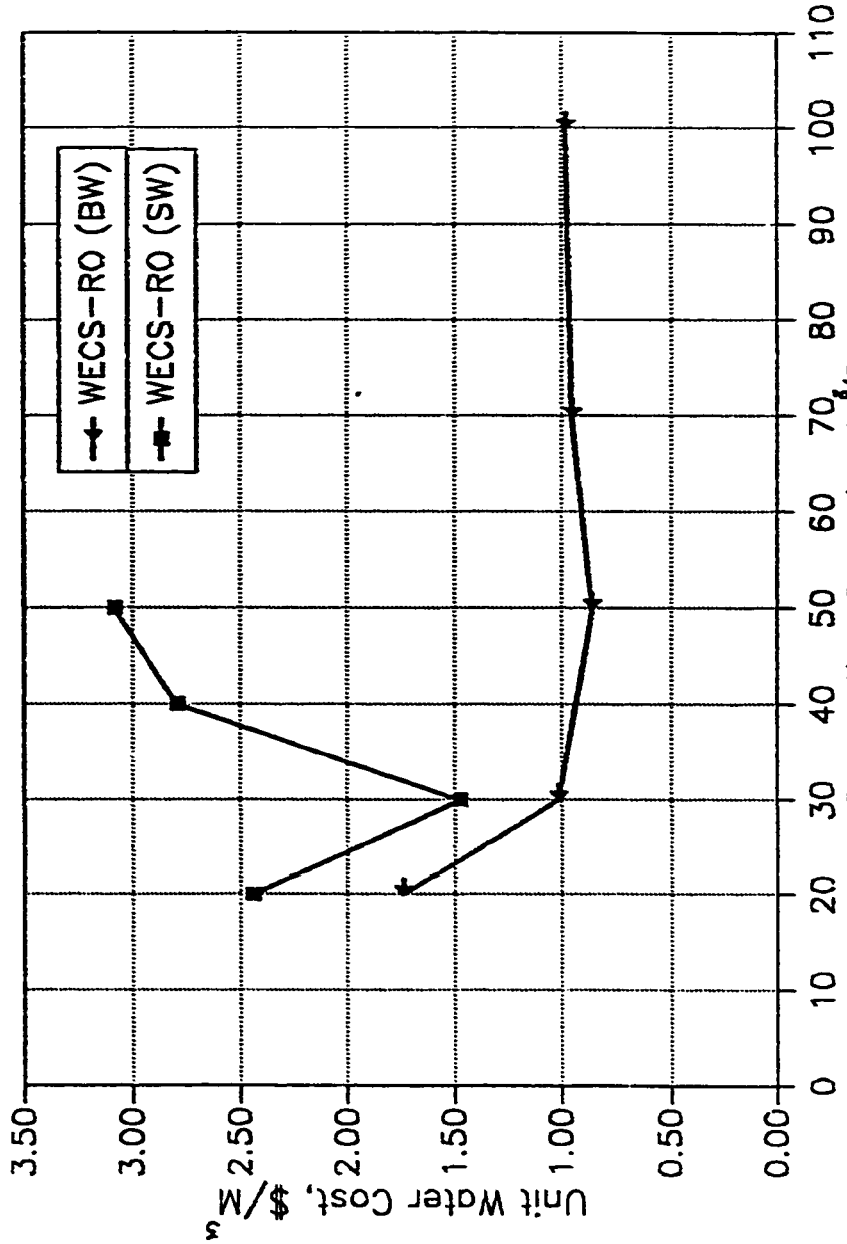

Figure (6.24) Water Cost Various WECS-RO Plants

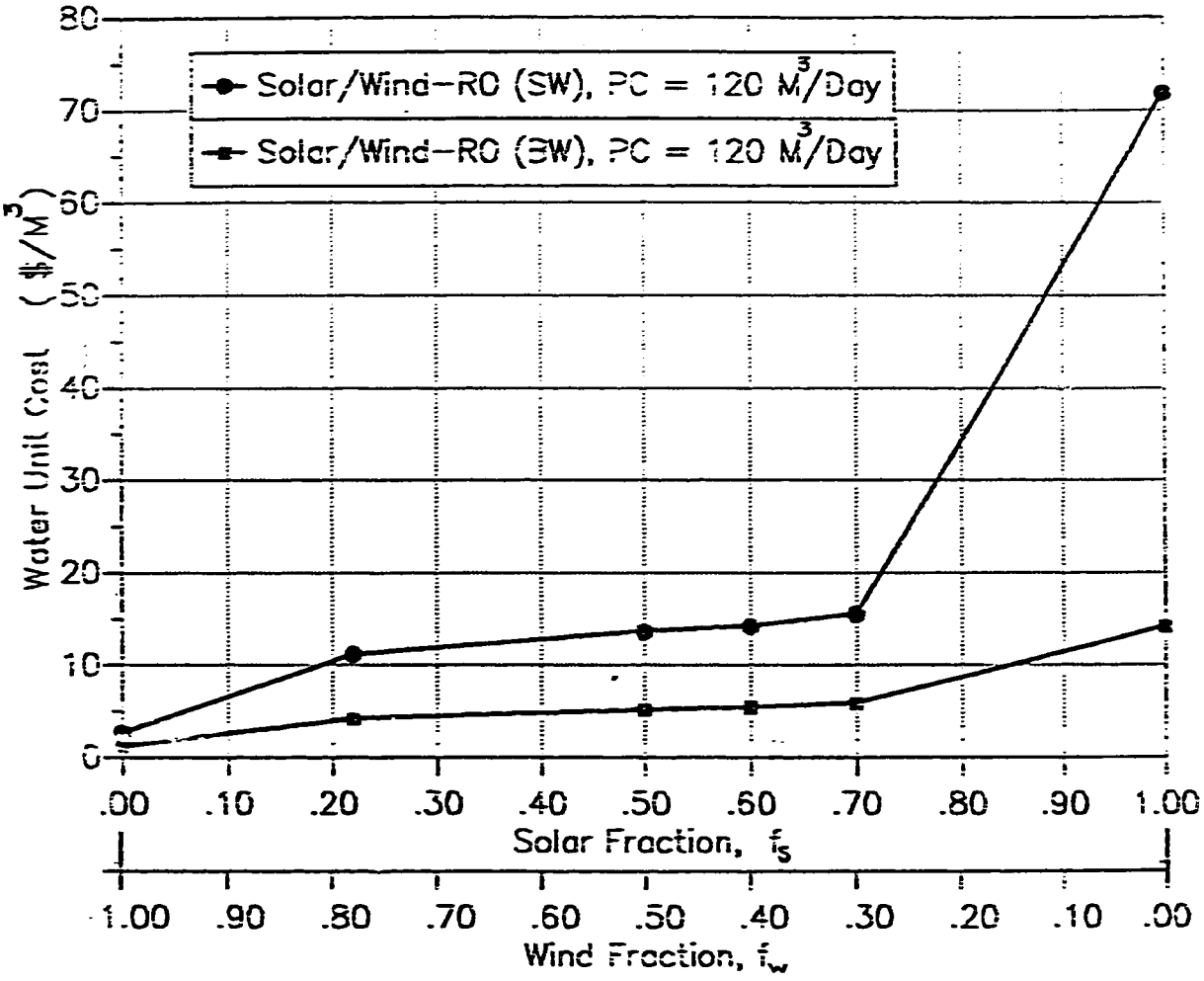

Figure (6.25) Water Cost for Various Solar/Wind-Operated RO Plants

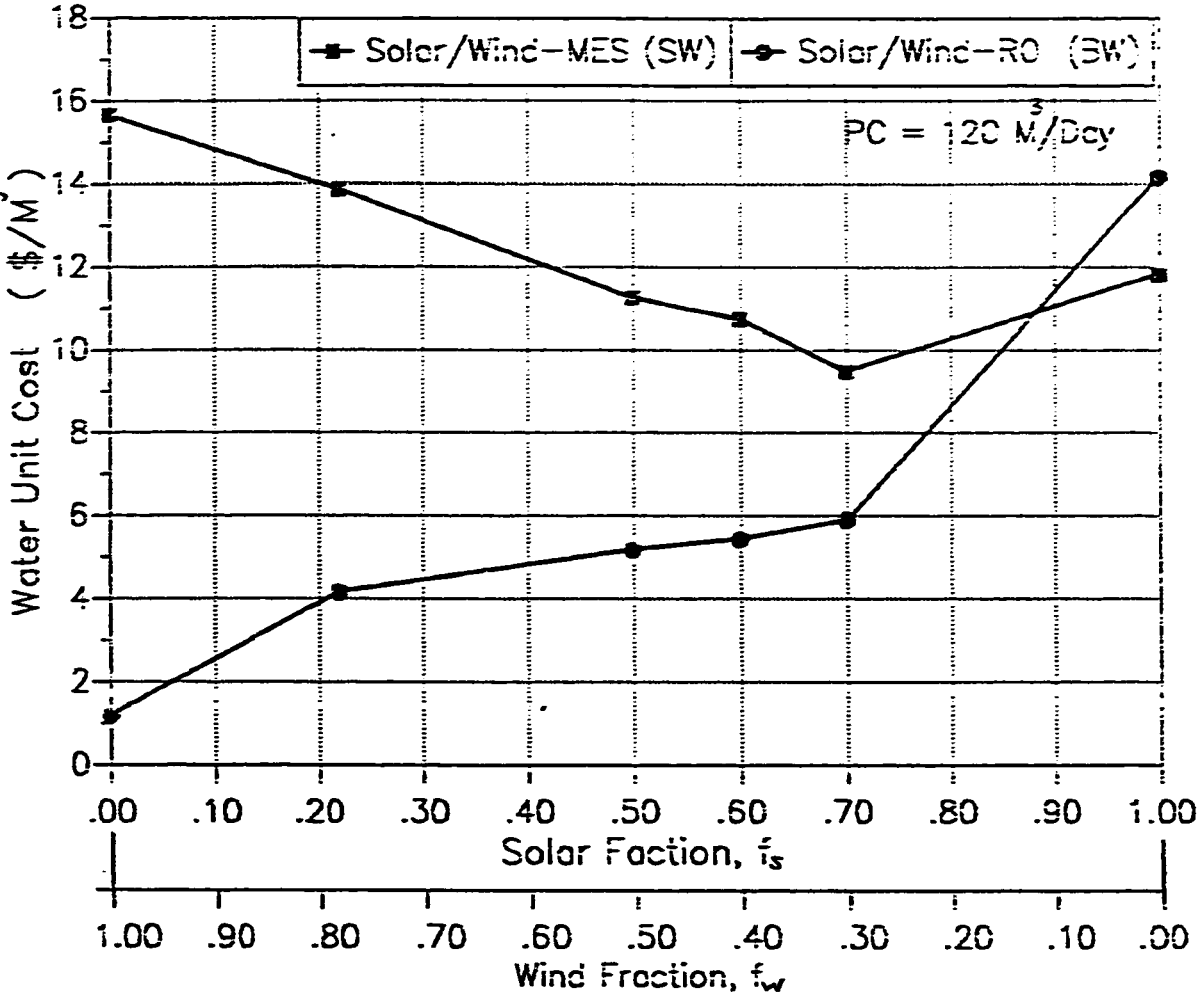

Figure (6.26) Water Unit Cost as a Function of Solar/Wind Fractions

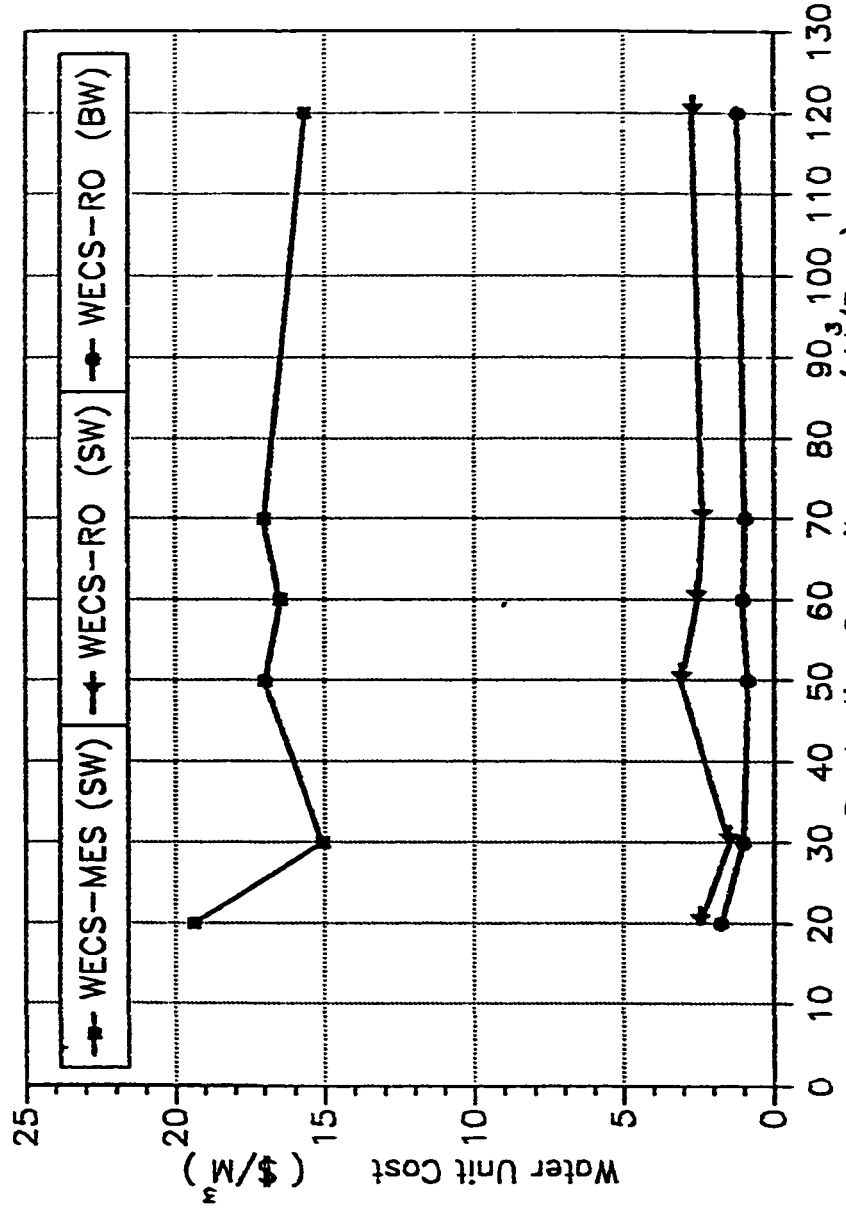

Figure (6.27) Water Cost for Different Wind-Operated Desalination Units

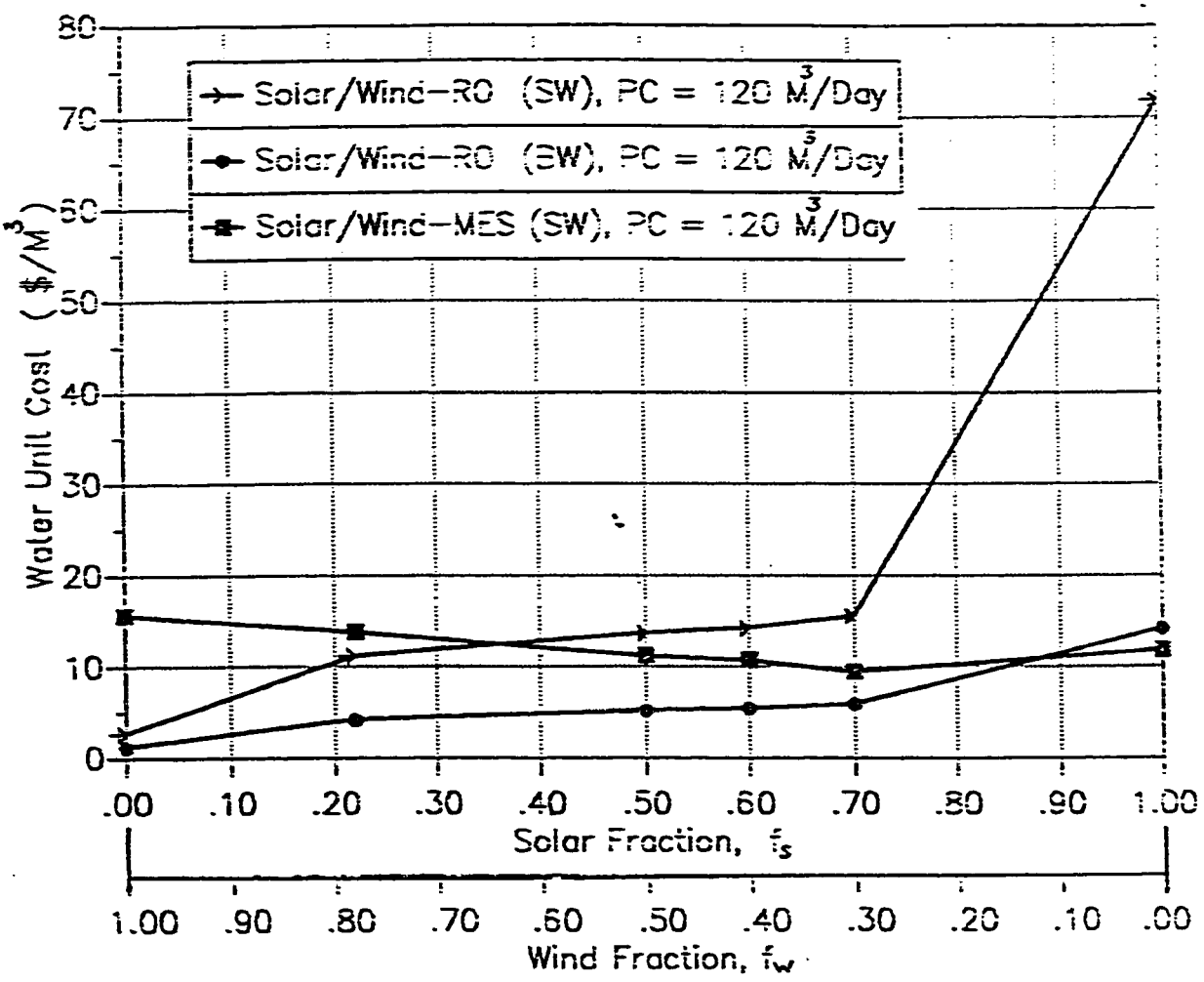

Figure (6.28) Water Cost for Typical Solar/Wind-Powered Desalination Plants

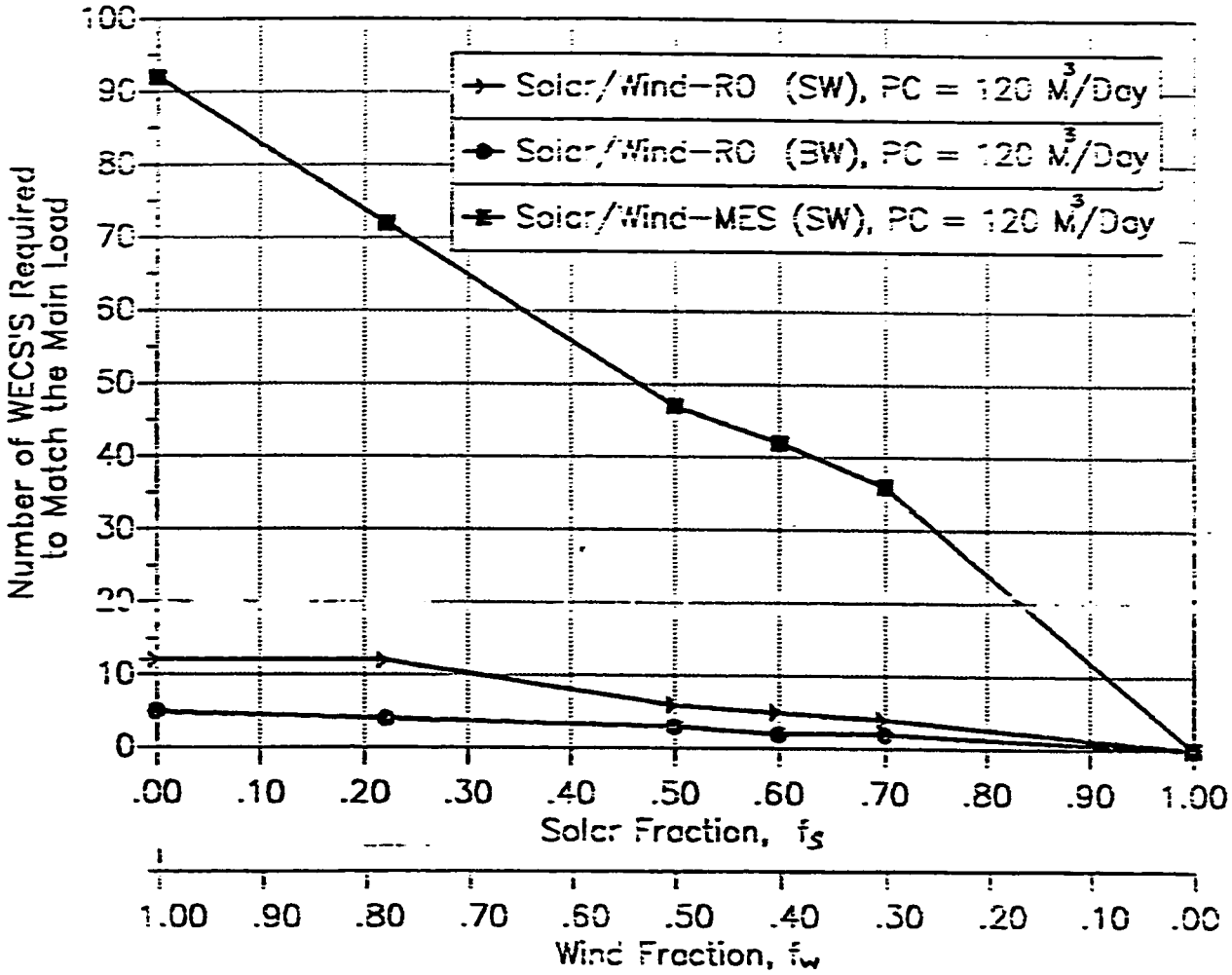

Figure (6.29) Size of WECS for Various Solar/Wind-Powered Desalinations Plants

from this figure that the size of WECS system used for seawater-RO process is twice as much as that for brackish water-RO process. This means that we need a land with an area equals approximately twice as much.

It is interesting at this stage to compare the resulting unit water cost of product water produced by the conventional (fuel-powered) desalination systems with that produced by the proposed solar/windpowered desalination systems. For conventional seawater distillation processes the unit water cost ranges between 0.57-1.69 $/m^3$ at production capacity ranging between 3800-380000 m^3/day as illustrated in table (3.12). However, the resulting unit water cost of the product water produced by the proposed non-conventional solar/wind-powered MES (configure1) is 11.8 $/m^3$ at production capacity equals to 120 m^3/day. This means that it costs about 7 times greater to produce one cubic meter of freshwater by the non-conventional system than to produce the same quantity by the conventional one. Low costs of fuel oil and the high investment costs of the evacuated-tube solar collectors are the main reasons for such discripancy.

On the other hand, desalting brackish water using conventional reverse osmosis systems yields a unit water cost ranging between 0.25-0.36 $/m^3$ at a production capacity ranging between 4000-190000 m^3/day as illustrated in table (3.12). Comparing this with the unit water cost of 0.87 $/m^3$ resulting from desalting brackish water using the non-conventional wind-powered RO system at a capacity equals to 100 m^3/day, yields that, the production cost of

freshwater using the former system is cheaper about three times as much than that of the latter system. The numbers representing the unit water costs of conventional systems are those based on moderate values of fuel oil costs.

In general, the issue of water desalination economics is not the only rational factor upon which conventional and non-conventional desalination systems are weighted. In cases where the fuel costs are high, or the fuel is scarce, the solar/wind-powered desalination systems become an attractive choice. This is also true for the application of desalination in remote locations where the conventional power is almost non-existent.

Recommendations

This study recommends that:

1. The WECS-RO system is to be used for desalting of brackish water and the combined solar/wind-MES system is to be used for desalting seawater (at low production capacities) in remote locations having similarities with Dhahran's climatic conditions.

2. The second-law based thermodynamics analysis is shown to be a great tool for evaluating desalination processes. Therefore, it is highly recommended that further investigations on the utilization of this tool, from practical standpoint, should be made.

3. It is also recommended that the entire design of the solar/wind-powered desalination system is based on the second-law of thermodynamics.

4. The procedure of calculating the irreversibilities and the second-law efficiency of desalination plants has been developed in this study and is recommended to be implemented using computer-based models.

5. It is found that the main sources of raising the cost of desalinated water using photovoltaic-RO system, is the high costs of the photovoltaic systems and their relatively poor electrical conversion efficiencies. Therefore, it is recommended that more efforts should be made to improve the positives of photovoltaic systems.

6. It is recommended that some study should be made on applications of other alternatives of solar/wind-energy conversion devices, such as, the pumped-hydro systems, for desalination.

7. It is also recommended that a solar/wind-powered desalination plant is installed at King Fahd University of Petroleum and Minerals for testing and demonstration purposes. This demonstration plant will greatly serve as a facility, both for providing potable water and academic research. Further areas in the field can be explored by graduate and undergraduate students using the proposed plant.

APPENDICES

APPENDIX A

THERMODYNAMIC PROPERTIES OF AQUEUS SODIUM CHLORIDE SOLUTIONS

Table A-1 The Specific Entropy of NaCl(aq), J/g.K [44]

t	P	m=0.1	m=0.25	m=0.5	m=0.75	m=1.0	m=2.0	m=3.0	m=4.0	m=5.0	m=6.0
°C	bar	mol/kg	mol/kg	mol/kg	mol/kg	mol/kg	mol/kg	mol/kg	mol/kg	mol/kg	mol/kg
0.0	1.0	3.513	3.507	3.492	3.475	3.457	3.376	3.289	3.202	3.117	3.036
10.0	1.0	3.663	3.654	3.637	3.617	3.597	3.500	3.416	3.325	3.236	3.152
20.0	1.0	3.807	3.797	3.777	3.755	3.732	3.637	3.539	3.444	3.352	3.265
25.0	1.0	3.878	3.866	3.845	3.822	3.798	3.699	3.600	3.502	3.409	3.321
30.0	1.0	3.947	3.935	3.912	3.888	3.864	3.761	3.659	3.559	3.465	3.375
40.0	1.0	4.081	4.060	4.043	4.018	3.991	3.882	3.775	3.671	3.573	3.481
50.0	1.0	4.212	4.197	4.171	4.143	4.114	3.999	3.887	3.780	3.679	3.584
60.0	1.0	4.338	4.323	4.294	4.264	4.234	4.113	3.996	3.885	3.781	3.683
70.0	1.0	4.461	4.444	4.414	4.382	4.350	4.224	4.102	3.987	3.880	3.780
80.0	1.0	4.581	4.563	4.530	4.497	4.463	4.331	4.205	4.086	3.976	3.873
90.0	1.0	4.697	4.678	4.644	4.609	4.574	4.436	4.305	4.183	4.069	3.964
100.0	1.0	4.811	4.790	4.754	4.718	4.681	4.538	4.402	4.277	4.160	4.052
110.0	1.4	4.922	4.900	4.862	4.824	4.786	4.637	4.497	4.368	4.248	4.138
120.0	2.0	5.030	5.007	4.968	4.928	4.888	4.734	4.590	4.457	4.335	4.222
130.0	2.7	5.136	5.112	5.071	5.029	4.988	4.828	4.680	4.544	4.418	4.303
140.0	3.6	5.240	5.215	5.172	5.128	5.086	4.921	4.768	4.629	4.500	4.383
150.0	4.8	5.342	5.316	5.271	5.226	5.181	5.011	4.855	4.711	4.580	4.460
160.0	6.2	5.442	5.414	5.368	5.321	5.275	5.100	4.939	4.792	4.658	4.536
170.0	7.9	5.540	5.512	5.463	5.415	5.367	5.186	5.021	4.871	4.734	4.610
180.0	10.0	5.637	5.607	5.557	5.507	5.458	5.271	5.102	4.949	4.809	4.682
190.0	12.5	5.732	5.701	5.649	5.597	5.546	5.355	5.181	5.024	4.882	4.753
200.0	15.5	5.826	5.794	5.740	5.686	5.634	5.437	5.259	5.099	4.954	4.822
210.0	19.1	5.919	5.885	5.829	5.774	5.720	5.517	5.335	5.172	5.024	4.890
220.0	23.2	6.011	5.976	5.918	5.861	5.805	5.597	5.410	5.243	5.092	4.956
230.0	28.0	6.102	6.066	6.005	5.946	5.889	5.675	5.484	5.313	5.160	5.021
240.0	33.4	6.193	6.155	6.092	6.031	5.972	5.752	5.557	5.383	5.226	5.085
250.0	39.7	6.283	6.243	6.178	6.115	6.054	5.828	5.628	5.451	5.291	5.148
260.0	46.9	6.373	6.331	6.264	6.199	6.136	5.903	5.699	5.517	5.355	5.209
270.0	55.0	6.462	6.419	6.349	6.282	6.217	5.978	5.769	5.584	5.418	5.270
280.0	64.1	6.553	6.507	6.434	6.364	6.297	6.052	5.838	5.649	5.480	5.329
290.0	74.4	6.643	6.596	6.520	6.447	6.377	6.125	5.906	5.713	5.542	5.388
300.0	85.8	6.735	6.685	6.605	6.529	6.457	6.197	5.973	5.777	5.602	5.446

Table A-1 The Specific Entropy of NaCl(aq), J/g.K (continued)

t	p	m=0.1	m=0.25	m=0.5	m=0.75	m=1.0	m=2.0	m=3.0	m=4.0	m=5.0	m=6.0
°C	bar	mol/kg	mol/kg	mol/kg	mol/kg	mol/kg	mol/kg	mol/kg	mol/kg	mol/kg	mol/kg
0.0	200.0	3.514	3.506	3.491	3.473	3.454	3.371	3.204	3.196	3.110	3.029
10.0	200.0	3.661	3.652	3.634	3.614	3.593	3.503	3.410	3.310	3.229	3.145
20.0	200.0	3.803	3.792	3.772	3.750	3.727	3.630	3.532	3.437	3.345	3.250
25.0	200.0	3.872	3.861	3.839	3.816	3.792	3.692	3.592	3.495	3.401	3.313
30.0	200.0	3.940	3.928	3.906	3.882	3.857	3.754	3.651	3.552	3.457	3.367
40.0	200.0	4.074	4.060	4.036	4.010	3.983	3.874	3.767	3.663	3.565	3.473
50.0	200.0	4.203	4.188	4.162	4.134	4.105	3.991	3.878	3.771	3.670	3.576
60.0	200.0	4.328	4.312	4.284	4.254	4.224	4.104	3.987	3.876	3.772	3.675
70.0	200.0	4.450	4.433	4.402	4.371	4.339	4.213	4.092	3.978	3.871	3.771
80.0	200.0	4.569	4.550	4.518	4.485	4.452	4.320	4.195	4.077	3.966	3.864
90.0	200.0	4.683	4.664	4.630	4.596	4.561	4.424	4.294	4.172	4.059	3.955
100.0	200.0	4.796	4.776	4.740	4.704	4.667	4.525	4.391	4.266	4.150	4.041
110.0	200.0	4.906	4.884	4.847	4.809	4.771	4.624	4.485	4.357	4.238	4.128
120.0	200.0	5.013	4.990	4.951	4.912	4.872	4.720	4.577	4.445	4.323	4.211
130.0	200.0	5.118	5.094	5.053	5.012	4.972	4.814	4.667	4.532	4.407	4.292
140.0	200.0	5.221	5.196	5.153	5.111	5.068	4.906	4.755	4.616	4.488	4.371
150.0	200.0	5.321	5.295	5.251	5.207	5.163	4.995	4.840	4.698	4.568	4.449
160.0	200.0	5.420	5.393	5.347	5.301	5.256	5.083	4.924	4.778	4.645	4.524
170.0	200.0	5.517	5.489	5.441	5.394	5.347	5.169	5.006	4.857	4.721	4.598
180.0	200.0	5.613	5.583	5.534	5.485	5.436	5.253	5.086	4.934	4.796	4.670
190.0	200.0	5.706	5.676	5.625	5.574	5.524	5.336	5.164	5.009	4.868	4.740
200.0	200.0	5.799	5.767	5.714	5.662	5.611	5.417	5.241	5.083	4.939	4.809
210.0	200.0	5.890	5.858	5.803	5.749	5.696	5.496	5.317	5.155	5.009	4.877
220.0	200.0	5.981	5.947	5.890	5.834	5.779	5.575	5.391	5.226	5.078	4.941
230.0	200.0	6.070	6.035	5.976	5.918	5.862	5.652	5.464	5.296	5.145	5.000
240.0	200.0	6.159	6.122	6.061	6.002	5.944	5.728	5.536	5.365	5.211	5.072
250.0	200.0	6.248	6.209	6.146	6.085	6.025	5.804	5.607	5.432	5.276	5.135
260.0	200.0	6.336	6.296	6.230	6.167	6.105	5.878	5.677	5.499	5.340	5.197
270.0	200.0	6.424	6.382	6.314	6.249	6.185	5.952	5.747	5.565	5.403	5.257
280.0	200.0	6.512	6.469	6.398	6.330	6.265	6.025	5.815	5.630	5.465	5.317
290.0	200.0	6.601	6.556	6.482	6.412	6.345	6.098	5.884	5.695	5.527	5.377
300.0	200.0	6.691	6.644	6.567	6.494	6.424	6.171	5.952	5.759	5.589	5.436

Table A-1 The Specific Entropy of NaCl(aq), J/g.K (continued)

t	P	m=0.1	m=0.25	m=0.5	m=0.75	m=1.0	m=2.0	m=3.0	m=4.0	m=5.0	m=6.0
°C	bar	mol/kg	mol/kg	mol/kg	mol/kg	mol/kg	mol/kg	mol/kg	mol/kg	mol/kg	mol/kg
0.0	400.0	3.513	3.505	3.409	3.471	3.451	3.366	3.270	3.190	3.104	3.022
10.0	400.0	3.658	3.648	3.629	3.609	3.588	3.497	3.403	3.311	3.223	3.138
20.0	400.0	3.798	3.787	3.766	3.744	3.720	3.623	3.525	3.430	3.338	3.251
25.0	400.0	3.866	3.855	3.833	3.810	3.785	3.685	3.585	3.488	3.394	3.306
30.0	400.0	3.934	3.922	3.899	3.875	3.850	3.746	3.644	3.544	3.449	3.360
40.0	400.0	4.066	4.052	4.028	4.002	3.975	3.866	3.759	3.655	3.557	3.465
50.0	400.0	4.194	4.179	4.153	4.125	4.096	3.982	3.870	3.763	3.662	3.567
60.0	400.0	4.318	4.302	4.274	4.244	4.214	4.094	3.978	3.867	3.763	3.666
70.0	400.0	4.439	4.422	4.391	4.360	4.329	4.203	4.083	3.969	3.862	3.762
80.0	400.0	4.556	4.538	4.506	4.473	4.440	4.309	4.184	4.067	3.957	3.855
90.0	400.0	4.670	4.651	4.618	4.583	4.549	4.413	4.283	4.162	4.050	3.946
100.0	400.0	4.782	4.761	4.726	4.690	4.654	4.513	4.380	4.255	4.140	4.033
110.0	400.0	4.890	4.869	4.832	4.795	4.757	4.611	4.474	4.346	4.227	4.118
120.0	400.0	4.997	4.974	4.936	4.897	4.858	4.707	4.565	4.434	4.313	4.201
130.0	400.0	5.100	5.077	5.037	4.996	4.956	4.800	4.654	4.520	4.396	4.282
140.0	400.0	5.202	5.178	5.136	5.094	5.052	4.891	4.741	4.604	4.477	4.360
150.0	400.0	5.302	5.276	5.233	5.189	5.146	4.980	4.826	4.685	4.556	4.437
160.0	400.0	5.399	5.373	5.328	5.283	5.238	5.067	4.909	4.765	4.633	4.512
170.0	400.0	5.495	5.468	5.421	5.374	5.328	5.152	4.991	4.843	4.708	4.585
180.0	400.0	5.589	5.560	5.512	5.464	5.416	5.235	5.070	4.919	4.782	4.657
190.0	400.0	5.681	5.652	5.602	5.552	5.503	5.317	5.148	4.994	4.854	4.727
200.0	400.0	5.772	5.742	5.690	5.638	5.588	5.397	5.224	5.067	4.925	4.795
210.0	400.0	5.862	5.830	5.776	5.723	5.671	5.476	5.299	5.139	4.994	4.863
220.0	400.0	5.951	5.917	5.862	5.807	5.754	5.553	5.372	5.209	5.062	4.928
230.0	400.0	6.038	6.003	5.946	5.890	5.835	5.628	5.444	5.278	5.128	4.993
240.0	400.0	6.124	6.089	6.029	5.971	5.914	5.703	5.514	5.346	5.194	5.057
250.0	400.0	6.210	6.173	6.112	6.052	5.993	5.776	5.584	5.412	5.258	5.119
260.0	400.0	6.295	6.257	6.193	6.131	6.071	5.849	5.652	5.477	5.321	5.180
270.0	400.0	6.380	6.340	6.274	6.210	6.148	5.920	5.720	5.542	5.383	5.241
280.0	400.0	6.464	6.422	6.354	6.288	6.225	5.991	5.786	5.606	5.445	5.301
290.0	400.0	6.548	6.505	6.434	6.366	6.301	6.061	5.852	5.668	5.505	5.360
300.0	400.0	6.632	6.587	6.514	6.444	6.376	6.130	5.917	5.731	5.566	5.419

Table A-2 The Specific Enthalpy of NaCl(aq), J/g [44]

t	P	m=0.1	m=0.25	m=0.5	m=0.75	m=1.0	m=2.0	m=3.0	m=4.0	m=5.0	m=6.0
°C	bar	mol/kg	mol/kg	mol/kg	mol/kg	mol/kg	mol/kg	mol/kg	mol/kg	mol/kg	mol/kg
0.0	1.0	-1985.7	-1960.2	-1939.0	-1912.4	-1885.9	-1780.4	-1702.3	-1625.2	-1555.5	-1491.6
10.0	1.0	-1944.1	-1927.1	-1899.5	-1872.0	-1847.0	-1751.6	-1667.0	-1591.1	-1522.3	-1459.2
20.0	1.0	-1902.6	-1886.0	-1859.2	-1833.2	-1808.0	-1714.6	-1631.5	-1556.7	-1488.9	-1426.6
25.0	1.0	-1881.8	-1865.5	-1839.0	-1813.3	-1788.4	-1696.1	-1613.7	-1539.5	-1472.1	-1410.3
30.0	1.0	-1861.1	-1845.0	-1818.8	-1793.4	-1768.8	-1677.5	-1595.9	-1522.3	-1455.4	-1393.9
40.0	1.0	-1819.5	-1803.9	-1778.4	-1753.6	-1729.6	-1640.2	-1560.1	-1487.0	-1421.8	-1361.2
50.0	1.0	-1778.0	-1762.8	-1737.9	-1713.8	-1690.4	-1602.9	-1524.4	-1453.3	-1388.3	-1328.5
60.0	1.0	-1736.5	-1721.6	-1697.5	-1673.9	-1651.1	-1565.6	-1488.6	-1418.7	-1354.8	-1295.8
70.0	1.0	-1694.9	-1680.5	-1657.0	-1634.0	-1611.7	-1528.2	-1452.8	-1384.2	-1321.3	-1263.3
80.0	1.0	-1653.3	-1639.3	-1616.4	-1594.1	-1572.4	-1490.8	-1417.0	-1349.7	-1287.9	-1230.7
90.0	1.0	-1611.6	-1598.0	-1575.8	-1554.1	-1532.9	-1453.4	-1381.1	-1315.2	-1254.4	-1198.2
100.0	1.0	-1569.8	-1556.7	-1535.1	-1514.0	-1493.4	-1415.9	-1345.3	-1280.6	-1221.0	-1165.7
110.0	1.4	-1527.8	-1515.1	-1494.2	-1473.8	-1453.8	-1378.3	-1309.4	-1246.0	-1187.6	-1133.2
120.0	2.0	-1485.7	-1473.4	-1453.2	-1433.4	-1414.0	-1340.6	-1273.4	-1211.5	-1154.1	-1100.7
130.0	2.7	-1443.4	-1431.6	-1412.1	-1392.9	-1374.2	-1302.9	-1237.4	-1176.8	-1120.6	-1068.2
140.0	3.6	-1400.9	-1389.6	-1370.8	-1352.3	-1334.2	-1265.1	-1201.3	-1142.2	-1087.2	-1035.7
150.0	4.8	-1358.2	-1347.3	-1329.3	-1311.5	-1294.0	-1227.2	-1165.1	-1107.5	-1053.6	-1003.2
160.0	6.2	-1315.2	-1304.8	-1287.6	-1270.5	-1253.7	-1189.1	-1128.9	-1072.7	-1020.1	-970.7
170.0	7.9	-1272.0	-1262.1	-1245.7	-1229.3	-1213.2	-1151.0	-1092.6	-1037.9	-986.5	-938.1
180.0	10.0	-1228.4	-1219.1	-1203.5	-1187.9	-1172.5	-1112.6	-1056.2	-1003.0	-952.9	-905.5
190.0	12.5	-1184.4	-1175.7	-1161.0	-1146.2	-1131.5	-1074.2	-1019.6	-968.0	-919.2	-872.9
200.0	15.5	-1140.1	-1132.0	-1118.1	-1104.2	-1090.3	-1035.5	-983.0	-933.0	-885.4	-840.2
210.0	19.1	-1095.3	-1087.8	-1074.9	-1061.8	-1048.7	-996.6	-946.1	-897.8	-851.6	-807.5
220.0	23.2	-1049.9	-1043.1	-1031.2	-1019.1	-1006.8	-957.4	-909.1	-862.4	-817.6	-774.7
230.0	28.0	-1004.0	-997.9	-987.1	-975.0	-964.4	-917.9	-871.0	-827.0	-783.6	-741.8
240.0	33.4	-957.3	-952.0	-942.3	-932.1	-921.6	-878.2	-834.4	-791.3	-749.4	-708.9
250.0	39.7	-909.9	-905.4	-896.9	-887.8	-878.3	-838.0	-796.6	-755.4	-715.0	-675.8
260.0	46.9	-861.5	-857.9	-850.8	-842.8	-834.3	-797.4	-758.5	-719.3	-680.5	-642.7
270.0	55.0	-812.1	-809.5	-803.9	-797.1	-789.8	-756.4	-720.1	-682.9	-645.8	-609.4
280.0	64.1	-761.5	-760.1	-756.0	-750.7	-744.5	-714.9	-681.3	-646.2	-610.8	-575.9
290.0	74.4	-709.5	-709.4	-707.1	-703.3	-698.5	-672.9	-642.1	-609.2	-575.6	-542.2
300.0	85.8	-655.9	-657.3	-657.1	-655.1	-651.7	-630.5	-602.6	-571.8	-539.9	-508.0

Table A-2 The Specific Enthalpy of NaCl(aq), J/g (continued)

t	p	m=0.1	m=0.25	m=0.5	m=0.75	m=1.0	m=2.0	m=3.0	m=4.0	m=5.0	m=6.0
°C	bar	mol/kg	mol/kg	mol/kg	mol/kg	mol/kg	mol/kg	mol/kg	mol/kg	mol/kg	mol/kg
0.0	200.0	-1965.9	-1940.6	-1920.7	-1893.7	-1867.6	-1771.3	-1686.0	-1609.6	-1540.4	-1477.0
10.0	200.0	-1925.0	-1900.3	-1881.0	-1854.7	-1829.2	-1734.8	-1650.9	-1575.6	-1507.3	-1444.7
20.0	200.0	-1884.1	-1867.8	-1841.2	-1815.5	-1790.6	-1698.1	-1615.6	-1541.4	-1474.0	-1412.2
25.0	200.0	-1863.7	-1847.5	-1821.3	-1795.9	-1771.2	-1679.6	-1597.9	-1524.3	-1457.3	-1395.9
30.0	200.0	-1843.1	-1827.2	-1801.3	-1776.2	-1751.8	-1661.2	-1580.2	-1507.1	-1440.6	-1379.6
40.0	200.0	-1802.1	-1786.5	-1761.3	-1736.7	-1712.9	-1624.2	-1544.6	-1472.7	-1407.2	-1346.9
50.0	200.0	-1761.0	-1745.8	-1721.2	-1697.2	-1674.0	-1587.1	-1509.1	-1438.4	-1373.8	-1314.4
60.0	200.0	-1719.9	-1705.1	-1681.1	-1657.7	-1635.0	-1550.0	-1473.5	-1404.0	-1340.4	-1281.8
70.0	200.0	-1678.7	-1664.4	-1641.0	-1618.2	-1596.0	-1512.9	-1437.9	-1369.6	-1307.1	-1249.3
80.0	200.0	-1637.5	-1623.6	-1600.8	-1578.6	-1556.9	-1475.7	-1402.3	-1335.3	-1273.8	-1216.8
90.0	200.0	-1596.2	-1582.7	-1560.5	-1538.9	-1517.8	-1438.5	-1366.6	-1300.9	-1240.5	-1184.4
100.0	200.0	-1554.8	-1541.7	-1520.2	-1499.1	-1478.6	-1401.3	-1331.0	-1266.5	-1207.2	-1152.1
110.0	200.0	-1513.3	-1500.6	-1479.7	-1459.3	-1439.3	-1364.0	-1295.3	-1232.2	-1173.9	-1119.7
120.0	200.0	-1471.7	-1459.4	-1439.2	-1419.4	-1400.0	-1326.7	-1259.6	-1197.8	-1140.7	-1087.4
130.0	200.0	-1429.9	-1418.0	-1398.5	-1379.3	-1360.5	-1289.3	-1223.8	-1163.4	-1107.4	-1055.2
140.0	200.0	-1388.0	-1376.5	-1357.7	-1339.2	-1321.0	-1251.9	-1188.1	-1129.1	-1074.2	-1022.9
150.0	200.0	-1345.8	-1334.9	-1316.8	-1298.9	-1281.4	-1214.4	-1152.3	-1094.7	-1041.0	-990.6
160.0	200.0	-1303.5	-1293.1	-1275.7	-1258.5	-1241.6	-1176.8	-1116.5	-1060.3	-1007.7	-958.4
170.0	200.0	-1261.0	-1251.1	-1234.5	-1218.0	-1201.7	-1139.1	-1080.6	-1025.8	-974.5	-926.2
180.0	200.0	-1218.3	-1208.8	-1193.0	-1177.3	-1161.7	-1101.4	-1044.7	-991.4	-941.2	-893.9
190.0	200.0	-1175.3	-1166.3	-1151.3	-1136.4	-1121.5	-1063.6	-1008.7	-956.9	-907.9	-861.6
200.0	200.0	-1131.9	-1123.6	-1109.4	-1095.2	-1081.1	-1025.6	-972.7	-922.3	-874.6	-829.3
210.0	200.0	-1088.2	-1080.5	-1067.2	-1053.8	-1040.4	-987.5	-936.5	-887.7	-841.3	-797.0
220.0	200.0	-1044.1	-1037.0	-1024.7	-1012.1	-999.5	-949.2	-900.2	-853.1	-807.9	-764.6
230.0	200.0	-999.5	-993.0	-981.7	-970.1	-958.3	-910.8	-863.9	-818.3	-774.4	-732.2
240.0	200.0	-954.3	-948.6	-938.3	-927.7	-916.8	-872.1	-827.3	-783.4	-740.8	-699.7
250.0	200.0	-908.5	-903.5	-894.4	-884.8	-874.8	-833.1	-790.5	-748.4	-707.1	-667.2
260.0	200.0	-862.0	-857.8	-849.9	-841.3	-832.3	-793.7	-753.5	-713.1	-673.3	-634.5
270.0	200.0	-814.6	-811.3	-804.7	-797.3	-789.3	-754.0	-716.2	-677.7	-639.4	-601.8
280.0	200.0	-766.2	-763.9	-758.7	-752.5	-745.6	-713.8	-678.6	-642.0	-605.2	-568.9
290.0	200.0	-716.5	-715.3	-711.7	-706.9	-701.2	-673.1	-640.5	-605.9	-570.7	-535.8
300.0	200.0	-665.4	-665.5	-663.7	-660.3	-655.9	-631.0	-601.9	-569.3	-535.8	-502.3

Table A-2 The Specific Enthalpy of NaCl(aq), J/g (continued)

t	p	m=0.1	m=0.25	m=0.5	m=0.75	m=1.0	m=2.0	m=3.0	m=4.0	m=5.0	m=6.0
°C	bar	mol/kg	mol/kg	mol/kg	mol/kg	mol/kg	mol/kg	mol/kg	mol/kg	mol/kg	mol/kg
0.0	400.0	-1946.5	-1929.5	-1902.0	-1875.3	-1849.6	-1754.4	-1669.9	-1594.1	-1525.4	-1462.4
10.0	400.0	-1906.3	-1889.7	-1862.0	-1836.8	-1811.6	-1710.1	-1634.9	-1560.2	-1492.3	-1430.2
20.0	400.0	-1865.9	-1849.0	-1823.5	-1790.0	-1773.3	-1681.6	-1599.8	-1526.1	-1459.1	-1397.7
25.0	400.0	-1845.7	-1829.7	-1803.7	-1770.5	-1754.1	-1663.3	-1582.1	-1509.0	-1442.5	-1381.5
30.0	400.0	-1825.4	-1809.6	-1783.9	-1759.0	-1734.8	-1644.9	-1564.5	-1491.9	-1425.8	-1365.2
40.0	400.0	-1784.7	-1769.3	-1744.2	-1719.9	-1696.2	-1608.1	-1529.1	-1457.7	-1392.6	-1332.7
50.0	400.0	-1744.0	-1729.0	-1704.5	-1680.7	-1657.6	-1571.3	-1493.7	-1423.5	-1359.3	-1300.2
60.0	400.0	-1703.2	-1688.6	-1664.7	-1641.5	-1618.9	-1534.4	-1458.3	-1389.2	-1326.0	-1267.7
70.0	400.0	-1662.4	-1648.2	-1624.9	-1602.2	-1580.2	-1497.5	-1422.9	-1355.0	-1292.8	-1235.3
80.0	400.0	-1621.6	-1607.7	-1585.0	-1562.9	-1541.4	-1460.6	-1387.4	-1320.8	-1259.5	-1202.9
90.0	400.0	-1580.7	-1567.2	-1545.1	-1523.5	-1502.5	-1423.6	-1352.0	-1286.6	-1226.4	-1170.6
100.0	400.0	-1539.7	-1526.6	-1505.1	-1484.1	-1463.6	-1386.6	-1316.5	-1252.4	-1193.2	-1138.4
110.0	400.0	-1498.5	-1485.8	-1465.0	-1444.6	-1424.7	-1349.6	-1281.0	-1218.2	-1160.1	-1106.2
120.0	400.0	-1457.3	-1445.0	-1424.8	-1405.0	-1385.6	-1312.5	-1245.5	-1184.0	-1127.0	-1074.0
130.0	400.0	-1415.9	-1404.1	-1384.5	-1365.3	-1346.5	-1275.3	-1210.0	-1149.8	-1093.9	-1041.9
140.0	400.0	-1374.4	-1363.0	-1344.1	-1325.5	-1307.3	-1238.2	-1174.5	-1115.6	-1060.9	-1009.8
150.0	400.0	-1332.8	-1321.8	-1303.6	-1285.7	-1268.1	-1201.0	-1138.9	-1081.4	-1027.8	-977.7
160.0	400.0	-1291.0	-1280.5	-1263.0	-1245.7	-1228.7	-1163.7	-1103.4	-1047.2	-994.8	-945.7
170.0	400.0	-1249.1	-1239.0	-1222.2	-1205.6	-1189.3	-1126.4	-1067.8	-1013.0	-961.8	-913.6
180.0	400.0	-1206.9	-1197.4	-1181.3	-1165.5	-1149.7	-1089.1	-1032.2	-978.8	-928.7	-881.5
190.0	400.0	-1164.6	-1155.5	-1140.3	-1125.1	-1110.1	-1051.7	-996.6	-944.6	-895.7	-849.5
200.0	400.0	-1122.0	-1113.5	-1099.0	-1084.6	-1070.3	-1014.2	-960.9	-910.4	-862.6	-817.4
210.0	400.0	-1079.1	-1071.2	-1057.6	-1043.9	-1030.3	-976.7	-925.2	-876.2	-829.6	-785.2
220.0	400.0	-1036.0	-1028.6	-1015.9	-1003.1	-990.2	-939.1	-889.5	-841.9	-796.5	-753.1
230.0	400.0	-992.4	-985.7	-973.9	-961.9	-949.0	-901.3	-853.7	-807.6	-763.3	-720.9
240.0	400.0	-948.5	-942.4	-931.6	-920.5	-909.3	-863.4	-817.8	-773.2	-730.1	-688.6
250.0	400.0	-904.1	-898.7	-889.0	-878.8	-868.4	-825.3	-781.8	-738.8	-696.8	-656.3
260.0	400.0	-859.2	-854.5	-845.9	-836.8	-827.2	-787.1	-745.6	-704.2	-663.5	-623.8
270.0	400.0	-813.8	-809.8	-802.4	-794.3	-785.7	-748.6	-709.4	-669.5	-630.0	-591.2
280.0	400.0	-767.6	-764.6	-758.4	-751.4	-743.0	-709.9	-672.9	-634.7	-596.3	-558.5
290.0	400.0	-720.7	-718.6	-713.8	-707.9	-701.4	-670.0	-636.1	-599.6	-562.4	-525.5
300.0	400.0	-672.9	-671.8	-668.5	-663.9	-658.5	-631.4	-599.0	-564.1	-528.2	-492.2

Table A-3 The Density of NaCl(aq), g/cm^3 [44]

t	P	m=0.1	m=0.25	m=0.5	m=0.75	m=1.0	m=2.0	m=3.0	m=4.0	m=5.0	m=6.0
°C	bar	mol/kg	mol/kg	mol/kg	mol/kg	mol/kg	mol/kg	mol/kg	mol/kg	mol/kg	mol/kg
0.0	1.0	1.00429	1.01086	1.02156	1.03200	1.04218	1.08058	1.11570	1.14810	1.17833	1.20697
10.0	1.0	1.00402	1.01032	1.02061	1.03065	1.04047	1.07769	1.11201	1.14389	1.17375	1.20203
20.0	1.0	1.00239	1.00851	1.01850	1.02827	1.03783	1.07421	1.10795	1.13940	1.16894	1.19688
25.0	1.0	1.00117	1.00722	1.01710	1.02676	1.03623	1.07228	1.10577	1.13705	1.16644	1.19423
30.0	1.0	0.99972	1.00571	1.01550	1.02507	1.03445	1.07022	1.10351	1.13463	1.16388	1.19152
40.0	1.0	0.99622	1.00212	1.01176	1.02119	1.03044	1.06577	1.09872	1.12958	1.15859	1.18597
50.0	1.0	0.99200	0.99784	1.00738	1.01672	1.02588	1.06089	1.09359	1.12425	1.15307	1.18023
60.0	1.0	0.98715	0.99296	1.00244	1.01172	1.02081	1.05561	1.08814	1.11865	1.14732	1.17432
70.0	1.0	0.98171	0.98748	0.99689	1.00611	1.01515	1.04976	1.08219	1.11267	1.14134	1.16836
80.0	1.0	0.97575	0.98152	0.99093	1.00013	1.00915	1.04371	1.07609	1.10653	1.13520	1.16221
90.0	1.0	0.96930	0.97508	0.98451	0.99373	1.00276	1.03733	1.06972	1.10017	1.12885	1.15588
100.0	1.0	0.96237	0.96819	0.97767	0.98692	0.99598	1.03064	1.06309	1.09359	1.12230	1.14936
110.0	1.4	0.95501	0.96089	0.97043	0.97974	0.98885	1.02367	1.05623	1.08681	1.11557	1.14267
120.0	2.0	0.94723	0.95316	0.96279	0.97210	0.98136	1.01640	1.04912	1.07981	1.10866	1.13580
130.0	2.7	0.93901	0.94503	0.95477	0.96425	0.97352	1.00884	1.04177	1.07260	1.10155	1.12874
140.0	3.6	0.93039	0.93649	0.94636	0.95596	0.96533	1.00099	1.03416	1.06518	1.09424	1.12151
150.0	4.8	0.92134	0.92755	0.93757	0.94730	0.95679	0.99283	1.02630	1.05754	1.08675	1.11411
160.0	6.2	0.91188	0.91820	0.92838	0.93826	0.94789	0.98437	1.01818	1.04967	1.07908	1.10654
170.0	7.9	0.90198	0.90843	0.91880	0.92884	0.93861	0.97559	1.00978	1.04158	1.07121	1.09882
180.0	10.0	0.89165	0.89824	0.90881	0.91902	0.92895	0.96647	1.00110	1.03325	1.06315	1.09095
190.0	12.5	0.88086	0.88760	0.89838	0.90879	0.91889	0.95700	0.99212	1.02467	1.05490	1.08296
200.0	15.5	0.86958	0.87649	0.88751	0.89812	0.90841	0.94716	0.98281	1.01583	1.04647	1.07485
210.0	19.1	0.85780	0.86489	0.87616	0.88699	0.89748	0.93692	0.97316	1.00673	1.03784	1.06665
220.0	23.2	0.84548	0.85276	0.86430	0.87537	0.88607	0.92625	0.96315	0.99733	1.02903	1.05837
230.0	28.0	0.83258	0.84007	0.85191	0.86323	0.87416	0.91514	0.95276	0.98763	1.02002	1.05003
240.0	33.4	0.81905	0.82677	0.83893	0.85053	0.86171	0.90354	0.94195	0.97762	1.01082	1.04165
250.0	39.7	0.80482	0.81281	0.82533	0.83723	0.84868	0.89144	0.93071	0.96728	1.00144	1.03327
260.0	46.9	0.78984	0.79813	0.81105	0.82328	0.83503	0.87880	0.91903	0.95661	0.99186	1.02490
270.0	55.0	0.77401	0.78265	0.79603	0.80865	0.82073	0.86562	0.90688	0.94559	0.98211	1.01656
280.0	64.1	0.75721	0.76627	0.78021	0.79327	0.80574	0.85188	0.89430	0.93424	0.97219	1.00828
290.0	74.4	0.73932	0.74890	0.76351	0.77712	0.79005	0.83764	0.88132	0.92262	0.96213	1.00005
300.0	85.8	0.72015	0.73039	0.74586	0.76015	0.77365	0.82299	0.86807	0.91081	0.95198	0.99187

Table A-3 The Density of NaCl(aq), g/cm^3 (continued)

t	P	m=0.1	m=0.25	m=0.5	m=0.75	m=1.0	m=2.0	m=3.0	m=4.0	m=5.0	m=6.0
°C	bar	mol/kg	mol/kg	mol/kg	mol/kg	mol/kg	mol/kg	mol/kg	mol/kg	mol/kg	mol/kg
0.0	200.0	1.01409	1.02052	1.03099	1.04120	1.05116	1.08876	1.12324	1.15517	1.18512	1.21369
10.0	200.0	1.01323	1.01942	1.02953	1.03939	1.04904	1.08563	1.11942	1.15090	1.18050	1.20867
20.0	200.0	1.01123	1.01726	1.02710	1.03672	1.04614	1.08199	1.11527	1.14638	1.17566	1.20346
25.0	200.0	1.00988	1.01585	1.02559	1.03511	1.04444	1.08000	1.11307	1.14402	1.17315	1.20079
30.0	200.0	1.00834	1.01425	1.02390	1.03335	1.04260	1.07790	1.11079	1.14159	1.17059	1.19808
40.0	200.0	1.00471	1.01054	1.02006	1.02937	1.03850	1.07340	1.10598	1.13654	1.16531	1.19253
50.0	200.0	1.00045	1.00622	1.01564	1.02487	1.03391	1.06852	1.10087	1.13123	1.15982	1.18682
60.0	200.0	0.99561	1.00135	1.01072	1.01988	1.02887	1.06327	1.09546	1.12568	1.15412	1.18095
70.0	200.0	0.99025	0.99596	1.00528	1.01440	1.02335	1.05761	1.08972	1.11989	1.14830	1.17507
80.0	200.0	0.98441	0.99013	0.99944	1.00855	1.01749	1.05171	1.08377	1.11391	1.14228	1.16903
90.0	200.0	0.97813	0.98386	0.99320	1.00233	1.01128	1.04552	1.07759	1.10772	1.13609	1.16282
100.0	200.0	0.97142	0.97718	0.98657	0.99573	1.00472	1.03905	1.07118	1.10134	1.12972	1.15644
110.0	200.0	0.96430	0.97011	0.97957	0.98879	0.99782	1.03231	1.06454	1.09476	1.12317	1.14988
120.0	200.0	0.95679	0.96267	0.97221	0.98151	0.99061	1.02531	1.05768	1.08799	1.11644	1.14315
130.0	200.0	0.94889	0.95485	0.96450	0.97389	0.98308	1.01805	1.05060	1.08103	1.10953	1.13624
140.0	200.0	0.94062	0.94666	0.95644	0.96595	0.97523	1.01052	1.04330	1.07387	1.10243	1.12915
150.0	200.0	0.93197	0.93811	0.94803	0.95766	0.96706	1.00272	1.03576	1.06651	1.09516	1.12188
160.0	200.0	0.92294	0.92919	0.93927	0.94904	0.95857	0.99465	1.02799	1.05893	1.08770	1.11444
170.0	200.0	0.91352	0.91989	0.93015	0.94007	0.94974	0.98628	1.01996	1.05115	1.08005	1.10682
180.0	200.0	0.90370	0.91021	0.92065	0.93075	0.94057	0.97761	1.01168	1.04314	1.07221	1.09904
190.0	200.0	0.89347	0.90012	0.91076	0.92104	0.93102	0.96862	1.00310	1.03489	1.06417	1.09111
200.0	200.0	0.88281	0.88960	0.90047	0.91093	0.92109	0.95927	0.99423	1.02638	1.05593	1.08302
210.0	200.0	0.87168	0.87864	0.88973	0.90040	0.91075	0.94956	0.98503	1.01760	1.04749	1.07480
220.0	200.0	0.86006	0.86719	0.87853	0.88942	0.89995	0.93943	0.97547	1.00853	1.03883	1.06646
230.0	200.0	0.84791	0.85523	0.86683	0.87794	0.88868	0.92886	0.96551	0.99914	1.02994	1.05800
240.0	200.0	0.83518	0.84270	0.85458	0.86592	0.87688	0.91780	0.95513	0.98941	1.02083	1.04946
250.0	200.0	0.82182	0.82955	0.84172	0.85332	0.86450	0.90622	0.94428	0.97929	1.01147	1.04084
260.0	200.0	0.80774	0.81571	0.82821	0.84008	0.85150	0.89404	0.93291	0.96877	1.00185	1.03217
270.0	200.0	0.79286	0.80110	0.81396	0.82612	0.83780	0.88124	0.92097	0.95780	0.99196	1.02347
280.0	200.0	0.77706	0.78562	0.79888	0.81138	0.82334	0.86774	0.90843	0.94635	0.98179	1.01477
290.0	200.0	0.76020	0.76914	0.78289	0.79577	0.80806	0.85353	0.89525	0.93440	0.97134	1.00609
300.0	200.0	0.74208	0.75151	0.76586	0.77921	0.79190	0.83859	0.88146	0.92196	0.96060	0.99743

Table A-3 The Density of NaCl(aq), g/cm^3 (continued)

t	p	m=0.1	m=0.25	m=0.5	m=0.75	m=1.0	m=2.0	m=3.0	m=4.0	m=5.0	m=6.0
°C	bar	mol/kg	mol/kg	mol/kg	mol/kg	mol/kg	mol/kg	mol/kg	mol/kg	mol/kg	mol/kg
0.0	400.0	1.02350	1.02979	1.04005	1.05005	1.05980	1.09666	1.13051	1.16203	1.19173	1.22023
10.0	400.0	1.02210	1.02819	1.03813	1.04783	1.05731	1.09331	1.12662	1.15772	1.18707	1.21512
20.0	400.0	1.01976	1.02570	1.03540	1.04489	1.05417	1.08953	1.12240	1.15317	1.18221	1.20986
25.0	400.0	1.01829	1.02418	1.03379	1.04319	1.05239	1.08749	1.12017	1.15080	1.17969	1.20718
30.0	400.0	1.01665	1.02249	1.03202	1.04134	1.05048	1.08535	1.11787	1.14836	1.17713	1.20446
40.0	400.0	1.01290	1.01866	1.02806	1.03727	1.04630	1.08080	1.11304	1.14332	1.17186	1.19892
50.0	400.0	1.00857	1.01428	1.02360	1.03272	1.04167	1.07591	1.10794	1.13803	1.16640	1.19324
60.0	400.0	1.00374	1.00942	1.01868	1.02775	1.03664	1.07069	1.10257	1.13253	1.16076	1.18742
70.0	400.0	0.99843	1.00409	1.01332	1.02236	1.03122	1.06516	1.09698	1.12688	1.15504	1.18160
80.0	400.0	0.99270	0.99835	1.00758	1.01661	1.02547	1.05938	1.09115	1.12102	1.14914	1.17565
90.0	400.0	0.98655	0.99223	1.00148	1.01053	1.01940	1.05333	1.08511	1.11497	1.14307	1.16956
100.0	400.0	0.98002	0.98573	0.99503	1.00411	1.01301	1.04704	1.07887	1.10875	1.13685	1.16331
110.0	400.0	0.97311	0.97887	0.98824	0.99738	1.00633	1.04050	1.07243	1.10236	1.13047	1.15690
120.0	400.0	0.96586	0.97168	0.98113	0.99034	0.99936	1.03374	1.06579	1.09579	1.12392	1.15033
130.0	400.0	0.95826	0.96415	0.97370	0.98301	0.99210	1.02674	1.05896	1.08905	1.11722	1.14359
140.0	400.0	0.95032	0.95630	0.96597	0.97538	0.98457	1.01951	1.05193	1.08215	1.11035	1.13668
150.0	400.0	0.94206	0.94812	0.95793	0.96746	0.97676	1.01205	1.04471	1.07506	1.10331	1.12961
160.0	400.0	0.93346	0.93963	0.94959	0.95925	0.96867	1.00435	1.03728	1.06780	1.09611	1.12237
170.0	400.0	0.92452	0.93081	0.94093	0.95074	0.96030	0.99640	1.02964	1.06035	1.08874	1.11496
180.0	400.0	0.91525	0.92166	0.93196	0.94193	0.95163	0.98820	1.02178	1.05271	1.08120	1.10738
190.0	400.0	0.90563	0.91217	0.92266	0.93280	0.94265	0.97974	1.01369	1.04487	1.07348	1.09965
200.0	400.0	0.89566	0.90233	0.91303	0.92334	0.93336	0.97098	1.00534	1.03681	1.06558	1.09177
210.0	400.0	0.88531	0.89213	0.90304	0.91354	0.92372	0.96193	0.99673	1.02853	1.05749	1.08374
220.0	400.0	0.87457	0.88154	0.89267	0.90337	0.91373	0.95254	0.98783	1.02000	1.04922	1.07557
230.0	400.0	0.86341	0.87055	0.88191	0.89281	0.90336	0.94280	0.97861	1.01121	1.04075	1.06728
240.0	400.0	0.85182	0.85913	0.87073	0.88184	0.89258	0.93267	0.96904	1.00213	1.03207	1.05889
250.0	400.0	0.83976	0.84725	0.85909	0.87042	0.88135	0.92211	0.95909	0.99274	1.02317	1.05039
260.0	400.0	0.82719	0.83487	0.84697	0.85851	0.86963	0.91109	0.94871	0.98300	1.01405	1.04183
270.0	400.0	0.81407	0.82195	0.83431	0.84607	0.85739	0.89954	0.93786	0.97287	1.00468	1.03321
280.0	400.0	0.80036	0.80844	0.82108	0.83306	0.84457	0.88742	0.92646	0.96231	0.99505	1.02456
290.0	400.0	0.78598	0.79429	0.80721	0.81941	0.83112	0.87466	0.91446	0.95126	0.98513	1.01593
300.0	400.0	0.77087	0.77943	0.79265	0.80508	0.81698	0.86118	0.90178	0.93965	0.97490	1.00735

APPENDIX B

COMPUTER PROGRAM FOR CALCULATING THE MONTHLY AVERAGE DAILY EXTRATERRESTERIAL RADIATION $\overline{H}_{on}$ FOR DHAHRAN CITY

```
      REAL BETA,FI,GAMA,DELTA(32),WS(32),GSC                            SOL00010
      REAL WSS(32),DELTAD(32)                                           SOL00020
      INTEGER MONTH,DAY,M(12),NN(32),HOH(32),SUM(12),HOHAV(12)          SOL00030
      GAMA = 0.0                                                        SOL00040
      BETA = 26.13                                                      SOL00050
C     FOR DHAHRAN CITY                                                  SOL00060
C     ----------------                                                  SOL00070
      GSC= 1353.0                                                       SOL00080
      FI= 26.13                                                         SOL00090
C                                                                       SOL00100
      FI = FI * (3.141593/180.0)                                        SOL00110
      BETA = BETA *(3.141593/180.0)                                     SOL00120
      GAMA = GAMA *(3.141593/180.0)                                     SOL00130
         WRITE(5,*)'                                                    SOL00140
         WRITE(5,*)'                                                    SOL00150
         WRITE(5,*)'    COMPUTATION OF HOH , DELTA AND HOH-BAR -        SOL00160
         WRITE(5,*)'    ---------------------------------------         SOL00170
         WRITE(5,*)'                                                    SOL00180
         WRITE(5,*)'                                                    SOL00190
         WRITE(5,*)'                                                    SOL00200
      DO 17 I=1,12                                                      SOL00210
         SUM(I)=0                                                       SOL00220
         HOHAV(I)=0                                                     SOL00230
17    CONTINUE                                                          SOL00240
C                                                                       SOL00250
C                                                                       SOL00260
      DO 10 MONTH=1,12                                                  SOL00270
         IF(MONTH.EQ.1) THEN                                            SOL00280
           M(MONTH)=31                                                  SOL00290
         ELSEIF(MONTH.EQ.2) THEN                                        SOL00300
           M(MONTH)=28                                                  SOL00310
         ELSEIF(MONTH.EQ.3) THEN                                        SOL00320
           M(MONTH)=31                                                  SOL00330
         ELSEIF(MONTH.EQ.4) THEN                                        SOL00340
           M(MONTH)=30                                                  SOL00350
        ELSEIF(MONTH.EQ.5) THEN                                         SOL00360
           M(MONTH)=31                                                  SOL00370
        ELSEIF(MONTH.EQ.6) THEN                                         SOL00380
           M(MONTH)=30                                                  SOL00390
        ELSEIF(MONTH.EQ.7) THEN                                         SOL00400
           M(MONTH)=31                                                  SOL00410
        ELSEIF(MONTH.EQ.8) THEN                                         SOL00420
           M(MONTH)=31                                                  SOL00430
        ELSEIF(MONTH.EQ.9) THEN                                         SOL00440
           M(MONTH)=30                                                  SOL00450
        ELSEIF(MONTH.EQ.10) THEN                                        SOL00460
           M(MONTH)=31                                                  SOL00470
        ELSEIF(MONTH.EQ.11) THEN                                        SOL00480
           M(MONTH)=31                                                  SOL00490
        ELSE                                                            SOL00500
           M(MONTH)=30                                                  SOL00510
        ENDIF                                                           SOL00520
        WRITE(5,11)MONTH                                                SOL00530
11      FORMAT(4X,'( MONTH = ',I2,')')                                  SOL00540
        WRITE(5,*)'    ---------------------------------'               SOL00550
        WRITE(5,7)
```

```
 7    FORMAT(7X,'DAY',8X,'DELTA',6X,'HOH ( J/M )')                    SOL00560
      WRITE(5,*)'    ---------------------------------'               SOL00570
      DO 20 DAY=1,M(MONTH)                                           SOL00580
         IF(MONTH.EQ.1) THEN                                         SOL00590
          NN(DAY) = DAY                                              SOL00600
         ELSEIF(MONTH.EQ.2) THEN                                     SOL00610
          NN(DAY) = DAY + 31                                         SOL00620
         ELSEIF(MONTH.EQ.3) THEN                                     SOL00630
          NN(DAY)= DAY + 59                                          SOL00640
         ELSEIF(MONTH.EQ.4) THEN                                     SOL00650
          NN(DAY)= DAY + 90                                          SOL00660
         ELSEIF(MONTH.EQ.5) THEN                                     SOL00670
          NN(DAY)=DAY + 120                                          SOL00680
         ELSEIF(MONTH.EQ.6) THEN                                     SOL00690
          NN(DAY)= DAY + 151                                         SOL00700
         ELSEIF(MONTH.EQ.7) THEN                                     SOL00710
          NN(DAY)= DAY + 181                                         SOL00720
         ELSEIF(MONTH.EQ.8) THEN                                     SOL00730
          NN(DAY)= DAY + 212                                         SOL00740
         ELSEIF(MONTH.EQ.9) THEN                                     SOL00750
          NN(DAY)= DAY + 243                                         SOL00760
         ELSEIF(MONTH.EQ.10) THEN                                    SOL00770
          NN(DAY)= DAY + 273                                         SOL00780
         ELSEIF(MONTH.EQ.11) THEN                                    SOL00790
          NN(DAY)= DAY + 304                                         SOL00800
        ELSE                                                         SOL00810
          NN(DAY)= DAY + 334                                         SOL00820
        ENDIF                                                        SOL00530
C                                                                    SOL00840
      DELTA(DAY)=23.45*(SIN(360.0*(284.0+NN(DAY))*3.141593/(180.0*   SOL00850
     *           365.0))*3.141593/180.0)                             SOL00860
      WS(DAY)= ACOS(-1*TAN(FI) * TAN(DELTA(DAY)))                    SOL00870
      WSS(DAY)=WS(DAY)*180.0/3.141593                                SOL00880
      DELTAD(DAY)=DELTA(DAY)*180.0/3.141593                          SOL00890
      HOH(DAY)=((24*3600*GSC)/3.141593)*(1.0+0.033*COS((360.0*NN(DAY SOL00900
     *         )*3.141593)/(365.0*180.0)))*(COS(FI)*COS(DELTA(DAY))* SOL00910
     *         SIN(WS(DAY))+WS(DAY)*SIN(FI)*SIN(DELTA(DAY)))         SOL00920
      HOH(DAY)=INT(HOH(DAY))                                         SOL00930
C                                                                    SOL00940
C     CALCULATION OF HOH-AVERAGE                                     SOL00950
      SUM(MONTH)=SUM(MONTH)+HOH(DAY)                                 SOL00960
      HOHAV(MONTH)=SUM(MONTH)/M(MONTH)                               SOL00970
C                                                                    SOL00980
C                                                                    SOL00990
      WRITE(5,9)DAY,DELTAD(DAY),HOH(DAY)                             SOL01000
 9    FORMAT(8X,I2,6X,' I',2X,F5.1,2X,' I',2X,I8)                    SOL01010
      WRITE(5,*)'    ---------------------------------'               SOL01020
20    CONTINUE                                                       SOL01030
      WRITE(5,23)HOHAV(MONTH)                                        SOL01040
23    FORMAT(6X,'I ','HOH-AVR. = ',I8,2X,'J/M'   ,'     I')          SOL01050
      WRITE(5,*)'     | AVERAGE DAY( N )=            I'             SOL01060
      WRITE(5,*)'     | AND HOH-BAR( H )=       J/M | '            SOL01070
      WRITE(5,*)'     ---------------------------- '                 SOL01080
      WRITE(5,*)'   '                                                SOL01090
      WRITE(5,*)'   '                                                SOL01100

      CONTINUE                                                       SOL01110
      END                                                            SOL01120
```

LIST OF REFERENCES

[1] Maurel, A., " Desalination by Reverse Osmosis Using Renewable Energies (SolarWind)," ***European Seminar- Athens 26-27-28***, Cadarache Centre Experiment, Sep. 1991.

[2] Altinbilek, H and Akyust, M. " Desalination for Municipal supply". Symposium on the Appropriate Applications of Solar Energy for the Arab Gulf States, ***Solar Water Desalination***, March 1981. pp. 142-156.

[3] Wojcik, C.K. et al, " Performance Study of Water Desalination Methods in Saudi Arabia," ***SANCST Project No. AR-1-057***, Final Report,1983.

[4] Anani, F. M. " Desalination Its Potentials and Limitations in the Economic Development Process of Saudi Arabia," ***Dissertation***, 1973.

[5] Gomkale, S. D. " Desalination Systems Based on Renewable Energy Sources- Status and Prospects," ***Solar Energy Society of India***, 1989, pp. 343-354.

[6] Maadhah, A.G. " Desalination of Seawater". ***Solar Water Desalination***, March 1981, pp. 69-93.

[7] Wojcik, C.K. and Maadha, A.G., " Water Desalination in Saudi Arabia," ***The Arabian Journal for Science and Engineering***, Vol.8, No.3, 1983, pp. 169-178.

[8] " Desalination By Renewable Energy Sources," ***The U.S.A.I.D. Desalination Manual***, ch.7, Aug. 1980.

[9] Cadwallader et al. " The Application of Wind Energy Systems to Desalination," ***Report No. OWRT/S--78/1***, Williamson Engineering Associates, Inc., Navarre, Fl. Apr. 1977.

[10] Khan. A.H., " Desalination Processes and Multistage Flash Distillation Practice," ***Elsevier Science Publishers***, New York, 1986, pp. 153-160.

[11] Gaggioli, R.A., " Thermodynamics : Second Law Analysis," ***Edited by Gaggioli, R.A.***, 1978, pp. 3-13.

[12] Al-Sulaiman, F.A. and Jamjoum F.A., " Applications of Wind Power on the East Coast of Saudi Arabia," ***Renewable Energy***, Pergamon Press, 1991, (in press).

[13] Callahan, J. et al, " Brackish Water Solar Desalination System for Soleras Program", ***Solar Water Desalination***, March 1981, pp. 198-225.

[14] Abdul-Aal H.K. and Al-Somait F., " Solar Energy Prospects in Saudi Arabia," ***Energy Communications***, 4(3), 1978, pp. 271-291.

[15] Crutcher, J.L. et al, " Photovoltaic Powered Seawater Desalination Systems Experience with Two Installations", ***Proceedings of the sixteenth IEEE Photovoltaic Specialist Conference*** , September 1982, pp. 1400-1404.

[16] Finnegan D.R. and Wanger W.M., " Process Selection Guide to Seawater Desalting," ***Desalination***, Vol.38, Nov.1981, pp. 29-43.

[17] Gerofi. J.P. and Fenton G.G., " Comparison of Solar RO and Solar Thermal Desalination Systems," ***Desalination***, Vol.39, Dec.1981, pp.

95-107.

[18] Ericsson, B. and Hallmans. B., " A Comparative Study of the Economics of RO and MSF in the Middle East." ***Desalination***, Vol.55, Nov.1985. pp. 441-458.

[19] Lawand, T.A., " The Economics of Wind Powered Desalination Systems," ***Report No. T-36***, Brace Research Institute of McGill University. Sep.1967.

[20] Petit, P.J. and Gaggioli, R.A., " Second Law Procedure for Evaluating Processes," ***Thermodynamics: Second Law Analysis***, Edited by Gaggioli, R.A., 1978, pp. 16-37.

[21] Gyftopoulos, E.P. and Widmer, T.F., " Availability Analysis : The Combined Energy and Entropy Balance," ***Thermodynamics: Second Law Analysis***, Edited by Gaggioli, R.A., 1978. pp. 62-75.

[22] London, A.L., " Economics and The Second Law : An Engineering View and Methodology," ***Inter. J. Heat Mass Transfer***, Vol.25, No.6, 1982, pp. 743-751.

[23] Gaggioli, R.A. et al, " Second Law Efficiency and Costing Analysis of A combined Power and Desalination Plant." ***Journal of Energy Resources Technology***, Vol.110, Jun. 1988. pp. 114-118.

[24] Garg, H.P. et al, " Potential Energy Storage as Pumped Hydro," ***Solar Thermal Energy Storage***, D. Reidel Publishing Co., 1985, pp. 31-34.

[25] Andrews, J.W., " Energy-Storage Requirements Reduced in Coupled Wind Solar Generating Systems ". *Solar Energy*, Vol.18, 1976, pp. 73-74.

[26] Jensen, J. and Tofield, B.C., " Advanced Batteries for Energy Storage." *International Conference on Energy Storage*, Apr. 1981. pp. 205-211.

[27] Darlington, A.D. et al, " Estimation of Size Requirements for Solar Photovoltaic Systems," *Conference (C15), at the Royal Institution*, May, 1978, pp. 59-65.

[28] Barra, L. et al, " An Analytical Method to Determine the Optimal Size of a Photovoltaic Plant," *Solar Energy*, Vol.33, No.6, 1984. pp. 509-514.

[29] Duffie, J.A. and Beckman. W.A., " Design of Active Systems By $\overline{\varphi}-f$ chart Method," *Solar Engineering of Thermal Processes*, John Wiley & Sons, Inc., 1991, pp. 720-730.

[30] El-Nashar, A.M., " Performance of the Solar Desalination Plant at Abu Dhabi," Symposium on the Appropriate Applications of Solar Energy for the Arab Gulf States, *Edited by Ayyash, S.Y.*, 1987, pp. 183-194.

[31] Tribus, M. and Evans, R. , " The Thermodynamics of Seawater Conversion" , *Report No. 62-53.* Feb. 1963.

[32] Maurel, A. , " Seawater and Brackish Water Desalination" , *Report No. SEDFMA/SEATN/86-0048*, Feb. 1986. pp 1-31.

[33] Luft, W. , " Solar Energy Water Desalination in the United States and Saudi Arabia" , *Report No. 1044.11* , Apr. 1981, pp 1-23.

[34] Nadler. M. et al, " Planning an Energy Efficient Solar Powered Desalination Plant" , ***Solar Water Desalination*** , Mar. 1981, pp 299-312.

[35] Kreith, F. and Luft, W. , " An Overview of Solar Desalination Technologies" , ***Solar Water Desalination*** , Mar. 1981, pp 12-32.

[36] Smulders, P.T. and Feron, P. , " Seawater Desalination and Wind Energy" , ***European Wind Energy Conference*** , Oct. 1984. pp 634-641.

[37] Lior, N. , " Principles of Desalination" , ***Solar Water Desalination*** , Mar. 1981, pp 1-11.

[38] Bushnak, A. , " Desalination by Reverse Osmosis" , ***Solar Water Desalination*** , Mar. 1981, pp 281-293.

[39] Hamester, H. et al, " Design of a Commercial Solar Powered Hybrid Desalination Plant for Seawater at Yanbu, Saudi Arabia" , ***Solar Water Desalination*** , Mar. 1981, pp 241-263.

[40] James, W.L. , " The Demonstration of a Solar Photovoltaic Reverse Osmosis Desalination Plant" , ***Report No. 18/1109***, Sep. 1986, pp 1-38.

[41] Petersen, G. et al, " A Wind-Powered Water Desalination Plant for a small Island Community at the German Coast of the North Sea - Desig and Working Experience" , ***Report No. GKSS 83/E/81*** Sep. 1983, pp 173-180.

[42] Al-Nashar, A. and Qamhiyeh, A. , " Simulation of the Performance of MES Evaporators Under Unsteady State Operating Conditions" ,

Desalination , Vol. 79. 1990, pp 65-83.

[43] Wylen. G.V. and Sonntag. R.E. . " Fundamentals of Classical Thermodynamics" , *John Wiley and Sons Inc.* , Mar. 1985, Third Edition.

[44] Pitzer. K. et al. " Thermodynamic Properties of Aqueous Sodium Chloride Solutions" , *J. Phys. Chem. Ref. Data* , Vol. 13. No. 1. 1984. pp. 1-100.

[45] Al-Hussain. M. , *Al-Khobar MSF Desalination Plant, Personal Communication* , 1992 .

[46] El-Nashar, A. , " Performance of the Solar Desalination Plant at Abu-Dhabi" , *Desalination* , Vol. 72, 1989, pp. 405-424.

[47] Darwish. M. , " Comparison Between Small Capacity Mechanical Vapor Compression (MVC) and Reverse Osmosis (RO) Desalination Plants" , *Desalination* , Vol. 78, 1990, pp. 313-326.

[48] El-Hadidi, M. and Shahid, S. " Meteorological Data for Dhahran" , *Energy Research Lab., KFUPM, Personal Communication*, 1992.

[49] Ansari, J. et al, " Wind Energy Atlas for the Kingdom of Saudi Arabia", 1986.

[50] El-Nashar. A. , " Computer Simulation of the Performance of a Solar Desalination Plant" , *Solar Energy*, Vol. 44, No.4, 1990, pp. 193-205.

[51] Bandopadhayay,P. . " Economic Evaluation of Wind Energy Applications for Remote Location Power Supply" , *Wind Engineering*,

Vol. 7, No.2, 1983.

[52] Auer, W., " Industrial Process Heat Applications Operational Field Test Oveview", ***Solar Water Desalination***, April 1983, p. 80.

[53] Feron, P., " The Use of Wind Power in Autonomous Reverse Osmosis Seawater Desalination" , ***Wind Engineering***, Vol. 9, No.3, 1985, pp. 196-197.